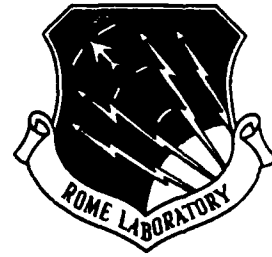


AD-A238 809



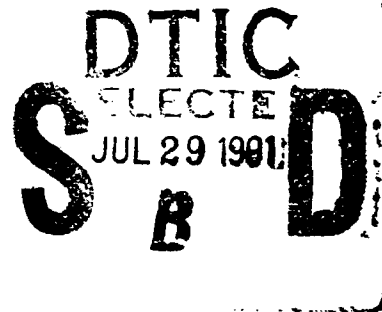
RL-TR-91-104
Final Technical Report
June 1991



APPLICATION OF THE MATRIX PENCIL APPROACH TO DIRECTION FINDING

Syracuse University

Braham Himed and Donald D. Weiner



APPROVED FOR PUBLIC RELEASE; DISTRIBUTION UNLIMITED.

91-05836

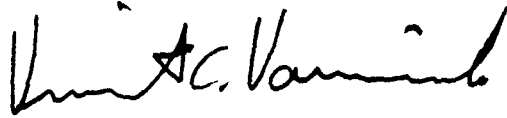
Rome Laboratory
Air Force Systems Command
Griffiss Air Force Base, NY 13441-5700

91 7 22 030

This report has been reviewed by the Rome Laboratory Public Affairs Office (PA) and is releasable to the National Technical Information Service (NTIS). At NTIS it will be releasable to the general public, including foreign nations.

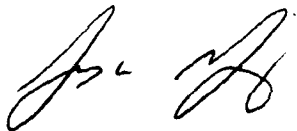
RL-TR-91-104 has been reviewed and is approved for publication.

APPROVED:



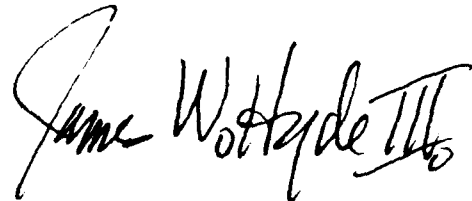
VINCENT C. VANNICOLA
Project Engineer

APPROVED:



JAMES W. YOUNGBERG, LtCol, USAF
Deputy Director of Surveillance

FOR THE COMMANDER:



JAMES W. HYDE III
Directorate of Plans & Programs

If your address has changed or if you wish to be removed from the Rome Laboratory mailing list, or if the addressee is no longer employed by your organization, please notify RL(OCTS) Griffiss AFB NY 13441-5700. This will assist us in maintaining a current mailing list.

Do not return copies of this report unless contractual obligations or notices on a specific document require that it be returned.

REPORT DOCUMENTATION PAGE

Form Approved
OMB No. 0704-0188

Public reporting burden for this collection of information is estimated to average 1 hour per response, including the time for reviewing instructions, searching existing data sources, gathering and maintaining the data needed, and completing and reviewing the collection of information. Send comments regarding this burden estimate or any other aspect of this collection of information, including suggestions for reducing this burden, to Washington Headquarters Service, Directorate for Information Operations and Reports, 1215 Jefferson Davis Highway, Suite 1204, Arlington, VA 22202-4302, and to the Office of Management and Budget, Paperwork Reduction Project (0704-0188), Washington, DC 20503.

1. AGENCY USE ONLY (Leave Blank)		2. REPORT DATE June 1991	3. REPORT TYPE AND DATES COVERED Final	
4. TITLE AND SUBTITLE APPLICATION OF THE MATRIX PENCIL APPROACH TO DIRECTION FINDING			5. FUNDING NUMBERS C - F30602-88-D-0027 TASK - A-9-1126 PE - 62702F PR - 4506 TA - 11 WU - P4	
6. AUTHOR(S) Braham Himed, Donald D. Weiner			8. PERFORMING ORGANIZATION REPORT NUMBER	
7. PERFORMING ORGANIZATION NAME(S) AND ADDRESS(ES) Syracuse University Department of Electrical & Computer Engineering 111 Link Hall Syracuse NY 13210			10. SPONSORING/MONITORING AGENCY REPORT NUMBER RL-TR-91-104	
9. SPONSORING/MONITORING AGENCY NAME(S) AND ADDRESS(ES) Rome Laboratory (OCTS) Griffiss AFB NY 13441-5700			11. SUPPLEMENTARY NOTES Rome Laboratory Project Engineer: Vincent C. Vannicola/OCTS/(315) 330-4437	
12a. DISTRIBUTION/AVAILABILITY STATEMENT Approved for public release; distribution unlimited.			12b. DISTRIBUTION CODE	
13. ABSTRACT (Maximum 200 words) The Matrix Pencil Approach (1) was shown to be an effective and efficient method for estimating the angles of arrival of multiple narrowband sources. It is classified as non search procedure. Therefore, it is computationally less complicated and eliminates problems encountered in search procedures with regard to memory storage and system calibration. Having collected the data from the outputs of a linear uniformly spaced array consisting of m sensors, the objective is to estimate the locations of the d sources (d m). The information about the parameters of interest are contained in the rank reducing values of a matrix pencil generated from the set of data.				
14. SUBJECT TERMS Signal Processing, Radar, Direction Finding, Electronics Engineering			15. NUMBER OF PAGES 202	
			16. PRICE CODE	
17. SECURITY CLASSIFICATION OF REPORT UNCLASSIFIED	18. SECURITY CLASSIFICATION OF THIS PAGE UNCLASSIFIED	19. SECURITY CLASSIFICATION OF ABSTRACT UNCLASSIFIED	20. LIMITATION OF ABSTRACT U/L	

ABSTRACT

The Matrix Pencil Approach [1] was shown to be an effective and efficient method for estimating the angles of arrival of multiple narrow-band sources. It is classified as a non search procedure. Therefore, it is computationally less complicated and eliminates problems encountered in search procedures with regard to memory storage and system calibration. Having collected the data from the outputs of a linear uniformly spaced array consisting of m sensors, the objective is to estimate the locations of the d sources ($d < m$). The information about the parameters of interest are contained in the rank reducing values of a matrix pencil generated from the set of data.

Several extensions of the Matrix Pencil Approach appear in this work. In the earlier work [1], a data window of length $L = m - d$ was used to form $(d + 1)$ vectors. Because this choice results in a minimum number of vectors to span the array, it fails to take into consideration the possible separation of the signal and noise subspaces. Thus, performance is drastically degraded at low values of signal to noise ratio (SNR). In this work it is shown that improved performance can be achieved using a data window of length $L = d$. Because this results in $(m - d + 1)$ vectors, which is the maximum number of vectors to span the array, identification of the noise subspace is possible. Previous developments of high resolution algorithms neglected the effects of mutual coupling which occurs between the elements of an array. We show that failure to account for mutual coupling results in poor performance. Concentrating our efforts on the non search procedures of ESPRIT and the Moving Window, we have successfully improved the performance of these methods by compensating for the mutual coupling. The problem of wideband signals is much more difficult and has been studied

by only a few investigators. Three methods dealing with the wideband case are proposed in this work. In the first method the wideband signals are modeled as sums of decaying exponentials. This model is suitable for non stationary signals. The natural frequencies of the sources are assumed to be unknown at the receiver. Therefore, the estimation procedure consists of estimating both natural frequencies and angles of arrival of the sources by means of two matrix pencils. However, an ambiguity problem arises as to which natural frequencies are to be associated with which angles of arrival. We show that a third matrix pencil removes this ambiguity. A second method is proposed where the wideband sources are assumed to be linear systems driven by white noise. This model is appropriate for stationary signals. The same array configuration as in the first case is used. The analysis is carried out on the unit circle using the Discrete Fourier Transform. The third approach makes use of the coherent signal subspace method (CSS) proposed by Wang and Kaveh [56] in conjunction with the moving window operator. Again the method performs relatively well when compared to ESPRIT. Finally, we have studied the effects of perturbation due to noise and due to sensor spacing. We have derived upper bounds for the Chordal Metric which is a measure between the true eigenvalue and the perturbed one. The chordal metric is shown to be a functional of the true and the perturbed angles of arrival.

Computer simulations are carried out for each of the analyses associated with respect to data window length, mutual coupling compensation, the three wideband methods, and the upper bounds in the chordal metric.

Accession For	
NTIS GRA&I	<input checked="" type="checkbox"/>
DTIC TAB	<input type="checkbox"/>
Unannounced	<input type="checkbox"/>
Justification _____	
By _____	
Distribution/	
Availability Codes	
Dist.	Avail and/or Special
A-1	



TABLE OF CONTENTS

	Page
ACKNOWLEDGMENTS	ii
LIST OF CONVENTIONS	v
LIST OF FIGURES	vi
CHAPTER 1 INTRODUCTION	1
1.1 Work Objectives	1
1.2 Signal Model	3
1.3 Literature Survey	5
1.4 Work Outline	18
CHAPTER 2 SIGNAL SUBSPACE PROCESSING	19
2.1 Principle	19
2.2 Pencil Theorem	21
2.2.1 Theorem	21
2.2.2 Determination of rank reducing values	22
2.3 Matrix Pencil Approach	25
2.3.1 ESPRIT	25
2.3.2 Moving Window	28
2.3.2.1 Original Version	30
2.3.2.2 New Version	33
2.3.2.3 Computer Simulation	34
CHAPTER 3 COMPENSATION FOR MUTUAL COUPLING	43
3.1 Model	44
3.2 Minimum Mean-Squared Error Estimation	50
3.3 Moving Window	51
3.4 ESPRIT	54
3.4.1 General Array	54
3.4.2 Linear Array	58
3.4.2.1 Overlapping Case	58
3.4.2.2 Non Overlapping Case	62
3.5 Computer Simulation	66
CHAPTER 4 EXTENSIONS TO WIDEBAND SIGNALS	80
4.1 Transient Signals	80
4.1.1 Computer Simulation	89
4.2 Wide Sense Stationary Signals	100
4.2.1 Computer Simulation	111
4.3 Fourier Approach	120
4.3.1 Computer Simulation	127
CHAPTER 5 PERTURBATION ANALYSIS	135
5.1 Chordal Metric	135
5.2 Perturbation Due to Noise	137
5.2.1 Moving Window	137
5.2.2 ESPRIT	139
5.2.2.1 General Case	140
5.2.2.2 Linear Overlapping Case	141

5.2.2.3	Linear Non Overlapping Case . . .	142
5.2.3	Computer Simulation	144
5.3	Perturbation Due to Sensor Spacing	149
5.3.1	Moving Window	149
5.3.2	ESPRIT	155
5.3.2.1	General Case	155
5.3.2.2	Linear Overlapping Case	159
5.3.2.2	Linear Non Overlapping Case	164
5.3.3	Computer Simulation	167
CHAPTER 6	CONCLUSION AND FUTURE WORK	173
6.1	Conclusion	173
6.2	Future Work	175
APPENDIX	177
REFERENCES	181

LIST OF CONVENTIONS

A	matrix A
A^H	transpose complex conjugate of A
A^+	pseudo-inverse of A
$\det(A)$	determinant of A
I	identity matrix
\underline{x}	vector \underline{x}
$ \underline{x} $	Euclidean norm of vector \underline{x}
$ A $	Euclidean norm of matrix A
$ A _f$	Frobenius norm of matrix A
$\langle \underline{x}, \underline{y} \rangle$	inner-product of vectors \underline{x} and \underline{y}
$E[\underline{X}]$	expected value of random vector \underline{X}
C	field of complex numbers
ε	belong to

LIST OF FIGURES

	Page
Fig. 1.1 Passive Angle of Arrival Estimation	2
Fig. 2.1 ESPRIT: General Array	26
Fig. 2.2 Moving Window of Length L	29
Fig. 2.3 Sample Mean of Angle Estimate at 16°	37
Fig. 2.4 Sample Mean of Angle Estimate at 24°	38
Fig. 2.5 Sample Variance of the Angle Estimate at 16°	39
Fig. 2.6 Sample Variance of the Angle Estimate at 24°	40
Fig. 2.7 Mean-Squared Error of the Angle Estimate at 16°	41
Fig. 2.8 Mean-Squared Error of the Angle Estimate at 24°	42
Fig. 3.1 Linear Array of m Dipoles	45
Fig. 3.2 Subsectioning of the m Dipoles	46
Fig. 3.3 ESPRIT: General Case	55
Fig. 3.4 ESPRIT: Linear Array	
3.4a Overlapping Case	59
3.4b Non Overlapping Case	59
Fig. 3.5 Sample Mean of the Angle Estimate at 16° Without Compensation	68
Fig. 3.6 Sample Mean of the Angle Estimate at 16° With Compensation Using MMSE Method	69
Fig. 3.7 Sample Mean of the Angle Estimate at 16° With Compensation Using Direct	70
Fig. 3.8 Mean-Squared Error of the Angle Estimate at 16° Without Compensation	71
Fig. 3.9 Mean-Squared Error of the Angle Estimate at 16° With Compensation Using MMSE Method	72
Fig. 3.10 Mean-Squared Error of the Angle Estimate at 16° With Compensation Using Direct	73
Fig. 3.11 Sample Mean of the Angle Estimate at 24° Without Compensation	74
Fig. 3.12 Sample Mean of the Angle Estimate at 24° With Compensation Using MMSE Method	75
Fig. 3.13 Sample Mean of the Angle Estimate at 24° With Compensation Using Direct	76
Fig. 3.14 Mean-Squared Error of the Angle Estimate at 24° Without Compensation	77
Fig. 3.15 Mean-Squared Error of the Angle Estimate at 24° With Compensation Using MMSE Method	78
Fig. 3.16 Mean-Squared Error of the Angle Estimate at 24° With Compensation Using Direct	79
Fig. 4.1 Wideband Array Configuration	82
Fig. 4.2 Emitter-Receiver Modeling	
4.2a l-th emitter source	101
4.2b Output of i-th Sensor to a Source Coming From Direction θ_1	101
4.2c Combination of the 2 Systems	101
Fig. 4.3 Sample Mean of the Angle Estimate at 16° (Transient Signals)	91
Fig. 4.4 Sample Variance of the Angle Estimate at 16° (Transient Signals)	92
Fig. 4.5 Mean-Squared Error of the Angle Estimate at 16° (Transient Signals)	93

Fig. 4.6	Sample Mean of the Angle Estimate at 24° (Transient Signals)	94
Fig. 4.7	Sample Variance of the Angle Estimate at 24° (Transient Signals)	95
Fig. 4.8	Mean-Squared Error of the Angle Estimate at 24° (Transient Signals)	96
Fig. 4.9	Sample Mean of the Angle Estimate at 16° (Wide Sense Stationary Signals)	112
Fig. 4.10	Sample Variance of the Angle Estimate at 16° (Wide Sense Stationary Signals)	113
Fig. 4.11	Mean-Squared Error of the Angle Estimate at 16° (Wide Sense Stationary Signals)	114
Fig. 4.12	Sample Mean of the Angle Estimate at 24° (Wide Sense Stationary Signals)	115
Fig. 4.13	Sample Variance of the Angle Estimate at 24° (Wide Sense Stationary Signals)	116
Fig. 4.14	Mean-Squared Error of the Angle Estimate at 24° (Wide Sense Stationary Signals)	117
Fig. 4.15	Sample Mean of the Angle Estimate at 16° (Fourier Approach)	129
Fig. 4.16	Sample Variance of the Angle Estimate at 16° (Fourier Approach)	130
Fig. 4.17	Mean-Squared Error of the Angle Estimate at 16° (Fourier Approach)	131
Fig. 4.18	Sample Mean of the Angle Estimate at 24° (Fourier Approach)	132
Fig. 4.19	Sample Variance of the Angle Estimate at 24° (Fourier Approach)	133
Fig. 4.20	Mean-Squared Error of the Angle Estimate at 24° (Fourier Approach)	134

CHAPTER 1

INTRODUCTION

1.1 RESEARCH OBJECTIVES

In this work, the problem of passive high resolution direction finding of multiple sources using a sensor array is addressed. This problem arises in such systems as radar, sonar, seismology, geophysics, etc. A direction finding system is referred to as passive when the signals received at the array are generated externally to the array. These signals can be either narrowband or broadband. In both cases, given measurements collected at the array output, the objective is to determine the number of targets (Detection) and estimate their parameters such as angles of arrival, natural frequencies, etc., (Estimation). A signal is classified as narrowband when the bandwidth of the impinging signals from the sources is much less than the reciprocal of the propagation time of the wavefronts across the array. When this condition does not hold, the signals are said to be wideband.

The problem of narrowband sources has been studied extensively. Solutions range from the classical ones such as the periodogram, the correlogram, etc. to subspace approaches such as MUSIC, ESPRIT, Matrix Pencil, etc. This work deals with the Matrix Pencil Approach [1]. For the sake of clarity, assume that d narrowband sources are present, m measurements are collected at the output of a linear uniformly spaced array of m elements and $m > d$ (Fig. 1-1). The Matrix Pencil approach is based on an invariance introduced by the geometry of the array (linear uniformly spaced). It is shown that the parameters of interest, i.e, the angles of arrival, are related to the rank reducing values of a matrix pencil generated from the

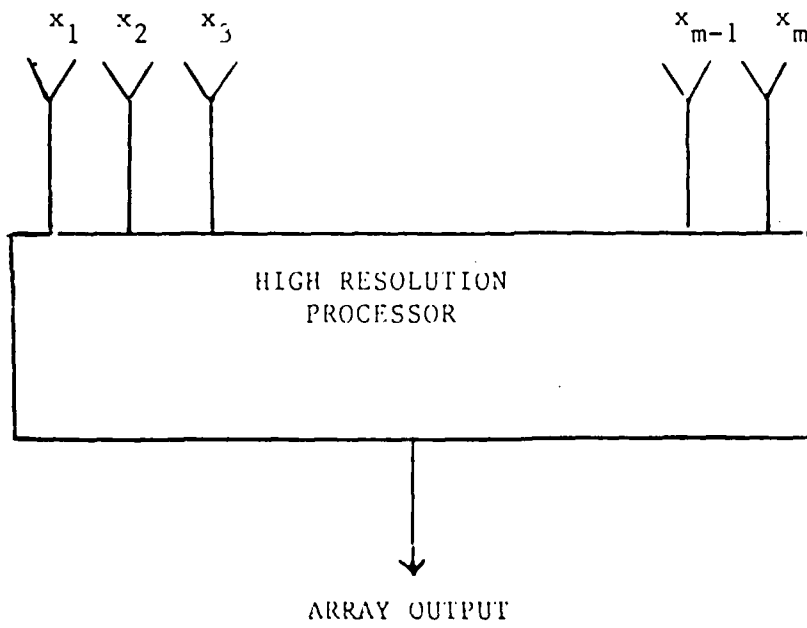
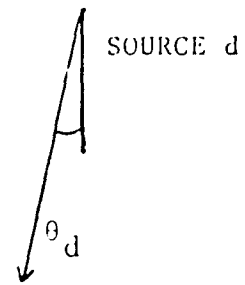
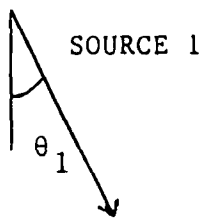


Fig. 1-1 Passive Angle of Arrival Estimation

data. The method is shown to hold even in the presence of fully correlated sources. However, the method, as applied in [1], did not fully take into account the separation of the noise and signal subspaces. The eigenvalues generated from the data, as applied in [1], were obtained using a dimensionality too small to allow for identification of the noise subspace. That is the reason why the method performed relatively poorly at low signal to noise ratios (SNR). We have devised a scheme which displays improved performance at low SNR. High resolution algorithms devised previously ignored mutual coupling which may exist between array elements. In effect, each element of the array was modeled as though it existed by itself. We have studied the effects of mutual coupling and we devised schemes to compensate for these effects. The case of wideband sources is much more complex and has been treated by only a few authors. In this dissertation, we extended the notion of the matrix pencil to the wideband case. Finally, previous algorithms assumed a perfect sensor spacing. We studied the performance of the matrix pencil for the case of small perturbations in the sensor spacing.

1.2 SIGNAL MODEL

Before reviewing the work that has been done previously, it is useful to develop expressions for the received signals and see how they simplify for the case of narrowband signals. For this, assume that we have a linear uniformly spaced array composed of m identical sensors. Let Δ be the sensor spacing and d the number of sources. These sources are assumed to be in the far field so that planar waves arrive at the array. It follows that the output of the i -th array element can be expressed as

$$x_i(t) = \sum_{k=1}^d a(\theta_k) s_k(t - \tau_{ik}) + n_i(t); \quad i=1, 2, \dots, m, \quad (1.2-1)$$

where

$a(\theta_k)$ is the gain pattern of the sensor at angle θ_k ,

$n_i(t)$ is the additive noise,

τ_{ik} is the time delay that source k takes to travel from the reference sensor to the i -th sensor. With respect to the first sensor τ_{ik} is given by

$$\tau_{ik} = (i-1)(\Delta/c)\sin(\theta_k), \quad (1.2-2)$$

where c is the propagation speed of the plane waves.

Let $s_k(t)$ be a modulated signal of the form

$$s_k(t) = g_k(t)\cos(\omega_0 t + \alpha_k(t)), \quad (1.2-3)$$

where all the sources are assumed to be emitting at the same carrier frequency ω_0 . Therefore, $s_k(t - \tau_{ik})$ is given by

$$s_k(t - \tau_{ik}) = g_k(t - \tau_{ik})\cos(\omega_0 t - \omega_0 \tau_{ik} + \alpha_k(t - \tau_{ik})). \quad (1.2-4)$$

Note that

$$\omega_0 \tau_{ik} = (i-1)\phi_k, \quad (1.2-5)$$

where

$$\phi_k = \omega_0(\Delta/c)\sin(\theta_k). \quad (1.2-6)$$

For narrowband signals, the modulation varies slowly relative to the carrier. In particular, assume that $g_k(t)$ and $\alpha_k(t)$ are essentially unchanged over the duration of the observation interval. Then

$$g_k(t - \tau_{ik}) \approx g_k(t) \quad (1.2-7)$$

and

$$\alpha_k(t - \tau_{ik}) \approx \alpha_k(t). \quad (1.2-8)$$

The expression for $s_k(t - \tau_{ik})$ simplifies to

$$s_k(t - \tau_{ik}) = g_k(t)\cos(\omega_0 t - (i-1)\phi_k + \alpha_k(t)). \quad (1.2-9)$$

Clearly, for narrowband signals, we see that the time delay results in a phase shift. When the signals $s_k(t)$ are broadband, $g_k(t-\tau_{ik})$ and $\alpha_k(t-\tau_{ik})$ can no longer be approximated by $g_k(t)$ and $\alpha_k(t)$, respectively.

For narrowband signals, note that $s_k(t-\tau_{ik})$ can be written as

$$s_k(t-\tau_{ik}) = \text{Re}\{ g_k(t) e^{j\alpha_k(t)} e^{-j(i-1)\phi_k} e^{j\omega_0 t} \} \quad (1.2-10)$$

where $\text{Re}\{.\}$ denotes the real part operator. Let $\tilde{s}_k(t)$ be the complex envelope of $s_k(t)$. Then

$$\tilde{s}_k(t) = g_k(t) e^{j\alpha_k(t)}. \quad (1.2-11)$$

Also define $\tilde{x}_i(t)$ and $\tilde{n}_i(t)$ as the complex envelopes of $x_i(t)$ and $n_i(t)$, respectively. It is easy to see that

$$\tilde{x}_i(t) = \sum_{k=1}^d a(\theta_k) \tilde{s}_k(t) e^{-j(i-1)\phi_k} + \tilde{n}_i(t); \quad i=1, 2, \dots, m. \quad (1.2-12)$$

In the remainder of this dissertation, we will drop the "~" and will assume that we are dealing with the complex envelopes of the corresponding signals. The expression for the received signal at the i -th sensor will be expressed as

$$x_i(t) = \sum_{k=1}^d a(\theta_k) s_k(t) e^{-j(i-1)\phi_k} + n_i(t); \quad i=1, 2, \dots, m. \quad (1.2-13)$$

1.3 LITERATURE SURVEY

The problem of estimating the angular locations of sources is of great importance and, over the years, has occupied many researchers. This problem is the spatial frequency analog of the temporal problem dealing with harmonic retrieval in additive noise. Consequently, research in direction finding has benefited a great deal from the advances made in spectral analysis. The periodogram [2,3] was seen as one of the most promising meth-

ods in determining the locations of sources where one has to plot the function

$$\hat{P}_{XX}(\phi) = (\Delta/m) \left| \sum_{k=1}^d x_i(t) e^{-ji\phi} \right|^2, \quad (1.3-1)$$

where $x_i(t)$ is the received signal at the i -th sensor, Δ is the sensor spacing and m is the total number of sensors. The periodogram has the advantage of being non parametric in the sense that it does not rely on knowledge of a model of the input processes. Also, it is robust in that it is relatively insensitive to signal parameters. It is also simple to implement. However, a disadvantage is that the physical size of the array has to be increased in order to achieve a better resolution. Typically, two sources that are separated by less than one standard beamwidth cannot be resolved. The standard beamwidth is defined as $\phi_B = 2\pi/m$.

Another way of estimating the power spectral density (p.s.d) is by using the autocorrelation sequence [4,5] defined as

$$\hat{r}_{XX}(l) = 1/(m-l) \sum_{n=1}^{(m-l)} x_{n+1}(t) x_n^*(t); \quad l=0, 1, \dots, (m-1). \quad (1.3-2)$$

When considering only a finite sequence, the power spectral density is estimated by the correlogram which is given by

$$\hat{P}_{XX}(\phi) = \Delta \sum_{l=-L}^L r_{XX}(l) e^{-jl\phi}, \quad (1.3-3)$$

where $L = (m/10)$ has been found to give good estimates of the terms in the autocorrelation sequence. Note that this may require an unacceptably large value of m . This value of L arises in an attempt to get good estimates of

$r_{xx}(l)$ for all lags in the sum.

Parametric spectral estimation techniques [6,7] have been introduced to overcome the limitations encountered with the periodogram or the correlogram. Here, the spatial samples $x_i(t)$ are taken as the samples from an autoregressive (AR) process of order p which, by definition, satisfies the linear difference equation

$$\hat{x}_n(t) = - \sum_{k=1}^p a_k x_{n-k}(t) + u_n, \quad (1.3-4)$$

where the coefficients a_k 's ; $k=1, \dots, p$, are constant parameters and u_n is a sample from a zero mean white Gaussian process with autocorrelation sequence

$$\hat{r}_{uu}(l) = \begin{cases} E[|u_n|^2] = \rho_{uu} & ; l=0 \\ 0 & ; l \neq 0 \end{cases} \quad (1.3-5)$$

In this approach, the angles of arrival are obtained as the maxima of the power spectral density

$$\hat{P}_{AR}(\phi) = (\Delta \rho_{uu}) \left\{ \left| 1 + \sum_{k=1}^p a_k e^{-jk\phi} \right|^{-2} \right\}, \quad (1.3-6)$$

where ρ_{uu} and a_k ; $k=1, 2, \dots, p$ are obtained by solving the Yule-Walker normal equations

$$\begin{bmatrix} \hat{r}_{xx}(0) & \hat{r}_{xx}^*(1) & \dots & \hat{r}_{xx}^*(p) \\ \hat{r}_{xx}(1) & \hat{r}_{xx}(0) & \dots & \hat{r}_{xx}^*(p-1) \\ \vdots & \vdots & \dots & \vdots \\ \hat{r}_{xx}(p) & \hat{r}_{xx}(p-1) & \dots & \hat{r}_{xx}(0) \end{bmatrix} \begin{bmatrix} 1 \\ a_1 \\ \vdots \\ a_p \end{bmatrix} = \begin{bmatrix} \rho_{uu} \\ 0 \\ \vdots \\ 0 \end{bmatrix}$$

and $\hat{r}_{xx}(l)$ is the autocorrelation estimator given by

$$\hat{r}_{xx}(l) = 1/(m-l) \sum_{n=1}^{(m-l)} x_{n+1}(t)x_n^*(t) ; l=0, 1, \dots, p. \quad (1.3-7)$$

Recall that the p.s.d in the correlogram method is given by

$$\hat{P}_{xx}(\phi) = \Delta \sum_{l=-L}^L \hat{r}_{xx}(l)e^{-jl\phi} , \quad (1.3-8)$$

which means that the autocorrelation sequence is assumed to be zero for $|l|>L$. This windowing is the reason for the poor resolution capability of the classical estimator. The AR p.s.d estimator uses the autocorrelation of the correlogram methods and extrapolates estimates of the autocorrelation sequence through

$$\begin{aligned} \hat{r}_{xx}(l) &= \sum_{k=-L}^L a_k \hat{r}_{xx}(l-k) ; l>0 \\ \hat{r}_{xx}(l) &= \hat{r}_{xx}^*(l) ; l<0 \end{aligned} \quad (1.3-9)$$

which results in a p.s.d given by

$$\hat{P}_{xx}(\phi) = \Delta \sum_{l=-\infty}^{\infty} \hat{r}_{xx}(l)e^{-jl\phi} . \quad (1.3-10)$$

This means that it extrapolates estimates of the entire autocorrelation sequence which explains the high resolution property of the AR p.s.d estimator. Burg [8] showed that the extrapolated autocorrelation function has maximum entropy. This results in the most random time series which has $\hat{r}_{xx}(0), \hat{r}_{xx}(1), \dots, \hat{r}_{xx}(p)$ as its first $(p+1)$ lag values.

Linear prediction techniques [9-11] can also be applied to the

direction finding problem. The idea here is to estimate the output of the n-th sensor as a linear combination of the other sensor outputs ; i.e,

$$\hat{x}_n(t) = - \sum_{k=1}^L a_k^f x_{n-k}(t) ; L < n \leq m \quad (1.3-11)$$

where L is the order of the prediction filter. The coefficients a_k^f are chosen such that the error $\rho = E[|x_n(t) - \hat{x}_n(t)|^2]$ is minimized. The minimization results in the minimum error variance given by

$$\rho_{\min} = r_{xx}(0) + \underline{r}_L^H \underline{a}.$$

The equations involved in the minimization can be expressed as

$$\begin{bmatrix} \hat{r}_{xx}(0) & \hat{r}_{xx}^*(1) & \dots & \hat{r}_{xx}^*(L) \\ \hat{r}_{xx}(1) & \hat{r}_{xx}(0) & \dots & \hat{r}_{xx}^*(L-1) \\ \vdots & \vdots & \ddots & \vdots \\ \hat{r}_{xx}(L) & \hat{r}_{xx}(L-1) & \dots & \hat{r}_{xx}(0) \end{bmatrix} \begin{bmatrix} 1 \\ a_1^f \\ \vdots \\ a_p^f \end{bmatrix} = \begin{bmatrix} \rho_{uu} \\ 0 \\ \vdots \\ 0 \end{bmatrix}.$$

These equations are identical to the Yule-Walker equations when $L=p$. Therefore, for $L=p$, the Yule-Walker equations arise in both the AR and linear forward prediction approaches. Backward linear prediction can also be introduced where

$$\hat{x}_{n-L}(t) = - \sum_{k=1}^L a_k^b x_{n-L-k}(t) . \quad (1.3-12)$$

Again, the coefficients a_k^b are chosen so as to minimize the error defined as $\rho = E[|x_{n-L}(t) - \hat{x}_{n-L}(t)|^2]$. This leads us to the same set of equations as before and it can be shown that $\rho_{\min}^f = \rho_{\min}^b$ and $(a_k^f) = (a_k^b)^*$ for $k=1, 2, \dots, L$. The forward-backward linear prediction (FBLP) is based on the use of least squares for estimating the AR parameters. This technique is also

known as the least squares method [12-15]. Here, we have to solve an over-determined set of equations of $2(m-p)$ equations in p unknowns, where p is the order of the filter.

If the available data sequence is very long, sequential estimation techniques are available for updating the AR parameter estimates. These techniques are useful for tracking sources with slowly varying angles of arrival. They are also known as adaptive algorithms. The least mean squares (LMS) adaptive algorithm [16] is based upon the gradient steepest descent adaptive procedure where the $(j+1)$ -th element is given by

$$\hat{x}_{j+1}(t) = - \sum_{k=1}^p a_k x_{j+1-k}(t) . \quad (1.3-13)$$

A minimization procedure is then developed which results in a $(j+1)$ -th error given by

$$e_{j+1}(p, j) = x_{j+1}(t) + (\underline{x}_j(p-1))^T \underline{a}_p(j) . \quad (1.3-14)$$

The LMS algorithm attempts to find the minimum of the mean-squared error quadratic surface. This search proceeds in a random fashion but, on the average, the LMS algorithm converges to the optimum coefficient vector. The condition for convergence is that the step size satisfies

$$0 < \xi < (1/p r_{xx}(0)) , \quad (1.3-15)$$

where

$$r_{xx}(0) = (1/j) \sum_{k=1}^j |x_k(t)|^2 . \quad (1.3-16)$$

Another way of dealing with long data sequences is to use a recursive least squares method (RLS) [17]. This method searches for the forward prediction error filter vector \underline{a}_p which minimizes the sum of the squared

errors subject to the constraint that the first component of \underline{a}_p is unity. This method leads to the same answer as in the LMS case. The only difference is that the adaptive gain is constant for the LMS whereas it is a spatially variant matrix for the RLS. The LMS appears to be more attractive than the RLS because of its robustness in its behavior, its insensitivity to perturbations and its computational flexibility. It requires a number of computations proportional to p whereas a number of computations proportional to p^2 is required for the RLS.

We have seen earlier how an AR process can be used to generate observed data samples. The spatial samples $x_i(t)$ can also be modeled as though they are generated by a moving average (MA) process [18] where by definition, we have

$$\hat{x}_n(t) = \sum_{k=1}^q b_k u_{n-k} + u_n = \sum_{k=0}^q b_k u_{n-k} , \quad (1.3-17)$$

where $b_0=1$, q is the order of the MA process and u_n are samples from a zero mean white noise process with autocorrelation sequence given by

$$r_{uu}(l) = \begin{cases} E[|u_n|^2] = \rho_{uu} & ; l=0 \\ 0 & ; l \neq 0 \end{cases} .$$

The power spectrum is then given by

$$\hat{P}(\phi) = (\Delta\lambda_{uu}) \left\{ \left| 1 + \sum_{k=1}^q b_k e^{-jk\phi} \right|^2 \right\}, \quad (1.3-18)$$

where $\phi = (\omega D/c) \sin(\theta)$. The angles of arrival are determined as the peaks of this spectrum. To avoid solution of a large number of nonlinear equations, the parameters b_k ; $k=1, 2, \dots, q$, can be estimated by approximating the

MA process with an equivalent AR process of order p where $p \gg q$. The parameters of these two processes are related by

$$a_1 + \sum_{n=1}^q b_n a_{1-n} \delta(l) = \begin{cases} 1 & ; l=0 \\ 0 & ; l \neq 0. \end{cases} \quad (1.3-19)$$

It can be shown that the MA model is not a high resolution spectral estimator because it does not model narrowband spectra very well.

AR and MA processes can be combined to form an ARMA process [20]. Here the spatial samples $\hat{x}_n(t)$ are modeled as samples from the process

$$\hat{x}_n(t) = - \sum_{k=1}^p a_k x_{n-k} + \sum_{k=0}^q b_k u_{n-k}, \quad (1.3-20)$$

where $b_0=1$, a_1, a_2, \dots, a_p and b_1, b_2, \dots, b_q are constant parameters. u_n is a sample from a zero mean white Gaussian process with

$$r_{uu}(l) = \begin{cases} E[|u_n|^2] = \rho_{uu} & ; l=0 \\ 0 & ; l \neq 0 \end{cases} .$$

The power spectrum is given by

$$\hat{P}_{xx}(\phi) = (\Delta\lambda_{uu}) \left\{ \left| 1 + \sum_{k=1}^q b_k e^{-jk\phi} \right|^2 \right\} \left\{ \left| 1 + \sum_{k=1}^p a_k e^{-jk\phi} \right|^{-2} \right\}. \quad (1.3-21)$$

The angles of arrival of the sources are determined as the peaks of this spectrum. Again, to avoid having to solve a set of nonlinear equations, the coefficients a_1, a_2, \dots, a_p and b_1, b_2, \dots, b_q can be estimated by approximating the ARMA process with an equivalent AR process of order $r \gg (p+q)$. A least squares procedure can then be used to solve for the moving average coefficients $1, \hat{b}_1(q), \hat{b}_2(q), \dots, \hat{b}_q(q)$. These ele-

ments are then used to solve for the coefficient 1, $\hat{a}_1(p)$, $\hat{a}_2(p)$, . . .
 ., $\hat{a}_p(p)$ knowing that

$$a_1 = c_1 + \sum_{n=1}^q b_n c_{1-n} \quad (1.3-22)$$

where c_k are the parameters of the equivalent AR process.

The minimum variance spectral estimator (MVSE), also known as Capon's maximum likelihood estimator [25], does not make use of the standard maximum likelihood estimate (MLE). Instead, a constrained optimization problem is solved. The MVSE generates a spectral estimate that describes relative component strengths over spatial frequency, but it is not a true p.s.d estimator. Let y_i be the response of a transversal filter with input $x_i(t)$. y_i is given by

$$y_i = \sum_{k=0}^p a_k x_{i-k}(t),$$

where a_k ; $k=1, 2, \dots, p$, are the filter coefficients. These coefficients are selected so as to minimize the variance $\rho = E[|y_i|^2]$, subject to the constraint that a desired spatial sinusoidal input does not experience distortion. It should be pointed out that this estimator is a non parametric estimator.

The beam forming (BF) [27] algorithm is suited to single sources where in effect, the observations are modeled as an MA (Moving Average) process.

Recently, subspace approaches have been introduced. These methods are based on an eigenvalue-eigenvector decomposition of the correlation matrix. This makes use of the fact that there is a relationship between the

eigenvectors of the spatial correlation matrix and the source angles of arrival. These methods are shown to yield asymptotically unbiased estimates of such signal parameters as angles of arrival, number of signals, etc. Schmidt [28] and, independently, Bienvenu [30] were the first to correctly exploit the measurement model in the case of a sensor array of arbitrary shapes. Schmidt's algorithm, called MUSIC (Multiple Signal Classification), identifies two distinct eigenspaces. The space associated with the smallest eigenvalue which appears with a multiplicity of $(m-d)$, where m is the number of sensors and d is the number of targets, assuming $m > d$, is called the noise subspace. The space associated with the d non zero eigenvalues is called the signal subspace. The angles of arrival of the sources are estimated via a search procedure which consists of choosing directional vectors and correlating them with the noise space generated by the noise eigenvectors corresponding to the noise eigenvalues. Since the noise space is orthogonal to the signal space, the angles of arrival are the peaks in the reciprocal of this correlation. Computationally, this algorithm is very inefficient. Another disadvantage of MUSIC is that it cannot handle completely correlated sources. A pre-processing technique called Spatial Smoothing [31], was then suggested for the case of a linear uniformly spaced array. Spatial Smoothing uses a set of L contiguous subarrays ($L < m$). $(m-L+1)$ correlation matrices are added up to form a new correlation matrix. This matrix is shown to be non singular. However, this processing decreases the effective aperture size which reduces the ability of the array to detect a sizable number of sources since the two are directly related.

Non search procedures were introduced to reduce such problems as computational complexity, storage, etc., which are inherent in search procedures. A non search procedure using MUSIC was initiated by Barabell [32]

for the case of a linear uniformly spaced array. Instead of plotting the MUSIC spectrum, a root finding procedure is developed, where the roots of the polynomial are functions of the parameters of interest. An improvement has been noticed, especially for the case of closely spaced targets.

Pisarenko's method [33] is based upon the fact that the covariance matrix has a smallest eigenvalue of multiplicity $(m-d)$. Thus, a repeated eigenanalysis is required to determine the multiplicity of the smallest eigenvalue. In practice, however, because the correlation matrix is evaluated from finite data samples, it is very difficult to count the multiplicity of the smallest eigenvalue. More sophisticated approaches based on statistical considerations have been developed [34-38]. Yet, the choice of a subjective threshold make these methods undesirable. Wax and Kailath [39] developed methods based on the information theoretic criteria introduced by Akaike (AIC) and by Schwartz and Rissanen (MDL). The number of signals is derived by minimizing the MDL or AIC functions. Recently, Zhao et. al. [40] showed that AIC is inconsistent and further suggested a family of consistent estimators of which MDL is a member.

ESPRIT (Estimation of Signal Parameters via a Rotational Invariance Technique) was later proposed by Roy and Kailath [43]. It is based on an invariance introduced by the array geometry. It is shown to be robust and computationally very efficient. The angles of arrival of the sources are directly related to the generalized eigenvalues of a matrix pencil formed from the data. However, the estimates obtained with this algorithm are very biased at low SNR. Although the original version of ESPRIT employed a least squares criterion, a total least squares procedure [44,45] was then devised to overcome this disadvantage.

Yet, ESPRIT can not be used in the case of completely correlated

sources. H. Ouibrahim has shown that ESPRIT is only one of several possible operators that could be used in the Matrix Pencil Approach [1]. Two other operators have been proposed which are referred to as the Summation Operator and Moving Window operator. The Moving Window operator is shown to hold even in the case of fully correlated sources, thus outperforming ESPRIT.

Ouibrahim also showed [46] that the Moving Window, Prony's method and Pisarenko's method are all equivalent in the sense that they check the dependence/independence of some data vectors. S. Mayrargue [47,48] showed that ESPRIT, TAM (Toeplitz Approximation Method) [49,50] and Tufts and Kumaresan's method [51,52] are all equivalent in the sense that they all solve the same multidimensional system.

All of this work was done for the case of narrowband signals. The case of wideband signals is much more difficult and has been studied by only a few people. Su and Morf. [53,54] suggested using a Modal Decomposition of the signals along with MUSIC to solve for the angles of arrival. A set of angles of arrival is obtained for each pole in the received spectrum. Thus, more signal parameters like poles and residues have to be estimated.

A different way of approaching the problem is to decompose the wideband signal into narrowband signals and then use the well known narrowband algorithms. At this stage two schemes were developed; post averaging schemes and pre-averaging schemes.

The first scheme was used by Wax et. al. [55]. They suggested a modified version of the MUSIC algorithm. The spatial spectral estimate was formed by averaging (either geometrically or arithmetically) the MUSIC inner products for each of the frequencies considered. This method is termed as Incoherent processing. It cannot be employed in the case of signals ex-

periencing multipath.

Wang and Kaveh [56] proposed a pre-processing scheme using linear transformations to combine the various sub-bands into one single band. This is called Coherent Wide-Band (CWB) processing. Only one eigendecomposition is then performed at this reference frequency. This algorithm outperforms the previous one in many ways such as computation, applicability in the case of coherent sources, etc. However, it suffers from the fact that preliminary estimates of the angles of arrival are needed in order to form the linear transformations. If these angles are clustered within a beamwidth, then the method performs well. Otherwise, spatial prefiltering is needed.

Another wideband method was introduced by Buckley and Griffiths [58] called BASS-ALE (Broad-Band Signal Subspace Spatial Spectrum Estimation). They generate a signal subspace using a "stacked" vector snapshot. The vectors obtained at each subband are stacked on top of one another. This algorithm is computationally more expensive than CWB.

A new coherent wide band algorithm was proposed by Kumaresan and Shaw [60]. They make use of a bilinear transformation to transform each sub-band into the reference band. This can be considered as a one step algorithm. Also it does not need the a priori knowledge of the angles of arrival. However, it can only be applied to electronically small arrays. Its performance deteriorates for targets near the endfires.

Recently, Ottersten and Kailath [61,62] proposed extending the ESPRIT algorithm to wide band signals. They use the same model as is described in Su and Morf [36] and ESPRIT is applied to determine the source locations for each of the signal poles.

1.4 WORK OUTLINE

The remainder of this work is organized as follows. Chapter 2 introduces the principles of signal subspace processing, the pencil theorem, (which is the basis of this work), and the Matrix Pencil approach. New ways for evaluating the generalized eigenvalues are also proposed. All of the algorithms discussed above assume an ideal sensor environment in which each sensor is assumed to exist by itself. Therefore, effects of reradiation from these sensors are completely neglected. Chapter 3 deals with the problem of mutual coupling between the sensors. Compensation techniques are developed for the Matrix Pencil Approach using the Moving Window and the ESPRIT operators. Chapter 4 is devoted to the extension of the Moving Window to the broadband case. Three methods are devised. The first is original in the sense that the Matrix Pencil approach is utilized with a signal model not used previously in other approaches. The signals are identified by their poles (natural frequencies) and their angles of arrival. The second method utilizes the same model used by Su and Morf. However the analysis is carried out completely in the time domain. The third makes use of the CWB of Wang and Kaveh. Chapter 5 analyzes the effects of the noise and perturbations due to sensor spacing. A measure is introduced and a geometric upper bound is derived for the Moving Window and ESPRIT operators. Conclusions and recommendations for future research are presented in chapter 6.

CHAPTER 2
SIGNAL SUBSPACE PROCESSING

2.1 PRINCIPLE

Assume there are d sources emitting signals $s_k(t)$; $k=1,2,\dots,d$, which are impinging on a linear array composed of m sensors. It is assumed that $d < m$. Let the superscript T denote transpose. The received signal at the i -th sensor can be modeled as

$$x_i(t) = \sum_{k=1}^d s_k(t) a_i(\theta_k) + n_i(t), \quad (2.1-1)$$

where

$a_i(\theta_k)$ is the relative response of the i -th sensor to the k -th source,

$s_k(t)$ is the complex envelope of the signal emitted by the k -th source,

n_i is the additive noise assumed to have zero mean and variance σ^2 .

In vector notation, this can be written as

$$\underline{X} = A \underline{S} + \underline{N} \quad (2.1-2)$$

where

$\underline{X}^T = [x_1, x_2, \dots, x_m] = (m \times 1)$ received signal vector,

$\underline{S}^T = [s_1, s_2, \dots, s_d] = (d \times 1)$ impinging signal vector,

$\underline{N}^T = [n_1, n_2, \dots, n_m] = (m \times 1)$ noise vector,

$A = [\underline{a}_1 \ \underline{a}_2 \ \dots \ \underline{a}_d] = (m \times d)$ direction matrix,

$\underline{a}_i^T = [a_1(\theta_i) \ a_2(\theta_i) \ \dots \ a_m(\theta_i)] = (m \times 1)$ i^{th} direction column

vector of A .

In all the subspace approaches that have been proposed the signals

and noise are assumed to be statistically independent and the noises n_i are assumed to be independent from sensor to sensor with a correlation matrix given by $\sigma^2 I$ where I is the identity matrix. Let the superscript H denote the Hermitian Transpose. The spatial covariance matrix is

$$\begin{aligned} R &= E[\underline{X} \underline{X}^H] = E[(\underline{AS} + \underline{N})(\underline{AS} + \underline{N})^H] \\ &= E[\underline{AS} \underline{S}^H A^H] + E[\underline{N} \underline{N}^H] \\ &= AE[\underline{S} \underline{S}^H] A^H + \sigma^2 I \end{aligned} \quad (2.1-3)$$

Let $S = E[\underline{S} \underline{S}^H]$. Then R can be written as

$$R = ASA^H + \sigma^2 I \quad (2.1-4)$$

where

R is an $(m \times m)$ matrix.

Let $\{\lambda_1 \geq \lambda_2 \geq \lambda_3 \geq \dots \geq \lambda_m\}$ be the set of eigenvalues of R . Let $\{\underline{V}_1, \underline{V}_2, \underline{V}_3, \dots, \underline{V}_m\}$ be the set of the corresponding eigenvectors.

If S is non singular and with the assumption that $m \geq d$, we can show that

1) the minimum eigenvalue of R is σ^2 with multiplicity $(m-d)$, i.e.,

$$\lambda_{d+1} = \lambda_{d+2} = \lambda_{d+3} = \dots = \lambda_m = \lambda_{\min} = \sigma^2.$$

2) the eigenvectors associated with the minimum eigenvalue, $\underline{V}_{d+1}, \underline{V}_{d+2}, \underline{V}_{d+3}, \dots, \underline{V}_m$, are orthogonal to the space spanned by the columns of A .

These results lead to the following direction finding approach :

- 1) determine the number of sources d from the multiplicity of λ_{\min} .
- 2) use the orthogonality relation between the direction vectors of the impinging sources and the eigenvectors corresponding to λ_{\min} to yield the directions of arrival of the sources. We just have to "search" for those direction vectors that are orthogonal to the eigenvectors cor-

responding to λ_{\min} . For this reason methods based on this approach are called search procedures.

2.2 PENCIL THEOREM

2.2.1 Theorem

Denote by C the field of all complex numbers. Consider two matrices M and N of size $(k \times p)$. The set

$$\{ M - \lambda N ; \lambda \in C \}$$

is said to be a matrix pencil. The matrices M and N are required to have the following decompositions

$$M = E F$$

$$N = E D F$$

where

E is a $(k \times d)$ matrix and $k \geq d$

F is a $(d \times p)$ matrix and $p \geq d$

D is a $(d \times d)$ diagonal matrix where d_{ii} denotes the i -th diagonal element.

If M and N are two matrices which have the decompositions cited above and if E , F and D are all of rank d , then the rank of the matrix pencil $M - \lambda N$ is decreased by 1 whenever

$$\lambda_i = (d_{ii})^{-1} ; i=1,2,\dots,d.$$

These values of λ_i are known as the generalized eigenvalues of the matrix pencil.

Proof

Since

$$M = EF$$

and

$$N=EDF,$$

$$M-\lambda N = EF-\lambda EDF = E(I-\lambda D)F.$$

Thus,

$$\text{rank}(M-\lambda N) = \text{rank}(E(I-\lambda D)F) = \min\{\text{rank}(E), \text{rank}(F), \text{rank}(I-\lambda D)\}.$$

However, by assumption

$$\text{rank}(E)=\text{rank}(F)=d$$

and

$\text{rank}(I-\lambda D)$ is of rank d as long as $(1-\lambda_i d_{ii}) \neq 0$; $i=1,2,\dots,d$.

If $(1-\lambda_i d_{ii})=0$, which implies that $\lambda_i=(d_{ii})^{-1}$, $\text{rank}(I-\lambda D)=d-1$. Therefore, the rank of $(M-\lambda N)$ is reduced by 1 whenever

$$\lambda_i=(d_{ii})^{-1} ; i=1,2,\dots,d.$$

2.2.2 Determination of rank reducing values

Note from above that two cases may occur. If $k=p$, M and N are square matrices. The set of the generalized eigenvalues of the pencil $M-\lambda N$ is defined to be the set of all elements λ_i such that

$$\det(M-\lambda_i N)=0.$$

When the generalized eigenvalues are distinct, the rank of $M-\lambda N$ is reduced by 1 whenever λ equals one of these values. In the case where $k>p$, M and N are non square matrices. $\det(M-\lambda_i N)$ no longer exists since the pencil is not square. For this reason we have to "make" the pencil matrix a square one. This can be done by premultiplying the pencil $M-\lambda N$ by either M^H or N^H . This can also be done by postmultiplying the pencil $M-\lambda N$ by either M^H or N^H . We obtain

$$M^H(M-\lambda N) = M^H M - \lambda M^H N$$

or

$$N^H(M-\lambda N) = N^H M - \lambda N^H N.$$

$M^H(M-\lambda N)$ and $N^H(M-\lambda N)$ are both square matrices ($p \times p$). Notice that

$$\begin{aligned} M^H(M-\lambda N) &= (EF)^H(EF-\lambda EDF) = F^H E^H E F - \lambda F^H E^H E D F \\ &= F^H E^H E (I-\lambda D) F \end{aligned}$$

and

$$\begin{aligned} N^H(M-\lambda N) &= (EDF)^H(EF-\lambda EDF) = F^H D^H E^H E F - \lambda F^H D^H E^H E D F \\ &= F^H D^H E^H E (I-\lambda D) F. \end{aligned}$$

Both equations have the decompositions required by the pencil theorem since

$$F^H E^H E \text{ and } F \text{ are of rank } d$$

and

$$F^H D^H E^H E \text{ and } F \text{ are of rank } d.$$

Because $(I-\lambda D)$ arises in all of these equations, we can say that the rank reducing values of the pencils $M^H(M-\lambda N)$ and $N^H(M-\lambda N)$ are identical to those of the pencil $(M-\lambda N)$.

Note that the pencils $M^H(M-\lambda N)$ and $N^H(M-\lambda N)$ have p generalized eigenvalues. However, there is a method which relies on a singular value decomposition (SVD) of the matrices M and N to obtain a matrix pencil which has exactly d generalized eigenvalues which in turn are the rank reducing values of the pencil $(M-\lambda N)$. The singular value decompositions of the matrices M and N result in

$$\begin{aligned} \text{and} \quad M &= U_m S_m V_m^H \\ N &= U_n S_n V_n^H, \end{aligned} \tag{2.2.2-1}$$

where

$$U_m = [\underline{U}_{m1} \quad \underline{U}_{m2} \quad \dots \quad \underline{U}_{mk}] = (k \times k)$$

$$\underline{U}_{mi} = i\text{-th right singular vector of } M = (k \times 1),$$

$$S_m = \left[\begin{array}{c|c} \Sigma_m & 0 \\ \hline 0 & 0 \end{array} \right] = (k \times p)$$

$$\Sigma_m = \text{diag} \{ \sigma_1 \sigma_2 \dots \sigma_d \} = (d \times d),$$

σ_i = i-th singular value of M

$$V_m = [\underline{V}_{m1} \ \underline{V}_{m2} \ \dots \ \underline{V}_{mp}] = (p \times p)$$

\underline{V}_{mi} = i-th left singular vector of M = (px1),

$$U_n = [\underline{U}_{n1} \ \underline{U}_{n2} \ \dots \ \underline{U}_{nk}] = (k \times k)$$

\underline{U}_{ni} = i-th right singular vector of N = (kx1),

$$S_n = \left[\begin{array}{c|c} \Sigma_n & 0 \\ \hline 0 & 0 \end{array} \right] = (k \times p)$$

$$\Sigma_n = \text{diag} \{ \sigma_1 \sigma_2 \dots \sigma_d \} = (d \times d),$$

σ_i = i-th singular value of N

$$V_n = [\underline{V}_{n1} \ \underline{V}_{n2} \ \dots \ \underline{V}_{np}] = (p \times p)$$

\underline{V}_{ni} = i-th left singular vector of N = (px1).

Collecting the d principal left and right singular eigenvectors (corresponding to the d non zero singular values), we have

$$\begin{aligned} M &= M^t = U_m^t \Sigma_m (V_m^t)^H \\ \text{and} \quad N &= N^t = U_n^t \Sigma_n (V_n^t)^H, \end{aligned} \tag{2.2.2-2}$$

where t denotes truncated and

$$U_m^t = [\underline{U}_{m1} \ \underline{U}_{m2} \ \dots \ \underline{U}_{md}] = (k \times d)$$

$$V_m^t = [\underline{V}_{m1} \ \underline{V}_{m2} \ \dots \ \underline{V}_{md}] = (d \times p)$$

$$U_n^t = [\underline{U}_{n1} \ \underline{U}_{n2} \ \dots \ \underline{U}_{nd}] = (k \times d)$$

$$V_n^t = [\underline{V}_{n1} \ \underline{V}_{n2} \ \dots \ \underline{V}_{nd}] = (d \times p).$$

Therefore,

$$(M - \lambda N) = (M^t - \lambda N^t) = (U_m^t \Sigma_m (V_m^t)^H - \lambda U_n^t \Sigma_n (V_n^t)^H). \tag{2.2.2-3}$$

Pre-multiplying and post-multiplying both sides of equation (2.2.2-3) by

$(U_n^t)^H$ and V_n^t respectively, we get

$$(U_n^t)^H (M^t - \lambda N^t) V_n^t = ((U_n^t)^H U_m^t \Sigma_m (V_m^t)^H V_n^t - \lambda \Sigma_n). \quad (2.2.2-4)$$

This pencil is square and is of dimensions $(d \times d)$ and thus has d rank reducing values which are exactly its generalized eigenvalues.

2.3 MATRIX PENCIL APPROACH

As was stated earlier, the matrix pencil approach is based upon the pencil theorem. Two matrices are formed from the data generated at the outputs of the sensor array. The generalized eigenvalues of the pencil thus formed are shown to contain the information about the locations of the targets. In this section we discuss two different operators.

2.3.1 ESPRIT

Consider a planar array of arbitrary geometry composed of $2m$ sensors arranged in pairs so as to form m doublets having the same directional orientation with respect to each other. The elements of each doublet have identical directional gain patterns and are translationally separated by a known displacement Δ (Fig. 2-1). Other than the obvious requirement that each sensor have non-zero gain in the directions of the emitting signals, the beam pattern of the elements in the doublet are totally arbitrary. Assume there are d ($m > 2d$) narrowband sources centered at frequency ω , and that the sources are located sufficiently far from the array such that the wavefronts impinging on the array are planar. Assume the sources are located at azimuthal angles θ_k , $k=1, 2, \dots, d$ and emitting signals whose complex envelopes are denoted by s_k , $k=1, 2, \dots, d$. Additive noise is present at all $2m$ sensors and is assumed to be stationary with zero-mean and variance σ^2 . The signals received at the two sensors in the i -th doublet can be expressed as

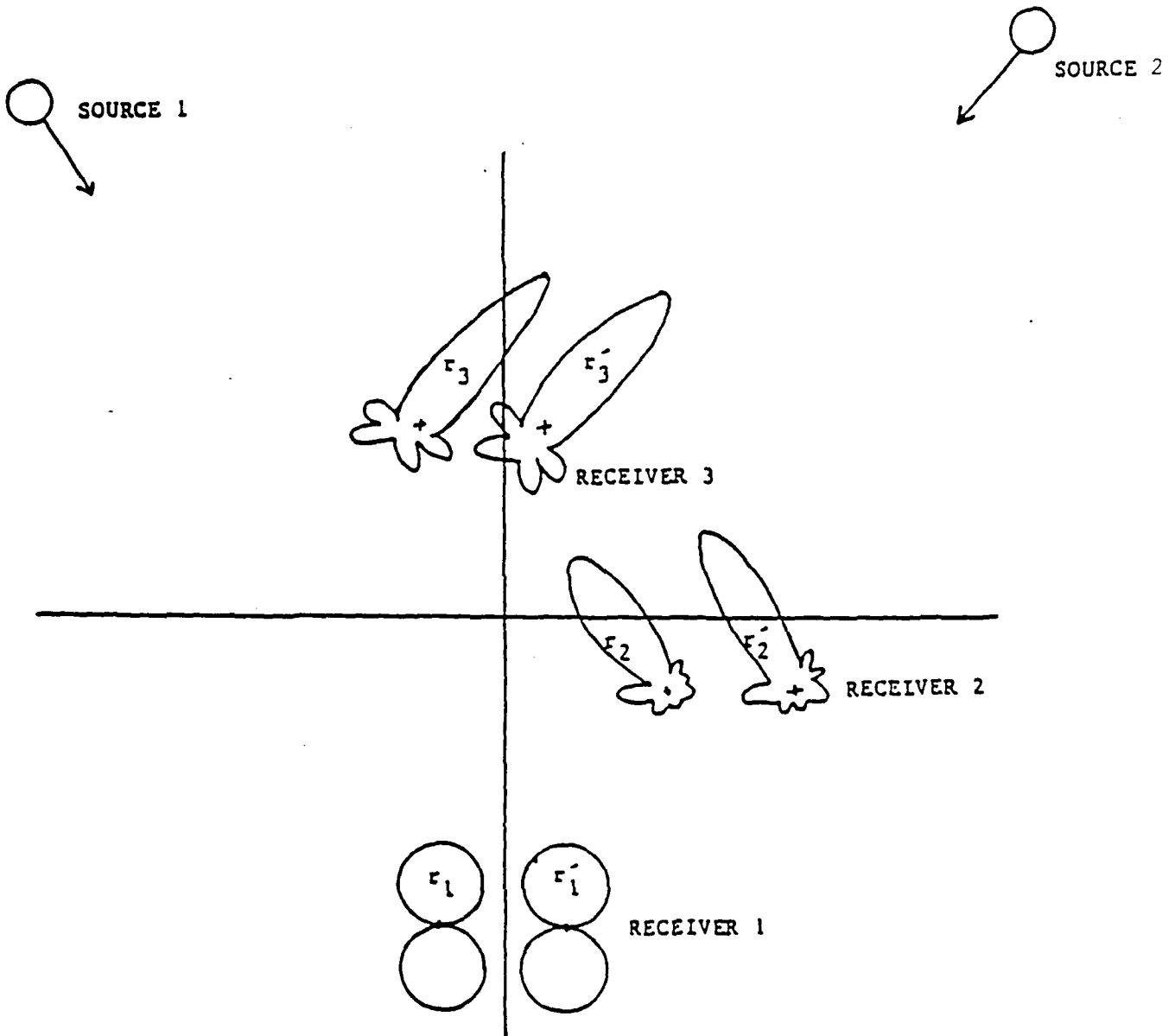


Fig. 2-1 ESPRIT (General Case)

$$v_i(t) = \sum_{k=1}^d s_k(t) g_i(\theta_k) + n_{ix}(t) = x_i(t) + n_{ix}(t) \quad (2.3-1)$$

$$w_i(t) = \sum_{k=1}^d s_k(t) e^{-j(\omega\Delta/c)\sin(\theta_k)} g_i(\theta_k) + n_{iy}(t) = y_i(t) + n_{iy}(t),$$

where $g_i(\theta_k)$ is the gain response of the i -th sensor to a source arriving at angle θ_k .

Two vectors \underline{V} and \underline{W} are then formed where

$$\underline{V}^T = [v_1 \ v_2 \ v_3 \ \dots \ v_m]$$

and

$$\underline{W}^T = [w_1 \ w_2 \ w_3 \ \dots \ w_m].$$

\underline{V} and \underline{W} can be written as

$$\begin{aligned} \underline{V} &= G\underline{S} + \underline{N}_x = \underline{X} + \underline{N}_x \\ \underline{W} &= G\phi\underline{S} + \underline{N}_y = \underline{Y} + \underline{N}_y, \end{aligned} \quad (2.3-2)$$

where G , ϕ , \underline{S} , \underline{N}_x and \underline{N}_y are the following matrices:

$$G = [g_1 \ g_2 \ \dots \ g_d] = (m \times d) \text{ gain matrix,}$$

$$g_i = [g_1(\theta_i) \ g_2(\theta_i) \ \dots \ g_m(\theta_i)] = (m \times 1) \text{ } i^{\text{th}} \text{ gain column vector of } G.$$

$$\underline{S}^T = [s_1 \ s_2 \ \dots \ s_d] = (d \times 1) \text{ impinging signal vector,}$$

$$\underline{N}_x^T = [n_{1x} \ n_{2x} \ \dots \ n_{mx}] = (m \times 1) \text{ noise vector,}$$

$$\underline{N}_y^T = [n_{1y} \ n_{2y} \ \dots \ n_{my}] = (m \times 1) \text{ noise vector,}$$

and

$$\phi = \text{diag}\{e^{j\phi_1} \ e^{j\phi_2} \ \dots \ e^{j\phi_d}\}$$

where

$$\phi_k = -(\omega\Delta/c)\sin(\theta_k), \quad k=1, 2, \dots, d. \quad (2.3-3)$$

Assuming that the signals and noise are statistically independent and that the noise components are uncorrelated from sensor to sensor, we have

$$E[\underline{V} \underline{V}^H] = GSG^H + \sigma^2 I$$

$$E[\underline{V} \underline{V}^H] = GS\Phi^H G^H \quad (2.3-4)$$

where I is the $(m \times m)$ identity matrix and $S = E[\underline{S} \underline{S}^H]$. Consider the matrices M and N , where

$$\begin{aligned} M &= E[\underline{V} \underline{V}^H] - \sigma^2 I = E[\underline{X} \underline{X}^H] = GSG^H \\ N &= E[\underline{V} \underline{W}^H] = E[\underline{X} \underline{Y}^H] = GS\Phi^H G^H . \end{aligned} \quad (2.3-5)$$

Consider the pencil $M - \lambda N$.

$$M - \lambda N = (GSG^H) - \lambda(GS\Phi^H G^H) = GS(I - \lambda\Phi^H)G^H. \quad (2.3-6)$$

In the case where the sources are not fully correlated (hence, S is not singular) and the direction of arrival of the sources are all distinct, M and N are of rank d . The rank of this pencil is reduced by 1 whenever

$$\lambda_k = e^{j\phi_k} = \exp\{-j(\omega\Delta/c)\sin(\theta_k)\} ; k=1, 2, \dots, d. \quad (2.3-7)$$

The angles of arrival are then given by

$$\theta_k = \sin^{-1}\{j \ln(\lambda_k) / (\omega\Delta)\} ; k=1, 2, \dots, d. \quad (2.3-8)$$

2.3.2 MOVING WINDOW

Assume we have a linear array composed of m identical sensors with uniform spacing D . Let there be $d \leq m$ narrowband sources located at azimuthal angles θ_k ; $k=1, 2, \dots, d$ (Fig. 2-2). Let the complex envelopes of the emitting signals be denoted by $s_k(t)$; $k=1, 2, \dots, d$. Assume the sources are in the far field such that planar wavefronts arrive at the array. With reference to the first sensor, the received signal at the i^{th} sensor is modeled as

$$v_i(t, \underline{\theta}) = \sum_{k=1}^d s_k(t) a_i(\theta_k) + n_i(t) = x_i + n_i ; i=1, 2, \dots, m \quad (2.3.2-1)$$

where

$$a_i(\theta_k) = a_k e^{j(i-1)\phi_k}$$

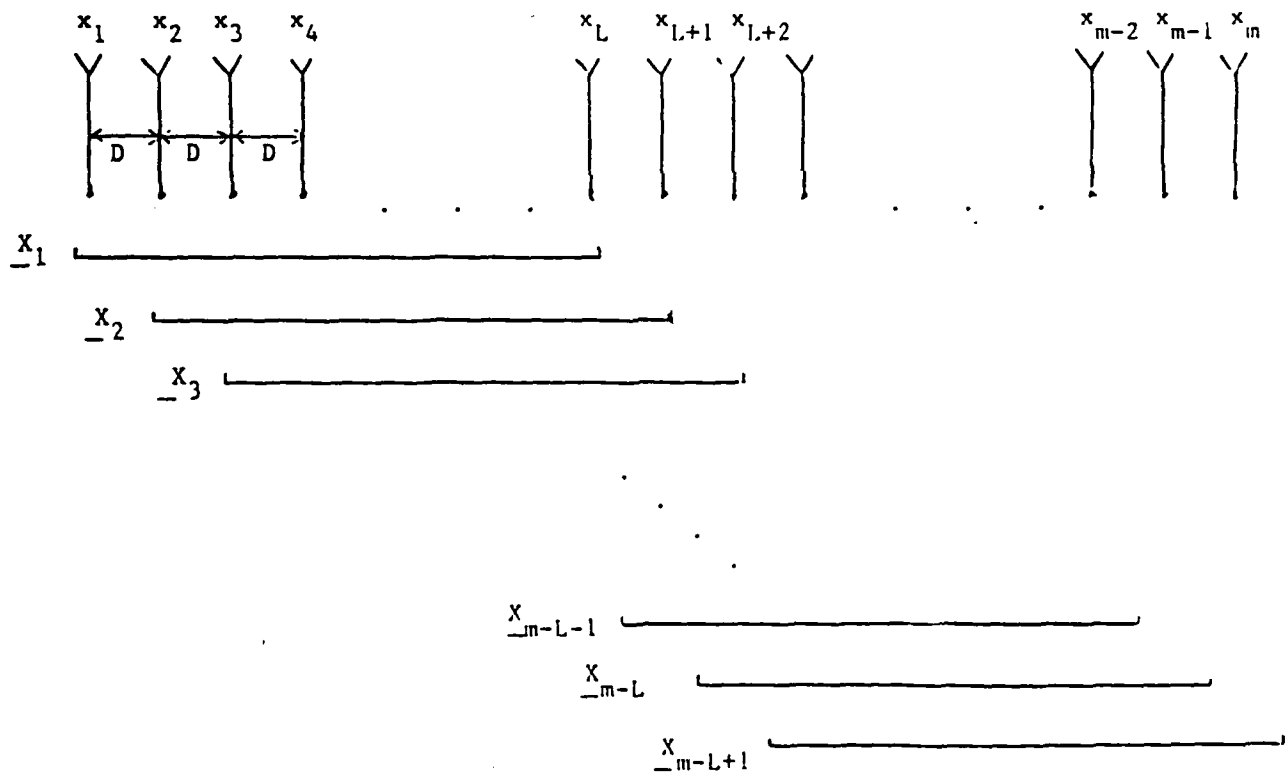
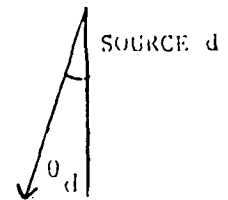
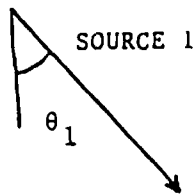


Fig. 2-2 Moving Window of Length L

$$\phi_k = -\omega D \sin(\theta_k) / c ; k=1, 2, \dots, d,$$

ω is the center frequency of the plane waves

c is the propagation speed of the waves

D is the sensor spacing

$a_k = a(\theta_k)$ is the beam pattern in the direction of the k -th emitter

and

$n_i(t)$ is the additive noise assumed to be zero-mean.

2.3.2.1 Original Version

In the original formulation of the matrix pencil approach using the moving window, Ouibrahim [1] generated $(d+1)$ vectors of length $(m-d)$. These vectors were then used to form two $(d \times d)$ matrices M and N . Unlike the ESPRIT approach, these matrices are of rank d even in the presence of fully correlated sources. The only restriction is that all sources have distinct angles of arrival. For this case, there will always be d generalized eigenvalues of the pencil $(M - \lambda N)$ regardless of the size of the sensor array. In the absence of noise, Ouibrahim's choice results in generalized eigenvalues whose corresponding eigenvectors span the signal subspace. However, in the presence of noise, the generalized eigenvalues are contaminated by the noise so that neither the signal nor the noise subspaces can be identified. This explains why the method performs badly for signal to noise ratios smaller than 15 dB. To overcome this deficiency, it is preferable to choose a window of length $L < (m-d)$ and then form $(m-L+1)$ vectors \underline{v}_n of length L where

$$\underline{v}_n^T = [v_n, v_{n+1}, \dots, v_{n+L-1}] ; n=1, \dots, (m-L+1).$$

The limits of L will be derived later. It can be shown that \underline{v}_n can be written as

$$\underline{V}_n = A_1 B \phi^{(n-1)} \underline{S} + \underline{N}_n = \underline{X}_n + \underline{N}_n \quad (2.3.2.1-1)$$

where

$$A_1 = \begin{bmatrix} 1 & 1 & \dots & 1 \\ e^{j\phi_1} & e^{j\phi_2} & \dots & e^{j\phi_d} \\ \vdots & \vdots & \ddots & \vdots \\ e^{j(L-1)\phi_1} & e^{j(L-1)\phi_2} & \dots & e^{j(L-1)\phi_d} \end{bmatrix}$$

$$\phi = \text{diag}\{e^{j\phi_1} \ e^{j\phi_2} \ \dots \ e^{j\phi_d}\}$$

$$B = \text{diag}\{a_1, a_2, \dots, a_d\}$$

$$\underline{S}^T = [s_1, s_2, \dots, s_d],$$

$$\underline{N}_n^T = [n_n, n_{n+1}, \dots, n_{n+L-1}].$$

The two matrices M_1 and N_1 are then formed

$$M_1 = \begin{bmatrix} \uparrow & \uparrow \\ | & | \\ \underline{V}_1 & \dots & \underline{V}_{(m-L)} \\ | & | \\ \downarrow & \downarrow \end{bmatrix} = \begin{bmatrix} v_1 & \dots & v_{(m-L)} \\ v_2 & \dots & v_{(m-L+1)} \\ \vdots & & \vdots \\ \vdots & & \vdots \\ v_L & \dots & v_{(m-1)} \end{bmatrix} \quad (2.3.2.1-2)$$

$$N_1 = \begin{bmatrix} \uparrow & \uparrow \\ | & | \\ \underline{V}_2 & \dots & \underline{V}_{(m-L+1)} \\ | & | \\ \downarrow & \downarrow \end{bmatrix} = \begin{bmatrix} v_2 & \dots & v_{(m-L+1)} \\ v_3 & \dots & v_{(m-L+2)} \\ \vdots & & \vdots \\ \vdots & & \vdots \\ v_{(L+1)} & \dots & v_m \end{bmatrix} \quad (2.3.2.1-3)$$

Using the expression for \underline{V}_n ; $n=1, 2, \dots, (m-L+1)$, the matrices M_1 and N_1 become

$$M_1 = [A_1 B \underline{S} \ A_1 B \phi \underline{S} \ \dots \ A_1 B \phi^{(m-L-1)} \underline{S}] + [\underline{N}_1 \ \underline{N}_2 \ \dots \ \underline{N}_{(m-L)}],$$

$$N_1 = [A_1 B \phi \underline{S} \ A_1 B \phi^2 \underline{S} \ \dots \ A_1 B \phi^{(m-L-1)} \underline{S}] + [\underline{N}_2 \ \underline{N}_3 \ \dots \ \underline{N}_{(m-L+1)}].$$

This can also be written as

$$M_1 = A_1 B [\underline{S} \ \phi \underline{S} \ \dots \ \phi^{(m-L-1)} \underline{S}] + [\underline{N}_1 \ \underline{N}_2 \ \dots \ \underline{N}_{(m-L)}],$$

$$N_1 = A_1 B \phi [\underline{S} \ \phi \underline{S} \ \dots \ \phi^{(m-L-1)} \underline{S}] + [\underline{N}_2 \ \underline{N}_3 \ \dots \ \underline{N}_{(m-L+1)}].$$

Let C be the matrix

$$C = [\underline{s} \ \phi \underline{s} \ \dots \ \phi^{(m-L)} \underline{s}]$$

It can be shown that C can be expressed as

$$C = D U,$$

where

$$D = \text{diag}\{s_1 \ s_2 \ \dots \ s_d\},$$

$$U = \begin{bmatrix} 1 & e^{j\phi_1} & \dots & e^{j(m-L-1)\phi_1} \\ 1 & e^{j\phi_2} & \dots & e^{j(m-L-1)\phi_2} \\ \vdots & \vdots & \ddots & \vdots \\ 1 & e^{j\phi_d} & \dots & e^{j(m-L-1)\phi_d} \end{bmatrix}$$

Let N' and N'' be the matrices

$$N' = [\underline{N}_1 \ \underline{N}_2 \ \dots \ \underline{N}_{(m-L)}],$$

$$N'' = [\underline{N}_2 \ \underline{N}_3 \ \dots \ \underline{N}_{(m-L+1)}].$$

Then

$$M_1 = A_1 B D U + N'$$

and

$$N_1 = A_1 B D \phi U + N''.$$

(2.3.2.1-4)

Assuming that the signals and noise are statistically independent and that the noise components are uncorrelated from sensor to sensor with zero mean and variance σ^2 , we get

$$E[M_1^H M_1] = U^H V U + L \sigma^2 I_{(m-L)} \quad (2.3.2.1-5)$$

$$E[N_1^H M_1] = U^H \phi^H V U + L \sigma^2 I_{1(m-L)} \quad (2.3.2.1-6)$$

where $I_{(m-L)}$ is the $(m-L) \times (m-L)$ identity matrix, $I_{1(m-L)}$ is the matrix

$$I_{1(m-L)} = \begin{bmatrix} 0 & 1 & 0 & 0 & \dots & 0 \\ 0 & 0 & 1 & 0 & \dots & 0 \\ 0 & 0 & 0 & 1 & \dots & 0 \\ \vdots & \vdots & \vdots & \vdots & \ddots & \vdots \\ 0 & 0 & 0 & 0 & \dots & 1 \\ 0 & 0 & 0 & 0 & \dots & 0 \end{bmatrix}$$

and V is the matrix $V = E[D^H B^H A_1^H A_1 B D]$. Defining

$$F_{pq} = \sum_{i=1}^L e^{j(i-1)(\phi_p - \phi_q)},$$

$$S_{pq} = E[s_q^* s_p],$$

$$a_{pq} = a_q^* s_p,$$

the matrix V can be written as

$$V = \begin{bmatrix} S_{11} a_{11} F_{11} & S_{21} a_{21} F_{21} & \dots & S_{d1} a_{d1} F_{d1} \\ S_{12} a_{12} F_{12} & S_{22} a_{22} F_{22} & \dots & S_{d2} a_{d2} F_{d2} \\ \vdots & \vdots & \ddots & \vdots \\ S_{1d} a_{1d} F_{1d} & S_{2d} a_{2d} F_{2d} & \dots & S_{dd} a_{dd} F_{dd} \end{bmatrix}.$$

Define the matrices M and N such that

$$M = E[M_1^H M_1] - L \sigma^2 I_{(m-L)} = U^H V U \quad (2.3.2.1-7)$$

$$N = E[N_1^H N_1] - L \sigma^2 I_{(m-L)} = U^H \Phi^H V U. \quad (2.3.2.1-8)$$

Note that M and N are $(m-L) \times (m-L)$ matrices. Assuming that $(m-L) \geq d$, M and N will always be of rank d. Therefore, the limits on L are

$$d \leq L \leq (m-d).$$

Consider the matrix pencil $M - \lambda N$.

$$M - \lambda N = U^H V U - \lambda U^H \Phi^H V U = U^H (I - \lambda \Phi^H) V U \quad (2.3.2.1-9)$$

which satisfies the requirements of the pencil theorem. Hence, the values of λ for which the rank of $M - \lambda N$ decreases by 1 are given by

$$\lambda_k = e^{j\phi_k}; \quad k=1, 2, \dots, d. \quad (2.3.2.1-10)$$

The angles of arrival are given by

$$\theta_k = \sin^{-1}\{j \text{cln}(\lambda_k) / \omega D\}; \quad k=1, 2, \dots, d. \quad (2.3.2.1-11)$$

2.3.2.2 New Version

From equations (2.3.2.1-2) and (2.3.2.1-3), we see that we can

form $(L+1)$ vectors \underline{z}_r of length $(m-L)$ where \underline{z}_r is given by

$$\underline{z}_r^T = \{v_r^*, v_{r+1}^*, \dots, v_{r+m-L-1}^*\}; r=1, \dots, (L+1),$$

and $*$ denotes complex conjugate. We have purposely chosen to take the conjugate so that we deal with correlation matrices of the form $E[\underline{z} \underline{z}^H]$. Note that this is the usual form for the correlation matrix of the vector \underline{z} . it follows that M_1 and N_1 are simply

$$M_1 = \begin{bmatrix} \leftarrow \underline{z}_1^H \rightarrow \\ \leftarrow \underline{z}_2^H \rightarrow \\ \vdots \\ \leftarrow \underline{z}_L^H \rightarrow \end{bmatrix} \text{ and } N_1 = \begin{bmatrix} \leftarrow \underline{z}_2^H \rightarrow \\ \leftarrow \underline{z}_3^H \rightarrow \\ \vdots \\ \leftarrow \underline{z}_{(L+1)}^H \rightarrow \end{bmatrix}.$$

Therefore,

$$E[M_1^H M_1] = \sum_{i=1}^L E[\underline{z}_i \underline{z}_i^H] \quad (2.3.2.2-1)$$

and

$$E[N_1^H M_1] = \sum_{i=1}^L E[\underline{z}_{(i+1)} \underline{z}_i^H]. \quad (2.3.2.2-2)$$

The advantage of formulating the matrix pencil approach using the moving window in this fashion will be seen later when mutual coupling is present at the sensor array. Using the original version, it was necessary to employ a minimum mean squared error estimation scheme to compensate for the mutuals. Using the new version, it was possible to devise a scheme that provided a direct compensation for the mutuals.

3. Computer Simulation of the Moving Window Approach

The model used in the computer simulation consisted of two incoherent sources ($d=2$) incident on a linear array of eight uniformly spaced sensors ($m=8$). For convenience, the sensors are assumed to be omnidirectional. The Rayleigh resolution of this array is given by

$$2/(m-1)(180/\pi) \approx 16.37^\circ.$$

The 2 sources were assumed to be located at $\theta_1=16^\circ$ and $\theta_2=24^\circ$. The angular separation of these sources is 8° which is half the Raleigh resolution. The amplitudes of the sources were generated as statistically independent complex random variables with zero mean and unit variance. The noise was also chosen to be complex Gaussian with zero mean and unit variance. The sensors were positioned at half wavelength so that $(\omega_0 D/c)=\pi$. 100 snapshots were taken for each of the 50 runs. The length of the window was varied from $L=d=2$ to $L=(m-d)=6$. In the plots of the sample variance and the mean-squared error, the y-axis is defined as

$$y=10 \log_{10}(.).$$

Let $\hat{\theta}_k$ be an estimate of θ obtained at the k-th run (K is the number of runs). The sample mean (ME), the sample variance (Var) and the mean-squared error (MSE) are defined respectively as

$$ME(\theta) = (1/K) \sum_{k=1}^K \hat{\theta}_k,$$

$$Var(\theta) = (1/K) \sum_{k=1}^K (\hat{\theta}_k - ME(\theta))^2,$$

$$MSE(\theta) = (1/K) \sum_{k=1}^K (\hat{\theta}_k - \theta)^2.$$

The results are shown in Fig. 2.3 to 2.8. From figures 2.3 and 2.4, note that above 15 dB, the choice of L is not important as far as the sample mean is concerned. However, below 15 dB, the performance of the Moving Window degrades considerably with the choice of $L=5$ and $L=6$ (Ouibrahim's choice). For $L=2, 3$ or 4 , the performance of the method is comparable. By choosing a window of length $L=2$ (smallest possible), an improvement of al-

most 23 dB is achieved at a signal to noise ratio of 5 dB in the sample variance and the mean-squared error. This improvement is due mainly to the recognition of both subspaces (signal and noise) and the use of the singular value decomposition (SVD). The SVD is known to be robust even in the case of very ill conditioned matrices. The reduction of the 2 matrices involved in the matrix pencil to the desired dimension (d) through the SVD allowed us to effectively use the IMSL routine (EIGZC) which computes the generalized eigenvalues.

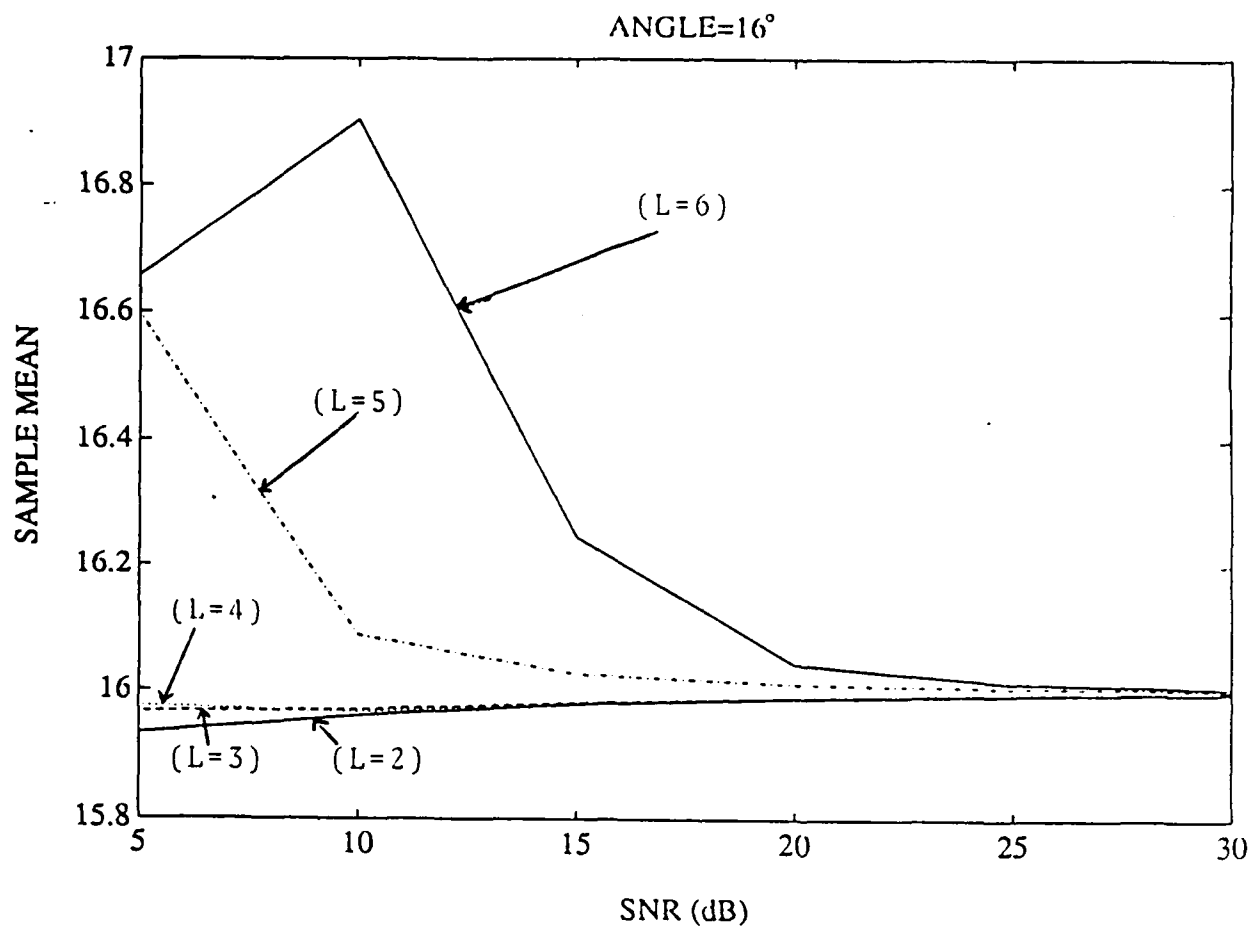


Fig. 2.3 Sample Mean of the Angle Estimate at 16°

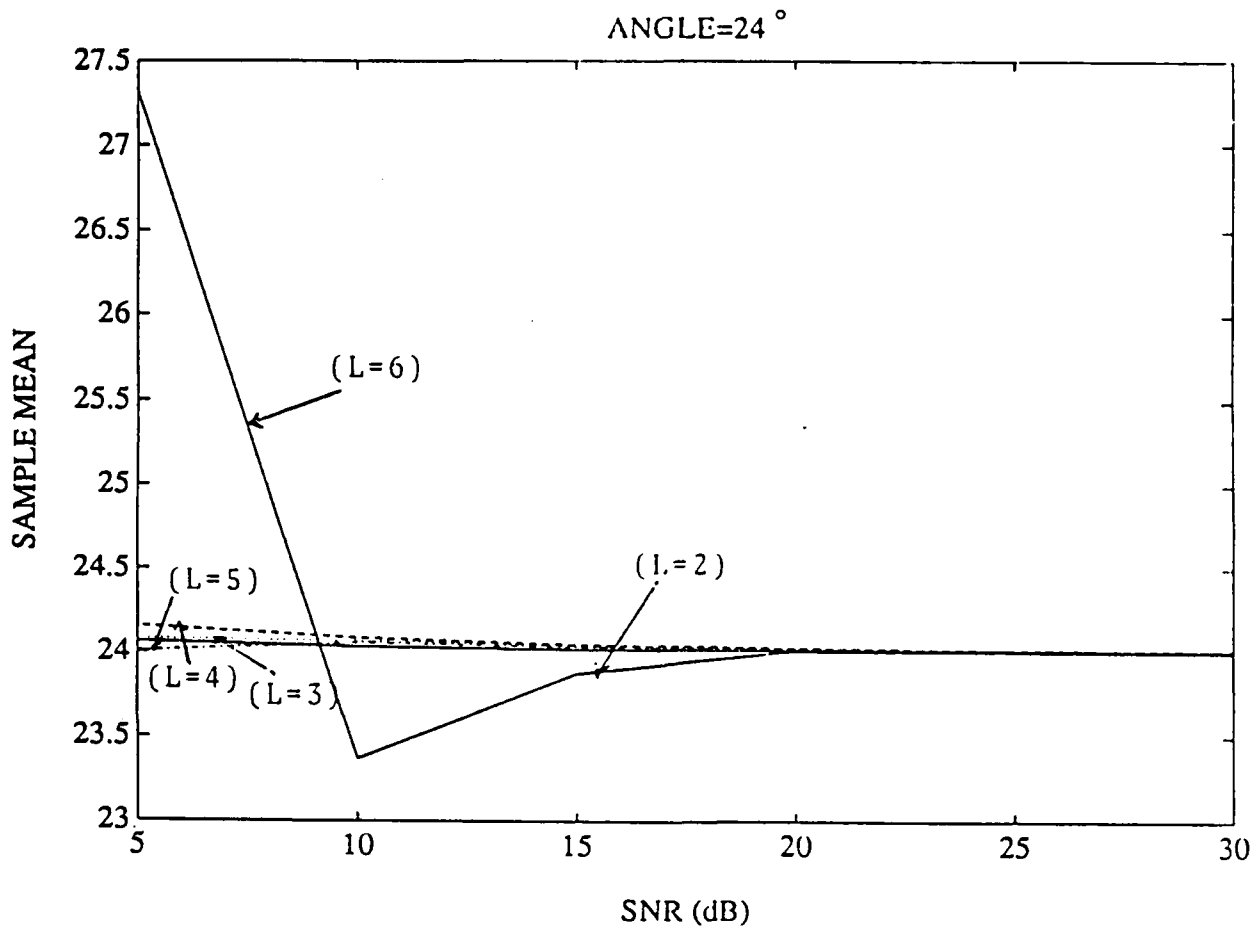


Fig. 2.4 Sample Mean of the Angle Estimate at 24°

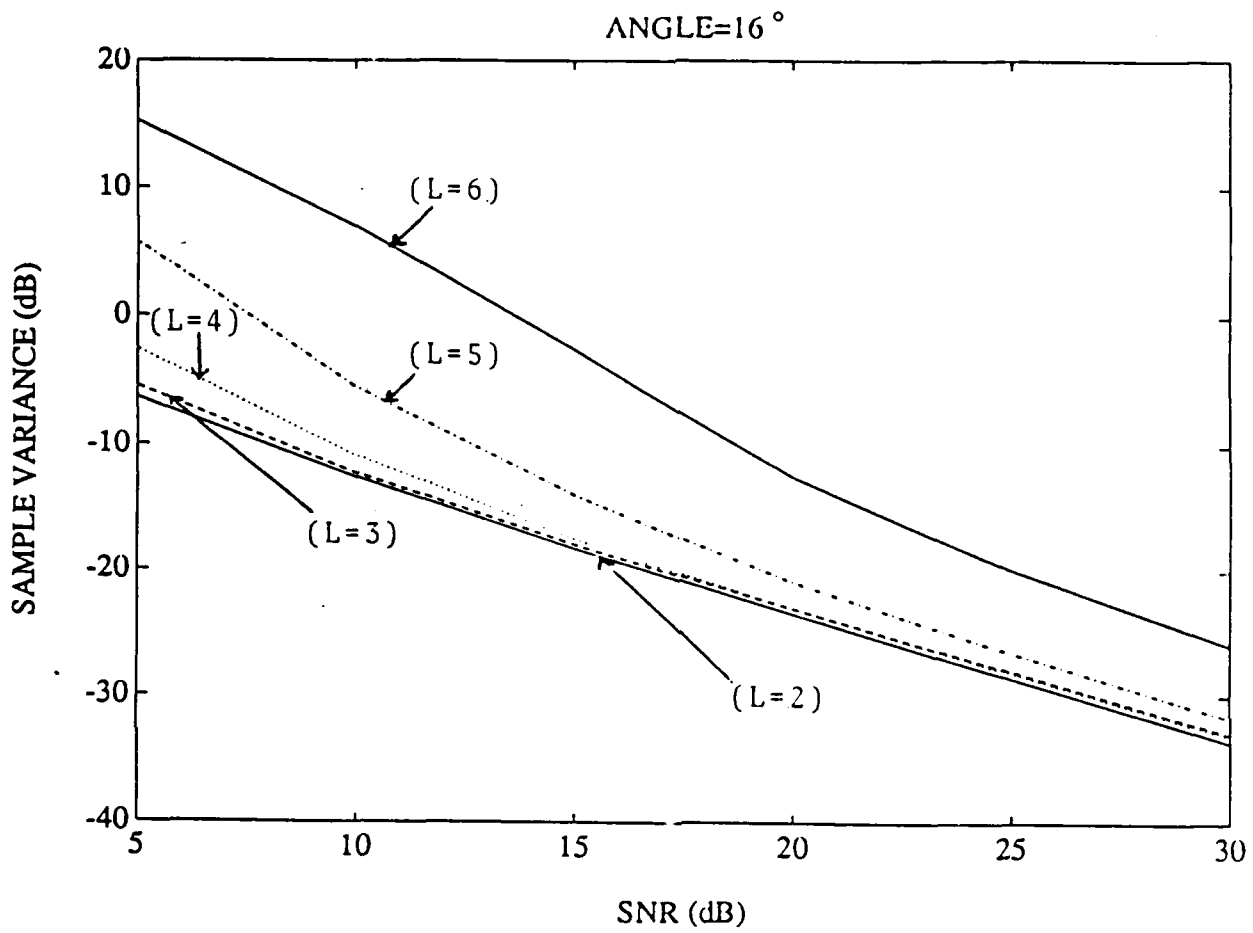


Fig. 2.5 Sample Variance of the Angle Estimate at 16°

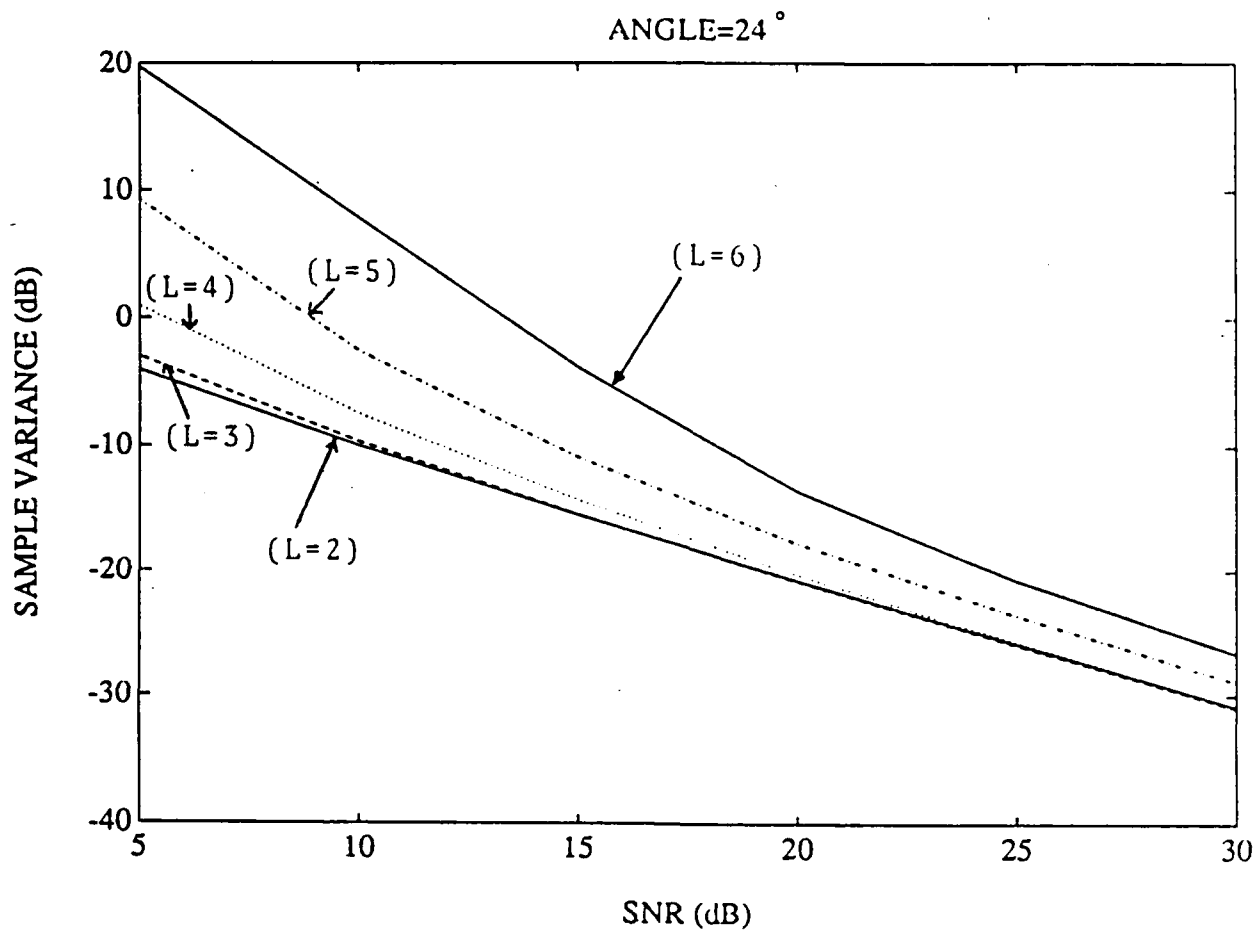


Fig. 2.6 Sample Variance of the Angle Estimate at 24°.

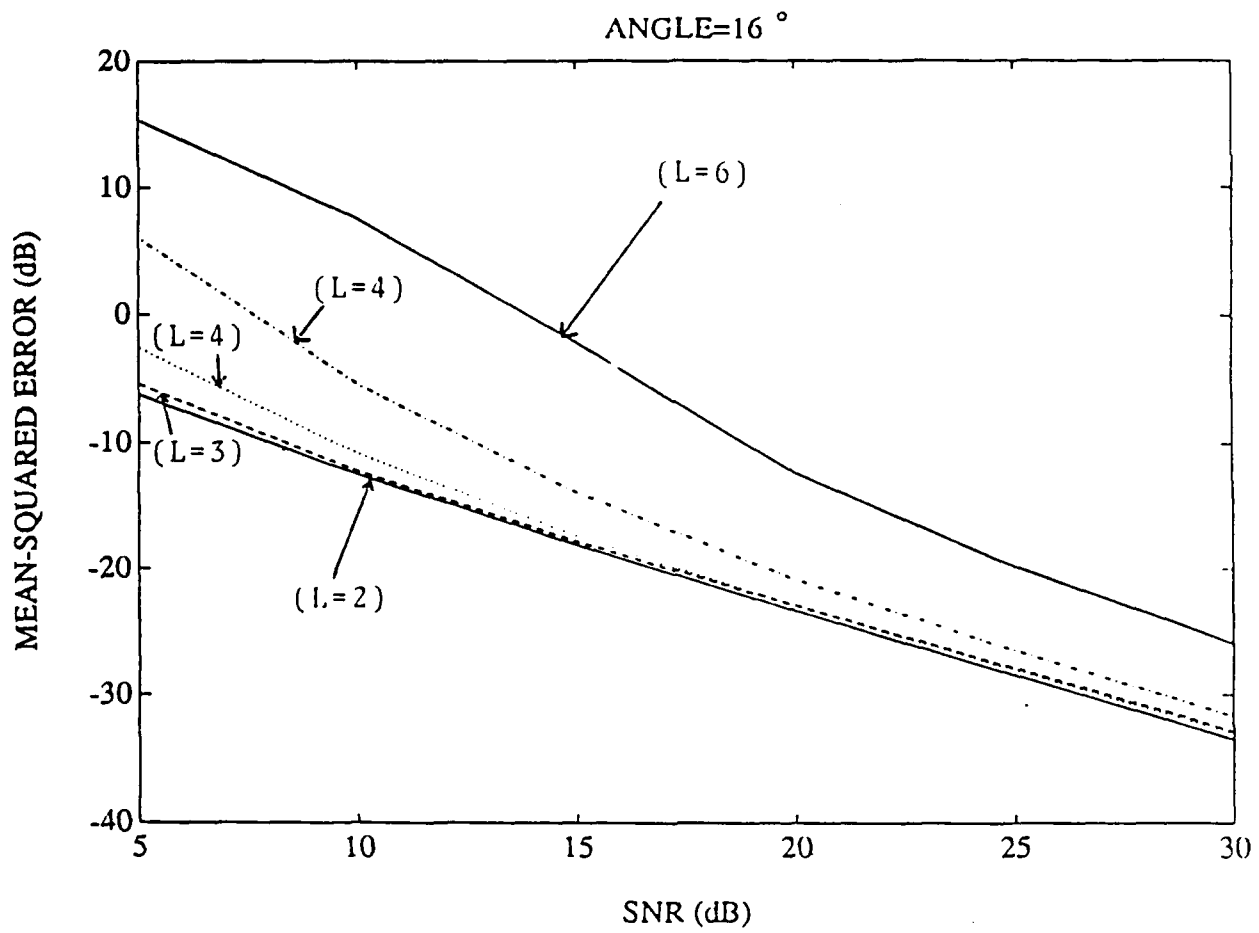


Fig. 2.7 Mean-Squared Error of the Angle Estimate at 16°.

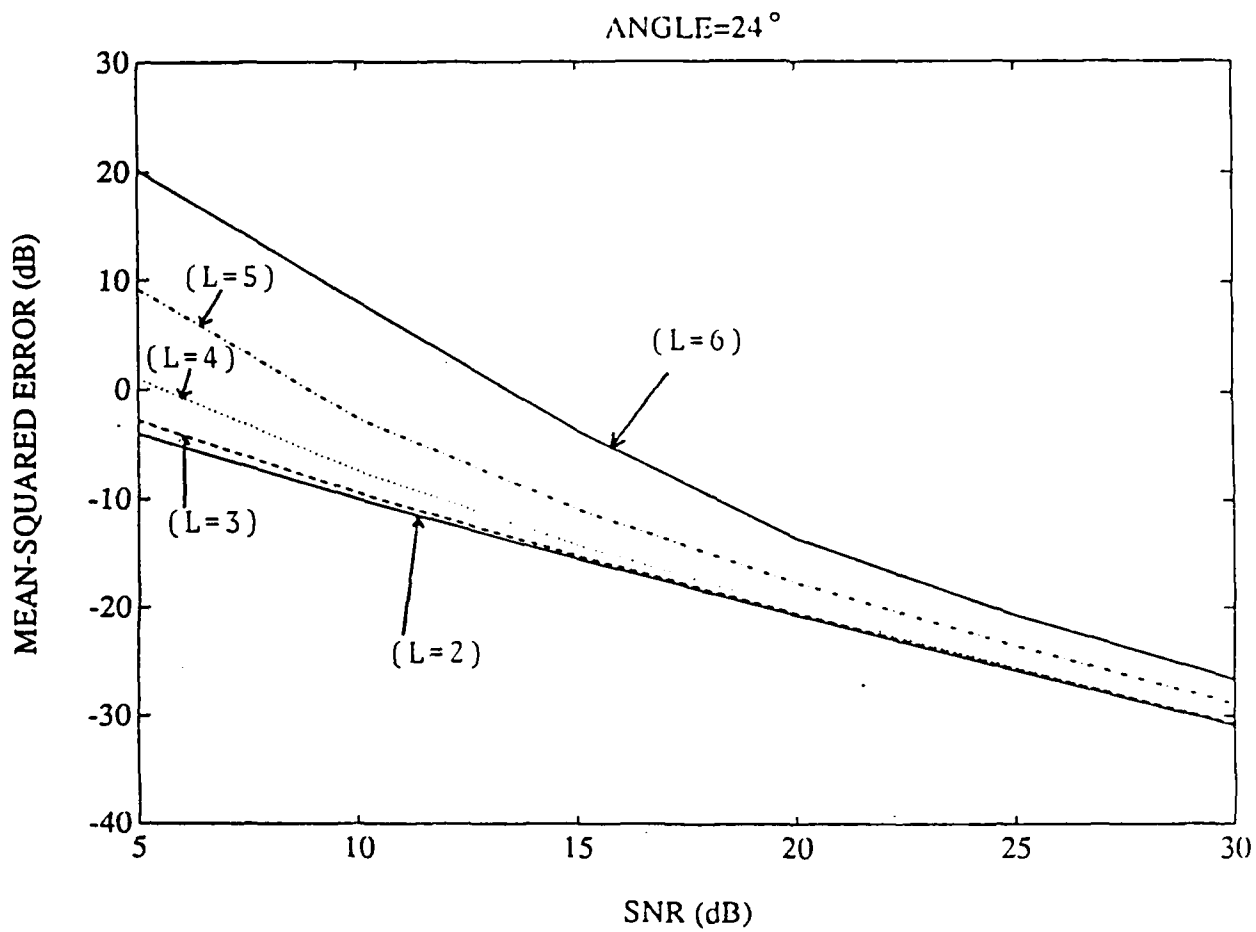


Fig. 2.8 Mean-Squared Error of the Angle Estimate at 24°.

CHAPTER 3

COMPENSATION FOR MUTUAL COUPLING

In the methods considered earlier, each sensor was treated as if it existed by itself. However, in practice, mutual coupling exists between the array sensors. Because the mutuals change the sensor impedances, the gain and radiation pattern of the array can be greatly distorted. In subspace methods this can significantly alter the eigensystems underlying the estimation procedures. Gupta and Ksienski [70] investigated the effects of mutual coupling on the performance of an adaptive array. In their treatment, the matrix Z_0 characterizing the mutual coupling between the sensors was determined using a mathematical model which models the antenna array consisting of m sensors as an $(m+1)$ terminal network. This matrix was then used to determine the sensor outputs that would have existed had there been no mutual coupling. A compensation scheme was then developed to study the method known as beamforming. Yeh and Leou [71] used the same mathematical model and applied it to the MUSIC algorithm. Recall, in the MUSIC algorithm, that one plots the inverse of the correlation between the noise subspace E_n and the directional vector $a(\theta)$, which we denote by $((E_n \cdot a(\theta))^2)^{-1}$. If mutual coupling is present, Yeh and Leou show that one has to plot the function $((E_n \cdot Z_0^{-1} \cdot a(\theta))^2)^{-1}$. Failure to do so results in severe degradation of the estimates. Shau [44] considered the case of deterministic signals in a noise free environment and eliminated the effects of mutual coupling for the method known as MFBLP (Modified Forward Backward Linear Prediction). In this chapter we develop algorithms to effectively compensate for the effects of mutual coupling when using the Matrix Pencil approach with ESPRIT and the Moving Window.

3.1 MODEL

Consider a linear array of m dipoles uniformly spaced at a distance D . Each dipole is of length t and has a radius r satisfying the condition $r \ll t$. A load is attached to the center gap of each dipole (Fig. 3-1). Assume there are d narrowband signals impinging on the array as planar wavefronts. The voltages induced by the assumed signals on the loads are the outputs of the dipoles. Induced currents will appear on the dipoles. These currents reradiate and generate scattered fields. The scattered fields then induce currents on the neighboring dipoles. The process of induction and reradiation causes the mutual coupling among the dipoles.

Using one sinusoidal expansion and weighting function per dipole, the method of moments [45,46] was used to obtain the matrix of mutuals (Fig. 3-2). Denote the current distribution by $J(z)$ (assuming longitudinal distribution and neglecting all other distributions) and the j -th expansion function by $f_j(z)$. Then

$$J(z) = \sum_{j=1}^m I(j) f_j(z) \quad (3.1-1)$$

where $I(j)$; $j=1, 2, \dots, m$, denotes the unknown current amplitude to be determined on each dipole. At a point (y,z) in the $Y-Z$ plane, the scattered field is given by

$$\Omega^{(s)}(y,z) = \sum_{j=1}^m I(j) E^{(j)}(y,z) \quad (3.1-2)$$

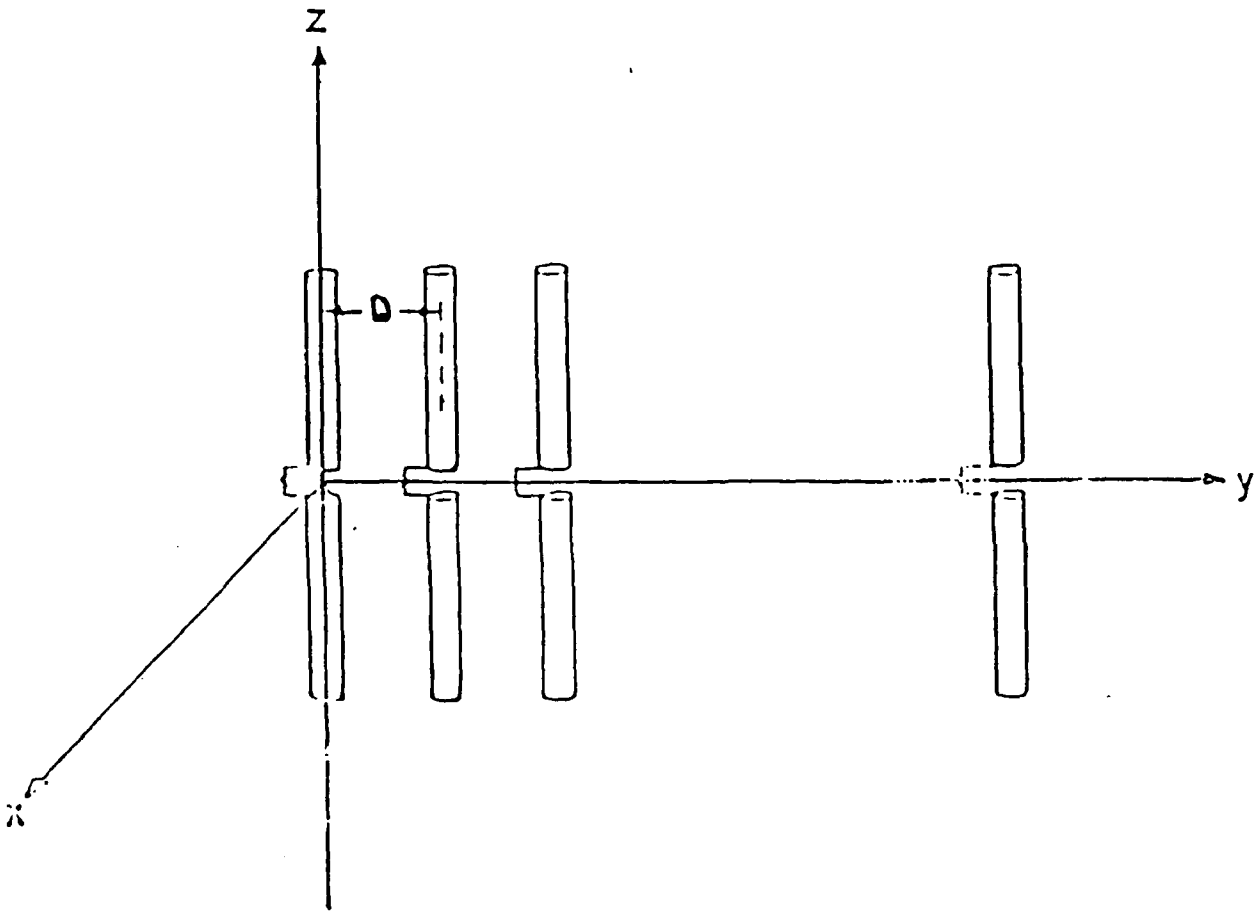


Fig. 3.1 Linear Array of m Dipoles.

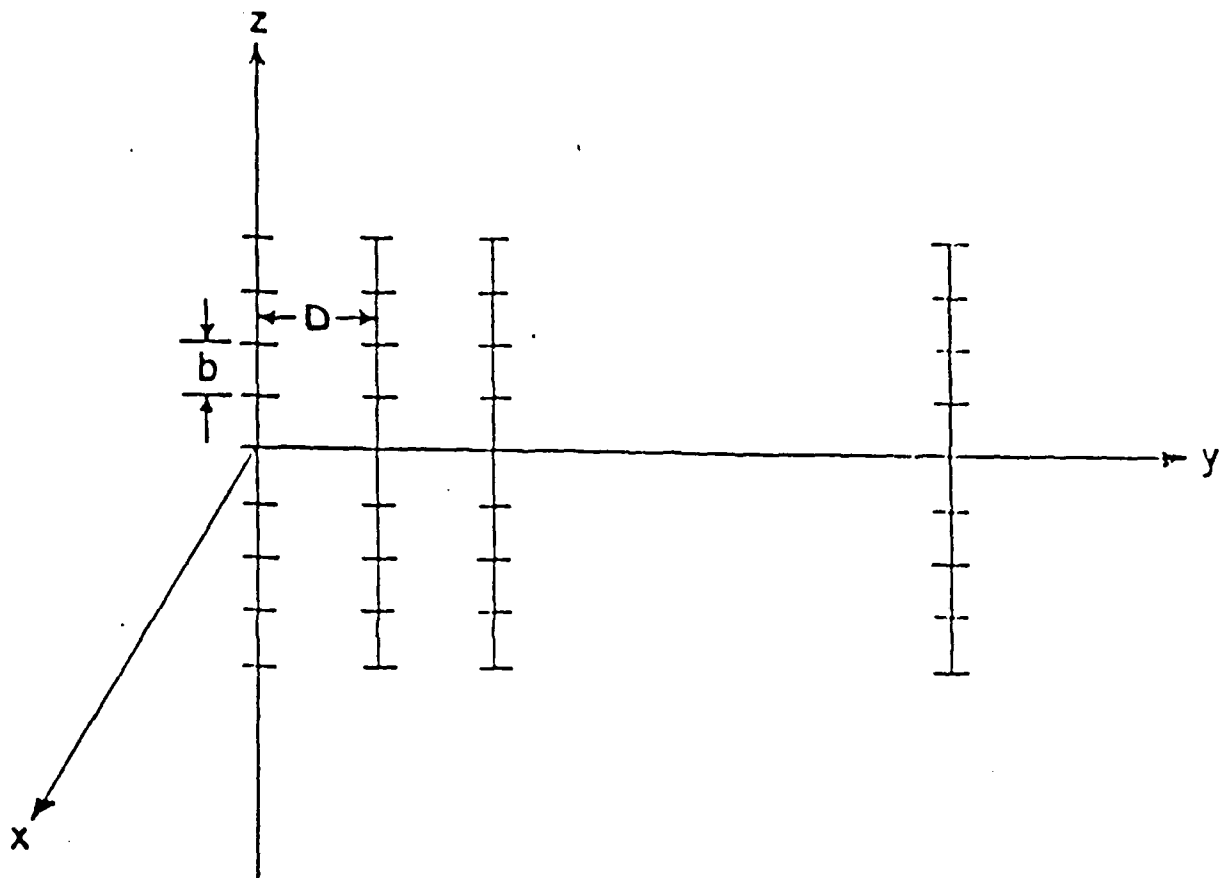


Fig. 3.2 Subsectioning of the m Dipoles.

where $E_j^{(s)}(y,z)$ is the scattered field from the j -th dipole. The total field will then be

$$E(y,z) = E^{(inc)}(y,z) + E^{(s)}(y,z) \quad (3.1-3)$$

where $E^{(inc)}$ is the incident field. Let E_z be the z -component of the total field. A generalized voltage $V(i)$ induced on the subsection spanned by the function $f_i(z)$ can be defined with respect to a weighting function $w_i(z)$ as

$$V(i) = F(E_z(y,z), w_i(z)) \quad (3.1-4)$$

where F is bilinear with respect to $E_z(y,z)$ and $w_i(y,z)$. Similarly, we define the voltage produced by the incident field on the i -th dipole by

$$v^{(inc)}(i) = F(E_z^{(inc)}(y,z), w_i(z)) \quad (3.1-5)$$

and the voltage produced by the scattered field on the i -th dipole by

$$v^{(s)}(i) = F(E_z^{(s)}(y,z), w_i(z)). \quad (3.1-6)$$

Thus, the total voltage introduced in the i -th dipole is

$$V(i) = v^{(inc)}(i) + v^{(s)}(i),$$

which, for metallic scatterers, becomes

$$V(i) = v^{(inc)}(i) + v^{(s)}(i) = 0$$

or

$$v^{(inc)}(i) = -v^{(s)}(i). \quad (3.1-7)$$

However,

$$\begin{aligned} v^{(s)}(i) &= F\left(\sum_{j=1}^m I(j) E_j^{(s)}(y,z), w_i(z)\right) \\ &= \sum_{j=1}^m I(j) F(E_j^{(s)}(y,z), w_i(z)). \end{aligned}$$

The total impedance between the i -th and j -th dipoles is defined to be

$$z^{ij} = -F(E_j^{(s)}(y,z), w_i(z)). \quad (3.1-8)$$

Thus,

$$v^{(s)}(i) = \sum_{j=1}^m -z^{ij} I(j) ; i=1,2,\dots,m. \quad (3.1-9)$$

In matrix notation

$$\underline{v}^{(s)} = -Z \underline{I} \quad (3.1-10)$$

where

$$\underline{v}^{(s)T} = [v^{(s)}(1), v^{(s)}(2), \dots, v^{(s)}(m)]$$

and

$$\underline{I}^T = [I(1), I(2), \dots, I(m)].$$

The total impedance matrix Z can be decomposed into two parts as

$$Z = Z_0 + Z_L$$

where

Z_0 is the generalized impedance matrix

and

Z_L is the load matrix.

Assuming that all loads are loaded with the same load z_1 , the matrix Z_L is given by

$$Z_L = \begin{bmatrix} z_1 & & & & \\ & z_1 & & & \\ & & \cdot & & \\ & & & \cdot & \\ & & & & \cdot \\ & 0 & & & & z_1 \end{bmatrix}.$$

The ij -th element of Z, therefore is

$$z^{ij} = z_{ij} + z_1 \delta_{ij},$$

where z_{ij} is the mutual impedance between the i -th and j -th dipoles. The total voltages induced on a load z_1 are given by

$$\underline{v}^{(L)} = Z_L \underline{I}$$

and

$$\underline{I} = Z_L^{-1} \underline{v}^{(L)}.$$

However,

$$\underline{v}^{(inc)} = Z \underline{I} = Z_0 Z_L^{-1} \underline{v}^{(L)} + \underline{v}^{(L)}$$

which implies that

$$\underline{v}^{(L)} = [I + Z_0 Z_L^{-1}]^{-1} \underline{v}^{(inc)}. \quad (3.1-11)$$

Let H be the matrix

$$H = [I + Z_0 Z_L^{-1}]. \quad (3.1-12)$$

H can be written as

$$H = \begin{bmatrix} 1+(z_{11}/z_1) & (z_{12}/z_1) & \dots & (z_{1m}/z_1) \\ (z_{21}/z_1) & 1+(z_{22}/z_1) & \dots & (z_{2m}/z_1) \\ \vdots & \vdots & & \vdots \\ \vdots & \vdots & & \vdots \\ (z_{m1}/z_1) & (z_{m2}/z_1) & \dots & 1+(z_{mm}/z_1) \end{bmatrix}.$$

Thus, when incident signals are impinging on the array and in the presence of additive noise, the output of the linear array will be

$$\underline{v}^{(L)} = H^{-1} \underline{v}^{(inc)} + \underline{N}.$$

For simplicity, let

$$\underline{X} = \underline{v}^{(inc)}$$

and

$$\underline{Y} = \underline{v}^{(L)}.$$

We now have a relationship between the incident signals and the outputs of the array which is

$$\underline{Y} = H^{-1} \underline{X} + \underline{N}. \quad (3.1-13)$$

3.2 MINIMUM MEAN-SQUARED ERROR ESTIMATION

If we try to use the vector \underline{Y} observed at the output of the array in the original formulation of the matrix pencil approach, it is not possible to obtain the decomposition needed for the matrix pencil. An estimate $\hat{\underline{X}}$ of \underline{X} is, therefore, generated. This estimate is also used in ESPRIT.

Assuming that the signals and noise are statistically independent and that the noise components are uncorrelated zero-mean random variables with variance σ^2 , the minimum mean-squared error linear estimator results when the error $(\underline{X} - \hat{\underline{X}})$ is orthogonal to the observed data \underline{Y} . Let $\hat{\underline{X}} = R \underline{Y}$, where R is to be determined. Thus, we have

$$E\{(\underline{X} - \hat{\underline{X}}) \underline{Y}^H\} = 0.$$

However $\hat{\underline{X}} = R \underline{Y}$ which implies that

$$E\{\underline{X} \underline{Y}^H\} = R E\{\underline{Y} \underline{Y}^H\}.$$

Recall that $\underline{Y} = H^{-1} \underline{X} + \underline{N}$. Thus,

$$E\{\underline{X} \underline{Y}^H\} = E\{\underline{X} (H^{-1} \underline{X} + \underline{N})^H\} = E\{\underline{X} \underline{X}^H\} (H^{-1})^H$$

and

$$\begin{aligned} E\{\underline{Y} \underline{Y}^H\} &= E\{(H^{-1} \underline{X} + \underline{N})(H^{-1} \underline{X} + \underline{N})^H\} \\ &= (H^{-1}) E\{\underline{X} \underline{X}^H\} (H^{-1})^H + \sigma^2 \underline{I}_m. \end{aligned}$$

Let C denote the correlation matrix of \underline{Y} . Then

$$C = E\{\underline{Y} \underline{Y}^H\} = (H^{-1}) E\{\underline{X} \underline{X}^H\} (H^{-1})^H + \sigma^2 \underline{I}_m.$$

Thus,

$$H (C - \sigma^2 \underline{I}_m) = E\{\underline{X} \underline{X}^H\} (H^{-1})^H = E\{\underline{X} \underline{Y}^H\}.$$

Therefore,

$$R = E\{\underline{X} \underline{Y}^H\} (E\{\underline{Y} \underline{Y}^H\})^{-1}$$

$$R = H (C - \sigma^2 \underline{I}_m) C^{-1}. \quad (3.2-1)$$

3.3 APPLICATION TO THE MOVING WINDOW

With the new formulation of the moving window, pre-processing the signals received at the output of the array will allow us to generate the signals that would have resulted had there been no mutual coupling. Recall that in the presence of mutual coupling, the received signal at the output of the array can be modeled as

$$\underline{Y} = H^{-1} \underline{X} + \underline{N}. \quad (3.3-1)$$

\underline{X} represents the vector of incident signals.

Let $HI = H^{-1}$. Consider the vector

$$\underline{Y}^* = HI^* \underline{X}^* + \underline{N}^* \quad (3.3-2)$$

where $*$ denotes complex conjugate. $(L+1)$ vectors \underline{Y}_n of length $(m-L)$ are then formed where

$$\underline{Y}_n^T = [y_n^* \ y_{(n+1)}^* \ y_{(n+2)}^* \ \dots \ y_{(n+m-L-1)}^*]$$

For the sake of clarity, let $m=5$ and $L=2$. Then

$$\begin{bmatrix} y_1^* \\ y_2^* \\ y_3^* \\ y_4^* \\ y_5^* \end{bmatrix} = \begin{bmatrix} hi_{11}^* & hi_{12}^* & hi_{13}^* & hi_{14}^* & hi_{15}^* \\ hi_{21}^* & hi_{22}^* & hi_{23}^* & hi_{24}^* & hi_{25}^* \\ hi_{31}^* & hi_{32}^* & hi_{33}^* & hi_{34}^* & hi_{35}^* \\ hi_{41}^* & hi_{42}^* & hi_{43}^* & hi_{44}^* & hi_{45}^* \\ hi_{51}^* & hi_{52}^* & hi_{53}^* & hi_{54}^* & hi_{55}^* \end{bmatrix} \begin{bmatrix} x_1^* \\ x_2^* \\ x_3^* \\ x_4^* \\ x_5^* \end{bmatrix} + \begin{bmatrix} n_1^* \\ n_2^* \\ n_3^* \\ n_4^* \\ n_5^* \end{bmatrix}.$$

Note that this matrix equation can be reformulated as

$$\begin{bmatrix} y_1^* \\ y_2^* \\ y_3^* \end{bmatrix} = \begin{bmatrix} hi_{11}^* & hi_{12}^* & hi_{13}^* \\ hi_{21}^* & hi_{22}^* & hi_{23}^* \\ hi_{31}^* & hi_{32}^* & hi_{33}^* \end{bmatrix} \begin{bmatrix} x_1^* \\ x_2^* \\ x_3^* \end{bmatrix} + \begin{bmatrix} 0 & 0 & hi_{14}^* \\ 0 & 0 & hi_{24}^* \\ 0 & 0 & hi_{34}^* \end{bmatrix} \begin{bmatrix} x_2^* \\ x_3^* \\ x_4^* \end{bmatrix} + \begin{bmatrix} 0 & 0 & hi_{15}^* \\ 0 & 0 & hi_{25}^* \\ 0 & 0 & hi_{35}^* \end{bmatrix} \begin{bmatrix} x_3^* \\ x_4^* \\ x_5^* \end{bmatrix} + \begin{bmatrix} n_1^* \\ n_2^* \\ n_3^* \end{bmatrix}$$

$$\begin{bmatrix} y_2^* \\ y_3^* \\ y_4^* \end{bmatrix} = \begin{bmatrix} hi_{21}^* & 0 & 0 \\ hi_{31}^* & 0 & 0 \\ hi_{41}^* & 0 & 0 \end{bmatrix} \begin{bmatrix} x_1^* \\ x_2^* \\ x_3^* \end{bmatrix} + \begin{bmatrix} hi_{22}^* & hi_{23}^* & hi_{24}^* \\ hi_{32}^* & hi_{33}^* & hi_{34}^* \\ hi_{42}^* & hi_{43}^* & hi_{44}^* \end{bmatrix} \begin{bmatrix} x_2^* \\ x_3^* \\ x_4^* \end{bmatrix} + \begin{bmatrix} 0 & 0 & hi_{25}^* \\ 0 & 0 & hi_{35}^* \\ 0 & 0 & hi_{45}^* \end{bmatrix} \begin{bmatrix} x_3^* \\ x_4^* \\ x_5^* \end{bmatrix} + \begin{bmatrix} n_2^* \\ n_3^* \\ n_4^* \end{bmatrix}$$

$$\begin{bmatrix} y_3^* \\ y_4^* \\ y_5^* \end{bmatrix} = \begin{bmatrix} hi_{31}^* & 0 & 0 \\ hi_{41}^* & 0 & 0 \\ hi_{51}^* & 0 & 0 \end{bmatrix} \begin{bmatrix} x_1^* \\ x_2^* \\ x_3^* \end{bmatrix} + \begin{bmatrix} hi_{32}^* & 0 & 0 \\ hi_{42}^* & 0 & 0 \\ hi_{52}^* & 0 & 0 \end{bmatrix} \begin{bmatrix} x_2^* \\ x_3^* \\ x_4^* \end{bmatrix} + \begin{bmatrix} hi_{33}^* & hi_{34}^* & hi_{35}^* \\ hi_{43}^* & hi_{44}^* & hi_{45}^* \\ hi_{53}^* & hi_{54}^* & hi_{55}^* \end{bmatrix} \begin{bmatrix} x_3^* \\ x_4^* \\ x_5^* \end{bmatrix} + \begin{bmatrix} n_3^* \\ n_4^* \\ n_5^* \end{bmatrix}$$

Using matrix notation, we have

$$\underline{Y}_1 = HI_{11} \underline{Z}_1 + HI_{12} \underline{Z}_2 + HI_{13} \underline{Z}_3 + \underline{N}_1,$$

$$\underline{Y}_2 = HI_{21} \underline{Z}_1 + HI_{22} \underline{Z}_2 + HI_{23} \underline{Z}_3 + \underline{N}_2,$$

$$\underline{Y}_3 = HI_{31} \underline{Z}_1 + HI_{32} \underline{Z}_2 + HI_{33} \underline{Z}_3 + \underline{N}_3.$$

For the general case, it can be shown that \underline{Y}_n can be written as

$$\underline{Y}_n = \sum_{i=1}^{(L+1)} HI_{ni} \underline{Z}_i + \underline{N}_n \quad (3.3-3)$$

where

$$\underline{Z}_i^T = [x_i^* \ x_{(i+1)}^* \ x_{(i+2)}^* \ \dots \ x_{(i+m-L-1)}^*] ; i=1, 2, \dots, (L+1)$$

$$\underline{N}_i^T = [n_i^* \ n_{(i+1)}^* \ n_{(i+2)}^* \ \dots \ n_{(i+m-L-1)}^*] ; i=1, 2, \dots, (L+1)$$

and

$$HI_{ni} = \begin{bmatrix} hi_{ni}^* & \dots & hi_{n(i+m-L-1)}^* \\ hi_{(n+1)i}^* & \dots & hi_{(n+1)(i+m-L-1)}^* \\ \vdots & \dots & \vdots \\ hi_{(n+m-L-1)i}^* & \dots & hi_{(n+m-L-1)(i+m-L-1)}^* \end{bmatrix} \text{ for } n=i$$

$$HI_{ni} = \begin{bmatrix} hi_{ni}^* & 0 & \dots & 0 \\ hi_{(n+1)i}^* & 0 & \dots & 0 \\ \vdots & \vdots & \dots & \vdots \\ hi_{(n+m-L-1)i}^* & 0 & \dots & 0 \end{bmatrix} \text{ for } n>i$$

$$HI_{ni} = \begin{bmatrix} 0 & 0 & \dots & 0 & hi_{n(i+m-L-1)}^* \\ 0 & 0 & \dots & 0 & hi_{(n+1)(i+m-L-1)}^* \\ \vdots & \vdots & \dots & \vdots & \vdots \\ 0 & 0 & \dots & hi_{(n+m-L-1)(i+m-L-1)}^* & \end{bmatrix} \text{ for } n<i$$

Note that HI_{ni} has dimensions $(m-L) \times (m-L)$. Let \underline{W} be the vector

$$\underline{W} = [\underline{Y}_1^T \underline{Y}_2^T \dots \underline{Y}_{(L+1)}^T]^T.$$

\underline{W} can be expressed as

$$\underline{W} = \begin{bmatrix} HI_{11} & HI_{12} & \dots & HI_{1(L+1)} \\ HI_{21} & HI_{22} & \dots & HI_{2(L+1)} \\ \vdots & \vdots & \ddots & \vdots \\ \vdots & \vdots & \ddots & \vdots \\ HI_{(L+1)1} & HI_{(L+1)2} & \dots & HI_{(L+1)(L+1)} \end{bmatrix} \begin{bmatrix} \underline{Z}_1 \\ \underline{Z}_2 \\ \vdots \\ \underline{Z}_{(L+1)} \end{bmatrix} + \begin{bmatrix} \underline{N}_1 \\ \underline{N}_2 \\ \vdots \\ \underline{N}_{(L+1)} \end{bmatrix}$$

This can also be written as

$$\underline{W} = \tilde{H}_1 \underline{Z} + \underline{N}' \quad (3.3-4)$$

Assuming the signals and noise to be statistically independent, we get

$$E[\underline{W} \underline{W}^H] = \tilde{H}_1 E[\underline{Z} \underline{Z}^H] \tilde{H}_1^H + E[\underline{N}' \underline{N}'^H]. \quad (3.3-5)$$

Therefore,

$$E[\underline{Z} \underline{Z}^H] = (\tilde{H}_1)^{-1} (E[\underline{W} \underline{W}^H] - E[\underline{N}' \underline{N}'^H]) ((\tilde{H}_1)^{-1})^H. \quad (3.3-6)$$

However $E[\underline{Z} \underline{Z}^H]$ can be expressed as

$$E[\underline{Z} \underline{Z}^H] = \begin{bmatrix} E[\underline{Z}_1 \underline{Z}_1^H] & E[\underline{Z}_1 \underline{Z}_2^H] & \dots & E[\underline{Z}_1 \underline{Z}_{(L+1)}^H] & E[\underline{Z}_1 \underline{Z}_{(L+1)}^H] \\ E[\underline{Z}_2 \underline{Z}_1^H] & E[\underline{Z}_2 \underline{Z}_2^H] & \dots & E[\underline{Z}_2 \underline{Z}_{(L+1)}^H] & E[\underline{Z}_2 \underline{Z}_{(L+1)}^H] \\ \vdots & \vdots & \ddots & \vdots & \vdots \\ \vdots & \vdots & \ddots & \vdots & \vdots \\ E[\underline{Z}_L \underline{Z}_1^H] & E[\underline{Z}_L \underline{Z}_2^H] & \dots & E[\underline{Z}_L \underline{Z}_L^H] & E[\underline{Z}_L \underline{Z}_{(L+1)}^H] \\ E[\underline{Z}_{(L+1)} \underline{Z}_1^H] & E[\underline{Z}_{(L+1)} \underline{Z}_2^H] & \dots & E[\underline{Z}_{(L+1)} \underline{Z}_L^H] & E[\underline{Z}_{(L+1)} \underline{Z}_{(L+1)}^H] \end{bmatrix}.$$

Thus, after partitioning the matrix $E[\underline{Z} \underline{Z}^H]$ into a total of $(L+1) \times (L+1)$ matrices, each having order $(m-L) \times (m-L)$, the matrices

$$M = \sum_{i=1}^L E[\underline{Z}_i \underline{Z}_i^H]$$

and

$$N = \sum_{i=1}^L E[Z_{(i+1)} Z_i^H].$$

needed in the formulation of the matrix pencil (see section 2.3.3) are readily obtained. By using such a formulation, we can effectively compensate for the effects of mutual coupling using the moving window. Recall that the i -th incident signal is given by

$$x_i(t, \theta) = \sum_{k=1}^d s_k(t) a_i(\theta_k); \quad i=1, 2, \dots, m$$

where

$$a_i(\theta_k) = a_k e^{j(i-1)\phi_k}$$

$$\phi_k = -\omega D \sin(\theta_k)/c; \quad k=1, 2, \dots, d,$$

ω is the center frequency of the plane waves

c is the propagation speed of the waves

D is the sensor spacing

$a_k = a(\theta_k)$ is the beam pattern in the direction of the k -th emitter

3.4 APPLICATION TO ESPRIT

Three different arrangements of the doublets are considered in this section.

3.4.1 General Array

We assume that we have $2m$ sensors so as to form m doublets. Further, we assume that each doublet is isolated from the others so that mutual coupling exists only between the two sensors within each doublet (Fig. 3.3). The observed signal at the i -th doublet can then be modeled as

$$\begin{bmatrix} v_i \\ w_i \end{bmatrix} = H_i^{-1} \begin{bmatrix} x_i \\ y_i \end{bmatrix} + \begin{bmatrix} n1_i \\ n2_i \end{bmatrix}; \quad i=1, 2, \dots, m. \quad (3.4.1-1)$$

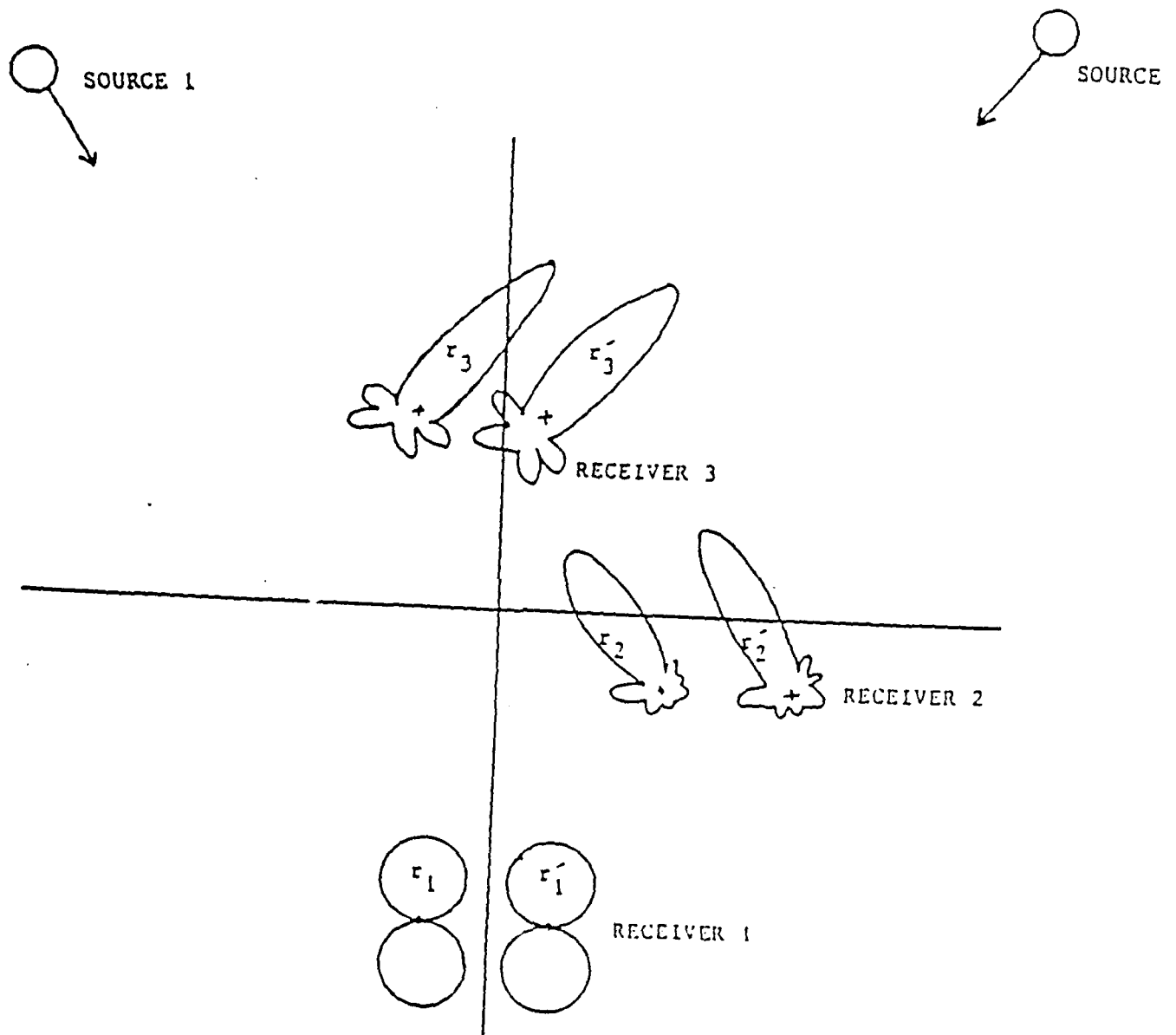


Fig. 3.3 ESPRIT- General Case

Let $HI_1 = H_1^{-1}$. HI_1 can be written as

$$\begin{bmatrix} hi11_i & hi12_i \\ hi21_i & hi22_i \end{bmatrix}.$$

Then

$$v_i = hi11_i x_i + hi12_i y_i + n1_i$$

and

(3.4.1-2)

$$w_i = hi21_i x_i + hi22_i y_i + n2_i.$$

Collecting all the v_i 's in a vector \underline{V} and all the w_i 's in a vector \underline{W} , we have

$$\begin{aligned} \underline{V} &= HI_{11} \underline{X} + HI_{12} \underline{Y} + \underline{N}_1 \\ \underline{W} &= HI_{21} \underline{X} + HI_{22} \underline{Y} + \underline{N}_2, \end{aligned} \quad (3.4.1-3)$$

where HI_{11} , HI_{12} , HI_{21} , HI_{22} , \underline{X} , \underline{Y} , \underline{N}_1 and \underline{N}_2 are given by

$$HI_{11} = \text{diag} \{hi11_1, hi11_2, \dots, hi11_m\},$$

$$HI_{12} = \text{diag} \{hi12_1, hi12_2, \dots, hi12_m\},$$

$$HI_{21} = \text{diag} \{hi21_1, hi21_2, \dots, hi21_m\},$$

$$HI_{22} = \text{diag} \{hi22_1, hi22_2, \dots, hi22_m\},$$

$$\underline{X} = [x_1, x_2, \dots, x_m]^T,$$

$$\underline{Y} = [y_1, y_2, \dots, y_m]^T,$$

$$\underline{N}_1 = [n1_1, n1_2, \dots, n1_m]^T,$$

$$\underline{N}_2 = [n2_1, n2_2, \dots, n2_m]^T.$$

Consider the vector \underline{Z} defined by

$$\underline{Z} = [\underline{V}^T \quad \underline{W}^T]^T.$$

\underline{Z} can be written as

$$\underline{Z} = \begin{bmatrix} HI_{11} & HI_{12} \\ HI_{21} & HI_{22} \end{bmatrix} \begin{bmatrix} \underline{X} \\ \underline{Y} \end{bmatrix} + \begin{bmatrix} \underline{N}_1 \\ \underline{N}_2 \end{bmatrix}. \quad (3.4.1-4)$$

Assuming that the signals and noise are statistically independent and that the noise components are uncorrelated from sensor to sensor with covariance matrix $\sigma^2 I_{2m}$, where I_{2m} is the $(2m \times 2m)$ identity matrix, then $C_{zz} = E[\underline{z} \underline{z}^H]$ is given by

$$C_{zz} = \begin{bmatrix} HI_{11} & HI_{12} \\ HI_{21} & HI_{22} \end{bmatrix} \begin{bmatrix} E[\underline{x} \underline{x}^H] & E[\underline{x} \underline{y}^H] \\ E[\underline{y} \underline{x}^H] & E[\underline{y} \underline{y}^H] \end{bmatrix} \begin{bmatrix} HI_{11} & HI_{12} \\ HI_{21} & HI_{22} \end{bmatrix}^H + \sigma^2 I_{2m}. \quad (3.4.1-5)$$

Let \tilde{H}_2 be the matrix

$$\tilde{H}_2 = \begin{bmatrix} HI_{11} & HI_{12} \\ HI_{21} & HI_{22} \end{bmatrix}.$$

Then

$$(\tilde{H}_2)^{-1} (C_{zz} - \sigma^2 I_{2m}) ((\tilde{H}_2)^{-1})^H = \begin{bmatrix} E[\underline{x} \underline{x}^H] & E[\underline{x} \underline{y}^H] \\ E[\underline{y} \underline{x}^H] & E[\underline{y} \underline{y}^H] \end{bmatrix}. \quad (3.4.1-6)$$

Having recovered the matrix on the right side of equation (3.4.1-6), the matrices $M = E[\underline{x} \underline{x}^H]$ and $N = E[\underline{y} \underline{y}^H]$ can be identified. Recall that incident signals are expressed as

$$x_i(t) = \sum_{k=1}^d s_k(t) g_i(\theta_k)$$

$$y_i(t) = \sum_{k=1}^d s_k(t) e^{-j(\omega \Delta/c) \sin(\theta_k)} g_i(\theta_k)$$

where $g_i(\theta_k)$ is the gain response of the i -th sensor to a source arriving at angle θ_k . The matrices M and N can be decomposed as

$$M = G S G^H \text{ and } N = G \Phi G^H, \quad (3.4.1-7)$$

where G , S and Φ are given by

$$\begin{aligned}
G &= [g_1 \ g_2 \ \dots \ g_d] = \text{gain matrix} \\
S &= B[S \ S^H], \\
\underline{S}^T &= [s_1 \ s_2 \ \dots \ s_d] = \text{impinging signal vector,} \\
\Phi &= \text{diag} [e^{j\phi_1}, e^{j\phi_2}, \dots, e^{j\phi_d}], \\
\phi_k &= -(\omega\Delta/c)\sin(\theta_k), \quad k=1, 2, \dots, d
\end{aligned}$$

Therefore, the effects of mutual coupling have been eliminated and the rank reducing values of the matrix pencil $(M-\lambda N)$ are given by

$$\lambda_k = e^{-j(\omega\Delta/c)\sin(\theta_k)}; \quad k=1, 2, \dots, d. \quad (3.4.1-8)$$

and the angles of arrival of the sources are given by

$$\theta_k = \sin^{-1}\{j\ln(\lambda_k)/(\omega\Delta/c)\}; \quad k=1, 2, \dots, d. \quad (3.4.1-9)$$

3.4.2 Linear Array

3.4.2.1 OVERLAPPING CASE

Consider a linear array of $(m+1)$ sensors and assume there are d ($d < m$) narrowband sources located at angles θ_k ; $k=1, \dots, d$. In this case we consider two sub-arrays consisting of the first m sensors and the last m sensors (Fig. 3.4a). The observed signal vector at the output of the array can be written as

$$\underline{Y} = H^{-1} \underline{X} + \underline{N}. \quad (3.4.2.1-1)$$

Let $HI = H^{-1}$. HI can be written as

$$\begin{bmatrix}
hi_{11} & hi_{12} & \dots & hi_{1(m+1)} \\
hi_{21} & hi_{22} & \dots & hi_{2(m+1)} \\
\vdots & \vdots & \dots & \vdots \\
\vdots & \vdots & \dots & \vdots \\
hi_{(m+1)1} & hi_{(m+1)2} & \dots & hi_{(m+1)(m+1)}
\end{bmatrix}.$$

Thus, if

$$\underline{Y}_1 = [y_1 \ y_2 \ \dots \ y_m]^T,$$

and

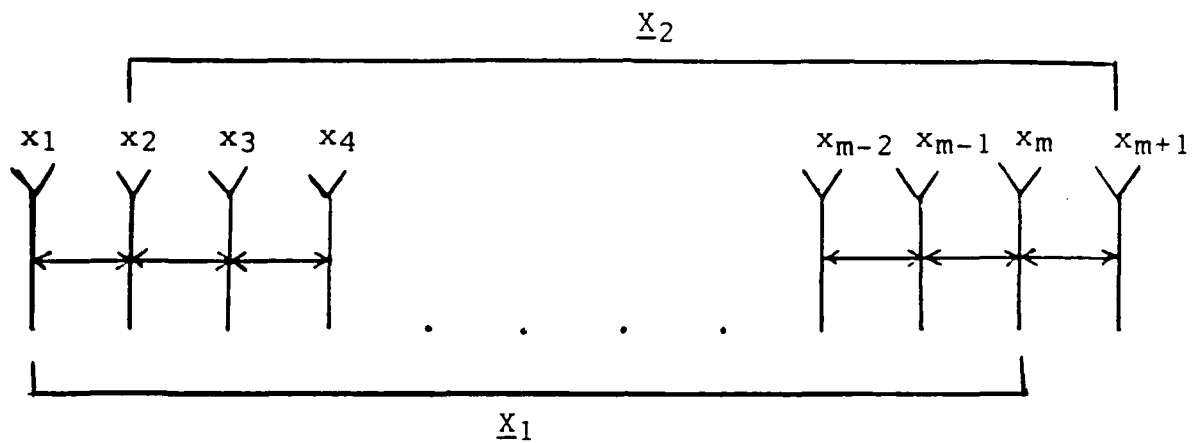


Fig. 3.4a ESPRIT : Linear Array
Overlapping Case.

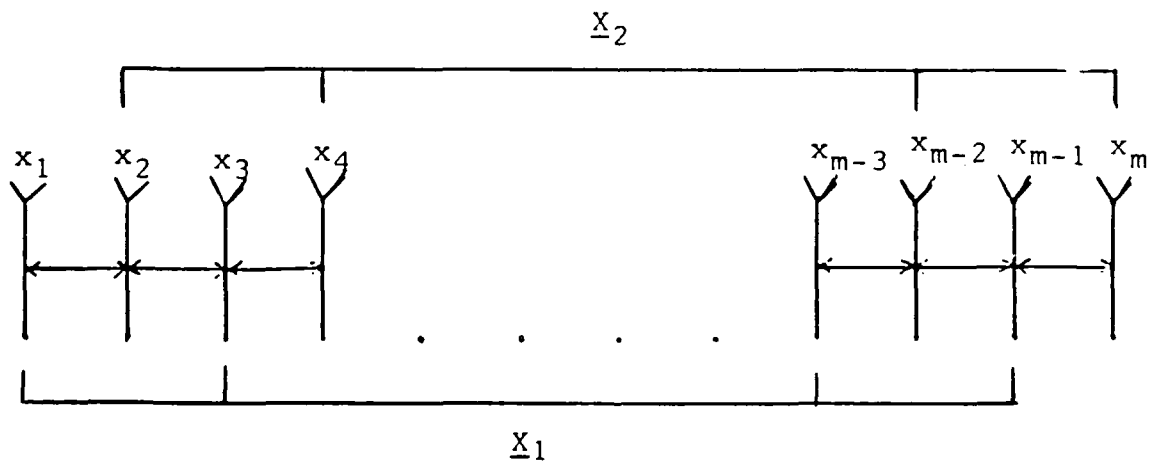


Fig. 3.4b ESPRIT : Linear Array
Non-Overlapping Case.

$$\underline{Y}_2 = [y_2 \ y_3 \ \dots \ y_{(m+1)}]^T,$$

we can write

$$\underline{Y}_1 = HI_{11} \underline{X}_1 + HI_{12} \underline{X}_2 + \underline{N}_1 \quad (3.4.2.1-2)$$

and

$$\underline{Y}_2 = HI_{21} \underline{X}_1 + HI_{22} \underline{X}_2 + \underline{N}_2, \quad (3.4.2.1-3)$$

where HI_{11} , HI_{12} , HI_{21} , HI_{22} , \underline{N}_1 , \underline{N}_2 , \underline{X}_1 and \underline{X}_2 are given by

$$\underline{X}_1 = [x_1 \ x_2 \ \dots \ x_m]^T,$$

$$\underline{X}_2 = [x_2 \ x_3 \ \dots \ x_{(m+1)}]^T.$$

$$HI_{11} = [hi_{111} \ hi_{112} \ \dots \ hi_{11m}],$$

$$hi_{11i} = [hi_{11i} \ hi_{12i} \ \dots \ hi_{mi}]^T; \ i=1, \dots, m,$$

$$HI_{12}^T = [0 \ 0 \ \dots \ 0 \ hi_{1(m+1)}],$$

$$HI_{21}^T = [hi_{221} \ 0 \ \dots \ 0],$$

$$HI_{22}^T = [hi_{222} \ hi_{223} \ \dots \ hi_{22(m+1)}],$$

$$hi_{22i} = [hi_{2i} \ hi_{3i} \ \dots \ hi_{(m+1)i}]^T; \ i=2, \dots, (m+1),$$

$$\underline{N}_1 = [n_1, \ n_2, \ \dots, \ n_m]^T,$$

$$\underline{N}_2 = [n_2, \ n_3, \ \dots, \ n_{(m+1)}]^T.$$

Consider the vector \underline{Z} defined as

$$\underline{Z} = [\underline{Y}_1^T \ \underline{Y}_2^T]^T.$$

\underline{Z} can be written as

$$\underline{Z} = \begin{bmatrix} HI_{11} & HI_{12} \\ HI_{21} & HI_{22} \end{bmatrix} \begin{bmatrix} \underline{X}_1 \\ \underline{X}_2 \end{bmatrix} + \begin{bmatrix} \underline{N}_1 \\ \underline{N}_2 \end{bmatrix}. \quad (3.4.2.1-4)$$

Assuming that the signals and noise are statistically independent and that the noise components are uncorrelated from sensor to sensor with variance σ^2 , then $C_{zz} = E[\underline{Z} \underline{Z}^H]$ is given by

$$C_{zz} = \begin{bmatrix} HI_{11} & HI_{12} \\ HI_{21} & HI_{22} \end{bmatrix} \begin{bmatrix} E[\underline{X}_1 \underline{X}_1^H] & E[\underline{X}_1 \underline{X}_2^H] \\ E[\underline{X}_2 \underline{X}_1^H] & E[\underline{X}_2 \underline{X}_2^H] \end{bmatrix} \begin{bmatrix} HI_{11} & HI_{12} \\ HI_{21} & HI_{22} \end{bmatrix}^H + \sigma^2 \begin{bmatrix} I_m & 0 \\ 0 & I_m \end{bmatrix}. \quad (3.4.2.1-5)$$

Let \tilde{H}_3 and $[\tilde{I}]$ be the matrices

$$\tilde{H}_3 = \begin{bmatrix} HI_{11} & HI_{12} \\ HI_{21} & HI_{22} \end{bmatrix}$$

and

$$[\tilde{I}] = \begin{bmatrix} I_m & I1_m \\ I2_m & I_m \end{bmatrix} .$$

where I_m is the identity matrix and $I1_m$ and $I2_m$ are

$$I1_m = \begin{bmatrix} 0 & 0 & 0 & \dots & 0 & 0 \\ 1 & 0 & 0 & \dots & 0 & 0 \\ 0 & 1 & 0 & \dots & 0 & 0 \\ \dots & \dots & \dots & \dots & \dots & \dots \\ 0 & 0 & 0 & \dots & 0 & 0 \\ 0 & 0 & 0 & \dots & 1 & 0 \end{bmatrix} , \quad I2_m = I1_m^T$$

Then

$$(\tilde{H}_3)^{-1} (C_{zz} - \sigma^2[\tilde{I}])(\tilde{H}_3)^{-1} H = \begin{bmatrix} E[\underline{X}_1 \underline{X}_1^H] & E[\underline{X}_1 \underline{X}_2^H] \\ E[\underline{X}_2 \underline{X}_1^H] & E[\underline{X}_2 \underline{X}_2^H] \end{bmatrix} . \quad (3.4.2.1-6)$$

Having recovered the matrix on the right side of equation (3.4.2.1-6), the matrices $M = E[\underline{X}_1 \underline{X}_1^H]$ and $N = E[\underline{X}_1 \underline{X}_2^H]$ can be identified. Recall that the i -th incident signal is given by

$$x_i(t, \theta) = \sum_{k=1}^d s_k(t) a_i(\theta_k); \quad i=1, 2, \dots, (m+1)$$

where

$$a_i(\theta_k) = a_k e^{j(i-1)\phi_k}$$

$$\phi_k = -\omega D \sin(\theta_k)/c; \quad k=1, 2, \dots, d,$$

ω is the center frequency of the plane waves

c is the propagation speed of the waves

D is the sensor spacing

$a_k = a(\theta_k)$ is the beam pattern in the direction of the k -th emitter.

It can be shown that M and N have the decompositions

$$M = ASA^H \text{ and } N = AS\Phi A^H \quad (3.4.2.1-7)$$

where A , S and Φ are the following matrices

$$S = E[\underline{S} \underline{S}^H],$$

$$\underline{S}^T = \{s_1, \dots, s_d\} \text{ impinging signal vector,}$$

$$A = [\underline{a}_1 \ \underline{a}_2 \ \dots \ \underline{a}_d]$$

$$\underline{a}_i = [a(\theta_i) \ a(\theta_i)e^{j\phi_i} \ \dots \ a(\theta_i)e^{jm\phi_i}],$$

$$\Phi = \text{diag} [e^{j\phi_1}, \dots, e^{j\phi_d}].$$

Therefore, the effects of mutual coupling have been eliminated and the rank reducing values of the matrix pencil $(M - \lambda N)$ are given by

$$\lambda_k = e^{-j(\omega\Delta/c)\sin(\theta_k)}; \ k=1,2, \dots, d. \quad (3.4.2.1-8)$$

The angles of arrival of the sources are given by

$$\theta_k = \sin^{-1}\{j \ln(\lambda_k)/(\omega\Delta/c)\}; \ i=1,2, \dots, d. \quad (3.4.2.1-9)$$

3.4.2.2 NON-OVERLAPPING CASE

In this case a linear array composed of $2m$ sensors is used. Two neighboring sensors are considered as a doublet so that m doublets are formed (Fig. 3.4b). Let there be d ($d < m$) sources. Again, the received signal at the output of the array is modeled as

$$\underline{Y} = HI \underline{X} + \underline{N} \quad (3.4.2.2-1)$$

where HI is given by

$$HI = \begin{bmatrix} hi_{11} & hi_{12} & \dots & hi_{1(2m)} \\ hi_{21} & hi_{22} & \dots & hi_{2(2m)} \\ \cdot & \cdot & \cdot & \cdot \\ \cdot & \cdot & \cdot & \cdot \\ hi_{(2m)1} & hi_{(2m)2} & \dots & hi_{(2m)(2m)} \end{bmatrix}.$$

Let v_i and w_i be the signals received at the i -th doublet. Then

and
$$v_i = y(2i-1) \quad ; \quad i=1, 2, \dots, m.$$

$$w_i = y(2i)$$

Collecting all the v_i 's in a vector \underline{V} and all the w_i 's in a vector \underline{W} , we have

$$\underline{V} = HI_{11} \underline{X}_1 + HI_{12} \underline{X}_2 + \underline{N}_1 \quad (3.4.2.2-2)$$

and

$$\underline{W} = HI_{21} \underline{X}_1 + HI_{22} \underline{X}_2 + \underline{N}_2, \quad (3.4.2.2-3)$$

where HI_{11} , HI_{12} , HI_{21} , HI_{22} , \underline{X}_1 , \underline{X}_2 , \underline{N}_1 and \underline{N}_2 are given by

$$\underline{X}_1 = [x_1 \ x_3 \ \dots \ x_{(2m-1)}]^T,$$

$$\underline{X}_2 = [x_2 \ x_4 \ \dots \ x_{(2m)}]^T,$$

$$HI_{11}^T = [hi_{111} \ hi_{112} \ \dots \ hi_{11m}],$$

$$hi_{11i} = [hi_{(2i-1)1} \ hi_{(2i-1)3} \ \dots \ hi_{(2i-1)(2m-1)}]; \quad i=1, 2, \dots, m,$$

$$HI_{12}^T = [hi_{121} \ hi_{122} \ \dots \ hi_{12m}],$$

$$hi_{12i} = [hi_{(2i-1)2} \ hi_{(2i-1)4} \ \dots \ hi_{(2i-1)(2m)}]; \quad i=1, 2, \dots, m,$$

$$HI_{21}^T = [hi_{211} \ hi_{212} \ \dots \ hi_{21m}],$$

$$hi_{21i} = [hi_{(2i)1} \ hi_{(2i)3} \ \dots \ hi_{(2i)(2m-1)}]; \quad i=1, 2, \dots, m,$$

$$HI_{22}^T = [hi_{221} \ hi_{222} \ \dots \ hi_{22m}],$$

$$hi_{22i} = [hi_{(2i)2} \ hi_{(2i)4} \ \dots \ hi_{(2i)(2m)}]; \quad i=1, 2, \dots, m,$$

$$\underline{N}_1 = [n_1, n_3, \dots, n_{(2m-1)}]^T,$$

$$\underline{N}_2 = [n_2, n_4, \dots, n_{2m}]^T.$$

Consider the vector \underline{z} defined as

$$\underline{z} = [\underline{v}^T \underline{w}^T]^T.$$

\underline{z} can be written as

$$\underline{z} = \begin{bmatrix} HI_{11} & HI_{12} \\ HI_{21} & HI_{22} \end{bmatrix} \begin{bmatrix} \underline{x}_1 \\ \underline{x}_2 \end{bmatrix} + \begin{bmatrix} \underline{N}_1 \\ \underline{N}_2 \end{bmatrix}. \quad (3.4.2.2-4)$$

Assuming that the signals and noise are statistically independent and that the noise components are uncorrelated from sensor to sensor with covariance matrix $\sigma^2 I_{2m}$ where I_{2m} is the $(2m \times 2m)$ identity matrix. Then $C_{zz} = E[\underline{z} \underline{z}^H]$ is given by

$$C_{zz} = \begin{bmatrix} HI_{11} & HI_{12} \\ HI_{21} & HI_{22} \end{bmatrix} \begin{bmatrix} E[\underline{x}_1 \underline{x}_1^H] & E[\underline{x}_1 \underline{x}_2^H] \\ E[\underline{x}_2 \underline{x}_1^H] & E[\underline{x}_2 \underline{x}_2^H] \end{bmatrix} \begin{bmatrix} HI_{11} & HI_{12} \\ HI_{21} & HI_{22} \end{bmatrix}^H + \sigma^2 I_{2m}. \quad (3.4.2.2-5)$$

Let \tilde{H}_4 be the matrix

$$\tilde{H}_4 = \begin{bmatrix} HI_{11} & HI_{12} \\ HI_{21} & HI_{22} \end{bmatrix}.$$

Then

$$(\tilde{H}_4)^{-1} (C_{zz} - \sigma^2 I_{2m}) ((\tilde{H}_4)^{-1})^H = \begin{bmatrix} E[\underline{x}_1 \underline{x}_1^H] & E[\underline{x}_1 \underline{x}_2^H] \\ E[\underline{x}_2 \underline{x}_1^H] & E[\underline{x}_2 \underline{x}_2^H] \end{bmatrix}. \quad (3.4.2.2-6)$$

Having recovered the matrix on the right side of equation (3.4.2.2-6), the matrices $M = E[\underline{x}_1 \underline{x}_1^H]$ and $N = E[\underline{x}_1 \underline{x}_2^H]$ can be identified. The i -th incident signal can be written as

$$x_i(t, \underline{\theta}) = \sum_{k=1}^d s_k(t) a_i(\theta_k); \quad i=1, 2, \dots, 2m$$

where

$$a_i(\theta_k) = a_k e^{j(i-1)\phi_k}$$

$$\phi_k = -\omega D \sin(\theta_k)/c ; k=1, 2, \dots, d,$$

ω is the center frequency of the plane waves

c is the propagation speed of the waves

D is the sensor spacing

$a_k = a(\theta_k)$ is the beam pattern in the direction of the k -th emitter.

M and N have the following decompositions

$$M = ASA^H \text{ and } N = A\Phi^H A^H, \quad (3.4.2.2-7)$$

where A , S and Φ are given by

$$A = [a_1 \ a_2 \ \dots \ a_d]$$

$$a_i = [a(\theta_i) \ a(\theta_i)e^{j2\phi_i} \ \dots \ a(\theta_i)e^{j(2m-2)\phi_i}],$$

$$S = E[S \ S^H],$$

$$\underline{S}^T = \{s_1, \dots, s_d\} \text{ impinging signal vector,}$$

$$\Phi = \text{diag} [e^{j\phi_1} \ e^{j\phi_2} \ \dots \ e^{j\phi_d}],$$

Therefore, the effects of mutual coupling have been eliminated and the rank reducing values of the matrix pencil $(M - \lambda N)$ are given by

$$\lambda_k = e^{-j(\omega D/c)\sin(\theta_k)}; k=1, 2, \dots, d. \quad (3.4.2.2-8)$$

The angles of arrival of the sources are thus

$$\theta_k = \sin^{-1}\{j \ln(\lambda_k)/(\omega D/c)\}; k=1, 2, \dots, d. \quad (3.4.2.2-9)$$

3.5 Computer Simulation

The scenario used for this simulation consisted of two incoherent sources ($d=2$) which are incident on a linear array consisting of eight uniformly spaced half wavelength dipoles ($m=8$). The sources are assumed to

be located at $\theta_1=16^\circ$ and $\theta_2=24^\circ$. The noise was simulated to be white Gaussian with zero-mean and unit variance. The sensor spacing was assumed to be half wavelength such that $\omega D/c = \pi$. The load impedance was taken to be the complex conjugate of the self impedance. The statistics were derived from 50 runs where 100 snapshots were taken in each run. The results are shown in Fig. 3-5 to 3-16. In these figures, (1) represents the moving window, (2) and (3) represent ESPRIT for the linear case when overlapping and non overlapping arrays are considered, respectively, and (4) corresponds to ESPRIT used in a general case. Without compensation, note that all algorithms fail to accurately locate the two sources due to the distortion introduced by the mutual coupling. With the compensating schemes developed here, all algorithms identify the locations of the two sources correctly. However, ESPRIT used in a Linear Overlapping Case performs much better than the remaining algorithms. This is due to a larger array aperture. However, our objective was not to perform a comparison between the different algorithms but to derive effective methods to compensate for the mutual coupling effects. This has been achieved and it is shown that compensation of the mutuals is likely to be a necessity if acceptable performance is to be obtained in practice. In the different figures for the mean-squared error and the variance, the y-axis is defined as

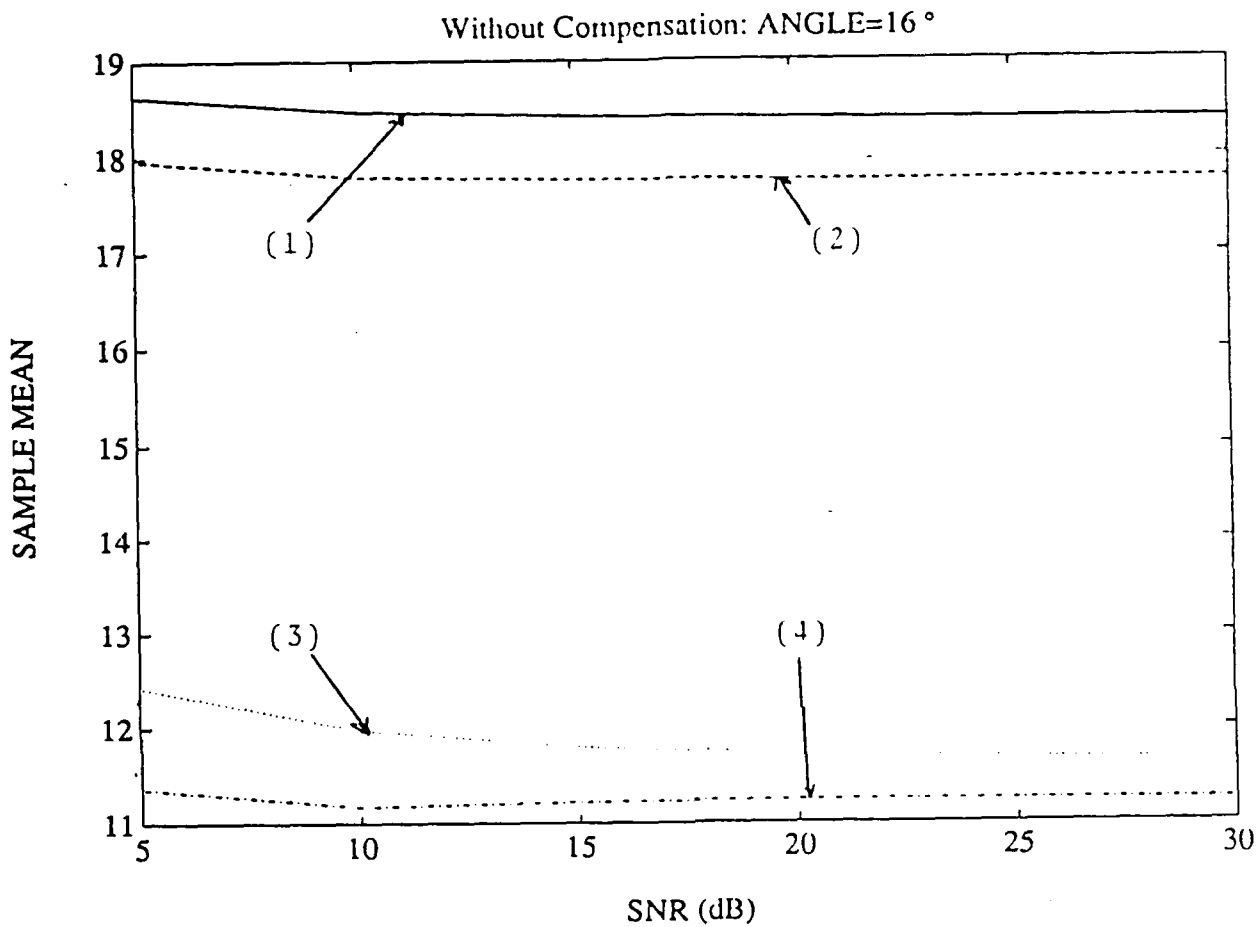
$$y=10 \log_{10}(.).$$

Let $\hat{\theta}_k$ be an estimate of θ obtained at the k-th run (K is the number of runs). The sample mean (ME), the sample variance (Var) and the mean-squared error (MSE) are defined respectively as

$$ME(\theta) = (1/K) \sum_{k=1}^K \hat{\theta}_k,$$

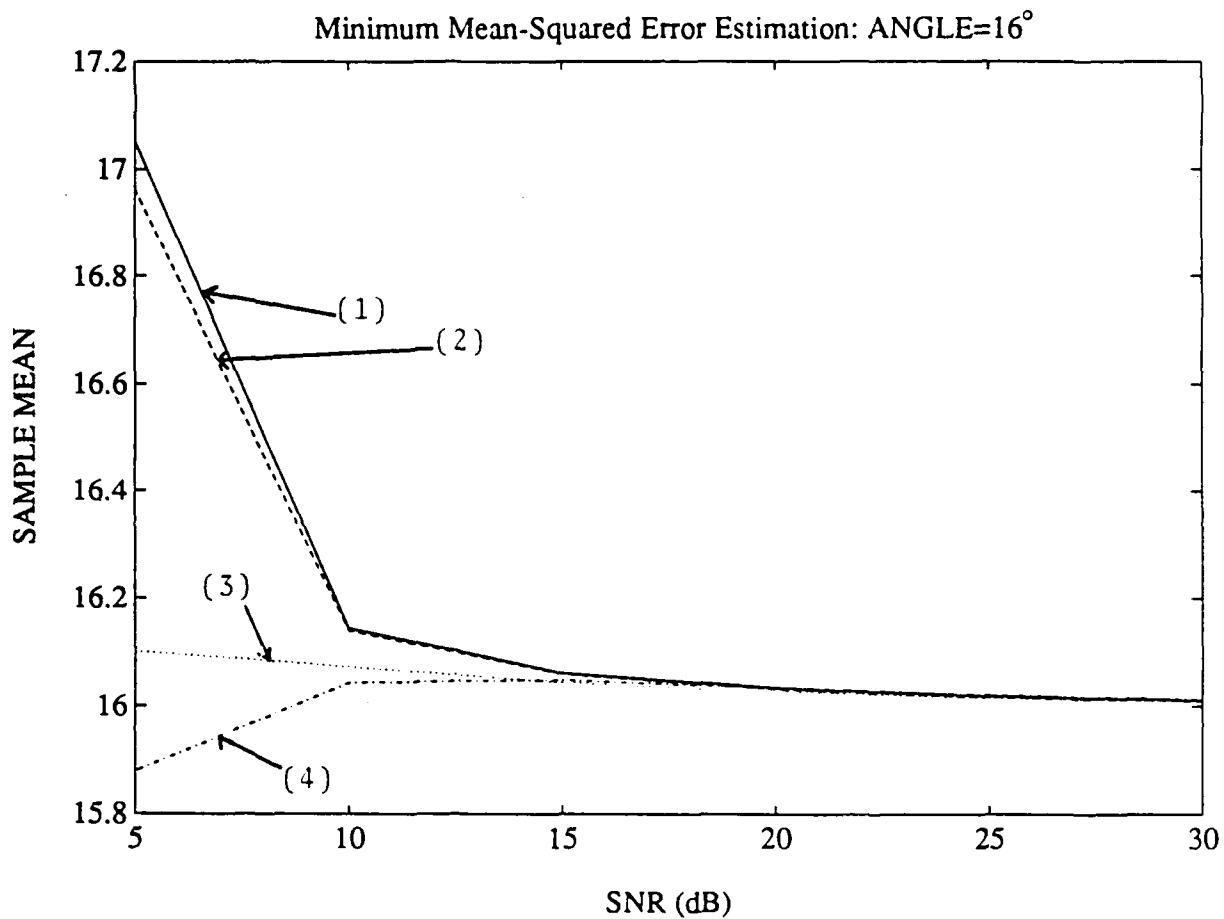
$$\text{Var}(\theta) = (1/K) \sum_{k=1}^K (\hat{\theta}_k - \text{ME}(\theta))^2,$$

$$\text{MSE}(\theta) = (1/K) \sum_{k=1}^K (\hat{\theta}_k - \theta)^2.$$



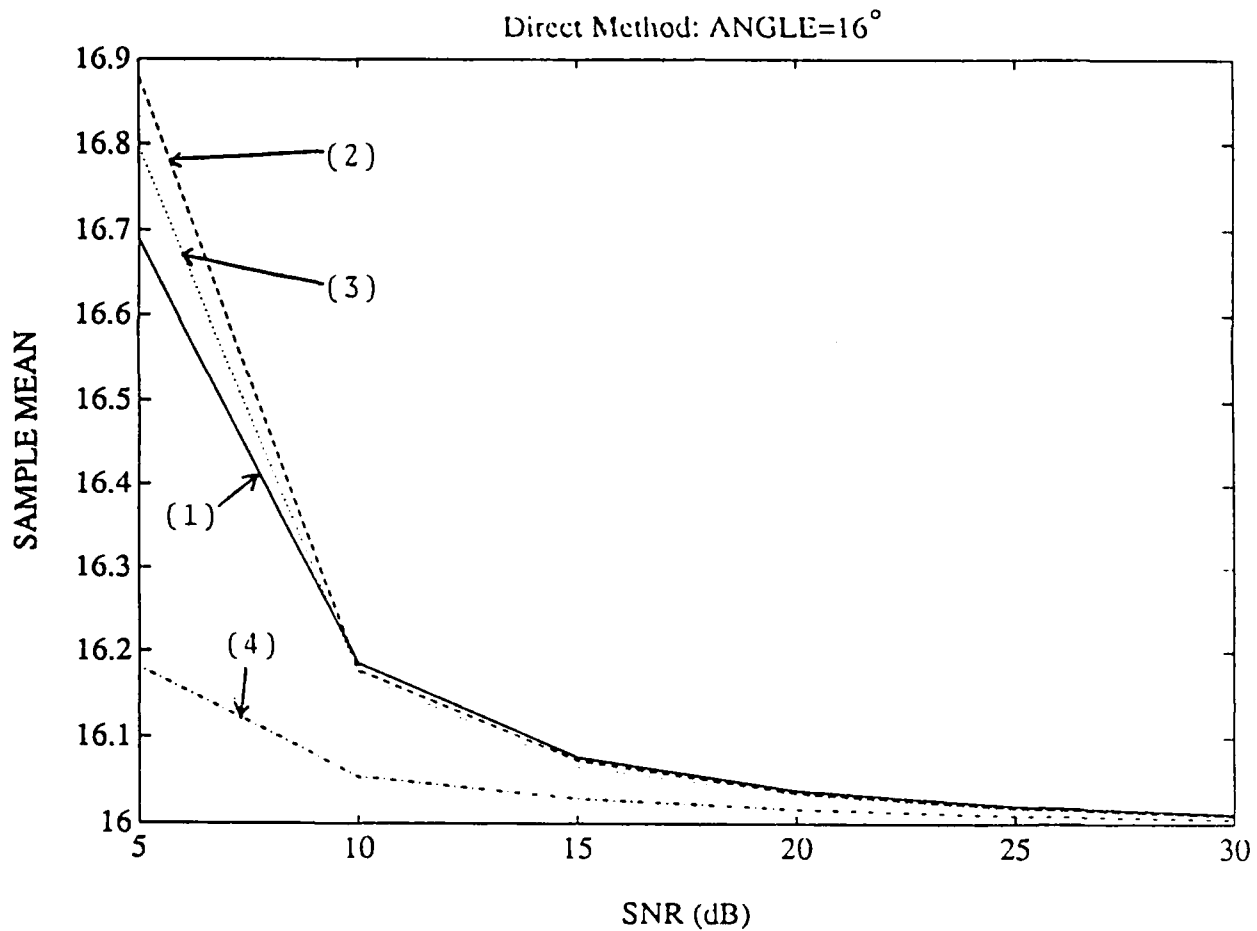
- (1)-Moving window
- (2)-ESPRIT: Linear Overlapping Case
- (3)-ESPRIT: Linear Non Overlapping Case
- (4)-ESPRIT: General Case.

Fig. 3.5 Sample Mean of the Angle Estimate at 16° Without Compensation for the Mutuals.



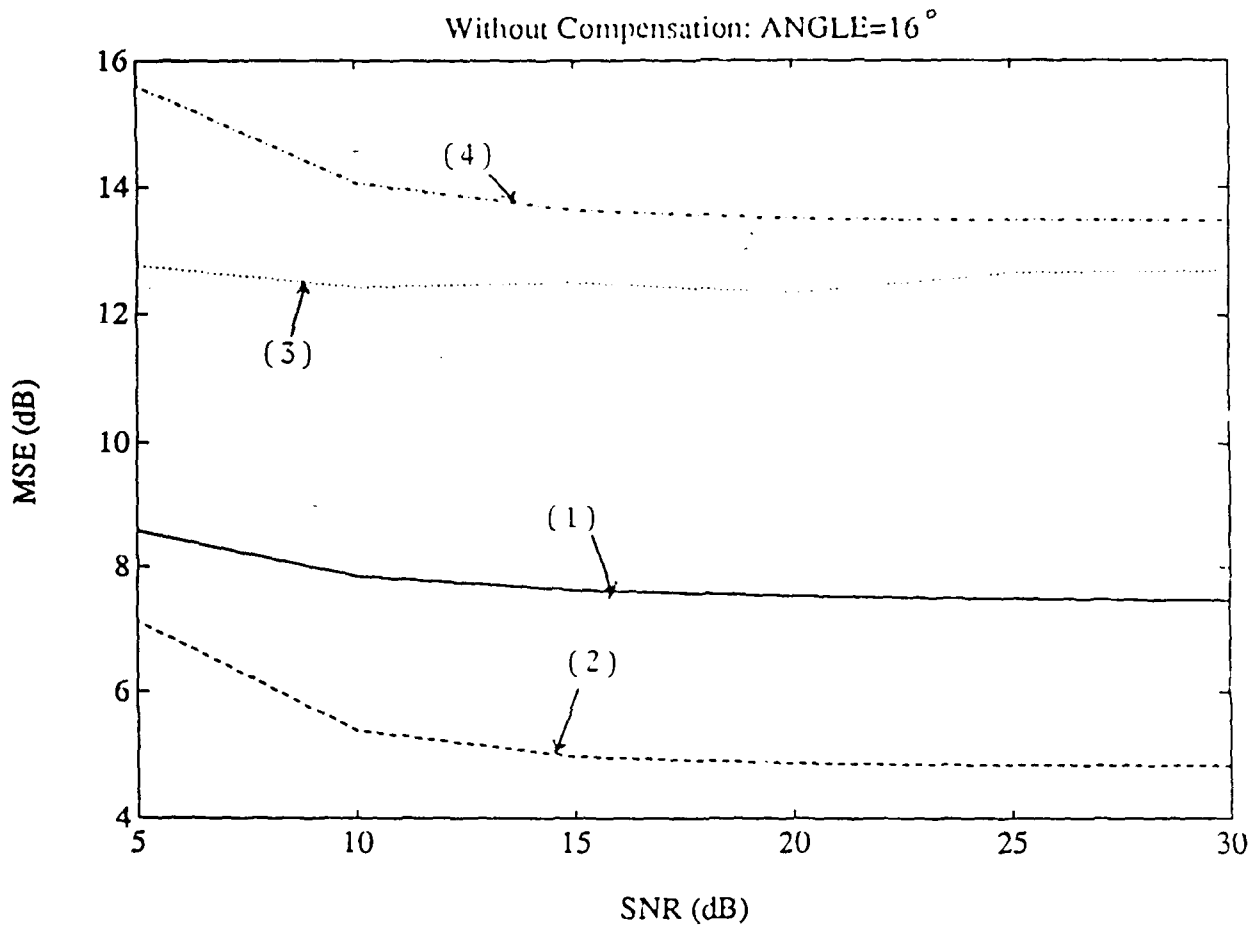
- (1)-Moving Window
- (2)-ESPRIT: Linear Overlapping Case
- (3)-ESPRIT: Linear Non-Overlapping Case
- (4)-ESPRIT: General case.

Fig. 3.6 Sample Mean of the Angle Estimate at 16° With Compensation for the Mutuals When Using a Minimum Mean-Squared Error Estimation.



- (1) -Moving Window
- (2) -ESPRIT: Linear Overlapping Case
- (3) -ESPRIT: Linear Non Overlapping Case
- (4) -ESPRIT: General case.

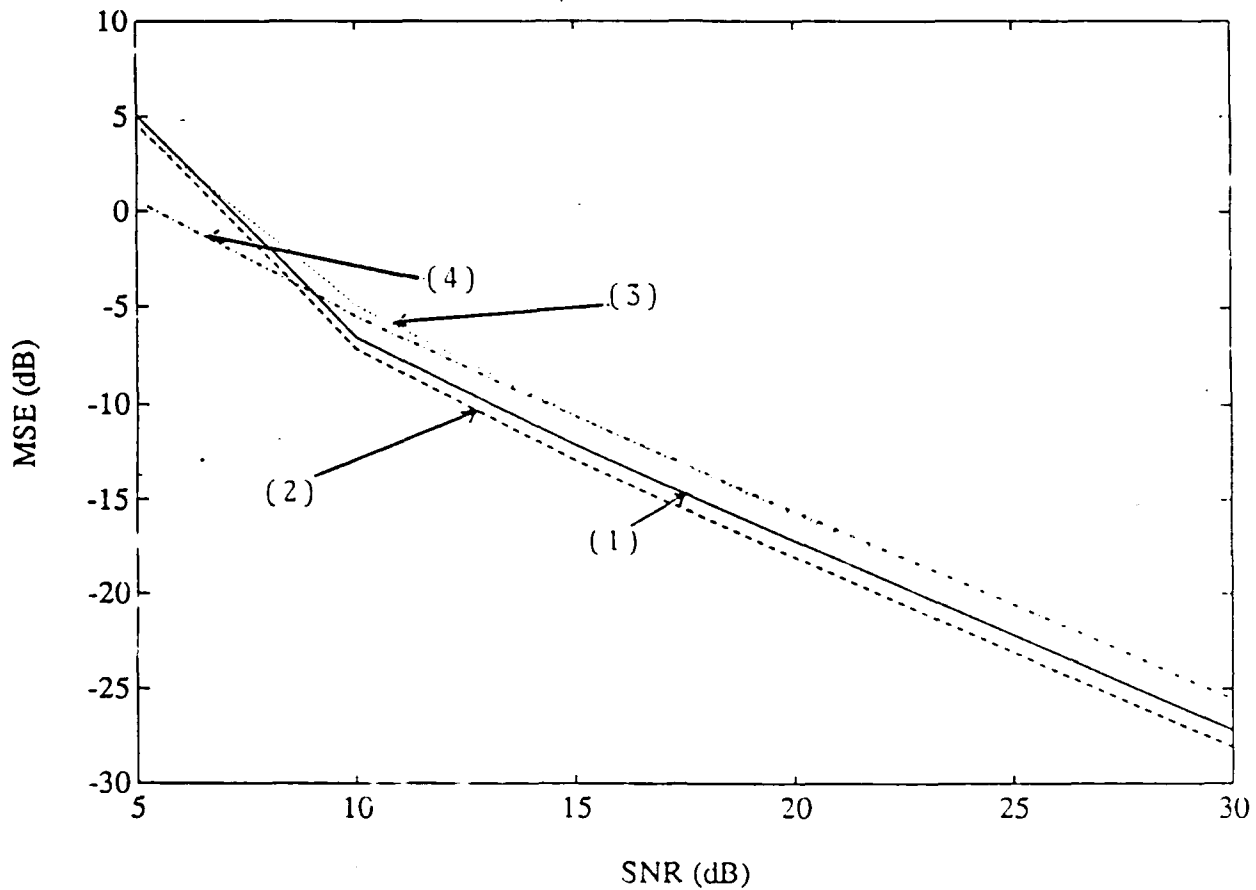
Fig. 3.7 Sample Mean of the Angle Estimate at 16° With Compensation for the Mutuals When Using the Direct Method.



- (1)-Moving Window
- (2)-ESPRIT: Linear Overlapping Case
- (3)-ESPRIT: Linear Non Overlapping Case
- (4)-ESPRIT: General Case.

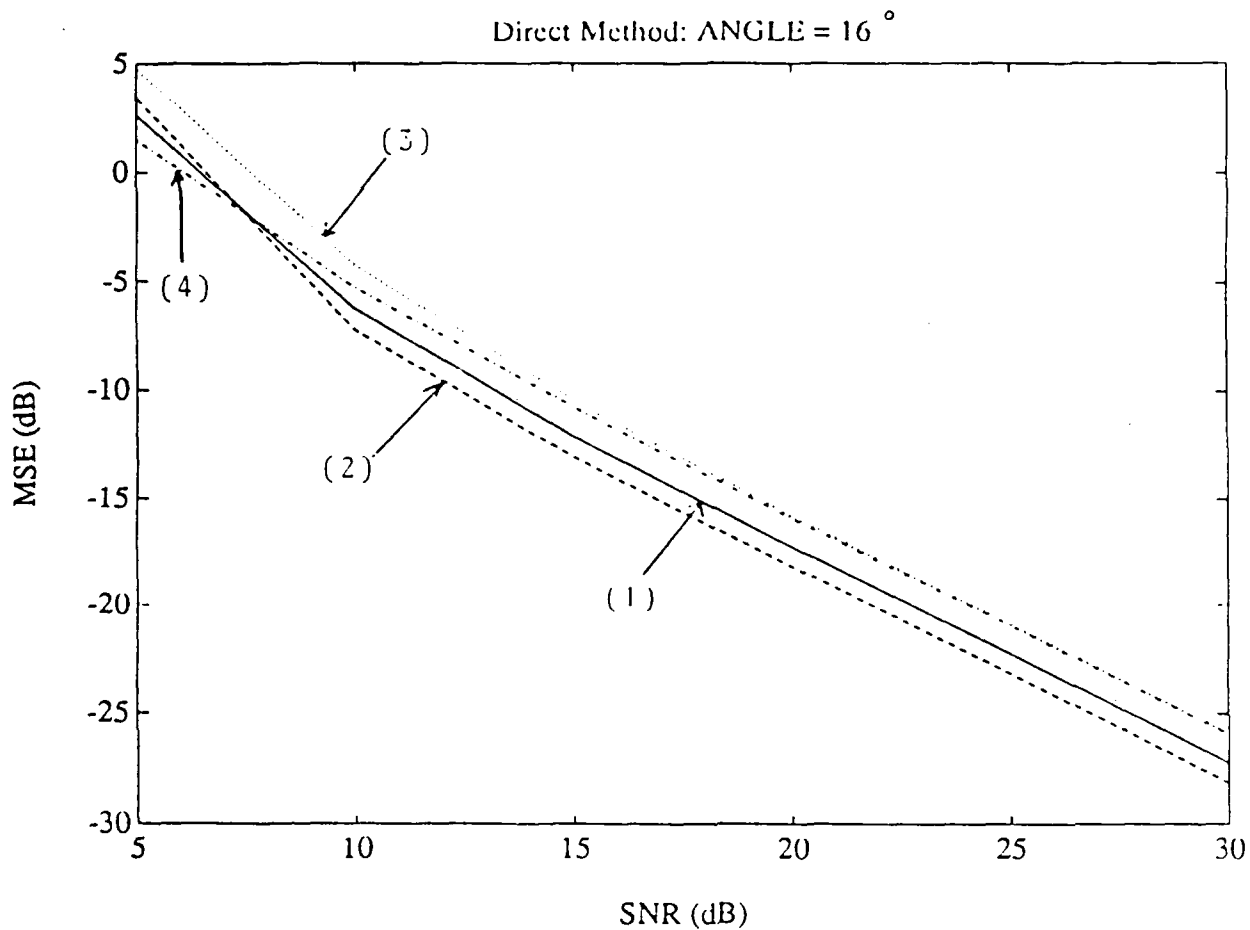
Fig. 3.8 Mean-Squared Error of the Angle Estimate at 16° Without Compensation for the Mutuals.

Minimum Mean-Squared Error Estimation: ANGLE = 16°



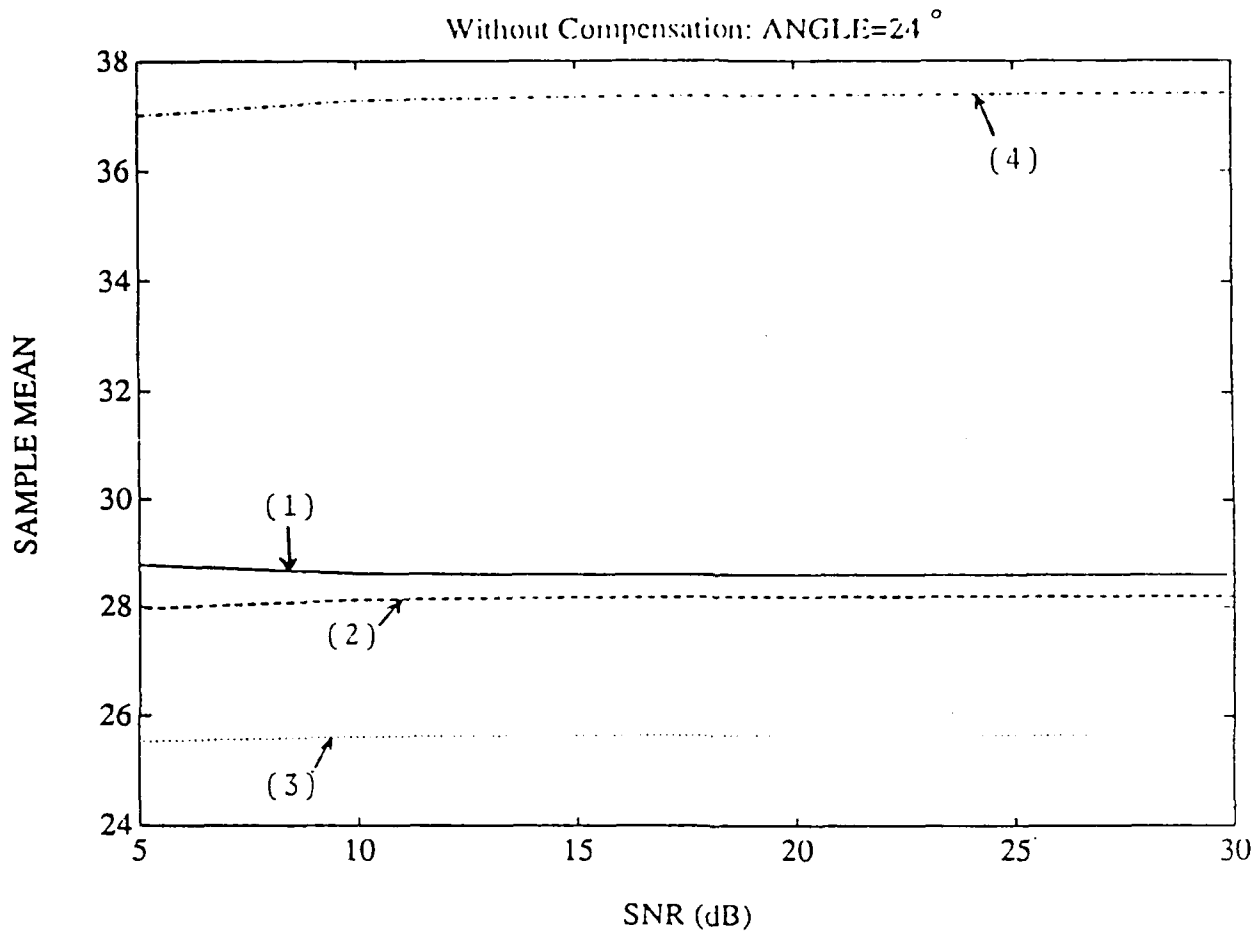
- (1)-Moving Window
- (2)-ESPRIT: Linear Overlapping Case
- (3)-ESPRIT: Linear Non Overlapping Case
- (4)-ESPRIT: General Case.

Fig. 3.9 Mean-Squared Error of the Angle Estimate at 16° With Compensation for the Mutuals When Using a Minimum Mean-Squared Error Estimation.



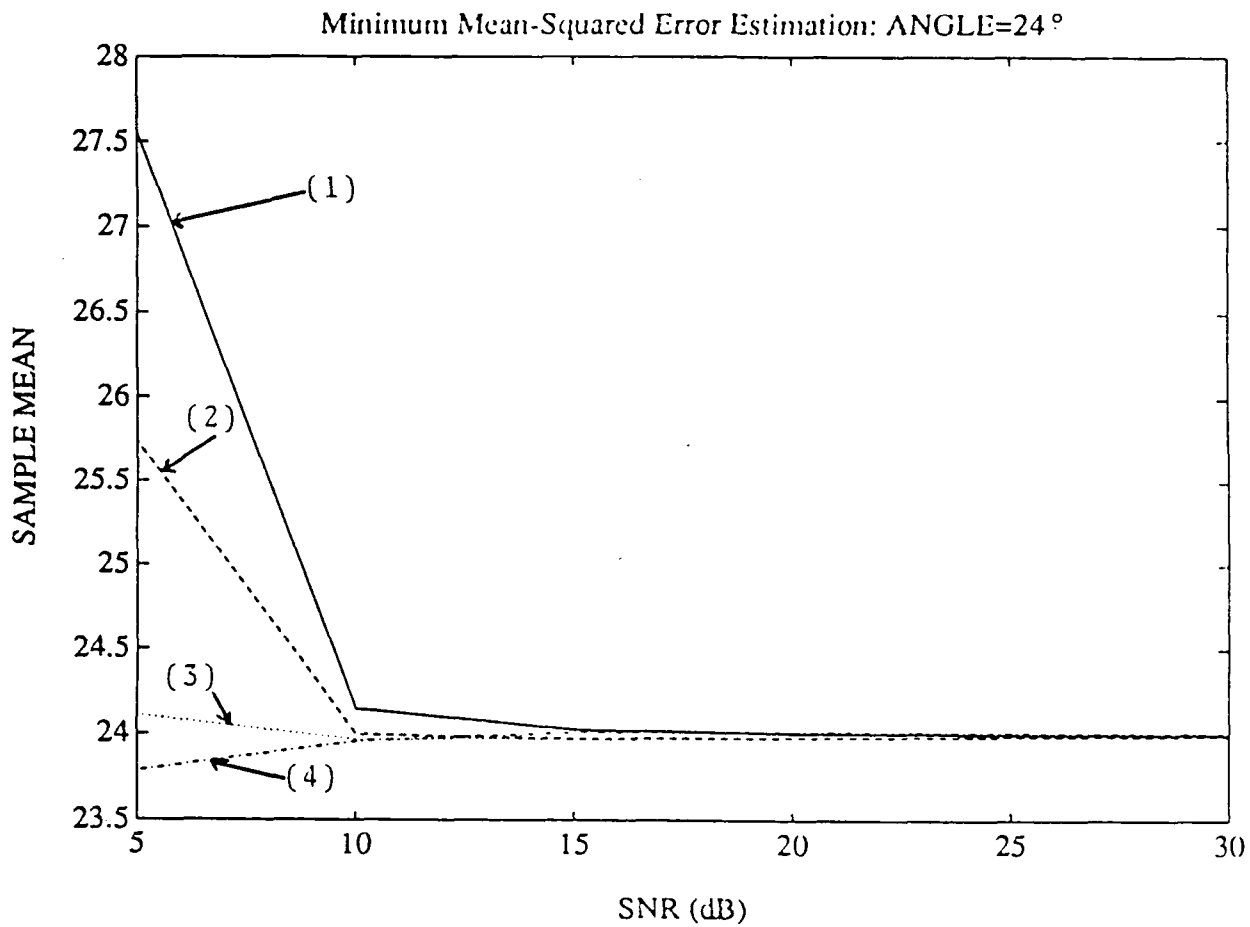
- (1) -Moving window
- (2) -ESPRIT: Linear Overlapping Case
- (3) -ESPRIT: Linear Non Overlapping Case
- (4) -ESPRIT: General Case.

Fig. 3.10 Mean-Squared Error of the Angle Estimate at 16° With Compensation for the Mutuals When Using the Direct Method.



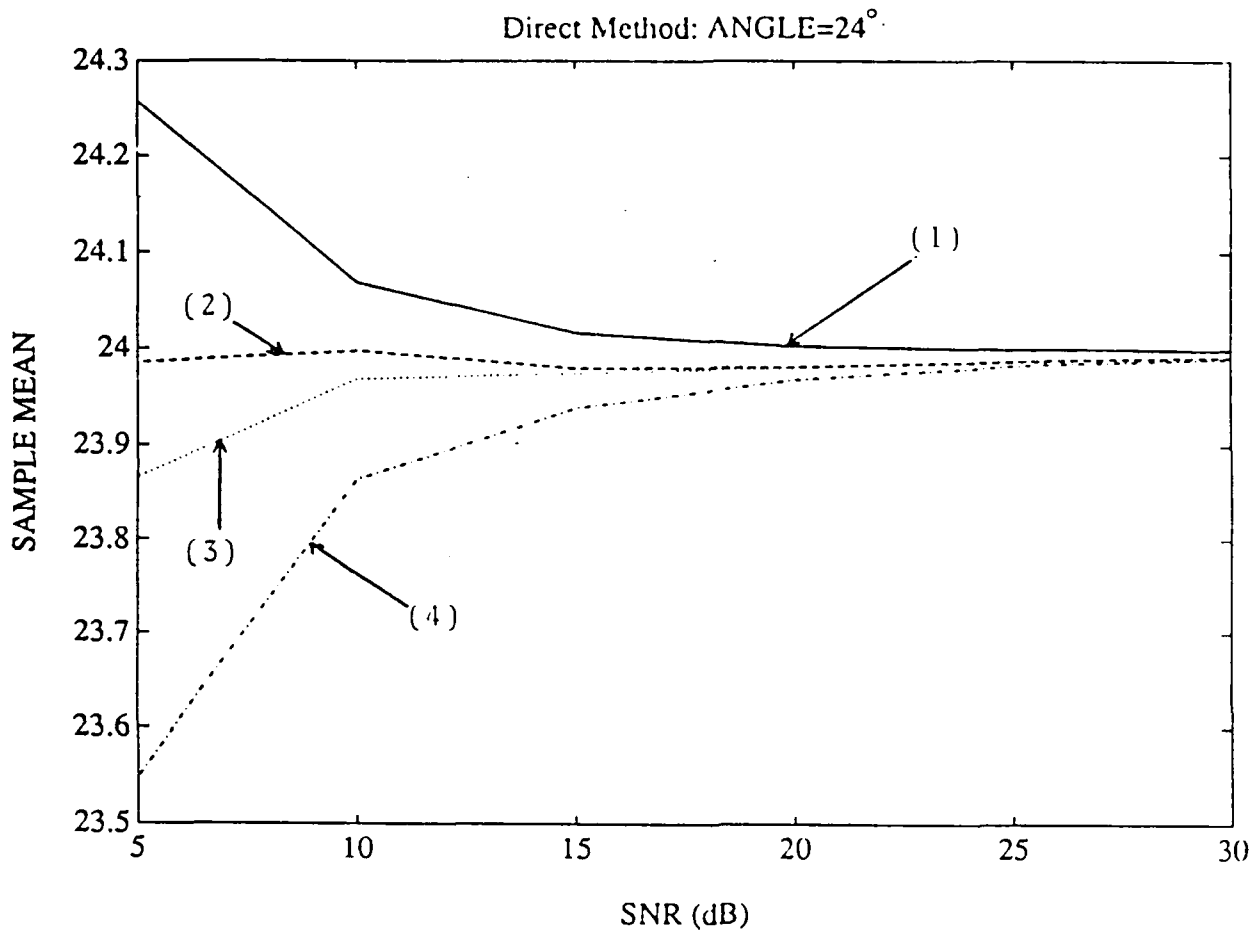
- (1) -Moving Window
- (2) -ESPRIT: Linear Overlapping Case
- (3) -ESPRIT: Linear Non Overlapping Case
- (4) -ESPRIT: General Case.

Fig. 3.11 Sample Mean of the Angle Estimate at 24° Without Compensation for the Mutuals.



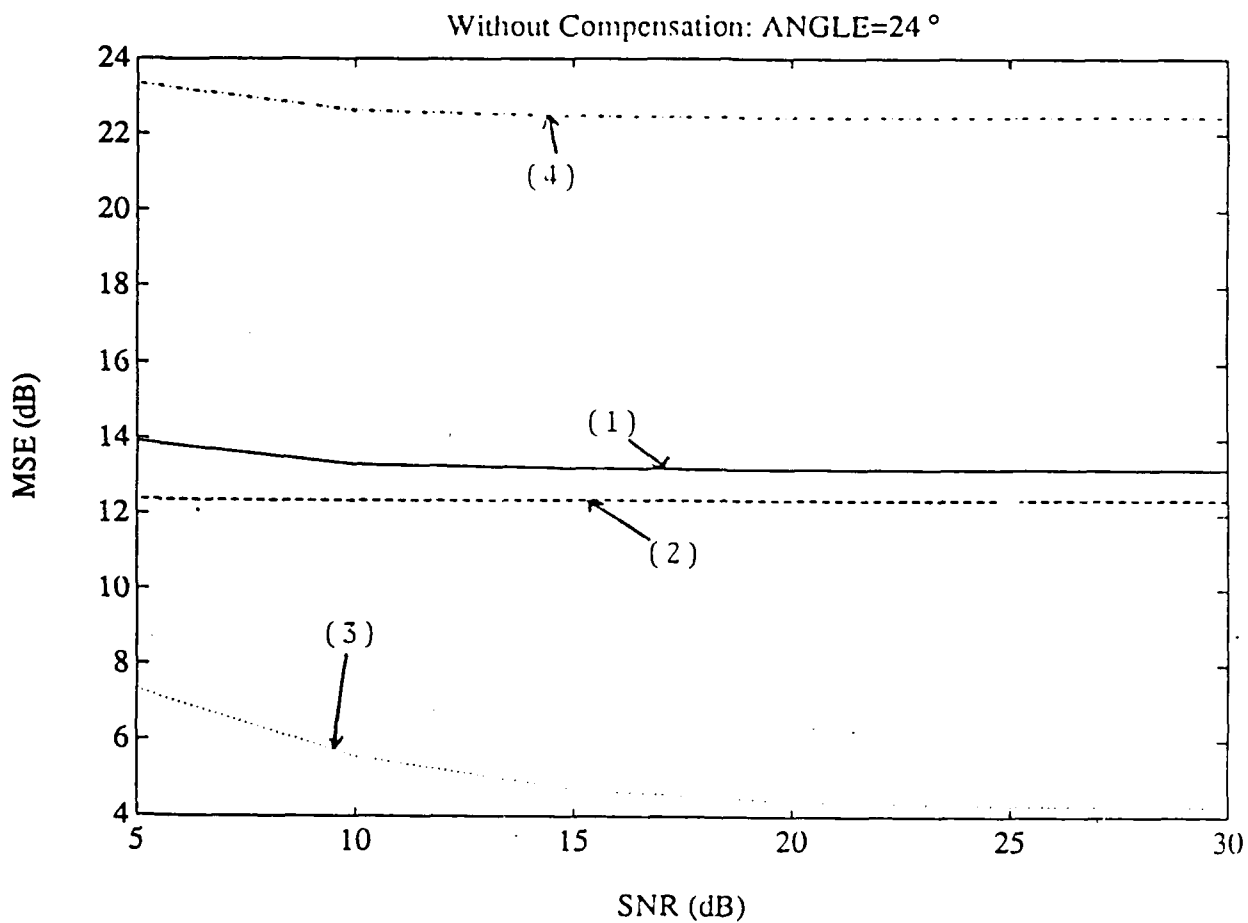
- (1)-Moving Window
- (2)-ESPRIT: Linear Overlapping Case
- (3)-ESPRIT: Linear Non Overlapping Case
- (4)-ESPRIT: General Case.

Fig. 3.12 Sample Mean of the Angle Estimate at 24° With Compensation for the Mutuals When Using a Minimum Mean-Squared Error Estimation.



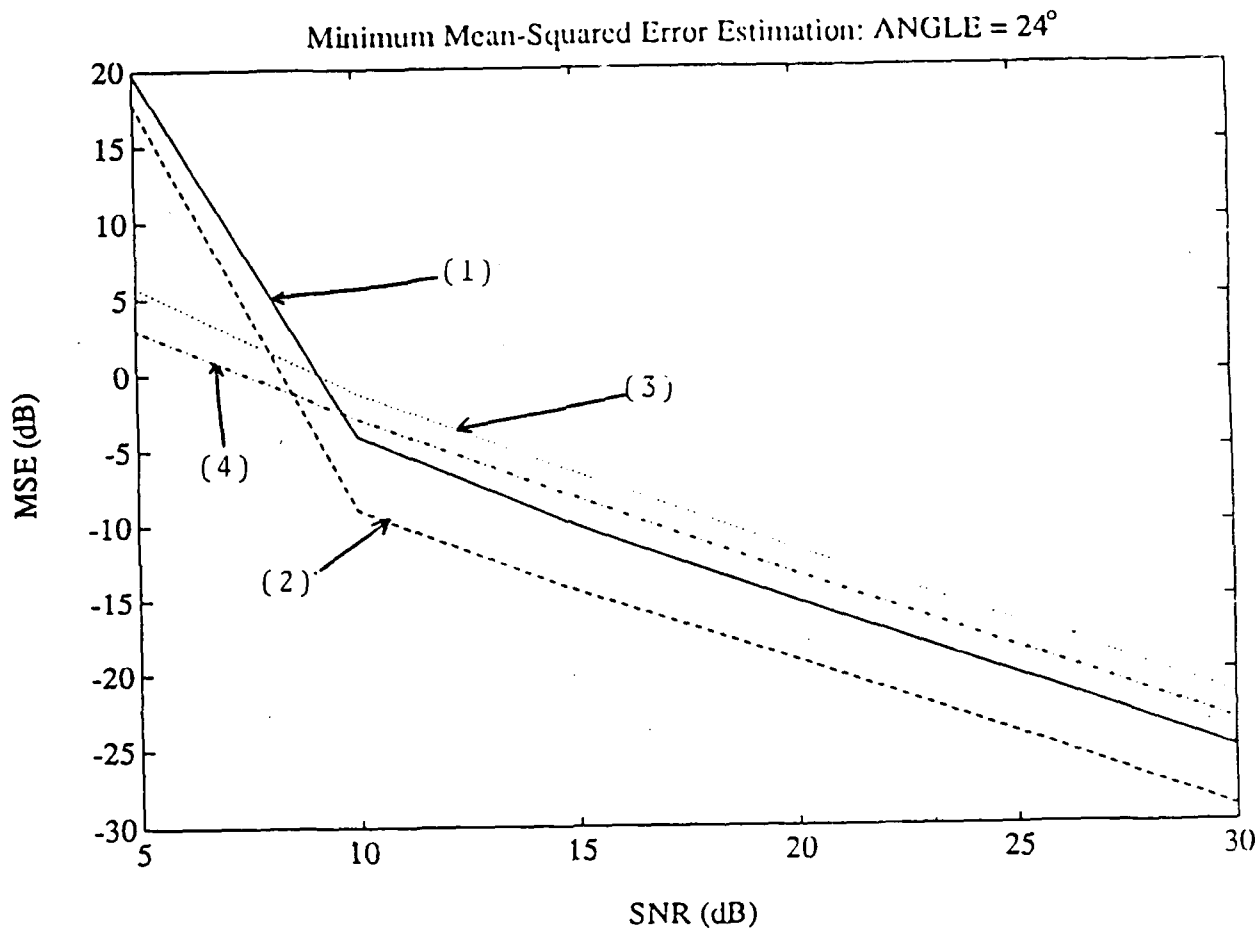
- (1) - Moving Window
- (2) - ESPRIT: Linear Overlapping Case
- (3) - ESPRIT: Linear Non Overlapping Case
- (4) - ESPRIT: General Case.

Fig. 3.13 Sample Mean of the Angle Estimate at 24° With Compensation for the Mutuals When Using the Direct Method.



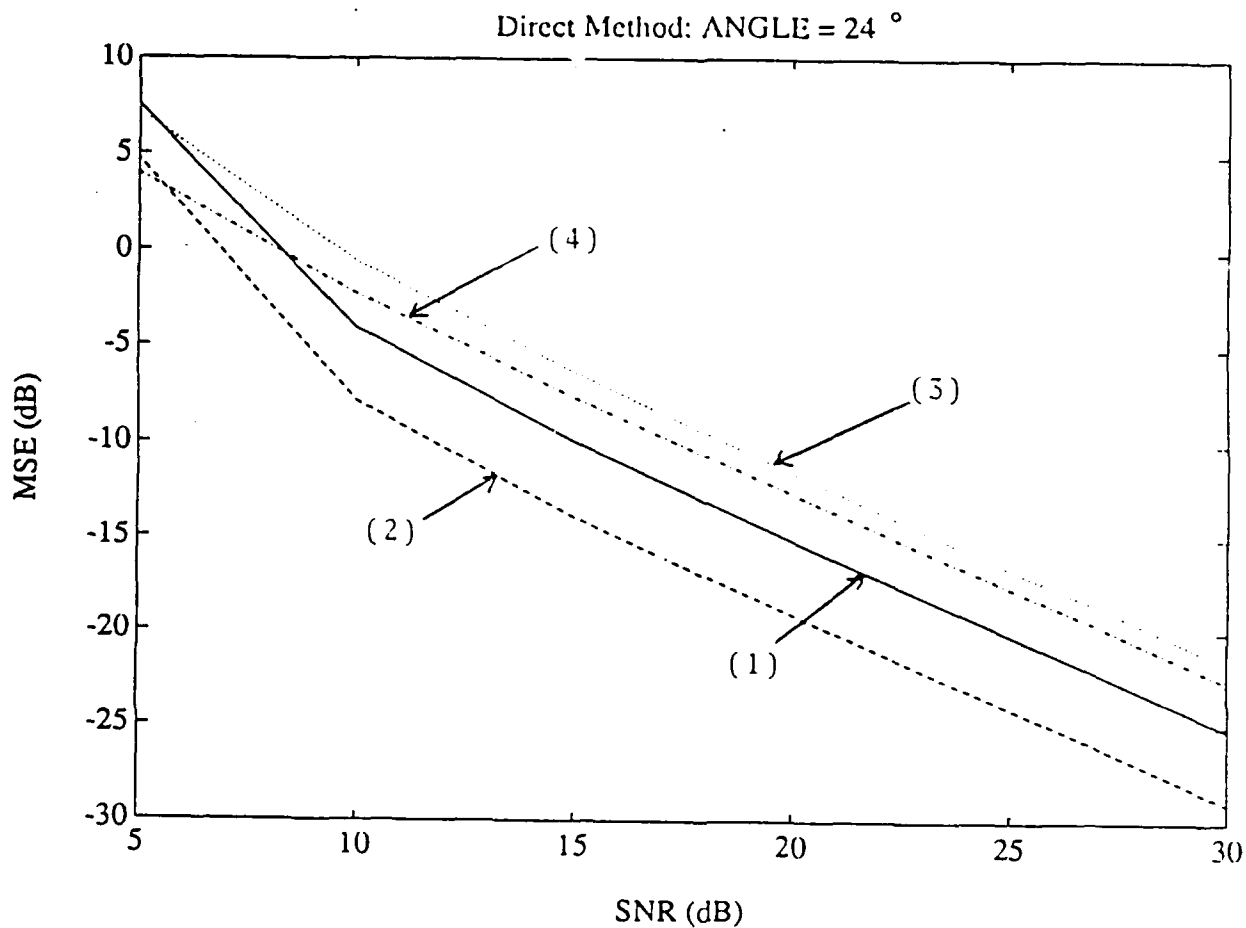
- (1) -Moving Window
- (2) -ESPRIT: Linear Overlapping Case
- (3) -ESPRIT: Linear Non Overlapping Case
- (4) -ESPRIT: General Case.

Fig. 3.14 Mean-Squared Error of the Angle Estimate at 24° Without Compensation for the Mutuals.



- (1) -Moving Window
- (2) -ESPRIT: Linear Overlapping Case
- (3) -ESPRIT: Linear Non Overlapping Case
- (4) -ESPRIT: General Case.

Fig. 3.15 Mean-Squared Error of the Angle Estimate at 24° With Compensation for the Mutuals When Using a Minimum Mean-Squared Error Estimation.



- (1) -Moving Window
- (2) -ESPRIT: Linear Overlapping Case
- (3) -ESPRIT: Linear Non Overlapping Case
- (4) -ESPRIT: General case.

Fig. 3.16 Mean-Squared Error of the Angle Estimate at 24° With Compensation for the Mutuals When Using the Direct Method.

CHAPTER 4

EXTENSIONS TO WIDEBAND SIGNALS

Different methods for estimating the angles of arrival of wideband signals can be developed depending upon the approach. In this section we devise three new techniques for the matrix pencil.

4.1 TRANSIENT SIGNALS

In this section we model each source as a sum of decaying exponentials. This representation is appropriate for non stationary signals. Consider a linear array which consists of m identical wideband sensors uniformly spaced at a distance Δ . Assume there are d broadband sources impinging on the array as planar wavefronts and emitting signals whose complex envelopes are denoted by $s_k(t)$. The signal received at the i -th sensor can be expressed as

$$x_i(t) = \sum_{k=1}^d a(\theta_k) s_k(t - \tau_{ik}) + n_i(t); \quad i=1, 2, \dots, m \quad (4.1-1)$$

where τ_{ik} is the time delay that source k takes to travel from the reference point to the i -th sensor. Taking the reference as the first sensor, τ_{ik} can be written as

$$\tau_{ik} = (i-1)(\Delta/c)\sin(\theta_k) \quad (4.1-2)$$

where c is the speed of propagation of the waves. Assume the k -th source can be represented by a sum of exponentials having natural frequencies p_{lk} ; $l=1, 2, \dots, M^{(k)}$. Thus, $s_k(t)$ can be written as

$$s_k(t) = \sum_{l=1}^{M(k)} b_{lk} e^{Plk t}, \quad (4.1-3)$$

where the coefficients b_{lk} are assumed to be random. Therefore, the received signal $x_i(t)$ can be expressed as

$$x_i(t) = \sum_{k=1}^d \sum_{l=1}^{M(k)} c_{lk} e^{(i-1)\phi_{lk}} + n_i(t); \quad i=1,2,\dots,m, \quad (4.1-4)$$

where

$$\phi_{lk} = -(\Delta/c)Plk \sin(\theta_k), \quad (4.1-5)$$

and

$$c_{lk} = a(\theta_k)b_{lk}e^{Plk t}. \quad (4.1-6)$$

Given the data collected at the output of the array, the problem is to estimate the angles of arrival of the sources. From the above data, a matrix pencil is generated. It is shown that the rank reducing values of this pencil are related to both the angles of arrival and the natural frequencies of the sources. The natural frequencies of the sources are assumed to be unknown at the receiver. Therefore, these natural frequencies have first to be estimated and then be used to solve for the angles of arrival. Thus, a simultaneous estimation of the natural frequencies and the angles of arrival is needed. To do so, the first sensor is followed by an equally spaced tapped delay line consisting of m taps with successive delays of T seconds. In addition the received signal at the i -th sensor is delayed by an amount of $(i-1)T$; $i=2, 3, \dots, m$, (Fig. 4-1). The signal at the output of the h -th delay following the first sensor is

$$y_h = x_1(t - (h-1)T) = \sum_{k=1}^d \sum_{l=1}^{M(k)} c_{lk} e^{(h-1)\gamma_{lk}} + n_1(t - (h-1)T); \quad h=0,1,\dots,(m-1) \quad (4.1-7)$$

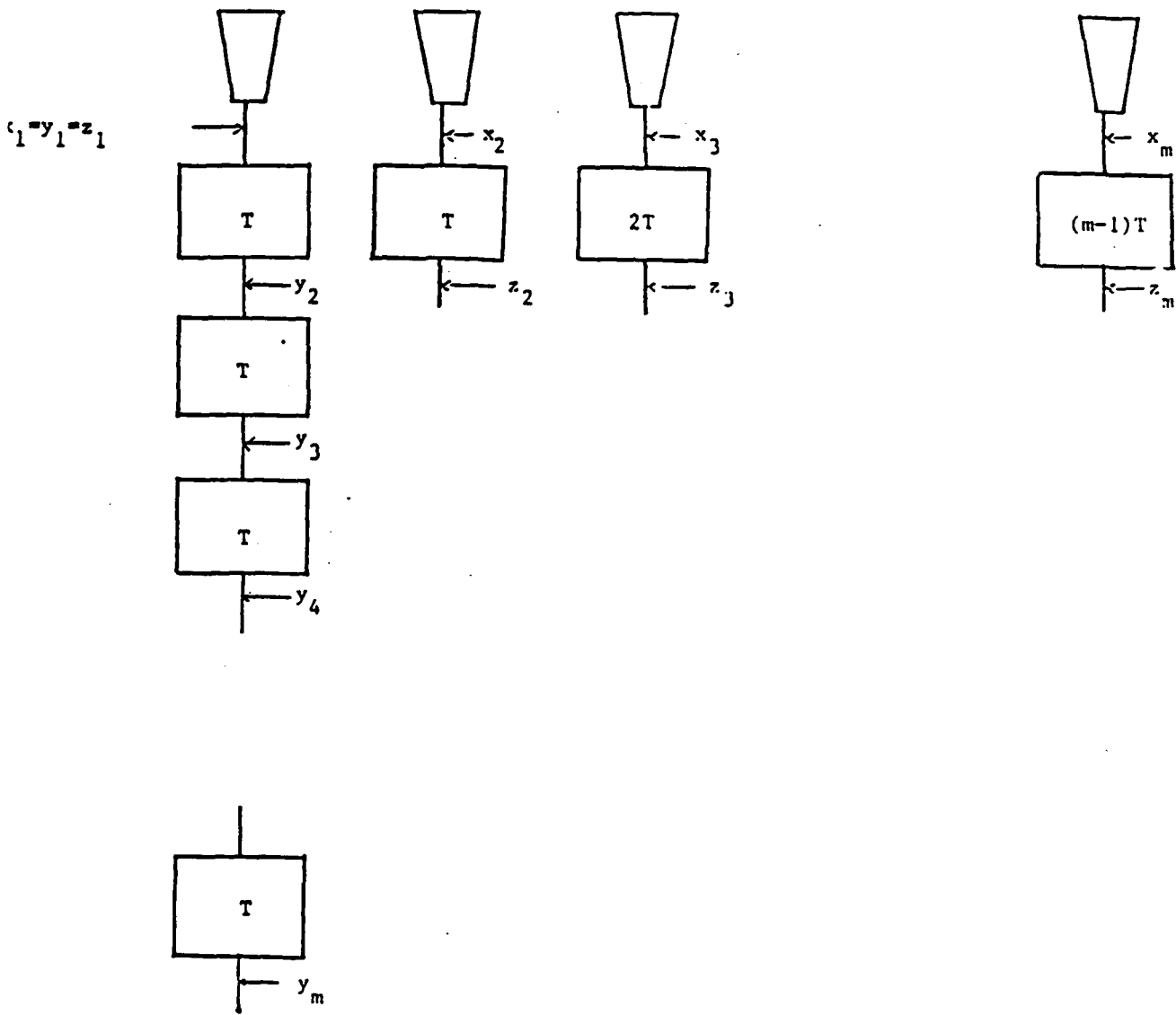


Fig. 4.1 Wideband Array Configuration.

where

$$\gamma_{lk} = -p_{lk}T. \quad (4.1-8)$$

The signal at the output of the delay connected to the i -th sensor can be expressed as

$$z_i = x_i(t - (i-1)T) = \sum_{k=1}^d \sum_{l=1}^M c_{lk} e^{(i-1)(\phi_{lk} + \gamma_{lk})} + n_i(t - (i-1)T); i=2, \dots, m. \quad (4.1-9)$$

Let

$$\psi_{ij} = (\phi_{ij} + \gamma_{ij}) \quad (4.1-10)$$

and

$$M = \sum_{k=1}^d M(k). \quad (4.1-11)$$

At this point we assume that all sources have distinct natural frequencies. This condition is relaxed later on. With the knowledge of the parameter M , we form $(m-L+1)$ vectors \underline{X}_n , $(m-L+1)$ vectors \underline{Y}_n and $(m-L+1)$ vectors \underline{Z}_n of length L where

$$M \leq L \leq (m-M)$$

and

$$\underline{X}_n = [x_n, x_{n+1}, \dots, x_{n+L-1}]^T, \quad n=1, 2, \dots, (m-L+1)$$

$$\underline{Y}_n = [y_n, y_{n+1}, \dots, y_{n+L-1}]^T, \quad n=1, 2, \dots, (m-L+1)$$

$$\underline{Z}_n = [z_n, z_{n+1}, \dots, z_{n+L-1}]^T, \quad n=1, 2, \dots, (m-L+1).$$

It can be shown that \underline{X}_n , \underline{Y}_n and \underline{Z}_n can be decomposed into

$$\underline{X}_n = A1\phi^{(n-1)} \underline{C} + \underline{NX}_n, \quad (4.1-12)$$

$$\underline{Y}_n = A2\Gamma^{(n-1)} \underline{C} + \underline{NY}_n, \quad (4.1-13)$$

$$\underline{Z}_n = A3\Psi^{(n-1)} \underline{C} + \underline{NZ}_n, \quad (4.1-14)$$

where $A1, A2, A3, \phi, \Gamma, \Psi, \underline{C}, \underline{NX}_n, \underline{NY}_n, \underline{NZ}_n$ are given by

$$A1 = [\underline{A1}_{1,1} \quad \underline{A1}_{2,1} \quad \dots \quad \underline{A1}_{M(d),d}],$$

$$\begin{aligned}
A_2 &= [\underline{A}_{21,1} \ \underline{A}_{22,1} \ \dots \ \underline{A}_{2M(d),d}], \\
A_3 &= [\underline{A}_{31,1} \ \underline{A}_{32,1} \ \dots \ \underline{A}_{3M(d),d}], \\
\underline{A}_{1i,j} &= [1 \ e^{\phi_{ij}} \ \dots \ e^{(L-1)\phi_{ij}}]^T, \\
\underline{A}_{2i,j} &= [1 \ e^{\gamma_{ij}} \ \dots \ e^{(L-1)\gamma_{ij}}]^T, \\
\underline{A}_{3i,j} &= [1 \ e^{\psi_{ij}} \ \dots \ e^{(L-1)\psi_{ij}}]^T, \\
\Phi &= \text{diag}\{ e^{\phi_{11}} \ \dots \ e^{\phi_{M(d)d}} \}, \\
\Gamma &= \text{diag}\{ e^{\gamma_{11}} \ \dots \ e^{\gamma_{M(d)d}} \}, \\
\Psi &= \text{diag}\{ e^{\psi_{11}} \ \dots \ e^{\psi_{M(d)d}} \}, \\
\underline{C} &= [c_{11}, c_{21}, \dots, c_{M(d)d}]^T, \\
\underline{N}_n &= [nx_n, nx_{n+1}, \dots, nx_{n+L-1}], \\
\underline{N}_y &= [ny_n, ny_{n+1}, \dots, ny_{n+L-1}], \\
\underline{N}_z &= [nz_n, nz_{n+1}, \dots, nz_{n+L-1}].
\end{aligned}$$

nx_i , ny_i and nz_i are introduced here for simplicity of notation. Actually, they are given by

$$\begin{aligned}
nx_i &= n_i(t), \\
ny_i &= n_i(t-(i-1)T),
\end{aligned}$$

and

$$nz_i = n_i(t-(i-1)T).$$

Note that $nx_1 = ny_1 = nz_1$. Six matrices M_1 , N_1 , P_1 , Q_1 , R_1 and S_1 are formed where

$$M_1 = \begin{bmatrix} \uparrow & & \uparrow \\ | & & | \\ \underline{X}_1 & \dots & \underline{X}_{(m-L)} \\ | & & | \\ \downarrow & & \downarrow \end{bmatrix}; \quad N_1 = \begin{bmatrix} \uparrow & & \uparrow \\ | & & | \\ \underline{X}_2 & \dots & \underline{X}_{(m-L+1)} \\ | & & | \\ \downarrow & & \downarrow \end{bmatrix}$$

$$P_1 = \begin{bmatrix} \uparrow & & \uparrow \\ \underline{Y}_1 & \dots & \underline{Y}_{(m-L)} \\ \downarrow & & \downarrow \end{bmatrix}; \quad Q_1 = \begin{bmatrix} \uparrow & & \uparrow \\ \underline{Y}_2 & \dots & \underline{Y}_{(m-L+1)} \\ \downarrow & & \downarrow \end{bmatrix}$$

$$R_1 = \begin{bmatrix} \uparrow & & \uparrow \\ \underline{Z}_1 & \dots & \underline{Z}_{(m-L)} \\ \downarrow & & \downarrow \end{bmatrix}; \quad S_1 = \begin{bmatrix} \uparrow & & \uparrow \\ \underline{Z}_2 & \dots & \underline{Z}_{(m-L+1)} \\ \downarrow & & \downarrow \end{bmatrix}.$$

M_1 can be rewritten as

$$M_1 = \begin{bmatrix} \uparrow & \uparrow & & \uparrow \\ \underline{A1C} & \underline{A1\phi C} & \dots & \underline{A1\phi^{(m-L-1)} C} \\ \downarrow & \downarrow & & \downarrow \end{bmatrix} + \begin{bmatrix} \uparrow & \uparrow & & \uparrow \\ \underline{NX}_1 & \underline{NX}_2 & \dots & \underline{NX}_{(m-L)} \\ \downarrow & \downarrow & & \downarrow \end{bmatrix},$$

$$M_1 = A1 [\underline{C} \ \underline{\phi C} \ \dots \ \underline{\phi^{(m-L-1)} C}] + [\underline{NX}_1 \ \underline{NX}_2 \ \dots \ \underline{NX}_{(m-L)}].$$

Similarly, it can be shown that

$$N_1 = A1\phi [\underline{C} \ \underline{\phi C} \ \dots \ \underline{\phi^{(m-L-1)} C}] + [\underline{NX}_2 \ \underline{NX}_3 \ \dots \ \underline{NX}_{(m-L+1)}],$$

$$P_1 = A2 [\underline{C} \ \underline{\Gamma C} \ \dots \ \underline{\Gamma^{(m-L-1)} C}] + [\underline{NY}_1 \ \underline{NY}_2 \ \dots \ \underline{NY}_{(m-L)}],$$

$$Q_1 = A2\Gamma [\underline{C} \ \underline{\Gamma C} \ \dots \ \underline{\Gamma^{(m-L-1)} C}] + [\underline{NY}_2 \ \underline{NY}_3 \ \dots \ \underline{NY}_{(m-L+1)}],$$

$$R_1 = A3 [\underline{C} \ \underline{\Psi C} \ \dots \ \underline{\Psi^{(m-L-1)} C}] + [\underline{NZ}_1 \ \underline{NZ}_2 \ \dots \ \underline{NZ}_{(m-L)}],$$

$$S_1 = A3\Psi [\underline{C} \ \underline{\Psi C} \ \dots \ \underline{\Psi^{(m-L-1)} C}] + [\underline{NZ}_2 \ \underline{NZ}_3 \ \dots \ \underline{NZ}_{(m-L+1)}].$$

These matrices have the following decompositions

$$M_1 = A1 C U1 + N1' \quad \text{and} \quad N_1 = A1 C \phi U1 + N1'' \quad , \quad (4.1-15)$$

$$P_1 = A2 C U2 + N2' \quad \text{and} \quad Q_1 = A2 C \Gamma U2 + N2'' \quad , \quad (4.1-16)$$

$$R_1 = A3 C U3 + N3' \quad \text{and} \quad S_1 = A3 C \Psi U3 + N3'' \quad (4.1-17)$$

where $U1, U2, U3, C, N1', N2', N3', N1'', N2''$ and $N3''$ are given by

$$U1^T = [\underline{U1}_{1,1} \ \underline{U1}_{2,1} \ \dots \ \underline{U1}_{M(d),d}],$$

$$\begin{aligned}
U2^T &= [\underline{U2}_{1,1} \ \underline{U2}_{2,1} \ \dots \ \underline{U2}_{M(d),d}], \\
U3^T &= [\underline{U3}_{1,1} \ \underline{U3}_{2,1} \ \dots \ \underline{U3}_{M(d),d}], \\
\underline{U1}_{i,j} &= [1 \ e^{\phi_{ij}} \ \dots \ e^{(m-L-1)\phi_{ij}}]^T, \\
\underline{U2}_{i,j} &= [1 \ e^{\gamma_{ij}} \ \dots \ e^{(m-L-1)\gamma_{ij}}]^T, \\
\underline{U3}_{i,j} &= [1 \ e^{\psi_{ij}} \ \dots \ e^{(m-L-1)\psi_{ij}}]^T, \\
C &= \text{diag} [c_{11}, c_{21}, \dots, c_{M(d)d}], \\
N1' &= [\underline{NX}_1 \ \underline{NX}_2 \ \dots \ \underline{NX}_{(m-L)}], \\
N2' &= [\underline{NY}_1 \ \underline{NY}_2 \ \dots \ \underline{NY}_{(m-L)}], \\
N3' &= [\underline{NZ}_1 \ \underline{NZ}_2 \ \dots \ \underline{NZ}_{(m-L)}], \\
N1'' &= [\underline{NX}_2 \ \underline{NX}_3 \ \dots \ \underline{NX}_{(m-L+1)}], \\
N2'' &= [\underline{NY}_2 \ \underline{NY}_3 \ \dots \ \underline{NY}_{(m-L+1)}], \\
N3'' &= [\underline{NZ}_2 \ \underline{NZ}_3 \ \dots \ \underline{NZ}_{(m-L+1)}].
\end{aligned}$$

Assuming the signals and noise to be statistically independent and that the noise components are uncorrelated from sensor to sensor, we get

$$\begin{aligned}
E[M_1^H M_1] &= U1^H V1 U1 + L \sigma^2 I_{(m-L)}, \\
E[N_1^H M_1] &= U1^H \phi^H V1 U1 + L \sigma^2 I_{1(m-L)}, \\
E[P_1^H P_1] &= U2^H V2 U2 + L \sigma^2 I_{(m-L)}, \\
E[P_1^H Q_1] &= U2^H \Gamma^H V2 U2 + L \sigma^2 I_{1(m-L)}, \\
E[R_1^H R_1] &= U3^H V3 U3 + L \sigma^2 I_{(m-L)}, \\
E[S_1^H R_1] &= U3^H \psi^H V3 U3 + L \sigma^2 I_{1(m-L)},
\end{aligned}$$

where $I_{(m-L)}$ is the $(m-L) \times (m-L)$ identity matrix and $I_{1(m-L)}$, $V1$, $V2$ and $V3$ are the matrices

$$I_{1(m-L)} = \begin{bmatrix} 0 & 1 & 0 & 0 & \dots & \dots & 0 \\ 0 & 0 & 1 & 0 & \dots & \dots & c \\ 0 & 0 & 0 & 1 & \dots & \dots & 0 \\ \dots & \dots & \dots & \dots & \dots & \dots & \dots \\ \dots & \dots & \dots & \dots & \dots & \dots & \dots \\ \dots & \dots & \dots & \dots & \dots & \dots & \dots \\ 0 & 0 & 0 & 0 & \dots & \dots & 1 \\ 0 & 0 & 0 & 0 & \dots & \dots & 0 \end{bmatrix},$$

$$V1 = E[C^H A_1^H A_1 C],$$

$$V2 = E[C^H A_2^H A_2 C],$$

$$V3 = E[C^H A_3^H A_3 C].$$

Now, let M, N, P, Q, R and S be the matrices

$$M = E[M_1^H M_1] - L\sigma^2 I_{(m-L)} = U1^H V1 U1, \quad (4.1-18)$$

$$N = E[N_1^H M_1] - L\sigma^2 I_{1(m-L)} = U1^H \Phi^H V1 U1, \quad (4.1-19)$$

$$P = E[P_1^H P_1] - L\sigma^2 I_{(m-L)} = U2^H V2 U2, \quad (4.1-20)$$

$$Q = E[Q_1^H P_1] - L\sigma^2 I_{1(m-L)} = U2^H \Gamma^H V2 U2, \quad (4.1-21)$$

$$R = E[R_1^H R_1] - L\sigma^2 I_{(m-L)} = U3^H V3 U3, \quad (4.1-22)$$

$$S = E[S_1^H R_1] - L\sigma^2 I_{1(m-L)} = U3^H \Psi^H V3 U3. \quad (4.1-23)$$

Consider the following three pencil matrices $(M - \lambda N)$, $(P - \eta Q)$ and $(R - \nu S)$.

Note that

$$(M - \lambda N) = (U1^H V1 U1) - \lambda (U1^H \Phi^H V1 U1) = U1^H (I - \lambda \Phi^H) V1 U1, \quad (4.1-24)$$

$$(P - \eta Q) = (U2^H V2 U2) - \eta (U2^H \Gamma^H V2 U2) = U2^H (I - \eta \Gamma^H) V2 U2, \quad (4.1-25)$$

$$(R - \nu S) = (U3^H V3 U3) - \nu (U3^H \Psi^H V3 U3) = U3^H (I - \nu \Psi^H) V3 U3. \quad (4.1-26)$$

The matrices U1, U2, U3, Φ , Γ , and Ψ are all of rank M as long as all the ϕ_{ij} 's are distinct and $L \geq M$. Defining

$$F_{pq,rs} = \sum_{i=1}^L \exp\{(i-1)(\phi_{pq}^* - \phi_{rs})\},$$

$$G_{pq,rs} = \sum_{i=1}^L \exp\{(i-1)(\gamma_{pq}^* - \gamma_{rs})\},$$

$$H_{pq,rs} = \sum_{i=1}^L \exp\{(i-1)(\psi_{pq}^* - \psi_{rs})\}$$

and

$$C_{pq,rs} = E[c_{pq}^* c_{rs}],$$

the matrices V1, V2 and V3 can be written as

$$\begin{aligned}
V1 &= \begin{bmatrix} C_{11,11} & F_{11,11} & \dots & C_{11,M(d)M(d)} & F_{11,M(d)M(d)} \\ C_{12,11} & F_{12,11} & \dots & C_{12,M(d)M(d)} & F_{12,M(d)M(d)} \\ \vdots & \vdots & \ddots & \vdots & \vdots \\ C_{M(d)M(d),11} & F_{M(d)M(d),11} & \dots & C_{M(d)M(d),M(d)M(d)} & F_{M(d)M(d),M(d)M(d)} \end{bmatrix}, \\
V2 &= \begin{bmatrix} C_{11,11} & G_{11,11} & \dots & C_{11,M(d)M(d)} & G_{11,M(d)M(d)} \\ C_{12,11} & G_{12,11} & \dots & C_{12,M(d)M(d)} & G_{12,M(d)M(d)} \\ \vdots & \vdots & \ddots & \vdots & \vdots \\ C_{M(d)M(d),11} & G_{M(d)M(d),11} & \dots & C_{M(d)M(d),M(d)M(d)} & G_{M(d)M(d),M(d)M(d)} \end{bmatrix}, \\
V3 &= \begin{bmatrix} C_{11,11} & H_{11,11} & \dots & C_{11,M(d)M(d)} & H_{11,M(d)M(d)} \\ C_{12,11} & H_{12,11} & \dots & C_{12,M(d)M(d)} & H_{12,M(d)M(d)} \\ \vdots & \vdots & \ddots & \vdots & \vdots \\ C_{M(d)M(d),11} & H_{M(d)M(d),11} & \dots & C_{M(d)M(d),M(d)M(d)} & H_{M(d)M(d),M(d)M(d)} \end{bmatrix}.
\end{aligned}$$

It is easy to see that the matrices V1, V2 and V3 are of rank M even in the presence of fully correlated sources. The rank of the pencil $(M-\lambda N)$ is decreased by 1 whenever

$$\begin{aligned}
\lambda_{ij} &= \exp\{-\phi_{ij}^*\} = \exp\{p_{ij}^*(\Delta/c)\sin(\theta_j)\}, & (4.1-27) \\
& \text{for } i=1, 2, \dots, M^{(k)}, \\
& \quad j,k=1, 2, \dots, d.
\end{aligned}$$

The rank of the pencil $(P-\eta Q)$ is decreased by 1 whenever

$$\begin{aligned}
\eta_{ij} &= \exp\{-\gamma_{ij}^*\} = \exp\{p_{ij}^*T\}, & (4.1-28) \\
& \text{for } i=1, 2, \dots, M^{(k)}, \\
& \quad j,k=1, 2, \dots, d.
\end{aligned}$$

The rank of the pencil $(R-\nu S)$ is decreased by 1 whenever

$$\begin{aligned}
\nu_{ij} &= \exp\{-\psi_{ij}^*\} = \exp\{p_{ij}^*(\Delta/c)\sin(\theta_j)\} \exp\{p_{ij}^*T\}, & (4.1-29) \\
& \text{for } i=1, 2, \dots, M^{(k)}, \\
& \quad j,k=1, 2, \dots, d.
\end{aligned}$$

Note that the first set of generalized eigenvalues gives us a set of coupled values of natural frequencies and angles of arrival. The second set

solves for the natural frequencies. With these two sets one might think that the problem is solved. However, there is some ambiguity in choosing which natural frequency goes with which angle of arrival. The third set solves this ambiguity since we can see that the set of these generalized eigenvalues is the product of the first and the second ;i.e;

$$v_{ij} = \lambda_{ij} \cdot \eta_{ij}. \quad (4.1-30)$$

Therefore, the ambiguity is removed by constructing a table of all the products of λ_{ij} and η_{nk} . These products are then compared with the values v_{rs} . Once a product is matched, that natural frequency is used to determine the angle of arrival of the source. In practice, due to numerical round off errors, a range of uncertainty remains since the products and the rank reducing values of the third set do not match exactly.

In the above algorithm, note that knowledge of the number of natural frequencies is important. If sources have common natural frequencies, then these frequencies would be counted only once. This means that the total number of distinct natural frequencies M should be replaced by a suitably reduced number.

4.1.1 COMPUTER SIMULATION

In this simulation, a linear uniformly spaced array consisting of 12 sensors was used. Two sources were assumed to be present and located at angles $\theta_1=16^\circ$ and $\theta_2=24^\circ$. Two cases were studied.

Case 1.		
Source	Angle of arrival	Natural frequencies
1	16°	0.25-j0.90 ; 0.25+j0.90
2	24°	0.12-j0.79 ; 0.12+j0.79

Case 2.		
Source	Angle of arrival	Natural frequencies
1	16°	0.25-j0.90 ; 0.25+j0.90
2	24°	0.25-j0.90 ; 0.25+j0.90

The sensor spacing was selected such that $\Delta/c=\pi/0.90$. The coefficients c_{1k} were assumed to be independent random variables. The additive noise was generated as white Gaussian with zero mean and unit variance. 100 snapshots were considered in each of the 50 runs simulated. The results of the angle estimates are shown in figures 4.3 to 4.8. It is clear from these figures that the estimates obtained from the second case (assuming 2 common poles) are much better than case (1). This is mainly due to the fact that the natural frequencies estimates are less biased in this case. The length of the window is smaller which results in a better noise reduction through the singular value decomposition (SVD). Tables 4.1 to 4.6 give the poles estimates with their variances. It is apparent here that due to the fact that fewer poles had to be estimated in the first case, the estimation procedure achieved a better performance than in the second case.

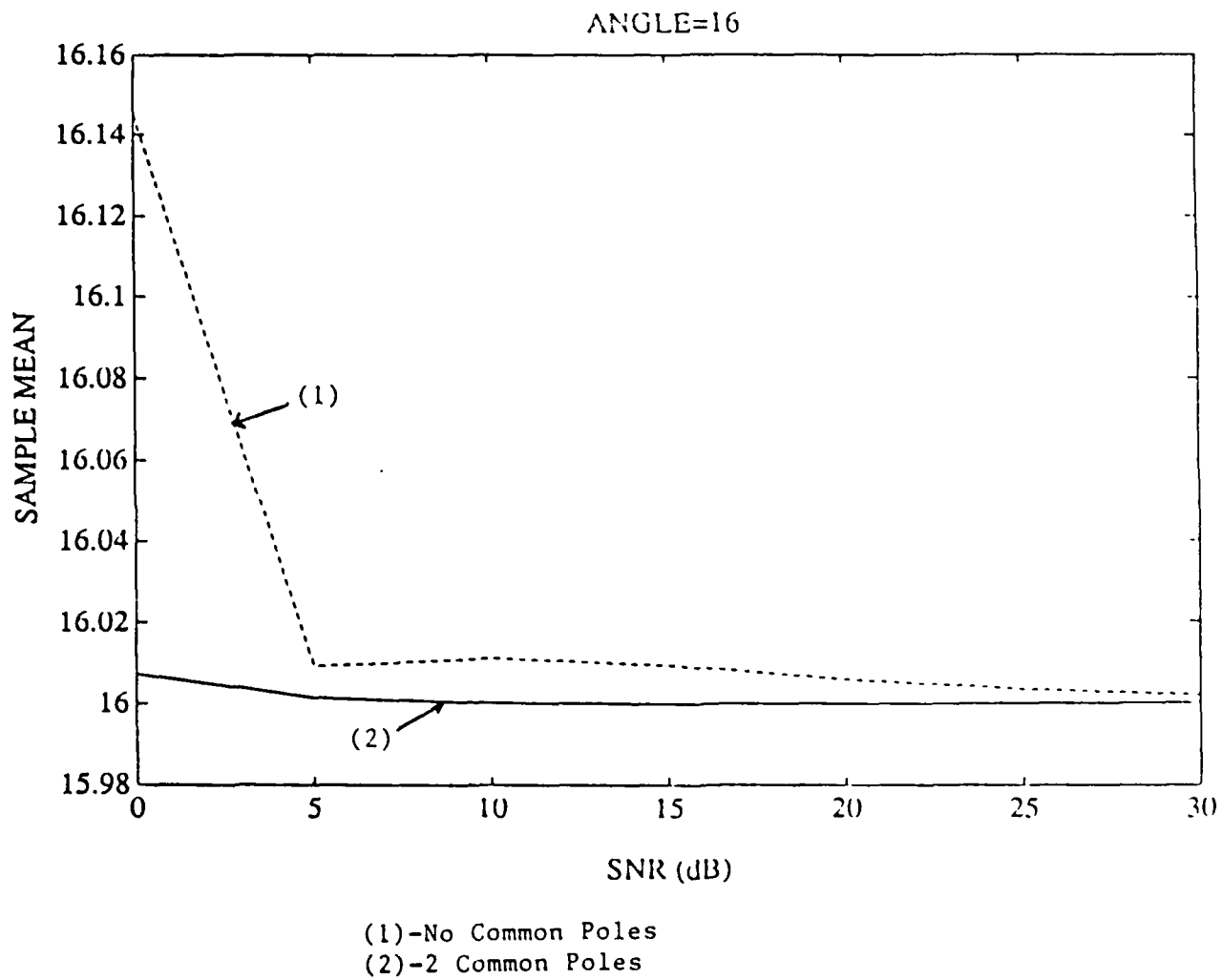


Fig. 4.3. Sample Mean of Angle at 16°
Transient Signals.

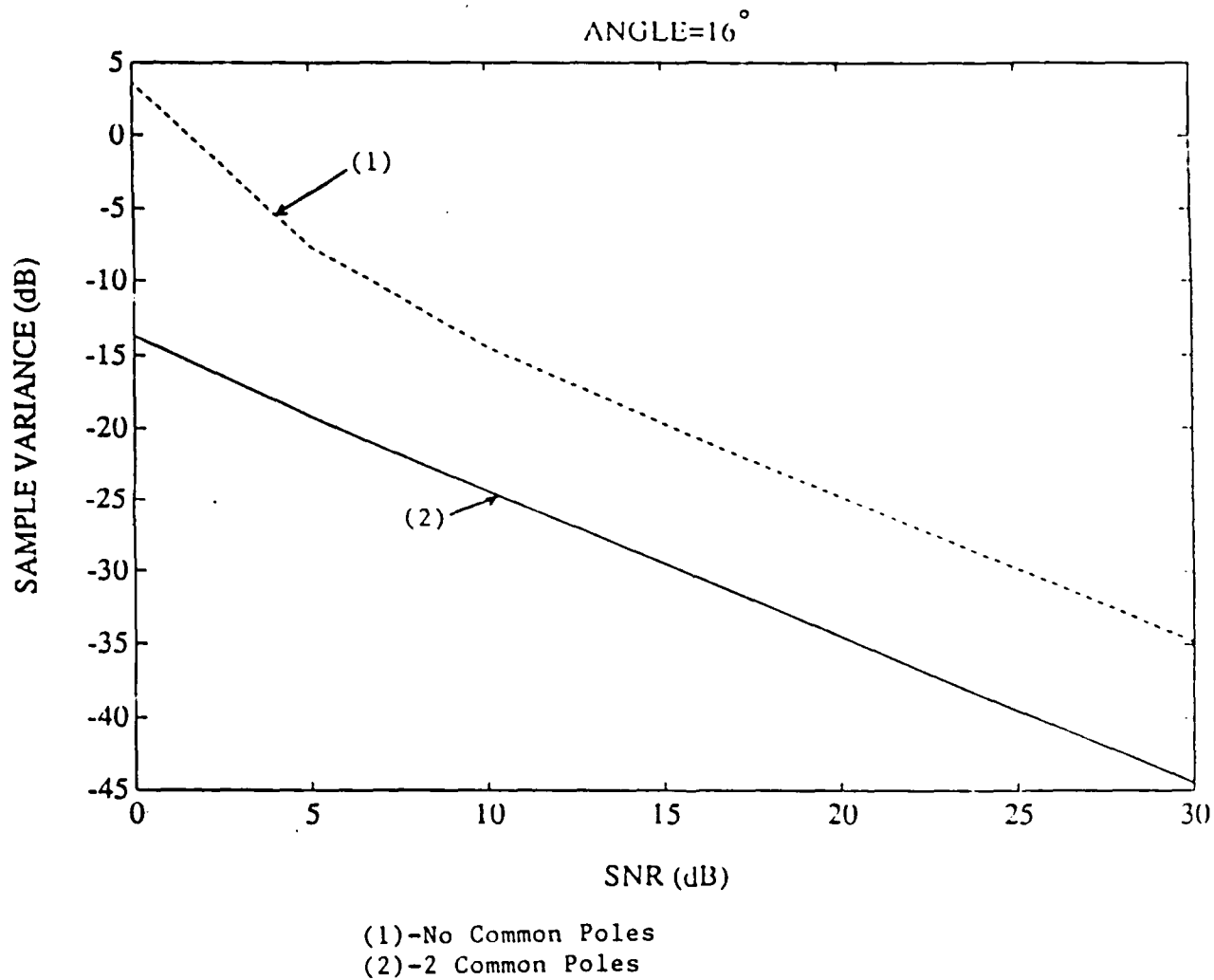


Fig. 4.4. Sample Variance of Angle at 16° Transient Signals.

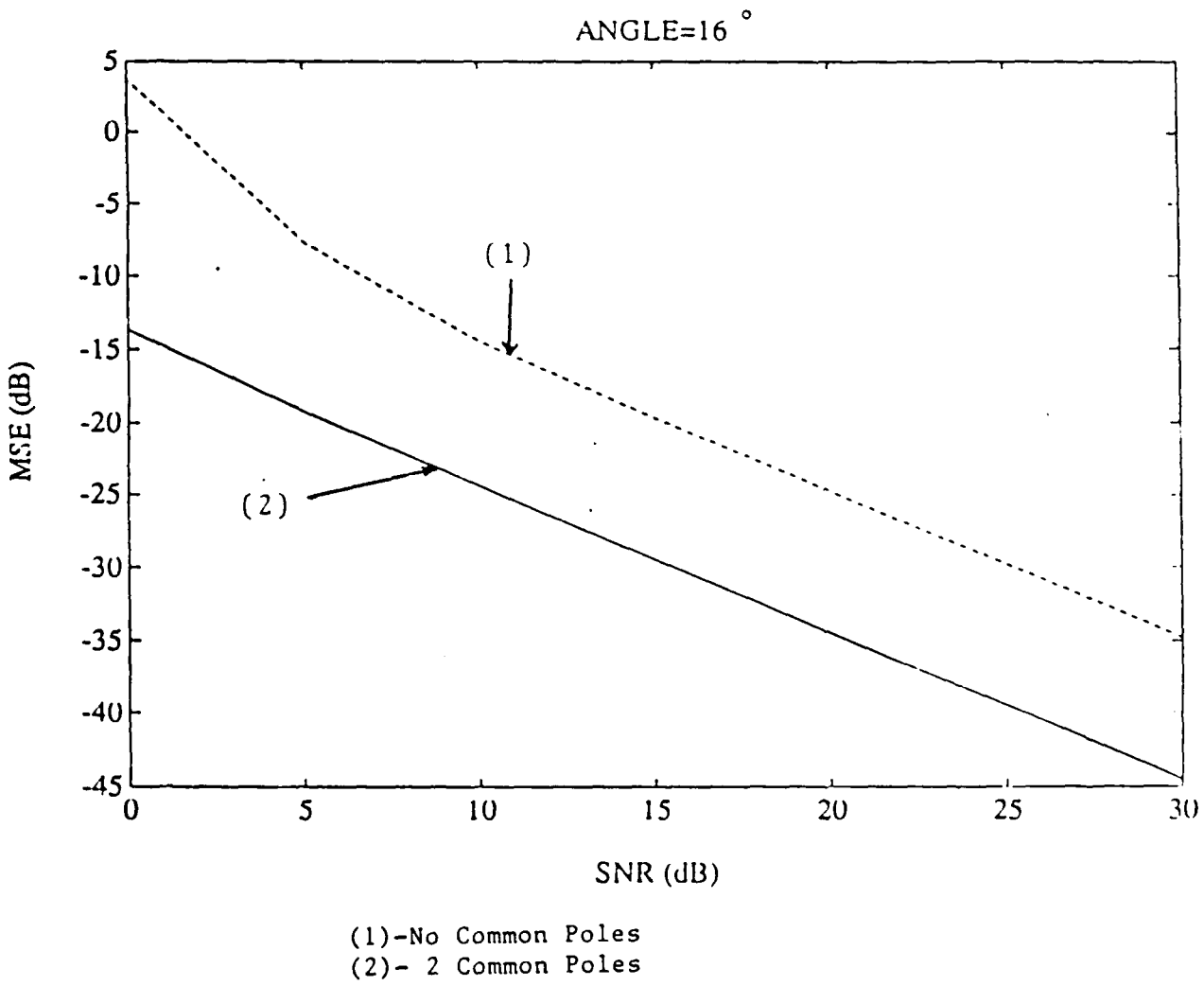


Fig. 4.5. Mean-Squared Error of Angle at 16°
Transient Signals.

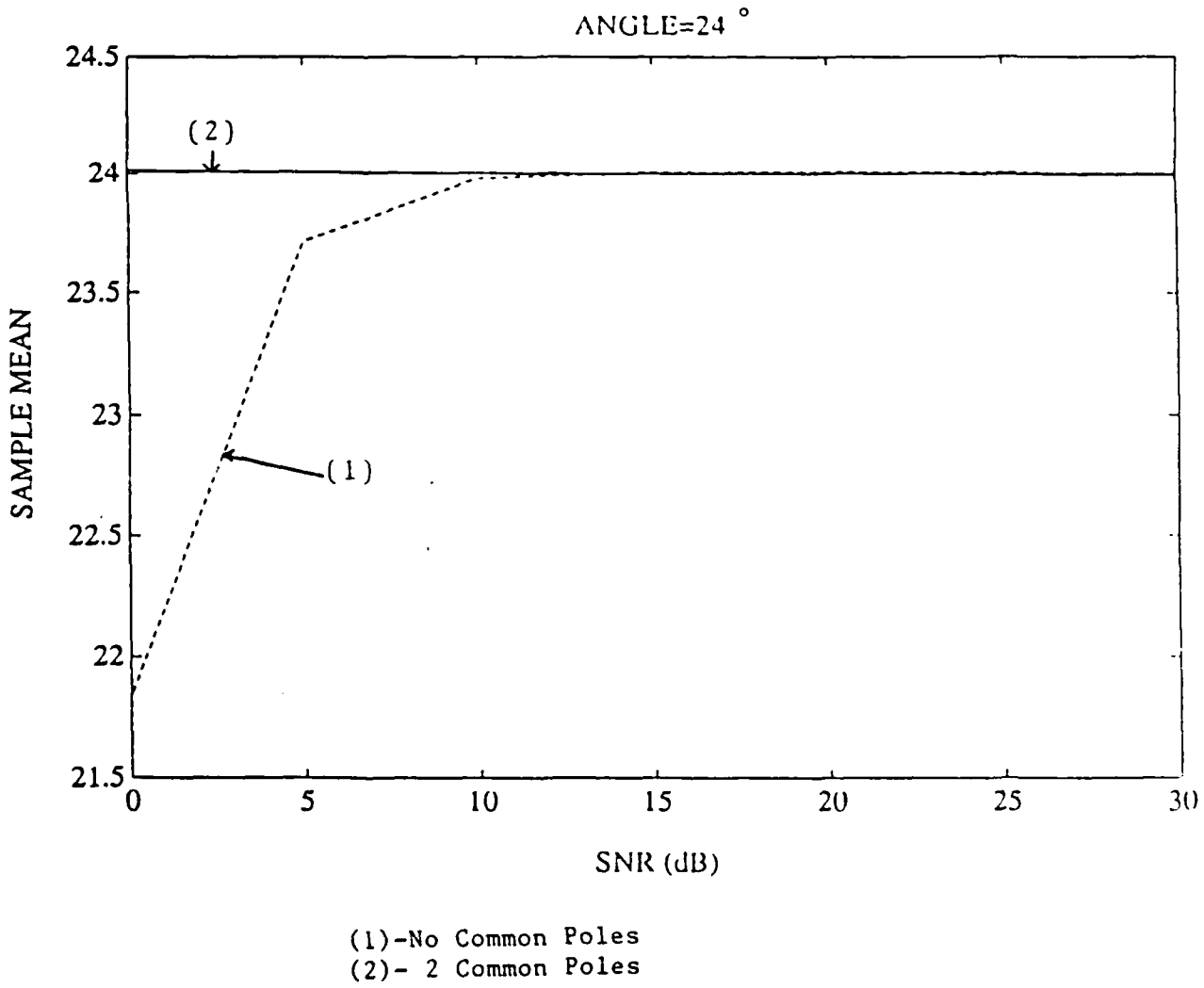


Fig. 4.6. Sample Mean of Angle at 24° Transient Signals.

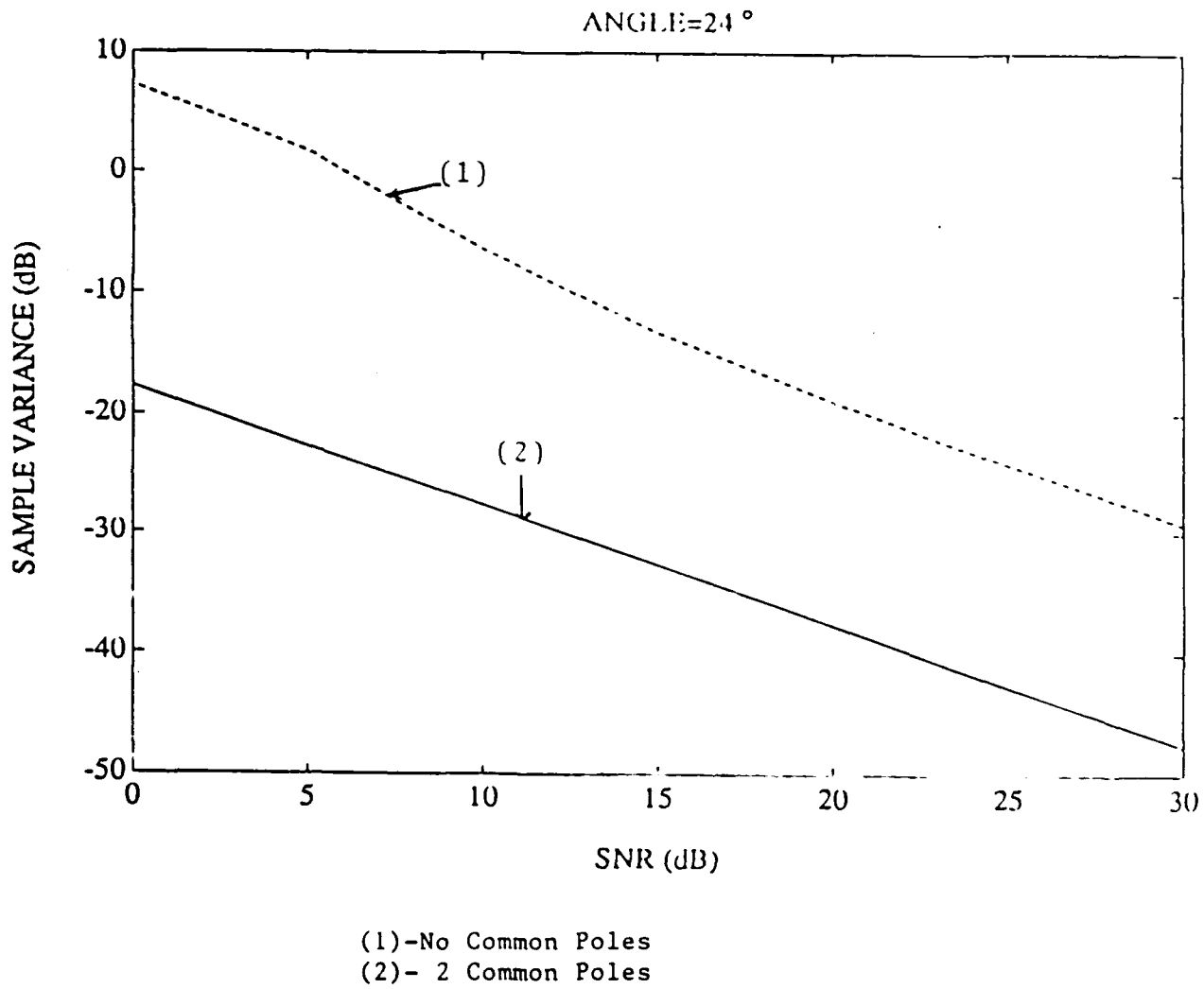
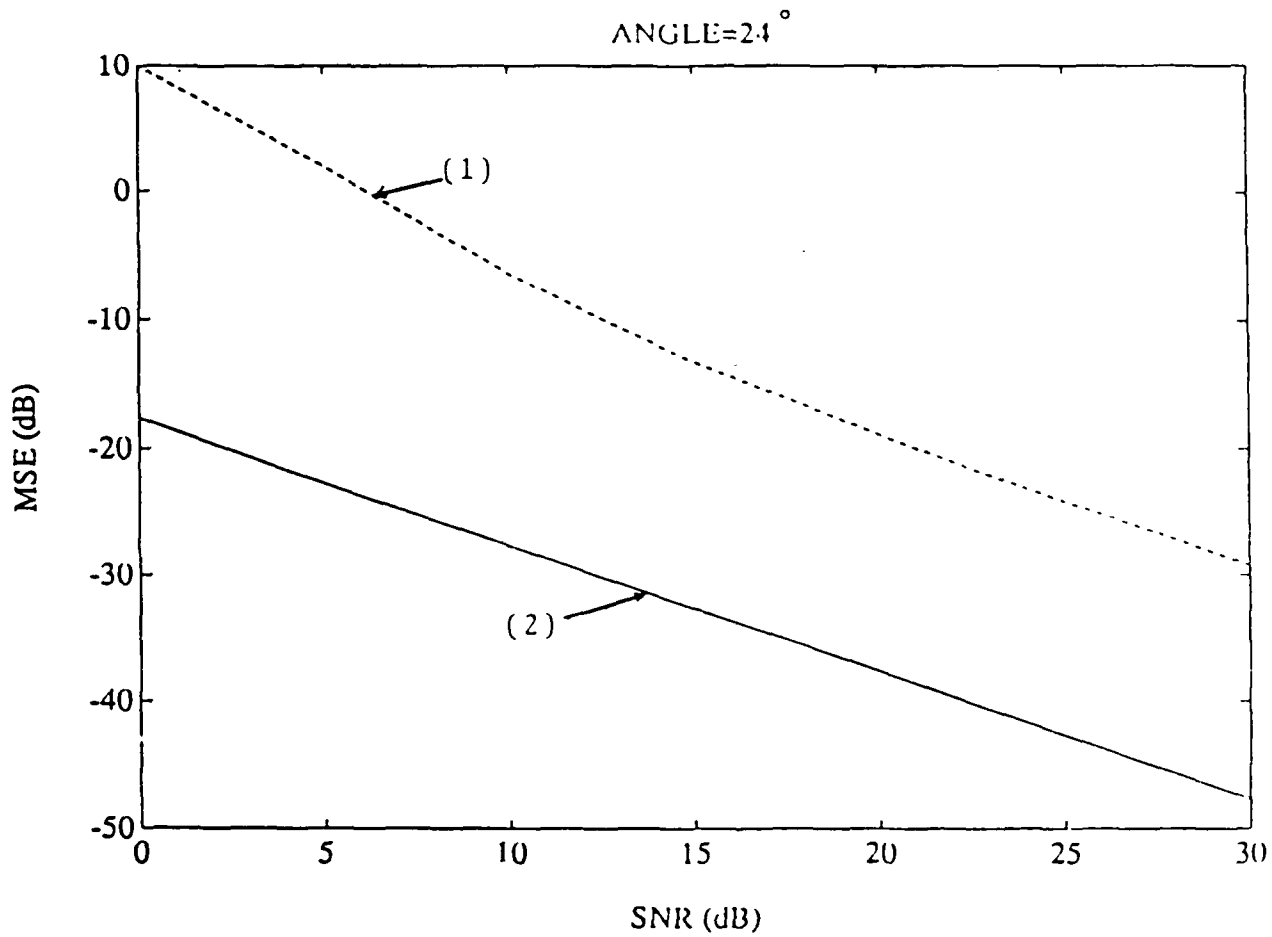


Fig. 4.7. Sample Variance of Angle at 24° Transient Signals.



(1)-No Common Poles
 (2)- 2 Common Poles

Fig. 4.8. Mean-Squared Error of Angle at 24° Transient Signals.

SNR (dB)	Sample Mean	Sample Variance
30	0.2500616-j0.9001127	7.8816270e-4
25	0.2501127-j0.9002026	1.4029399e-3
20	0.2502106-j0.9003684	2.5036666e-3
15	0.2504140-j0.9006952	4.5110551e-3
10	0.2509581-j0.9014653	1.9616835e-2
5	0.2519363-j0.9021969	1.9616835e-2
0	0.2310321-j0.9690142	0.1542990

Table 4.1
Sample Mean and Variance of the pole $p_{11}=0.25-j0.90$.
(No Common poles)

SNR (dB)	Sample Mean	Sample Variance
30	0.2499895+j0.8999775	8.9807872e-4
25	0.2499841+j0.8999586	1.6006386e-3
20	0.2499823+j0.8999237	2.6825261e-3
15	0.2500210+j0.8998682	5.1696543e-3
10	0.2503774+j0.8998694	9.6555240e-3
5	0.2538730+j0.9004380	2.2066321e-2
0	0.2310484+j0.9300936	9.0392388e-2

Table 4.2
Sample Mean and Variance of the pole $p_{12}=0.25+j0.90$.
(No Common poles)

SNR (dB)	Sample Mean	Sample Variance
30	0.1198686-j0.7899920	1.9208038e-4
25	0.1197963-j0.7900143	3.4073265e-3
20	0.1197361-j0.7901177	6.0717780e-3
15	0.1198721-j0.7905209	1.1008599e-3
10	0.1211890-j0.7921247	2.1280421e-2
5	0.1356790-j0.8039448	4.8372950e-2
0	0.2179931-j0.8058360	0.1220230

Table 4.3
Sample Mean and Variance of the pole $p_{11}=0.12-j0.79$.
(No Common poles)

SNR (dB)	Sample Mean	Sample Variance
30	0.1198654+j0.7897864	1.6900700e-3
25	0.1197749+j0.7896364	3.0200828e-3
20	0.1196503+j0.7894068	5.4612877e-3
15	0.1195874+j0.7891387	1.0212054e-2
10	0.1204553+j0.7893061	2.0683207e-2
5	0.1317147+j0.7937539	5.0145626e-2
0	0.2189744+j0.8155535	0.1081801

Table 4.4
Sample Mean and Variance of the pole $p_{11}=0.12-j0.79$.
(No Common poles)

SNR (dB)	Sample Mean	Sample Variance
30	0.2500181-j0.8999961	1.5507222e-4
25	0.2500326-j0.8999931	2.7576982e-4
20	0.2500592-j0.8999881	4.9048965e-4
15	0.2501090-j0.8999797	8.7285927e-4
10	0.2502059-j0.8999674	1.5552028e-3
5	0.2504041-j0.8999538	2.7789618e-3
0	0.2508400-j0.8999541	4.9983687e-3

Table 4.5
Sample Mean and Variance of the pole $p_{11}=0.25-j0.90$.
(2 Common poles)

SNR (dB)	Sample Mean	Sample Variance
30	0.2500219+j0.9000132	1.5080629e-4
25	0.2500393+j0.9000236	2.6813077e-4
20	0.2500712+j0.9000421	4.7654871e-4
15	0.2501304+j0.9000752	8.4674195e-4
10	0.2502445+j0.9002433	1.5038936e-3
5	0.2504744+j0.9002433	2.6707526e-3
0	0.2509713+j0.9004447	4.7491789e-3

Table 4.6
Sample Mean and Variance of the pole $p_{11}=0.25+j0.90$.
(2 Common poles)

4.2 WIDE SENSE STATIONARY SIGNALS

Consider the same configuration as in section 4.1. Let m be the number of wideband sensors in the linear uniformly spaced array and Δ be the sensor spacing. Assume there are d ($d < m$) wideband sources located in the far field so that planar waves arrive at the array. The sources $s_l(k)$ are modeled as the stationary output of a finite dimensional linear system driven by white noise sequences $e_l(k)$; $l=1, 2, \dots, d$, and k is a discrete time index [53,54]. Denote the transfer function of the l -th linear system as $h_l(z)$. Let the spatial array be modeled in terms of the impulse response of each element in the array. The array response to a unit impulse arriving at the array from direction θ will then be represented as the impulse response of this system. The combination for the l -th source can therefore be modeled as a single system, $a_l(z)$, driven by a white noise source sequence (Fig. 4.2). Let $g_i(k, \theta_l)$ be the response of the i -th sensor to a unit impulse coming from direction θ_l . The received signal at the i -th sensor can then be written as

$$x_i(k) = \sum_{l=1}^d g_i(k, \theta_l) * s_l(k) + n_i(k); \quad i=1, 2, \dots, m \quad (4.2-1)$$

$$x_i(k) = \sum_{l=1}^d g_i(k, \theta_l) * h_l(k) * e_l(k) + n_i(k); \quad i=1, 2, \dots, m \quad (4.2-2)$$

where $n_i(k)$ is the additive noise assumed to be uncorrelated with the emitter signals and $*$ denote the operation of convolution. Define $a_i(k, \theta_l)$ as

$$a_i^{(1)}(k, \theta_l) = g_i(k, \theta_l) * h_l(k). \quad (4.2.3)$$

Let $A^{(1)}(z)$ be the z -transform of $a^{(1)}(k)$. Assume this transfer function to be a rational function with the degree of the numerator being less than the degree of the denominator. It can be expressed as

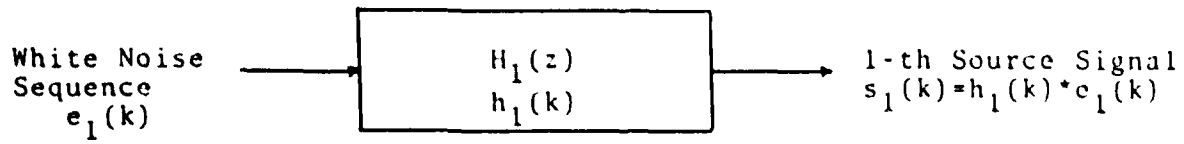


Fig. 4.2a 1-th emitter source



Fig. 4.2b Output of i-th sensor to a source coming from direction θ_1

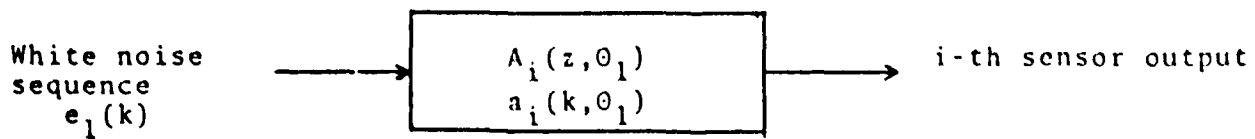


Fig. 4.2c Combination of the two systems.

$$A^{(1)}(z) = \sum_{r=1}^{M^{(1)}} h_{1r} / (1 - p_{1r} z^{-1}) \quad (4.2-4)$$

where p_{1r} is a complex number with magnitude less than 1. Note that these poles do not belong to $h_1(k)$ nor to $g_1(k, \theta_1)$. They are however, a mixture of both. We will loosely refer to them as poles of the sources. Thus, $a^{(1)}(k)$ can be written as

$$a^{(1)}(k) = \sum_{r=1}^{M^{(1)}} h_{1r} (p_{1r})^k. \quad (4.2-5)$$

However, $a_i^{(1)}(k, \theta_1)$ is related to $a^{(1)}(k)$ through

$$a_i^{(1)}(k, \theta_1) = a^{(1)}[k - (i-1)(\Delta/cT_s)\sin(\theta_1)] \quad (4.2-6)$$

where T_s is the sampling period and c is the propagation velocity of the plane waves. Substituting for the expression of $a^{(1)}(k)$, $a_i^{(1)}(k, \theta_1)$ can then be written as

$$a_i^{(1)}(k, \theta_1) = \sum_{r=1}^{M^{(1)}} h_{1r} (p_{1r})^k (p_{1r})^{-(i-1)(\Delta/cT_s)\sin(\theta_1)}. \quad (4.2-7)$$

Let ϕ_{1r} be

$$\phi_{1r} = (p_{1r})^{-(\Delta/cT_s)\sin(\theta_1)}. \quad (4.2-8)$$

$a_i(k, \theta_1)$ can then be rewritten as

$$a_i(k, \theta_1) = \sum_{r=1}^{M^{(1)}} h_{1r} (p_{1r})^k (\phi_{1r})^{(i-1)}. \quad (4.2-9)$$

Assuming an N point sequence, the received signal at the i -th sensor can be expressed as

$$x_i(k) = \sum_{l=1}^d \sum_{r=1}^{M(l)} h_{lr} (\phi_{lr})^{(i-1)} (p_{lr})^k * e_l(k) + n_i(k) \quad (4.2-10)$$

$i=1, 2, \dots, m$
 $k=0, 1, \dots, (N-1)$

Let $X_i(n)$ be the discrete Fourier transform of $x_i(k)$. This is given as

$$X_i(n) = \sum_{k=0}^{N-1} x_i(k) e^{-j(2\pi/N)nk} \quad (4.2-11)$$

$$X_i(n) = \sum_{k=0}^{N-1} \left\{ \sum_{l=1}^d \sum_{r=1}^{M(l)} h_{lr} (\phi_{lr})^{(i-1)} (p_{lr})^k * e_l(k) \right\} e^{-j(2\pi/N)nk} + \sum_{k=0}^{N-1} n_i(k) e^{-j(2\pi/N)nk} \quad (4.2-12)$$

$i=1, 2, \dots, m$
 $n=0, 1, \dots, (N-1)$

Let $\text{DFT}\{.\}$ denote the discrete Fourier transform operator. Then, by definition,

$$H_{lr}(n) = h_{lr} \sum_{k=0}^{N-1} (p_{lr})^k e^{-j(2\pi/N)nk} = h_{lr} \text{DFT}\{(p_{lr})^k\},$$

$$S_l(n) = \text{DFT}\{e_l(k)\},$$

$$N_i(n) = \text{DFT}\{n_i(k)\}.$$

It follows that

$$X_i(n) = \sum_{l=1}^d \sum_{r=1}^{M(l)} H_{lr}(n) (\phi_{lr})^{(i-1)} S_l(n) + N_i(n) \quad (4.2-13)$$

$i=1, 2, \dots, m$
 $n=0, 1, \dots, (N-1).$

Given this set of data, the objective is to solve for the angles of arrival of the sources. It can be shown that the rank reducing values of the matrix

pencil generated from this data are functions of both the angles of arrival and the poles of the sources. However, the poles of the sources are assumed to be unknown at the receiver. Thus, these poles have first to be estimated and then be used to solve for the angles of arrival. That is the reason why the same configuration as in section 4.1 can be used to solve this problem. Therefore, the first sensor is followed by an equally spaced tapped delay line consisting of m taps with successive delays of T seconds. In addition the received signal at the i -th sensor is delayed by an amount of $(i-1)T$; $i=2, 3, \dots, m$ (Fig. 4.1). The signal at the output of the h -th delay following the first sensor is

$$y_h(k) = x_1(k - (h-1)T) \\ = \sum_{l=1}^d \sum_{r=1}^{M(l)} h_{lr} (p_{lr})^k (p_{lr})^{-(h-1)T} * e_1(k - (h-1)T) + n_1(k - (h-1)T) \quad (4.2-14)$$

$$= \sum_{l=1}^d \sum_{r=1}^{M(l)} h_{lr} (p_{lr})^k (\gamma_{lr})^{(h-1)} * e_1(k - (h-1)T) + n_1(k - (h-1)T) \quad (4.2-15)$$

where

$$\gamma_{lr} = -p_{lr}^T. \quad (4.2-16)$$

The signal at the output of the delay connected to the i -th sensor can be expressed as

$$z_s(k) = x_s(k - (s-1)T) \\ = \sum_{l=1}^d \sum_{r=1}^{M(k)} h_{lr} (p_{lr})^k (\phi_{lr} \gamma_{lr})^{(s-1)} * e_1(k - (s-1)T) + n_s(k - (s-1)T) \quad (4.2-17)$$

Let

$$\psi_{lr} = (\phi_{lr})(\gamma_{lr}). \quad (4.2-18)$$

It can be shown that the discrete Fourier transforms $Y_h(n)$ and $Z_s(n)$ of

$y_h(k)$ and $z_s(k)$ are respectively

$$Y_h(n) = \sum_{l=1}^d \sum_{r=1}^{M(l)} H_{lr}(n) (\gamma_{lr})^{(h-1)} S_l'(n) + N_h'(n) \quad (4.2-19)$$

$$\begin{aligned} h &= 1, 2, \dots, m \\ n &= 0, 1, \dots, (N-1) \end{aligned}$$

$$Z_s(n) = \sum_{l=1}^d \sum_{r=1}^{M(l)} H_{lr}(n) (\phi_{lr} \gamma_{lr})^{(s-1)} S_l''(n) + N_h''(n) \quad (4.2-20)$$

$$\begin{aligned} s &= 1, 2, \dots, m \\ n &= 0, 1, \dots, (N-1) \end{aligned}$$

Assuming that the sources do not share any common pole, let M be

$$M = \sum_{l=1}^d M(l) \quad (4.2-18)$$

As in section 4.1, given M , we form $(m-L+1)$ vectors \underline{X}_n , $(m-L+1)$ vectors \underline{Y}_n and $(m-L+1)$ vectors \underline{Z}_n of length L where

$$M \leq L \leq (m-M)$$

and

$$\underline{X}_v(n) = [x_v(n), x_{v+1}(n), \dots, x_{v+L-1}(n)]^T, \quad v=1, 2, \dots, (m-L+1)$$

$$\underline{Y}_v(n) = [y_v(n), y_{v+1}(n), \dots, y_{v+L-1}(n)]^T, \quad v=1, 2, \dots, (m-L+1)$$

$$\underline{Z}_v(n) = [z_v(n), z_{v+1}(n), \dots, z_{v+L-1}(n)]^T, \quad v=1, 2, \dots, (m-L+1).$$

It can be shown that \underline{X}_v , \underline{Y}_v and \underline{Z}_v can be decomposed into

$$\underline{X}_v(n) = A_1 H(n) \phi^{(v-1)} \underline{S}(n) + \underline{NX}_v(n), \quad (4.1-19)$$

$$\underline{Y}_v(n) = A_2 H(n) \Gamma^{(v-1)} \underline{S}'(n) + \underline{NY}_v(n), \quad (4.1-20)$$

$$\underline{Z}_v(n) = A_3 H(n) \Psi^{(v-1)} \underline{S}''(n) + \underline{NZ}_v(n), \quad (4.1-21)$$

where $A_1, A_2, A_3, \phi, \Gamma, \Psi, C, \underline{NX}_v, \underline{NY}_v, \underline{NZ}_v$ are given by

$$A_1 = [\underline{A}_{1,1} \quad \underline{A}_{1,2} \quad \dots \quad \underline{A}_{1M(d),d}],$$

$$A_2 = [\underline{A}_{2,1} \quad \underline{A}_{2,2} \quad \dots \quad \underline{A}_{2M(d),d}],$$

$$A_3 = [\underline{A}_{3,1} \quad \underline{A}_{3,2} \quad \dots \quad \underline{A}_{3M(d),d}],$$

$$\begin{aligned}
\underline{A1}_{i,j} &= [1 \ \phi_{ij} \ \dots \ (\phi_{ij})^{L-1}]^T, \\
\underline{A2}_{i,j} &= [1 \ \gamma_{ij} \ \dots \ (\gamma_{ij})^{L-1}]^T, \\
\underline{A3}_{i,j} &= [1 \ \psi_{ij} \ \dots \ (\psi_{ij})^{L-1}]^T, \\
H(n) &= \text{diag}\{ H_{1,1}(n) \ H_{1,2}(n) \ \dots \ H_{d,M}(d) \}, \\
\Phi &= \text{diag}\{ \phi_{11} \ \dots \ \phi_{dM}(d) \}, \\
\Gamma &= \text{diag}\{ \gamma_{11} \ \dots \ \gamma_{dM}(d) \}, \\
\Psi &= \text{diag}\{ \psi_{11} \ \dots \ \psi_{dM}(d) \}, \\
\underline{S}(n) &= [S_1(n) \ \dots \ S_1(n) \ \dots \ S_d(n) \ \dots \ S_d(n)]^T, \\
\underline{S}'(n) &= [S_1'(n) \ \dots \ S_1'(n) \ \dots \ S_d'(n) \ \dots \ S_d'(n)]^T, \\
\underline{S}''(n) &= [S_1''(n) \ \dots \ S_1''(n) \ \dots \ S_d''(n) \ \dots \ S_d''(n)]^T, \\
\underline{NX}_v(n) &= [N_{x_v}(n), N_{x_{v+1}}(n), \dots, N_{x_{v+L-1}}(n)], \\
\underline{NY}_v(n) &= [N_{y_v}(n), N_{y_{v+1}}(n), \dots, N_{y_{v+L-1}}(n)], \\
\underline{NZ}_v(n) &= [N_{z_v}(n), N_{z_{v+1}}(n), \dots, N_{z_{v+L-1}}(n)].
\end{aligned}$$

$N_{x_i}(n)$, $N_{y_i}(n)$ and $N_{z_i}(n)$ are introduced here for simplicity of notation.

They are given by

$$\begin{aligned}
N_{x_i}(n) &= N_i(n), \\
N_{y_i}(n) &= \text{DFT}\{n_1(k-(i-1)T)\},
\end{aligned}$$

and

$$N_{z_i}(n) = \text{DFT}\{n_1(k-(i-1)T)\}.$$

Six matrices M_1 , N_1 , P_1 , Q_1 , R_1 and S_1 are formed where

$$M_1(n) = \begin{bmatrix} \uparrow & & \uparrow \\ | & & | \\ \underline{X}_1(n) \ \dots \ \underline{X}_{(m-L)}(n) & & \\ | & & | \\ \downarrow & & \downarrow \end{bmatrix}; \quad N_1(n) = \begin{bmatrix} \uparrow & & \uparrow \\ | & & | \\ \underline{X}_2(n) \ \dots \ \underline{X}_{(m-L+1)}(n) & & \\ | & & | \\ \downarrow & & \downarrow \end{bmatrix}$$

$$P_1(n) = \begin{bmatrix} \uparrow & & \uparrow \\ \underline{Y}_1(n) & \dots & \underline{Y}_{(m-L)}(n) \\ \downarrow & & \downarrow \end{bmatrix}; \quad Q_1(n) = \begin{bmatrix} \uparrow & & \uparrow \\ \underline{Y}_2(n) & \dots & \underline{Y}_{(m-L+1)}(n) \\ \downarrow & & \downarrow \end{bmatrix}$$

$$R_1(n) = \begin{bmatrix} \uparrow & & \uparrow \\ \underline{Z}_1(n) & \dots & \underline{Z}_{(m-L)}(n) \\ \downarrow & & \downarrow \end{bmatrix}; \quad S_1(n) = \begin{bmatrix} \uparrow & & \uparrow \\ \underline{Z}_2(n) & \dots & \underline{Z}_{(m-L+1)}(n) \\ \downarrow & & \downarrow \end{bmatrix}$$

These matrices have the following decompositions

$$M_1(n) = A_1 H(n) S(n) U_1(n) + N_1'(n); \quad N_1(n) = A_1 H(n) \Phi U_1(n) + N_1''(n), \quad (4.2-22)$$

$$P_1(n) = A_2 H(n) S'(n) U_2(n) + N_2'(n); \quad Q_1(n) = A_2 H(n) \Gamma U_2(n) + N_2''(n), \quad (4.2-23)$$

$$R_1(n) = A_3 H(n) S''(n) U_3(n) + N_3'(n); \quad S_1(n) = A_3 H(n) \Psi U_3(n) + N_3''(n), \quad (4.2-24)$$

where $U_1, U_2, U_3, S(n), S'(n), S''(n), N_1'(n), N_2'(n), N_3'(n), N_1''(n),$

$N_2''(n)$ and $N_3''(n)$ are given by

$$U_1^T = [\underline{U}_{1,1} \quad \underline{U}_{1,2} \quad \dots \quad \underline{U}_{d,M}(d)],$$

$$U_2^T = [\underline{U}_{2,1} \quad \underline{U}_{2,2} \quad \dots \quad \underline{U}_{d,M}(d)],$$

$$U_3^T = [\underline{U}_{3,1} \quad \underline{U}_{3,2} \quad \dots \quad \underline{U}_{d,M}(d)],$$

$$\underline{U}_{1,j} = [1 \quad \phi_{ij} \quad \dots \quad (\phi_{ij})^{(m-L+1)}]^T,$$

$$\underline{U}_{2,j} = [1 \quad \gamma_{ij} \quad \dots \quad (\gamma_{ij})^{(m-L+1)}]^T,$$

$$\underline{U}_{3,j} = [1 \quad \psi_{ij} \quad \dots \quad (\psi_{ij})^{(m-L+1)}]^T,$$

$$S(n) = \text{diag}\{ S_{11}(n) \quad S_{12}(n) \quad \dots \quad S_{dM}(d)(n) \},$$

$$S'(n) = \text{diag}\{ S_{11}'(n) \quad S_{12}'(n) \quad \dots \quad S_{dM}(d)'(n) \},$$

$$S''(n) = \text{diag}\{ S_{11}''(n) \quad S_{12}''(n) \quad \dots \quad S_{dM}(d)''(n) \},$$

$$N_1'(n) = [\underline{N}X_1(n) \quad \underline{N}X_2(n) \quad \dots \quad \underline{N}X_{(m-L)}(n)],$$

$$N_2'(n) = [\underline{N}Y_1(n) \quad \underline{N}Y_2(n) \quad \dots \quad \underline{N}Y_{(m-L)}(n)],$$

$$N_3'(n) = [\underline{N}Z_1(n) \quad \underline{N}Z_2(n) \quad \dots \quad \underline{N}Z_{(m-L)}(n)],$$

$$N_1''(n) = [\underline{N}X_2(n) \quad \underline{N}X_3(n) \quad \dots \quad \underline{N}X_{(m-L+1)}(n)],$$

$$N2^n(n) = [\underline{NY}_2(n) \ \underline{NY}_3(n) \ \dots \ \underline{NY}_{(m-L+1)}(n)],$$

$$N3^n(n) = [\underline{NZ}_2(n) \ \underline{NZ}_3(n) \ \dots \ \underline{NZ}_{(m-L+1)}(n)].$$

Assuming the signals and noise to be statistically independent and that the noise components are uncorrelated from sensor to sensor, we get

$$E[M_1^H(n)M_1(n)] = (1/N) \sum_{n=0}^{N-1} M_1^H(n)M_1(n) \quad (4.2-25)$$

$$E[M_1^H(n)M_1(n)] = U1^H V1 U1 + L N \sigma^2 I_{(m-L)} ,$$

$$E[N_1^H(n)M_1(n)] = U1^H \Phi^H V1 U1 + L N \sigma^2 I_{(m-L)} ,$$

$$E[P_1^H(n)P_1(n)] = U2^H V2 U2 + L N \sigma^2 I_{(m-L)} ,$$

$$E[P_1^H(n)Q_1(n)] = U2^H \Gamma^H V2 U2 + L N \sigma^2 I_{(m-L)} ,$$

$$E[R_1^H(n)R_1(n)] = U3^H V3 U3 + L N \sigma^2 I_{(m-L)} ,$$

$$E[S_1^H(n)R_1(n)] = U3^H \Psi^H V3 U3 + L N \sigma^2 I_{(m-L)} ,$$

where $I_{(m-L)}$ is the $(m-L) \times (m-L)$ identity matrix and $I_{(m-L)}$, $V1$, $V2$ and $V3$ are the matrices

$$I_{(m-L)} = \begin{bmatrix} 0 & 1 & 0 & 0 & \dots & \dots & 0 \\ 0 & 0 & 1 & 0 & \dots & \dots & 0 \\ 0 & 0 & 0 & 1 & \dots & \dots & 0 \\ \vdots & \vdots & \vdots & \vdots & \ddots & \ddots & \vdots \\ \vdots & \vdots & \vdots & \vdots & \vdots & \vdots & \vdots \\ 0 & 0 & 0 & 0 & \dots & \dots & 1 \\ 0 & 0 & 0 & 0 & \dots & \dots & 0 \end{bmatrix} ,$$

$$M_1(n) = A1 H(n) S(n) U1(n) + N1'(n)$$

$$V1 = E[S^H(n)H^H(n))A_1^H(n)A_1(n)H(n)S(n)] ,$$

$$V2 = E[S'^H(n)H^H(n))A_1^H(n)A_1(n)H(n)S'(n)] ,$$

$$V1 = E[S^H(n)H^H(n))A_1^H(n)A_1(n)H(n)S^n(n)] .$$

Now, let M , N , P , Q , R and S be the matrices

$$M = E[M_1^H M_1] - L \sigma^2 I_{(m-L)} = U1^H V1 U1 , \quad (4.2-26)$$

$$N = E[N_1^H M_1] - L \sigma^2 I_{(m-L)} = U1^H \Phi^H V1 U1 , \quad (4.2-27)$$

$$P = E[P_1^H P_1] - L\sigma^2 I_{(m-L)} = U_2^H V_2 U_2, \quad (4.2-28)$$

$$Q = E[Q_1^H P_1] - L\sigma^2 I_{1(m-L)} = U_2^H \Gamma^H V_2 U_2, \quad (4.2-29)$$

$$R = E[R_1^H R_1] - L\sigma^2 I_{(m-L)} = U_3^H V_3 U_3, \quad (4.2-30)$$

$$S = E[S_1^H R_1] - L\sigma^2 I_{1(m-L)} = U_3^H \Psi^H V_3 U_3. \quad (4.2-31)$$

Consider the following three pencil matrices $(M-\lambda N)$, $(P-\eta Q)$ and $(R-\nu S)$.

Note that

$$(M-\lambda N) = (U_1^H V_1 U_1) - \lambda (U_1^H \Phi^H V_1 U_1) = U_1^H (I - \lambda \Phi^H) V_1 U_1, \quad (4.2-32)$$

$$(P-\eta Q) = (U_2^H V_2 U_2) - \eta (U_2^H \Gamma^H V_2 U_2) = U_2^H (I - \eta \Gamma^H) V_2 U_2, \quad (4.2-33)$$

$$(R-\nu S) = (U_3^H V_3 U_3) - \nu (U_3^H \Psi^H V_3 U_3) = U_3^H (I - \nu \Psi^H) V_3 U_3. \quad (4.2-34)$$

The matrices $U_1, U_2, U_3, \Phi, \Gamma,$ and Ψ are all of rank M as long as all the ϕ_{ij} 's, the γ_{ij} 's, the ψ_{ij} 's are distinct and $L \geq M$. Defining

$$E_{pq,rs} = \sum_{i=1}^L (\phi_{pq}^* - \phi_{rs})(i-1),$$

$$F_{pq,rs} = \sum_{i=1}^L (\gamma_{pq}^* - \gamma_{rs})(i-1),$$

$$G_{pq,rs} = \sum_{i=1}^L (\psi_{pq}^* - \psi_{rs})(i-1)$$

$$C1_{pq,rs} = E[S_{pq}^*(n) S_{rs}(n)] H_{pq}^*(n) H_{rs}(n),$$

$$C2_{pq,rs} = E[S'_{pq}{}^*(n) S'_{rs}(n)] H_{pq}^*(n) H_{rs}(n),$$

$$C2_{pq,rs} = E[S''_{pq}{}^*(n) S''_{rs}(n)] H_{pq}^*(n) H_{rs}(n),$$

the matrices V_1, V_2 and V_3 can be written as

$$V_1 = \begin{bmatrix} C1_{11,11} E_{11,11} & \dots & C1_{11,M(d)M(d)} E_{11,M(d)M(d)} \\ C1_{12,11} E_{12,11} & \dots & C1_{12,M(d)M(d)} E_{12,M(d)M(d)} \\ \vdots & \vdots & \vdots \\ \vdots & \vdots & \vdots \\ C1_{M(d)M(d),11} E_{M(d)M(d),11} & \dots & C1_{M(d)M(d),M(d)M(d)} E_{M(d)M(d),M(d)M(d)} \end{bmatrix},$$

$$\begin{aligned}
V2 = & \begin{bmatrix} C2_{11,11}F_{11,11} & \dots & C2_{11,M(d)M(d)}F_{11,M(d)M(d)} \\ C2_{12,11}F_{12,11} & \dots & C2_{12,M(d)M(d)}F_{12,M(d)M(d)} \\ \vdots & \dots & \vdots \\ \vdots & \dots & \vdots \\ C2_{M(d)M(d),11}F_{M(d)M(d),11} & \dots & C2_{M(d)M(d),M(d)M(d)}F_{M(d)M(d),M(d)M(d)} \end{bmatrix}, \\
V3 = & \begin{bmatrix} C3_{11,11}G_{11,11} & \dots & C3_{11,M(d)M(d)}G_{11,M(d)M(d)} \\ C3_{12,11}G_{12,11} & \dots & C3_{12,M(d)M(d)}G_{12,M(d)M(d)} \\ \vdots & \dots & \vdots \\ \vdots & \dots & \vdots \\ C3_{M(d)M(d),11}G_{M(d)M(d),11} & \dots & C3_{M(d)M(d),M(d)M(d)}G_{M(d)M(d),M(d)M(d)} \end{bmatrix},
\end{aligned}$$

It can be seen that the matrices $V1$, $V2$ and $V3$ are of rank M . The rank of the pencil $(M-\lambda N)$ is decreased by 1 whenever

$$\begin{aligned}
\lambda_{ij} = 1/(\phi_{ij}^*) = (p_{ij}^*)(\Delta/cT_s)\sin(\theta_j), \quad (4.2.35) \\
\text{for } i=1, 2, \dots, M(1), \\
j,k=1, 2, \dots, d.
\end{aligned}$$

The rank of the pencil $(P-\eta Q)$ is decreased by 1 whenever

$$\begin{aligned}
\eta_{ij} = 1/(\gamma_{ij}^*) = (p_{ij}^*)^T, \quad (4.2.36) \\
\text{for } i=1, 2, \dots, M(1), \\
j,k=1, 2, \dots, d.
\end{aligned}$$

The rank of the pencil $(R-\nu S)$ is decreased by 1 whenever

$$\begin{aligned}
\nu_{ij} = 1/(\psi_{ij}^*) = (p_{ij}^*)(\Delta/cT_s)\sin(\theta_j) (p_{ij}^*)^T, \quad (4.2-37) \\
\text{for } i=1, 2, \dots, M(1), \\
j,k=1, 2, \dots, d.
\end{aligned}$$

As was noted in section 4.1, from the first set of generalized eigenvalues, we obtain a set of coupled values of poles and angles of arrival. The second set solves for the poles. The third set allows us to identify which poles go with which angles of arrival since

$$\nu_{ij} = \lambda_{ij} \cdot \eta_{ij}. \quad (4.2-38)$$

This way, we have successfully solved for the angles of arrival and the poles of the sources using a model of wide sense stationary signals.

4.2.1 COMPUTER SIMULATION

The scenario used for this simulation consisted of 12 sensors uniformly spaced at a distance Δ . Again, the 2 sources were assumed to be located at angles $\theta_1=16^\circ$ and $\theta_2=24^\circ$. Two cases were studied.

Case A

In this case, the emitter signals are assumed to have been generated by passing sequences of white noise through linear systems with impulse response given by $h_1(k)=(p_{11})^k+(p_{12})^k$ for one source where $p_{11}=0.12+j0.79$ and $p_{12}=p_{11}^*$, and $h_2(k)=(p_{21})^k+(p_{22})^k$ for the other source with $p_{21}=0.25+j0.90$ and $p_{22}=p_{21}^*$. Again, the received data was first Fourier decomposed using 128 snapshots and the statistics were derived using 50 runs.

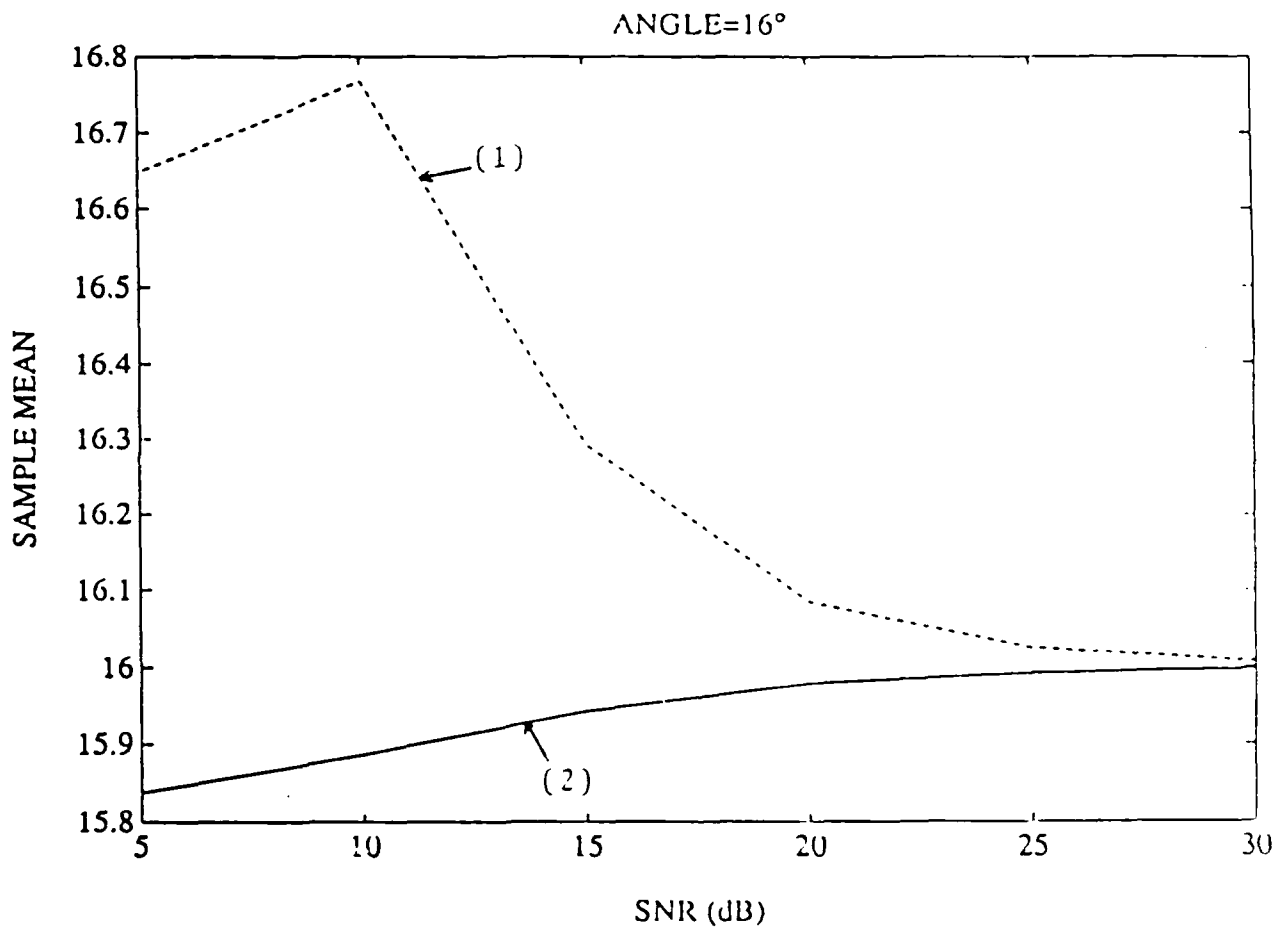
Case B

In this case, the two sources are assumed to have identical spectra. The emitter signals are generated by passing two independent white Gaussian noise sequences through a linear system whose impulse response is given by

$$h(k)=(p_{11})^k+(p_{12})^k$$

where $p_{11}=0.12+j0.79$ and $p_{12}=p_{11}^*$. The received data was first Fourier decomposed using 128 snapshots and the algorithm was runs 50 times.

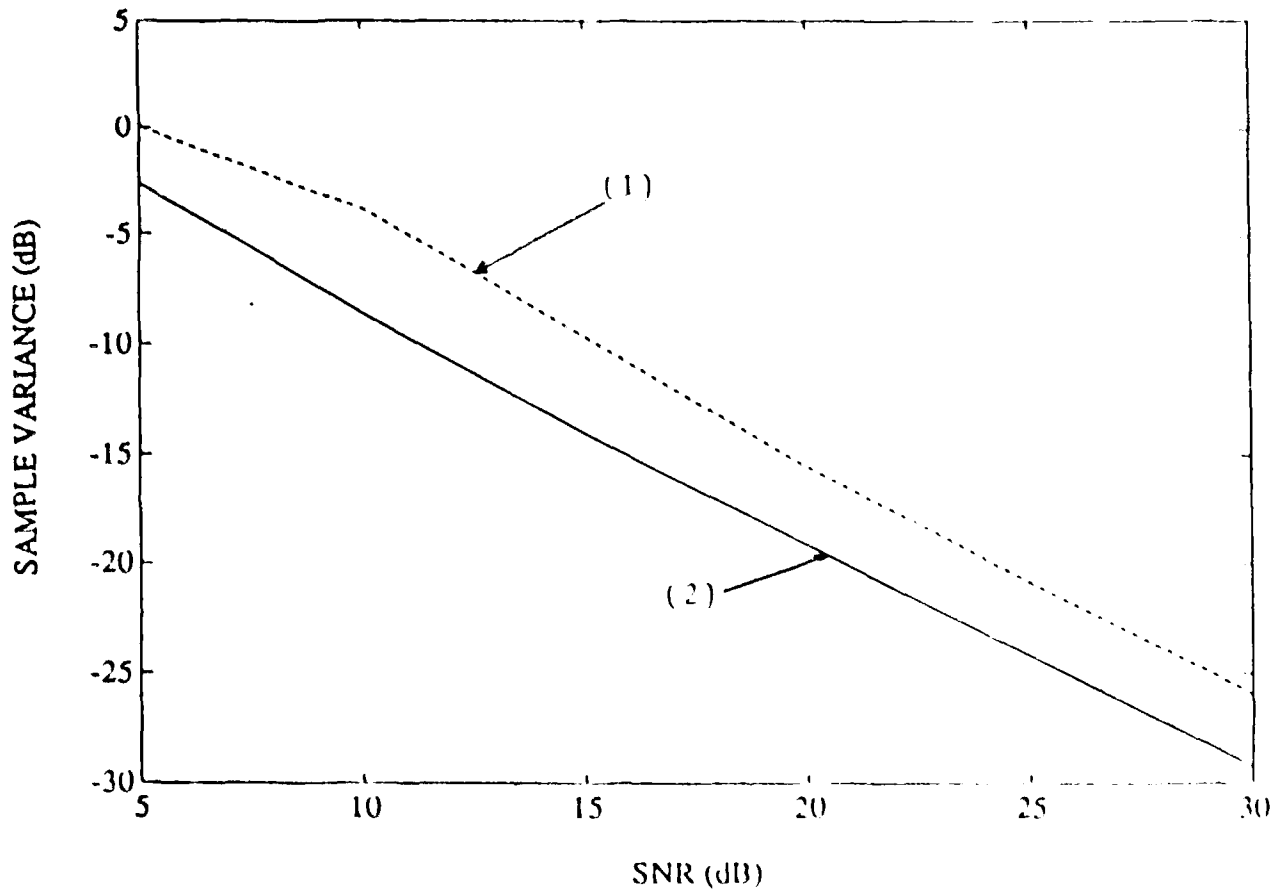
The results are plotted in figures 4.8 to 4.14 and tables 4.7 to 4.12. In these plots, (1) denotes the estimates for Case A whereas (2) corresponds to Case B. Both methods identify the poles of the sources with their angles of arrival, however, the second method gives better estimates due to the fact that the poles are estimated more efficiently. We have used the smallest window possible which is $L=2$ in this case whereas a window of length $L=4$ was used in the first case.



(1)-No Common Poles
 (2)- 2 Common Poles

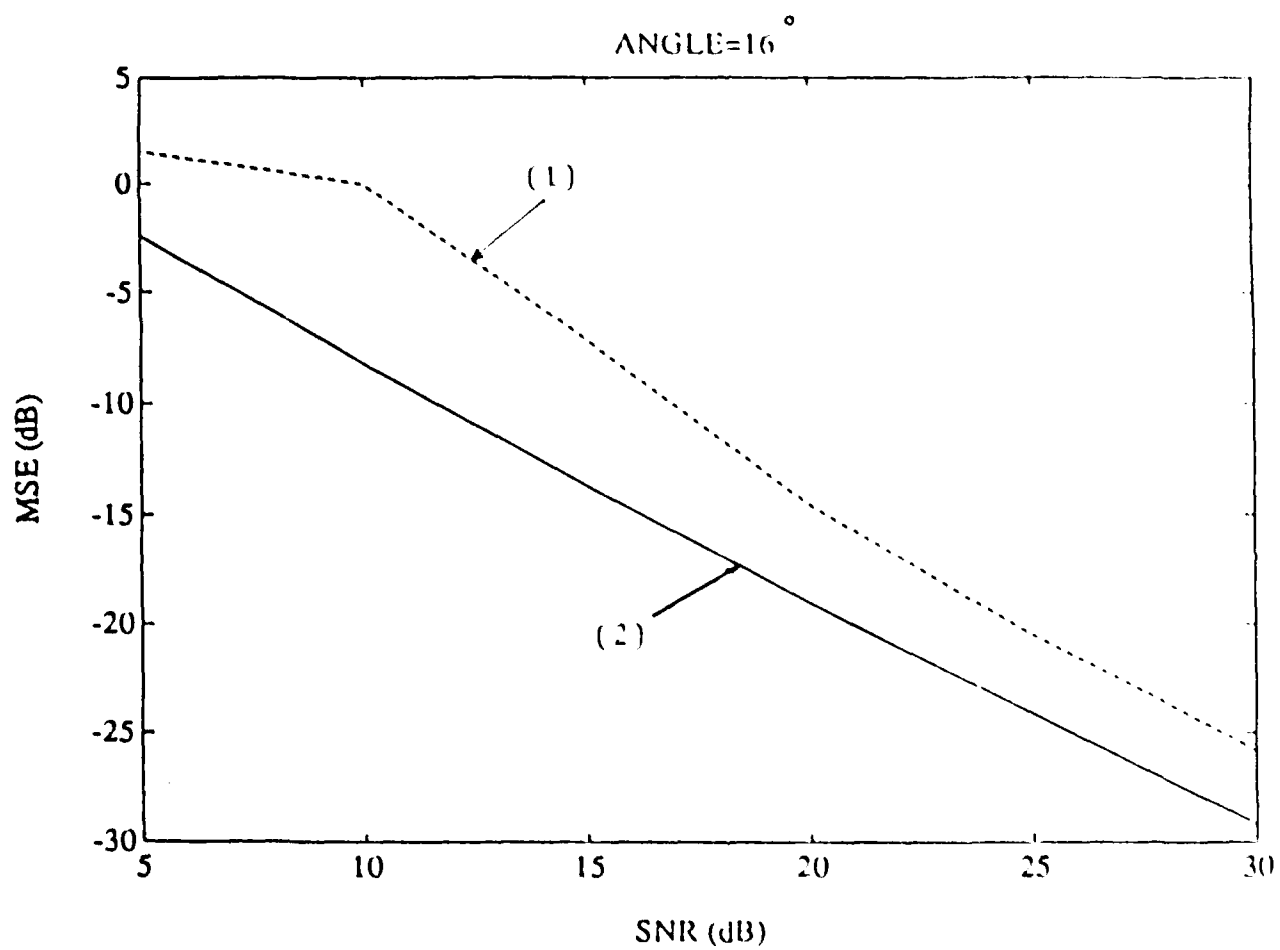
Fig. 4.9. Sample Mean of Angle at 16°
 Wide Sense Stationary Signals.

ANGLE=16



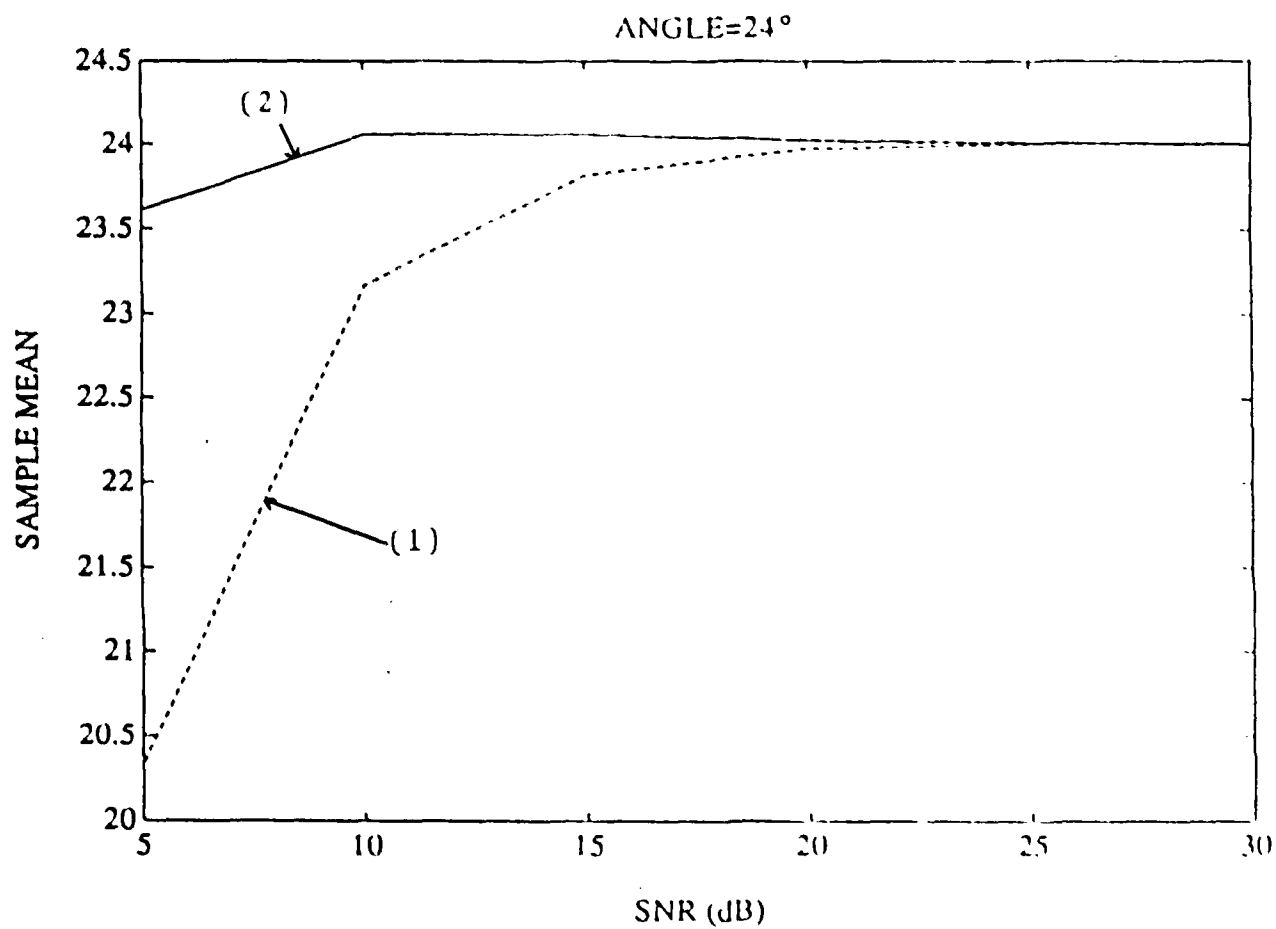
- (1) - No Common Poles
- (2) - 2 Common Poles

Fig. 4.10. Sample Variance of Angle at 16° Wide Sense Stationary Signals.



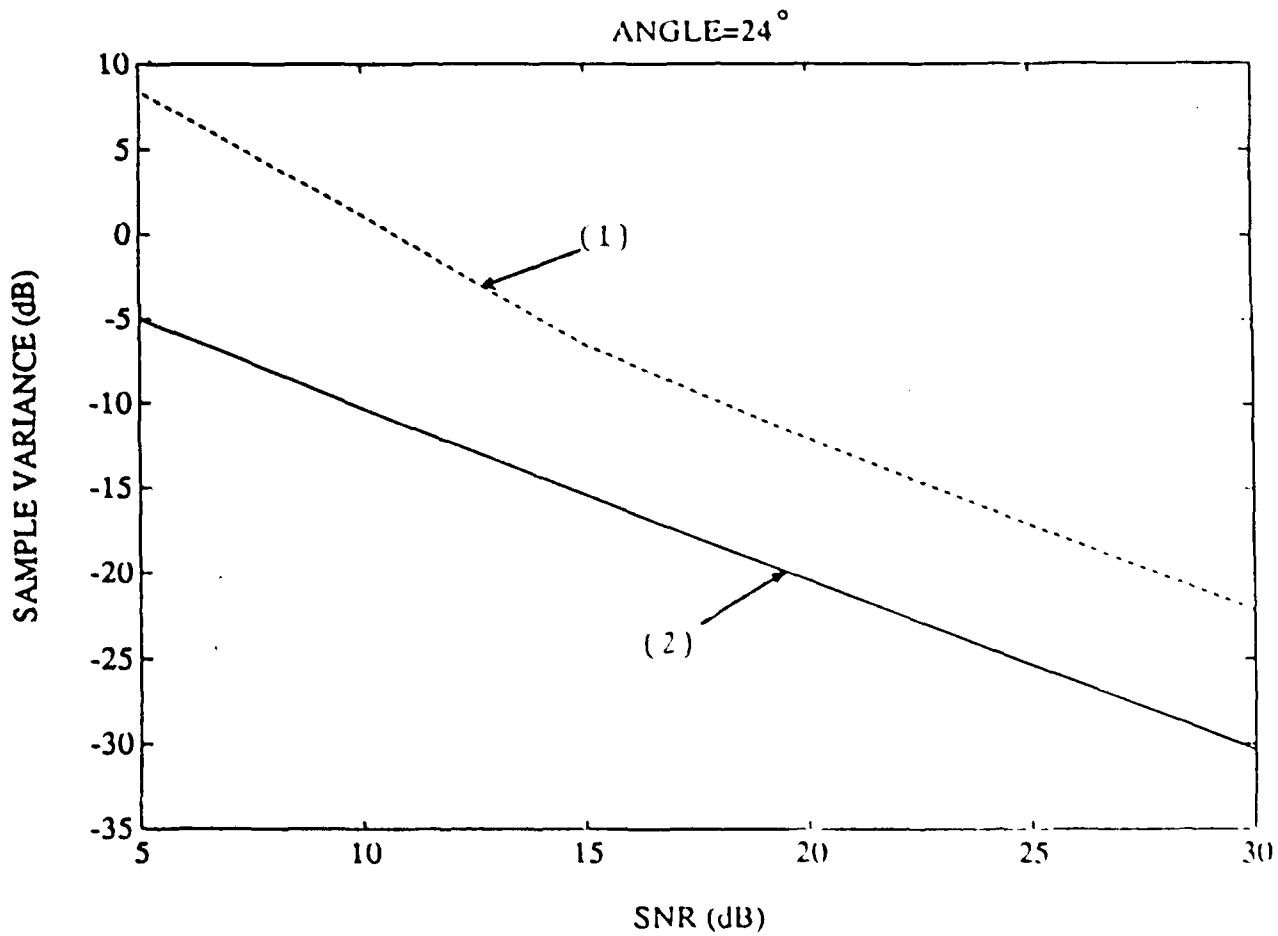
(1)-No Common Poles
 (2)- 2 Common Poles

Fig. 4.11. Mean-Squared Error of Angle at 16°
 Wide Sense Stationary Signals.



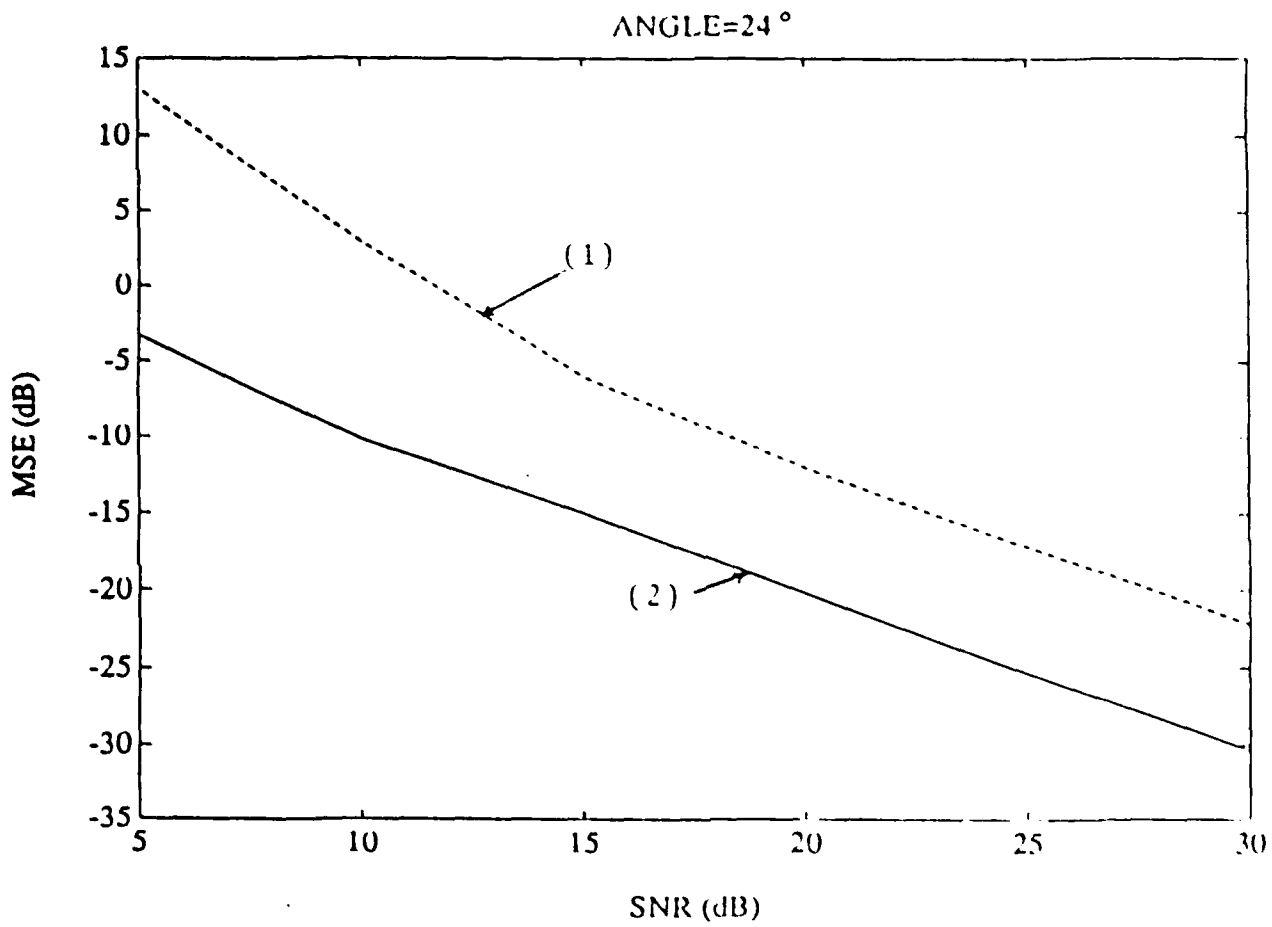
(1)-No Common Poles
 (2)- 2 Common Poles

Fig. 4.12. Sample Mean of Angle at 24°
 Wide Sense Stationary Signals.



- (1)-No Common Poles
- (2)- 2Common Poles

Fig. 4.13. Sample Variance of Angle at 24°
Wide Sense Stationary Signals.



(1)-No Common Poles
 (2)- 2 Common Poles

Fig. 4.14. Mean-Squared Error of Angle at 24°
 Wide Sense Stationary Signals.

SNR (dB)	Sample Mean	Sample Variance
30	0.2499700-j0.8999654	6.5221090e-4
25	0.2499475-j0.8997493	1.1575040e-3
20	0.2498654-j0.8989769	2.0493467e-3
15	0.2496969-j0.8965538	3.6088992e-3
10	0.2471662-j0.8881544	1.0184543e-2
5	0.1563175-j0.8014570	5.5371519e-2

Table 4.7
Sample Mean and Variance of the pole $p_{22}=0.25-j0.90$.
(No Common poles)

SNR (dB)	Sample Mean	Sample Variance
30	0.2500927+j0.8998703	5.1895110e-4
25	0.2501507+j0.8995793	1.0371592e-3
20	0.2502299+j0.8986719	1.8526319e-3
15	0.2503528+j0.8959982	3.3094636e-3
10	0.2429177+j0.8831745	1.9341080e-2
5	0.1579504+j0.8077933	5.6961089e-2

Table 4.8
Sample Mean and Variance of the pole $p_{21}=0.25+j0.90$.
(No Common poles)

SNR (dB)	Sample Mean	Sample Variance
30	0.1200390-j0.7898036	4.9322803e-4
25	0.1200731-j0.7895529	8.7595923e-4
20	0.1201505-j0.7889045	1.5568603e-3
15	0.1204159-j0.7871953	2.7756214e-3
10	0.1218340-j0.7832218	4.9832738e-3
5	0.1287750-j0.7795519	8.9591751e-3

Table 4.9
Sample Mean and Variance of the pole $p_{12}=0.12-j0.79$.
(No Common poles)

SNR (dB)	Sample Mean	Sample Variance
30	0.1199508+j0.7900655	4.9638440e-4
25	0.1199184+j0.7900197	8.8051870e-4
20	0.1198816+j0.7897383	1.5633145e-3
15	0.1199524+j0.7886938	2.7888690e-3
10	0.1210258+j0.7859387	5.0294539e-3
5	0.1271952+j0.7843727	8.9402702e-3

Table 4.10
Sample Mean and Variance of the pole $p_{11}=0.12+j0.79$.
(No Common poles)

SNR (dB)	Sample Mean	Sample Variance
30	0.1200018-j0.7899857	1.0762867e-4
25	0.1200033-j0.7899747	1.9138129e-4
20	0.1200061-j0.7899654	3.4014991e-4
15	0.1200114-j0.7899263	6.0441019e-4
10	0.1200223-j0.7898808	1.0735721e-3
5	0.1200452-j0.7898291	1.9071890e-3

Table 4.11
Sample Mean and Variance of the pole $p_{12}=p_{22}=0.12-j0.79$.
(2 Common poles)

SNR (dB)	Sample Mean	Sample Variance
30	0.1199916+j0.7900093	1.3058618e-4
25	0.1199852+j0.7900167	2.3202586e-4
20	0.1199739+j0.7900308	4.1216239e-4
15	0.1199542+j0.7900584	7.3149381e-4
10	0.1199203+j0.7901148	1.2967319e-3
5	0.1198631+j0.7902434	2.2957609e-3

Table 4.12
Sample Mean and Variance of the pole $p_{11}=p_{21}=0.12+j0.79$.
(2 Common poles)

4.3 FOURIER APPROACH

Consider the problem of estimating the angles of arrival of wideband signals. The notion of Fourier coefficients is used here in conjunction with the matrix pencil approach. Assume that all incoming signals have approximately the same bandwidth B . Let T be an observation interval and denote by ω_L and ω_H , the lowest and highest frequencies contained in B . In practice the frequency content is determined by Fourier decomposition of the received signals. The received signal at the i -th sensor can be modeled as

$$x_i(t) = \sum_{k=1}^d a(\theta_k) s_k(t - \tau_{ik}) + n_i(t); \quad i=1,2,\dots,m, \quad (4.3-1)$$

where τ_{ik} is

$$\tau_{ik} = (i-1)(\Delta/c)\sin(\theta_k).$$

Define the Fourier coefficients as

$$X_i(\omega_r) = (T)^{1/2} \int_{-T/2}^{T/2} x_i(t) \exp[-j\omega_r t] dt, \quad (4.3-2)$$

where R is the number of subbands, $\Delta\omega = (\omega_H + \omega_L)/R =$ width of each subband,

$\omega_r = (2\pi/T)(r_1 + r)$, r_1 is a suitably chosen integer such that

$(2\pi/T)r_1 = (\omega_L + \Delta\omega/2)$ and $(2\pi/T)(r_1 + R) = (\omega_H - \Delta\omega/2)$.

Taking the Fourier coefficients of both sides of equation (4.3-1),

we get

$$X_i(\omega_r) = \sum_{k=1}^d a(\theta_k) S_k(\omega_r) e^{j(i-1)\phi_k(\omega_r)} + N_i(\omega_r); \quad i=1,2,\dots,m, \quad (4.3-3)$$

$$r=1,2,\dots,R$$

where

$$\phi_k(\omega_r) = -(\omega_r)(\Delta/c)\sin(\theta_k). \quad (4.3-4)$$

Given this set of Fourier coefficients, $(m-L+1)$ vectors $\underline{X}_n(\omega_r)$ of length L are formed where

$$d \leq L \leq (m-d),$$

$$\underline{X}_n(\omega_r) = [X_n(\omega_r) X_{n+1}(\omega_r) \dots X_{n+L-1}(\omega_r)]^T; \quad n=1, 2, \dots, (m-L+1). \\ r=1, 2, \dots, R$$

It can be shown that $\underline{X}_n(\omega_r)$ can be put in the form

$$\underline{X}_n(\omega_r) = A(\omega_r) \phi^{(n-1)}(\omega_r) B \underline{S}(\omega_r) + \underline{N}_n(\omega_r), \quad (4.3-5)$$

where

$$A(\omega_r) = \begin{bmatrix} 1 & 1 & \dots & 1 \\ e^{j\phi_1(\omega_r)} & e^{j\phi_2(\omega_r)} & \dots & e^{j\phi_d(\omega_r)} \\ \vdots & \vdots & \dots & \vdots \\ \vdots & \vdots & \dots & \vdots \\ e^{j(L-1)\phi_1(\omega_r)} & e^{j(L-1)\phi_2(\omega_r)} & \dots & e^{j(L-1)\phi_d(\omega_r)} \end{bmatrix},$$

$$a_k = a(\theta_k),$$

$$B = \text{diag} \{a_1 \ a_2 \ \dots \ a_d \},$$

$$\phi(\omega_r) = \text{diag} \{ e^{j\phi_1(\omega_r)} \ e^{j\phi_2(\omega_r)} \ \dots \ e^{j\phi_d(\omega_r)} \},$$

$$\underline{S}(\omega_r) = [S_1(\omega_r) \ S_2(\omega_r) \ \dots \ S_d(\omega_r)]$$

and

$$\underline{N}_n^T(\omega_r) = [N_n(\omega_r) \ \dots \ N_{n+L-1}(\omega_r)].$$

Non singular transformation matrices $T_n(\omega_r)$ of dimension $(L \times L)$ are then used in such a way that

$$T_n(\omega_r) A(\omega_r) \phi^{(n-1)}(\omega_r) = A(\omega_0) \phi^{(n-1)}(\omega_0), \quad (4.3-6)$$

where ω_0 is a conveniently chosen frequency. In this fashion all the power in the corresponding sub bands is "moved" to a single band. This process is

termed in the literature as focusing. It is desirable to solve equation (4.3-6) for $T_n(\omega_T)$. However, $A(\omega_T)\Phi^{(n-1)}(\omega_T)$ is of dimension $(L \times d)$ and, therefore, does not possess an inverse. Without loss of generality, it is possible to augment $A(\omega_T)\Phi^{(n-1)}(\omega_T)$ by a matrix $W(\omega_T)$ of dimension $(L \times (L-d))$ so as to generate the non singular square $(L \times L)$ matrix

$$[A(\omega_T)\Phi^{(n-1)}(\omega_T) W(\omega_T)].$$

At ω_0 , this matrix becomes

$$[A(\omega_0)\Phi^{(n-1)}(\omega_0) W(\omega_0)].$$

An equivalent equation for equation (4.3-6) is then given by

$$T_n(\omega_T)[A(\omega_T)\Phi^{(n-1)}(\omega_T) W(\omega_T)] = [A(\omega_0)\Phi^{(n-1)}(\omega_0) W(\omega_0)].$$

It follows that

$$T_n(\omega_T) = [A(\omega_0)\Phi^{(n-1)}(\omega_0) W(\omega_0)][A(\omega_T)\Phi^{(n-1)}(\omega_T) W(\omega_T)]^{-1}.$$

Let $\beta_1, \beta_2, \dots, \beta_d$ be preliminary estimates of the angles of arrival $\theta_1, \theta_2, \dots, \theta_d$ obtained by some simple low resolution technique such as the periodogram. Define

$$\hat{\phi}_k(\omega_T) = -(\omega_T)(\Delta/c)\sin(\beta_k).$$

$A(\omega_T)$ is then approximated by the matrix

$$A_\beta(\omega_T) = \begin{bmatrix} 1 & \dots & 1 \\ \exp\{j\hat{\phi}_1(\omega_T)\} & \dots & \exp\{j\hat{\phi}_d(\omega_T)\} \\ \vdots & \dots & \vdots \\ \vdots & \dots & \vdots \\ \exp\{j(L-1)\hat{\phi}_1(\omega_T)\} & \dots & \exp\{j(L-1)\hat{\phi}_d(\omega_T)\} \end{bmatrix}.$$

$A_\beta(\omega_0)$ is obtained from $A_\beta(\omega_T)$ by replacing ω_T with ω_0 . The desired transformations are then given approximately by

$$\hat{T}_n(\omega_T) = [A_\beta(\omega_0)\Phi_\beta^{(n-1)}(\omega_0) W(\omega_0)][A_\beta(\omega_T)\Phi_\beta^{(n-1)}(\omega_T) W(\omega_T)]^{-1}.$$

To prevent matrices from being singular, W is chosen to have the same form as A but is evaluated at distinct angles different from $\beta_1, \beta_2, \dots, \beta_d$.

If it happens that all the true angles of arrival are within the neighborhood of a single angle β , the approximate transformation matrices are diagonal and are of the form

$$T_n(\omega_r) = e^{-j(n-1)(\omega_0 - \omega_r)(\Delta/c)\sin(\beta)} T_1(\omega_r)$$

where

$$T_1(\omega_r) = \text{diag}\{ 1 e^{-j(\omega_0 - \omega_r)(\Delta/c)\sin(\beta)} \dots e^{-j(L-1)(\omega_0 - \omega_r)(\Delta/c)\sin(\beta)} \}.$$

Applying these transformation to every vector, we obtain

$$\begin{aligned} T_n(\omega_r) \underline{X}_n(\omega_r) &= T_n(\omega_r) \underline{A}(\omega_r) \phi^{(n-1)}(\omega_r) \underline{B} \underline{S}(\omega_r) + T_n(\omega_r) \underline{N}_n(\omega_r) \\ &= \underline{A}(\omega_0) \phi^{(n-1)}(\omega_0) \underline{B} \underline{S}(\omega_r) + T_n(\omega_r) \underline{N}_n(\omega_r). \end{aligned} \quad (4.3-7)$$

With respect to the R sub-bands, consider

$$\underline{X}_n(\omega_0) = (1/R) \sum_{r=1}^R T_n(\omega_r) \underline{X}_n(\omega_r). \quad (4.3-8)$$

Let \underline{S}' and \underline{N}'_n be

$$\underline{S}' = (1/R) \sum_{r=1}^R \underline{S}(\omega_r) = [S'_1 \ S'_2 \ \dots \ S'_d]^T, \quad (4.3-9)$$

$$\underline{N}'_n = (1/R) \sum_{r=1}^R T_n(\omega_r) \underline{N}_n(\omega_r) = [N'_{n1} \ N'_{n2} \ \dots \ N'_{n(L-1)}]^T. \quad (4.3-10)$$

Therefore, $\underline{X}_n(\omega_0)$ can be expressed as

$$\underline{X}_n(\omega_0) = \underline{A}(\omega_0) \phi^{(n-1)}(\omega_0) \underline{B} \underline{S}' + \underline{N}'_n. \quad (4.3-11)$$

In the remainder of this discussion the dependence on ω_0 is assumed. The two matrices M_1 and N_1 are then formed where

$$M_1 = \begin{bmatrix} \uparrow & \uparrow & & \uparrow \\ | & | & & | \\ \underline{X}_1 & \underline{X}_2 & \dots & \underline{X}_{(m-L)} \\ | & | & & | \\ \downarrow & \downarrow & & \downarrow \end{bmatrix}; \quad N_1 = \begin{bmatrix} \uparrow & \uparrow & & \uparrow \\ | & | & & | \\ \underline{X}_2 & \underline{X}_3 & \dots & \underline{X}_{(m-L+1)} \\ | & | & & | \\ \downarrow & \downarrow & & \downarrow \end{bmatrix}.$$

These can be decomposed as

$$M_1 = \begin{bmatrix} \uparrow & \uparrow & & \uparrow \\ \underline{AB\underline{S}'} & \underline{AB\phi\underline{S}'} & \dots & \underline{AB\phi^{(m-L-1)}\underline{S}'} \\ \downarrow & \downarrow & & \downarrow \end{bmatrix} + N' \quad (4.3-12)$$

$$N_1 = \begin{bmatrix} \uparrow & \uparrow & & \uparrow \\ \underline{AB\phi\underline{S}'} & \underline{AB\phi^2\underline{S}'} & \dots & \underline{AB\phi^{(m-L)}\underline{S}'} \\ \downarrow & \downarrow & & \downarrow \end{bmatrix} + N'' \quad (4.3-13)$$

where

$$N' = \begin{bmatrix} \uparrow & \uparrow & & \uparrow \\ \underline{N_1'} & \underline{N_2'} & \dots & \underline{N_{(m-L)}'} \\ \downarrow & \downarrow & & \downarrow \end{bmatrix},$$

$$N'' = \begin{bmatrix} \uparrow & \uparrow & & \uparrow \\ \underline{N_2'} & \underline{N_3'} & \dots & \underline{N_{(m-L+1)'}} \\ \downarrow & \downarrow & & \downarrow \end{bmatrix}.$$

Simplification of M_1 and N_1 results in

$$M_1 = \underline{AB}[\underline{S}' \ \underline{\phi\underline{S}'} \ \dots \ \underline{\phi^{(m-L-1)}\underline{S}'}] + N',$$

$$N_1 = \underline{AB\phi}[\underline{S}' \ \underline{\phi^2\underline{S}'} \ \dots \ \underline{\phi^{(m-L-1)}\underline{S}'}] + N''.$$

Let F be the matrix

$$F = \begin{bmatrix} \uparrow & \uparrow & & \uparrow \\ \underline{S} & \underline{\phi\underline{S}} & \dots & \underline{\phi^{(m-L-1)}\underline{S}} \\ \downarrow & \downarrow & & \downarrow \end{bmatrix}.$$

The matrix F can be written as

$$F = D U,$$

where

$$D = \text{diag}\{ S'_1 S'_2 \dots S'_d \},$$

$$U = \begin{bmatrix} 1 e^{j\phi_1} \dots e^{j(m-L-1)\phi_1} \\ 1 e^{j\phi_2} \dots e^{j(m-L-1)\phi_2} \\ \vdots \vdots \vdots \\ 1 e^{j\phi_d} \dots e^{j(m-L-1)\phi_d} \end{bmatrix}.$$

Then

$$M_1 = AB D U + N' \quad (4.3-14)$$

and

$$N_1 = A B D U + N'' \quad (4.3-15)$$

Assuming that the signals and noise are statistically independent and that the noise components are uncorrelated from sensor to sensor, we get

$$E[M_1^H M_1] = U^H V U + E[N' H N'] \quad (4.3-16)$$

$$E[N_1^H M_1] = U^H A^H B^H V U + E[N'' H N'] \quad (4.3-17)$$

where V is the matrix $V = E[D^H B^H A^H A B D]$. Defining

$$F_{pq} = \sum_{i=1}^L e^{j(i-1)(\phi_p - \phi_q)},$$

$$S_{pq} = E[S_q^* S_p],$$

$$a_{pq} = a_q^* S_p,$$

the matrix V becomes

$$V = \begin{bmatrix} S_{11} a_{11} F_{11} & \dots & S_{d1} a_{d1} F_{d1} \\ S_{12} a_{12} F_{12} & \dots & S_{d2} a_{d2} F_{d2} \\ \vdots & \vdots & \vdots \\ S_{1d} a_{1d} F_{1d} & \dots & S_{dd} a_{dd} F_{dd} \end{bmatrix}.$$

Note that the matrix V is of rank d even in the presence of fully correlated sources. Define the matrices M and N as

$$M = E[M_1^H M_1] - E[N' H N'] = U^H V U \quad (4.3-18)$$

and

$$N = E[N_1^H M_1] - E[N_1^H N_1] = U^H \Phi^H V U. \quad (4.3-19)$$

The matrix pencil then becomes

$$M - \lambda N = U^H V U - \lambda U^H \Phi^H V U = U^H (I - \lambda \Phi^H) V U \quad (4.3-20)$$

which satisfies the requirements of the pencil theorem. Hence, the values of λ for which the rank of $M - \lambda N$ decreases by 1 are given by

$$\lambda_k = e^{j\phi_k}; \quad k=1,2,\dots,d. \quad (4.3-21)$$

The angles of arrival are given by

$$\theta_k = \sin^{-1}\{j \operatorname{cln}(\lambda_k) / \omega_0 \Delta\}; \quad k=1,2,\dots,d. \quad (4.3-22)$$

4.3.1 SIMULATION 3

Several possibilities exist for choosing the transformation matrices T_n [58]. It can be shown that a diagonal transformation leads to the simplest analysis. Assuming the sources to be clustered within the proximity of one location β , the transformation matrices $T_n(\omega_r)$ then become

$$T_n(\omega_r) = e^{-j(n-1)(\omega_0 - \omega_r)(\Delta/c)\sin(\beta)} T_1(\omega_r)$$

where

$$T_1(\omega_r) = \operatorname{diag}\{1, e^{-j(\omega_0 - \omega_r)(\Delta/c)\sin(\beta)}, \dots, e^{-j(L-1)(\omega_0 - \omega_r)(\Delta/c)\sin(\beta)}\}.$$

With this transformation it follows that

$$T_n(\omega_r) A(\omega_r) \Phi^{(n-1)}(\omega_r) = A(\omega_0) \Phi^{(n-1)}(\omega_0).$$

Assuming that the noise components are uncorrelated from sensor to sensor and from sub-band to sub-band with zero mean and variance σ^2 , it can be shown that

$$E[N_1^H N_1] = R \sigma^2 I_{(m-L)d}$$

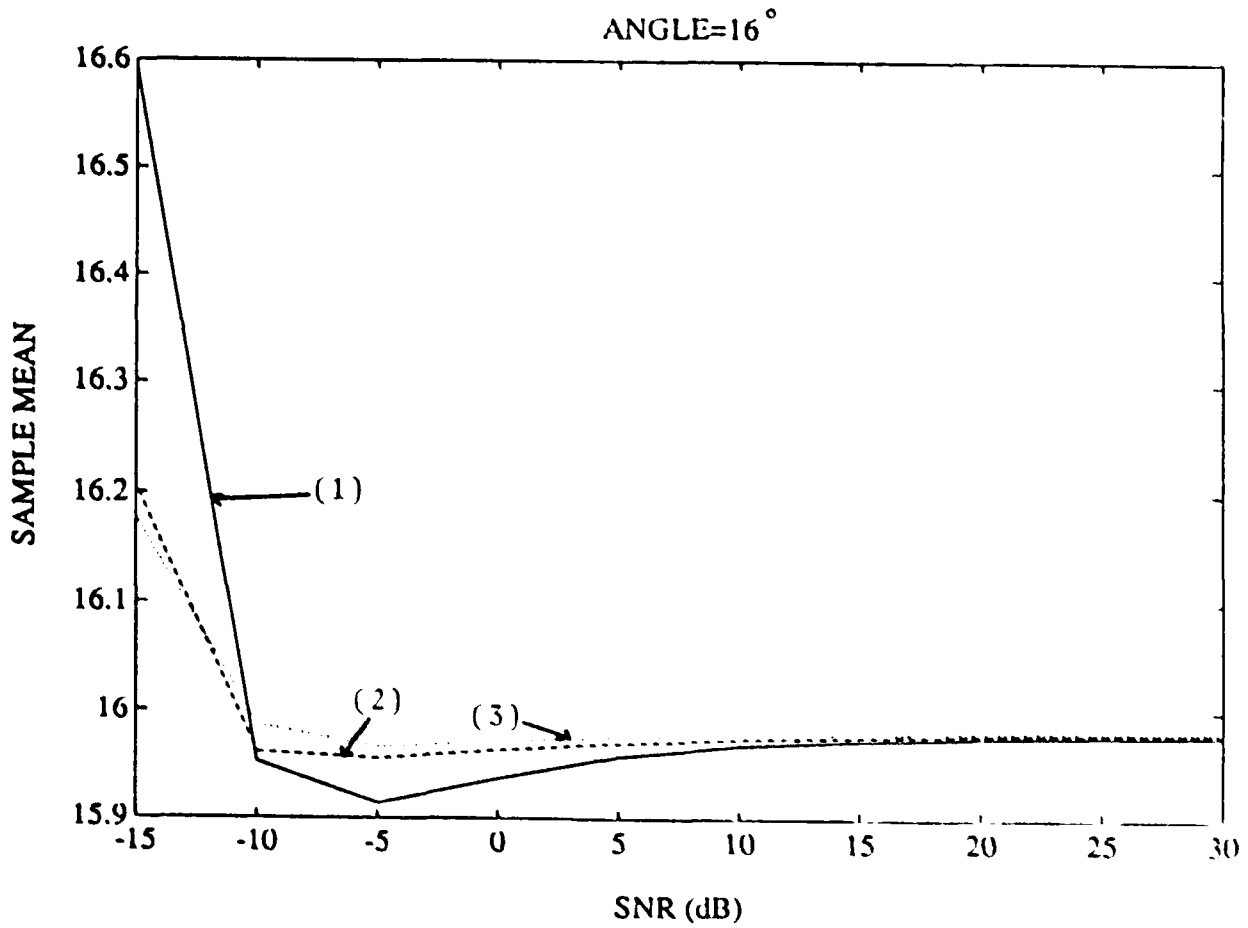
$$E[N_1^H N_1] = R \sigma^2 I_{(m-L)}$$

where $I_{(m-L)}$ is the $(m-L) \times (m-L)$ identity matrix and $I_{(m-L)d}$ is the matrix

$$I1_{(m-1)} = \begin{bmatrix} 0 & 1 & 0 & 0 & \dots & 0 \\ 0 & 0 & 1 & 0 & \dots & 0 \\ 0 & 0 & 0 & 1 & \dots & 0 \\ \dots & \dots & \dots & \dots & \dots & \dots \\ \dots & \dots & \dots & \dots & \dots & \dots \\ \dots & \dots & \dots & \dots & \dots & \dots \\ 0 & 0 & 0 & 0 & \dots & 1 \\ 0 & 0 & 0 & 0 & \dots & 0 \end{bmatrix} .$$

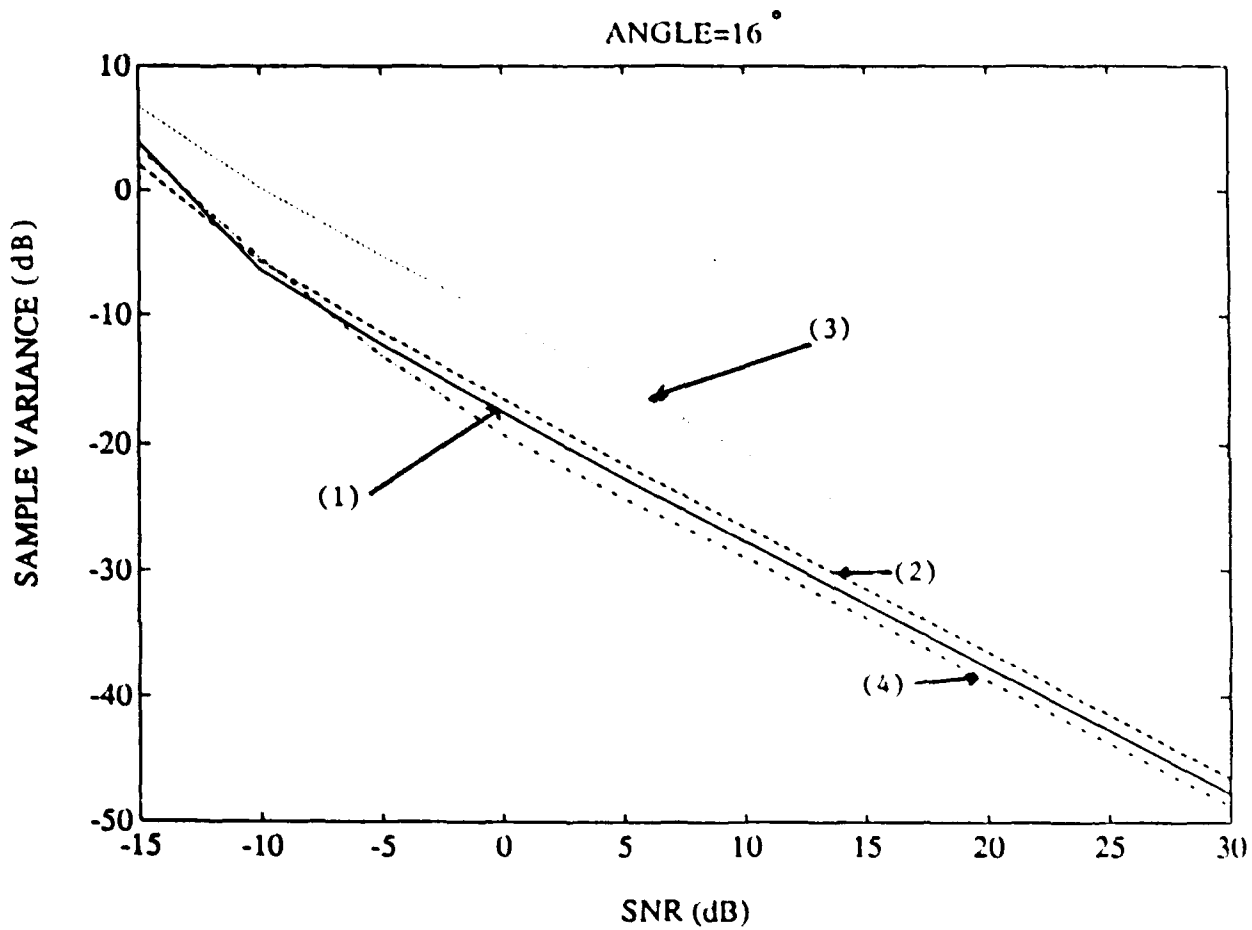
In the simulations, we have considered a linear array consisting of 8 sensors uniformly spaced at a distance $\Delta=c/(2 f_0)$. Following the example in [57], the two sources were assumed to be located at 16° and 24° and to have ideal rectangular spectra of bandwidth $B=40$ Hz centered at $f_0=100$ Hz. The broadband signals were first decomposed into 33 narrowband components. 100 snapshots were taken for each of the 50 runs. As in chapter 3, ESPRIT can be used either with overlapping subarrays or non overlapping subarrays. In the first case, the subarray \underline{X} consists of the first 7 sensors and the subarray \underline{Y} consists of the last 7 sensors. In the second case, two adjacent sensors were considered as a pair. The results of the simulation are plotted in figures 4.15 to 4.20. In these figures, the Moving Window is represented by (1), ESPRIT overlapping case by (2) and ESPRIT non overlapping case by (3). (4) represents the Cramer-Rao lower bound (CRLB) which is described in the appendix.

Note that the estimates obtained through moving window have small bias and their variances approach the CRLB very closely especially at high SNR. We have thus shown that the moving window can be applied in conjunction with CSS and that it performs slightly better than ESPRIT.



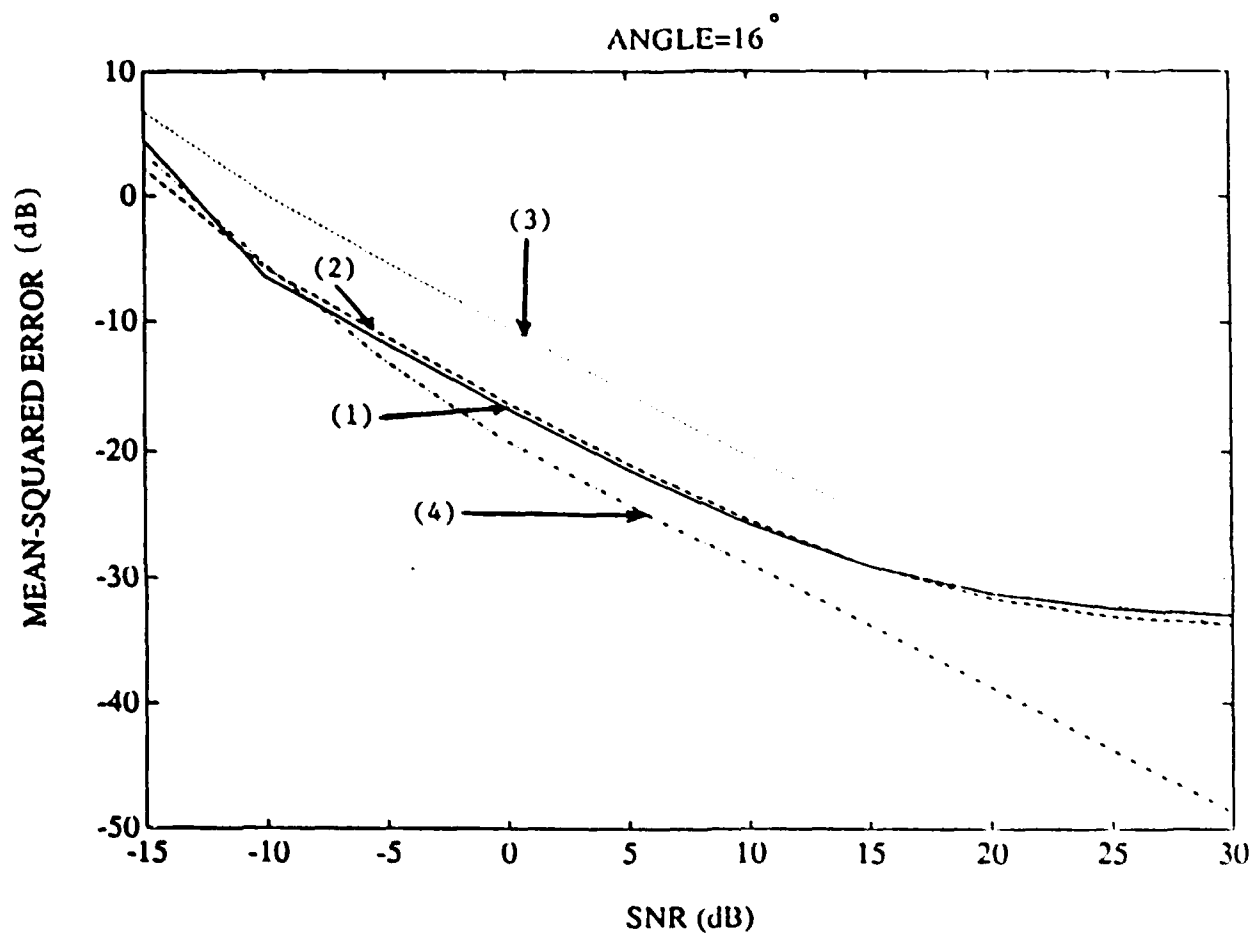
- (1)-Moving Window
- (2)-ESPRIT: Linear Overlapping Case
- (3)-ESPRIT: Linear Non Overlapping Case

Fig. 4.15. Sample Mean of Angle at 16°
Fourier Approach.



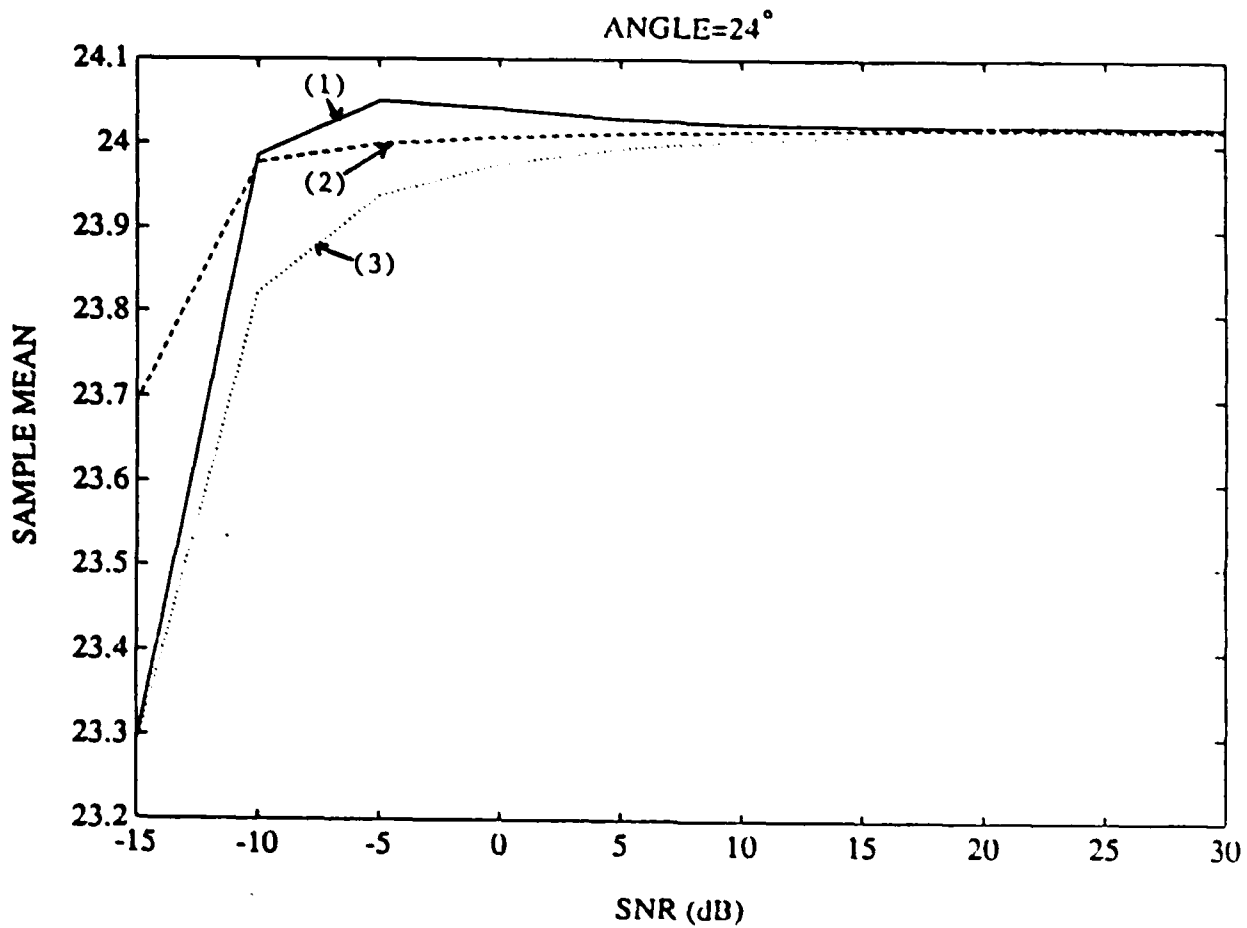
- (1)-Moving Window
- (2)-ESPRIT: Linear Overlapping Case
- (3)-ESPRIT: Linear Non Overlapping Case
- (4)-CRLB

Fig. 4.16. Sample Variance of Angle Estimate at 16°
Fourier Approach.



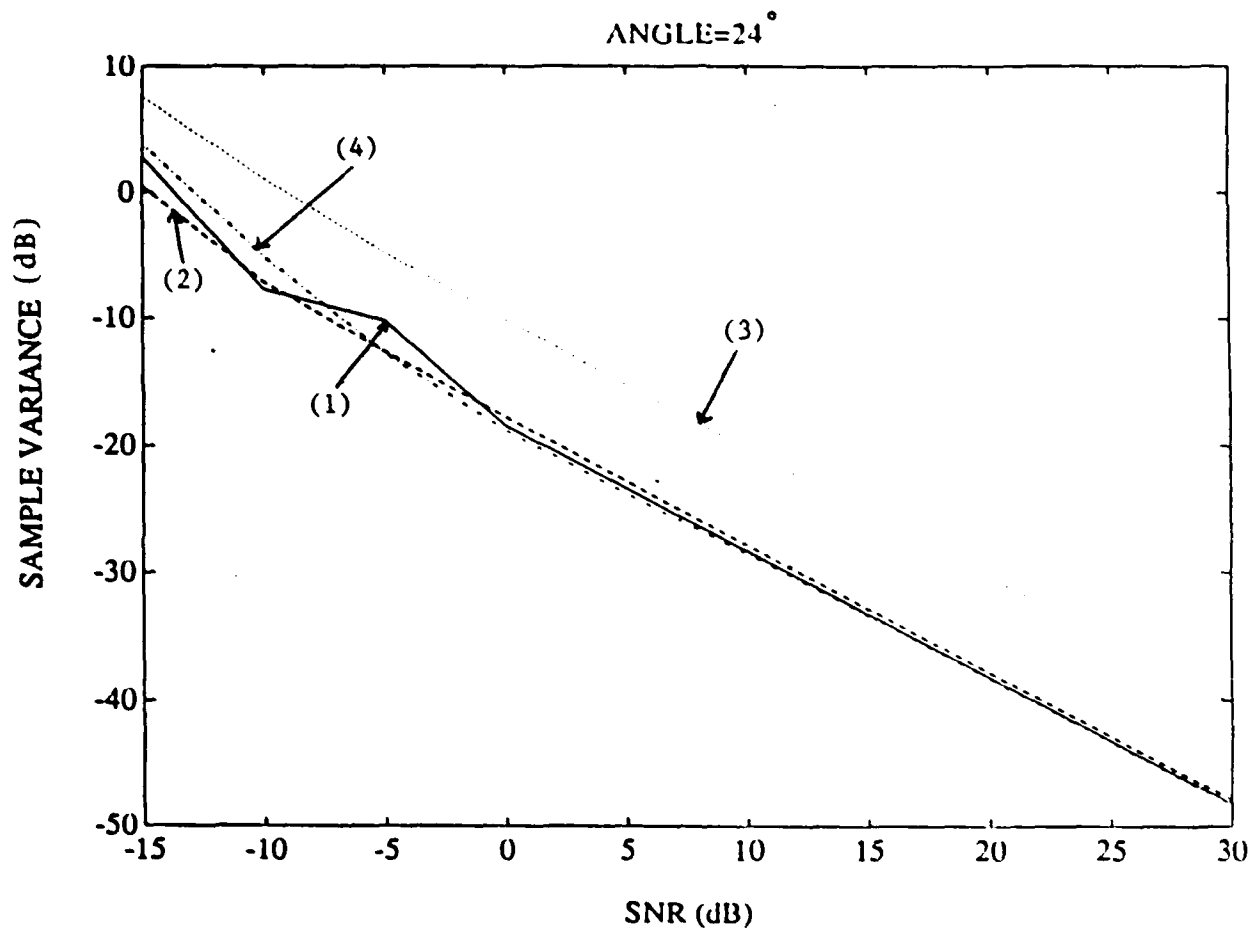
- (1)-Moving Window
- (2)-ESPRIT: Linear Overlapping Case
- (3)-ESPRIT: Linear Non Overlapping Case
- (4)-CRLB

Fig. 4.17. Mean-Squared Error of Angle at 16°
Fourier Approach.



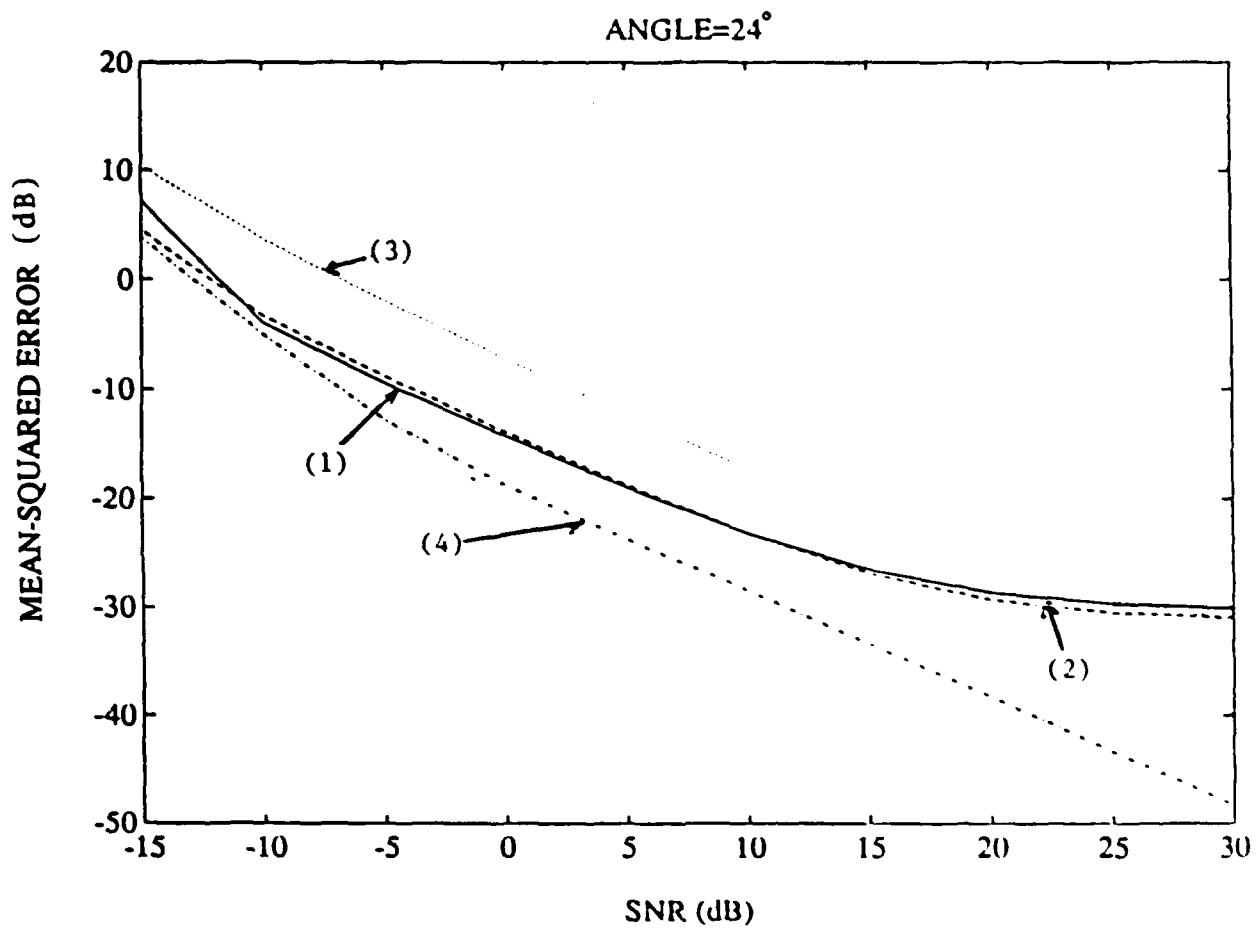
- (1)-Moving Window
- (2)-ESPRIT: Linear Overlapping Case
- (3)-ESPRIT: Linear Non Overlapping Case

Fig. 4.18. Sample Mean of Angle Estimate at 24°
Fourier Approach.



- (1)-Moving Window
- (2)-ESPRIT: Linear Overlapping Case
- (3)-ESPRIT: Linear Non Overlapping Case
- (4)-CRLB

Fig. 4.19. Sample Variance of Angle at 24°
Fourier Approach.



- (1)-Moving Window
- (2)-ESPRIT: Linear Overlapping Case
- (3)-ESPRIT: Linear Non Overlapping Case
- (4)-CRLB

Fig. 4.20. Mean-Squared Error of Angle at 24°
Fourier Approach.

CHAPTER 5

PERTURBATION ANALYSIS

The methods described previously assume that additive noise can be suppressed through noise compensation. Also, the uniform spacing between the sensor elements of an array is assumed to be known. In practice, however, it is likely that the noise compensation will be non ideal and that the sensor elements will be perturbed from their uniform spacing. In this section, performance degradation is investigated due to imperfect compensation of the additive noise. The case of offsets in the sensor spacing is studied in a similar fashion. The chordal metric [85] is introduced as a measure of the distance between the true and perturbed eigenvalues. Theoretical upper bounds are derived for the chordal metric for both the Moving Window and ESPRIT.

5.1 Chordal Metric

Let C denote the field of all complex numbers. Consider the eigenvalue problems

$$M \underline{x} = \lambda N \underline{x} \quad (5.1-1)$$

and

$$\underline{y}^H M = \lambda \underline{y}^H N \quad (5.1-2)$$

where H denotes complex conjugate transpose. \underline{x} and \underline{y} are called the right and left eigenvector, respectively, of the pencil formed by M and N . Solution for \underline{y} proceeds by solving

$$M^H \underline{y} = \lambda^* N^H \underline{y} .$$

Introduce the Euclidian matrix norm defined as

$$\|M\| = \sup_{\|\underline{x}\|=1} \|\underline{Mx}\| = \sup_{\|\underline{x}\|=1} \{ \underline{x}^H (M^H M) \underline{x} \}^{1/2} .$$

We are interested in the generalized eigenvalue problem

$$\tilde{M} \tilde{x} = \tilde{\lambda} \tilde{N} \tilde{x} \quad (5.1-3)$$

where

$$\tilde{M} = M + \Delta M = M + E \quad (5.1-4)$$

$$\tilde{N} = N + \Delta N = N + F. \quad (5.1-5)$$

Let α_i and β_i be the quantity

$$\alpha_i = \gamma_i {}^H M x_i \quad (5.1-6)$$

and

$$\beta_i = \gamma_i {}^H N x_i, \quad (5.1-7)$$

where x_i and γ_i are the i -th right and the i -th left eigenvectors of the pencil formed by M and N . It follows from equation (5.1-1) that

$$\lambda_i = \alpha_i / \beta_i. \quad (5.1-8)$$

Stewart [85] showed that small perturbations in M and N result in

$$\tilde{\lambda}_i = \frac{\alpha_i + \gamma_i {}^H E x_i + O(\epsilon^2)}{\beta_i + \gamma_i {}^H F x_i + O(\epsilon^2)} = \frac{\alpha_i' + O(\epsilon^2)}{\beta_i' + O(\epsilon^2)} \quad (5.1-9)$$

where

$$\lim_{\epsilon \rightarrow 0} \frac{O(\epsilon^2)}{\epsilon} = 0.$$

Define the chordal metric as

$$\chi(\lambda_i, \tilde{\lambda}_i) = \frac{|\lambda_i - \tilde{\lambda}_i|}{\sqrt{1 + |\lambda_i|^2} \sqrt{1 + |\tilde{\lambda}_i|^2}}. \quad (5.1-10)$$

With this definition it was shown [85] that

$$\chi(\lambda_i, \tilde{\lambda}_i) \leq \epsilon / \gamma_i + O(\epsilon^2) \quad (5.1-11)$$

where

$$\epsilon = \sqrt{||E||^2 + ||F||^2} \quad (5.1-12)$$

and

$$\gamma_1 = \sqrt{\alpha_1^2 + \beta_1^2} \quad (5.1-13)$$

In our applications, the eigenvalue λ_1 is related to the angle of arrival θ_1 through the equation

$$\lambda_1 = \exp\{j(\omega\Delta/c)\sin(\theta_1)\}.$$

The perturbed eigenvalue $\tilde{\lambda}_1$ then corresponds to an angle of arrival $\tilde{\theta}_1$ given by

$$\tilde{\lambda}_1 = \exp\{j(\omega\Delta/c)\sin(\tilde{\theta}_1)\}.$$

Let $\phi_1 = (\omega\Delta/c)\sin(\theta_1)$ and $\tilde{\phi}_1 = (\omega\Delta/c)\sin(\tilde{\theta}_1)$. It can be shown that

$$|\lambda_1 - \tilde{\lambda}_1| = 2 \sin\{(\phi_1 - \tilde{\phi}_1)/2\}. \quad (5.1-14)$$

Note that $|\lambda_1| = 1$ and $|\tilde{\lambda}_1| = 1$. Therefore, equation (5.1.10) reduces to

$$\chi(\lambda_1, \tilde{\lambda}_1) = \sin\{(\phi_1 - \tilde{\phi}_1)/2\}. \quad (5.1-15)$$

which implies that

$$\tilde{\theta}_1 = \sin^{-1}\{\sin(\theta_1) \pm (2c/\omega\Delta)\sin^{-1}\{\chi(\lambda_1, \tilde{\lambda}_1)\}\}. \quad (5.1-16)$$

Hence, given the value of the chordal metric, it is possible to determine the perturbed angle of arrival by using equation (5.1-16).

5.2 PERTUBATION DUE TO NOISE

In this section we study the effects of non ideal noise compensation on the performance of the Matrix Pencil Approach. To compensate for the noise, it was shown in chapter 2 that it is necessary to know the noise covariance matrix. However, in practice, the noise covariance matrix is not known exactly. To obtain a measure of the perturbation in the eigenvalues, upper bounds are derived for both the moving window and ESPRIT operators.

5.2.1 MOVING WINDOW

For the Moving Window operator discussed in chapter 2, two matrices $E[M_1^H M_1]$ and $E[N_1^H M_1]$ are formed where

$$E[M_1^H M_1] = U^H V U + L\sigma^2 I_{(m-L)} \quad (5.2.1-1)$$

$$E[N_1^H M_1] = U^H \Phi^H V U + L\sigma^2 I_{1(m-L)} \quad (5.2.1-2)$$

where U , V and U^H are $(m-L) \times (m-L)$ non-singular matrices and $I_{(m-L)}$ is the $(m-L) \times (m-L)$ identity matrix and $I_{1(m-L)}$ is the $(m-L) \times (m-1)$ matrix

$$I_{1(m-L)} = \begin{bmatrix} 0 & 1 & 0 & 0 & \dots & \dots & 0 \\ 0 & 0 & 1 & 0 & \dots & \dots & 0 \\ 0 & 0 & 0 & 1 & \dots & \dots & 0 \\ \vdots & \vdots & \vdots & \vdots & \ddots & \ddots & \vdots \\ \vdots & \vdots & \vdots & \vdots & \vdots & \vdots & \vdots \\ 0 & 0 & 0 & 0 & \dots & \dots & 1 \\ 0 & 0 & 0 & 0 & \dots & \dots & 0 \end{bmatrix} .$$

Let

$$\tilde{M} = E[M_1^H M_1]$$

$$\tilde{N} = E[N_1^H M_1]$$

$$M = U^H V U$$

$$E = L\sigma^2 I_{(m-L)}$$

$$N = U^H \Phi^H V U$$

$$F = L\sigma^2 I_{1(m-L)} .$$

As a worst case, assume noise correction is not attempted. Thus,

$$\tilde{M} = M + \Delta M = M + E \quad (5.2.1-4)$$

$$\tilde{N} = N + \Delta N = N + F. \quad (5.2.1.5)$$

In order to use the bound on the chordal metric, one needs to evaluate the euclidean norms of the matrices E and F . for this purpose, consider

$$||\underline{E}\underline{x}||^2 = \{(\underline{E}\underline{x})^H(\underline{E}\underline{x})\} = \underline{x}^H(E^H E)\underline{x} .$$

Maximizing $||\underline{E}\underline{x}||$ is the same as maximizing the quadratic form $\underline{x}^H(E^H E)\underline{x}$.

Given a Hermitian matrix M , it is known that the maximum value of the quotient,

$$\frac{\underline{x}^H M \underline{x}}{\underline{x}^H \underline{x}} ,$$

is equal to the largest eigenvalue of M . Therefore, under the constraint

$\underline{x}^H \underline{x} = 1$, the maximum value of $\underline{x}^H (E^H E) \underline{x}$ is equal to the maximum eigenvalue of $E^H E$. Since $E = L \sigma^2 I_{(m-L)}$, then $E^H E = L^2 \sigma^4 I_{(m-L)}$. The largest eigenvalue of this matrix is $L^2 \sigma^4$. Hence,

$$||E|| = L \sigma^2. \quad (5.2.1-6)$$

Similarly, because $F = L \sigma^2 I_{(m-L)}$, $F^H F$ is the following matrix

$$F^H F = L^2 \sigma^4 \begin{bmatrix} 0 & 0 & \dots & 0 & 0 \\ 0 & 1 & \dots & 0 & 0 \\ \vdots & \vdots & \vdots & \vdots & \vdots \\ 0 & 0 & \dots & 1 & 0 \\ 0 & 0 & \dots & 0 & 1 \end{bmatrix}.$$

The largest eigenvalue of this matrix is also $L^2 \sigma^4$. Thus

$$||F|| = L \sigma^2. \quad (5.2.1-7)$$

Therefore,

$$\epsilon = \sqrt{||E||^2 + ||F||^2} = L \sigma^2 \sqrt{2}. \quad (5.2.1-8)$$

For $\epsilon \rightarrow 0$; i.e., $\sigma^2 \ll (1/L(2)^{1/2})$, the bound on the chordal metric then becomes

$$\chi(\lambda_1, \tilde{\lambda}_1) \leq L \sigma^2 \sqrt{\frac{2}{((\underline{y}_1^H \underline{M} \underline{x}_1)^2 + (\underline{y}_1^H \underline{N} \underline{x}_1)^2)}} \quad (5.2.1-9)$$

5.2.2 ESPRIT

ESPRIT can be employed in a variety of situations. The general case involves isolated doublets located randomly in the plane. However, when a linear uniformly spaced array is used, two schemes are possible depending upon whether the doublets overlap or not. For a given number of sensor elements, the overlapping case has the advantage of having a larger aperture size and thus a better resolution.

5.2.2.1 General Case

For the general case of ESPRIT presented in chapter 2, two matrices were formed from the data vectors \underline{X} and \underline{Y} such that

$$E[\underline{X} \underline{X}^H] = A_1 S A_1^H + \sigma^2 I_m \quad (5.2.2.1-1)$$

$$E[\underline{X} \underline{Y}^H] = A_1 S \Phi^H A_1^H \quad (5.2.2.1-2)$$

Let

$$\tilde{M} = E[\underline{X} \underline{X}^H]$$

$$\tilde{N} = E[\underline{X} \underline{Y}^H]$$

$$M = A_1 S A_1^H$$

$$E = \sigma^2 I_m$$

$$N = A_1 S \Phi^H A_1^H$$

$$F = 0.$$

Thus, assuming noise correction is not attempted,

$$\tilde{M} = M + \Delta M = M + E$$

$$\tilde{N} = N + \Delta N = N + F.$$

We know that $||E||$ and $||F||$ are equal to the square root of the largest eigenvalue of $E^H E$ and $F^H F$, respectively. Since $E = \sigma^2 I_m$ and $F = 0$, $E^H E = \sigma^4 I_m$ and $F^H F = 0$. The largest eigenvalue of these matrices are σ^4 and 0. Therefore,

$$||E|| = \sigma^2 \quad (5.2.2.1-3)$$

$$||F|| = 0. \quad (5.2.2.1-4)$$

Thus,

$$\epsilon = \sqrt{||E||^2 + ||F||^2} = \sigma^2. \quad (5.2.2.1-5)$$

For $\epsilon \rightarrow 0$, the bound on the chordal metric becomes

$$x(\lambda_1, \tilde{\lambda}_1) \leq \frac{\sigma^2}{\sqrt{((\underline{y}_i^H \underline{M} \underline{x}_i)^2 + (\underline{y}_i^H \underline{N} \underline{x}_i)^2)}} \quad (5.2.2.1-6)$$

5.2.2.2 Linear Array: Overlapping Doublets Case

In this case a linear array composed of m sensors is used. The signal received at the i -th sensor can be modeled as

$$y_i(t, \underline{\theta}) = \sum_{k=1}^d a_k s_k(t) e^{j(i-1)\phi_k} + n_i(t); i=1, 2, \dots, m, \quad (5.2.2.2-1)$$

where

$$\phi_k = (\omega \Delta / c) \sin(\theta_k), \quad k=1, 2, \dots, d \quad (5.2.2.2-2)$$

and

$n_i(t)$ is the additive noise.

Two overlapping subarrays \underline{Y}_1 and \underline{Y}_2 are then formed where

$$\underline{Y}_1 = [y_1 \ y_2 \ \dots \ y_{(m-1)}]^T \quad (5.2.2.2-3)$$

$$\underline{Y}_2 = [y_2 \ y_3 \ \dots \ y_m]^T. \quad (5.2.2.2-4)$$

In chapter 3, it was shown that

$$E[\underline{Y}_1 \underline{Y}_1^H] = \underline{A}_2 \underline{B} \underline{S} \underline{B}^H \underline{A}_2^H + \sigma^2 \underline{I}_{(m-1)} \quad (5.2.2.2-5)$$

$$E[\underline{Y}_1 \underline{Y}_2^H] = \underline{A}_2 \underline{B} \underline{S} \underline{B}^H \underline{A}_2^H + \sigma^2 \underline{I}_{2(m-1)} \quad (5.2.2.2-6)$$

where $\underline{I}_{(m-1)}$ is the $(m-1) \times (m-1)$ identity matrix and $\underline{I}_{2(m-1)}$ is the $(m-1) \times (m-1)$ matrix shown below

$$\underline{I}_{1(m-1)} = \begin{bmatrix} 0 & 0 & 0 & 0 & \dots & 0 & 0 \\ 1 & 0 & 0 & 0 & \dots & 0 & 0 \\ 0 & 1 & 0 & 0 & \dots & 0 & 0 \\ \vdots & \vdots & \vdots & \vdots & \ddots & \vdots & \vdots \\ \vdots & \vdots & \vdots & \vdots & \ddots & \vdots & \vdots \\ 0 & 0 & 0 & 0 & \dots & 0 & 0 \\ 0 & 0 & 0 & 0 & \dots & 1 & 0 \end{bmatrix}.$$

Let

$$\tilde{M} = E\{Y_1 Y_1^H\}$$

$$\tilde{N} = E\{Y_1 Y_2^H\}$$

$$M = A_2 B S B^H A_2^H$$

$$E = \sigma^2 I_{(m-1)}$$

$$N = A_2 B S^H B^H A_2^H$$

$$F = \sigma^2 I_{1(m-1)}$$

Thus, assuming no compensation for the noise,

$$\tilde{M} = M + \Delta M = M + E$$

$$\tilde{N} = N + \Delta N = N + F.$$

As before, we know that $||E||$ and $||F||$ are equal to the square root of the largest eigenvalue of $E^H E$ and $F^H F$, respectively. It follows that

$$||E|| = \sigma^2 \quad (5.2.2.2-7)$$

and

$$||F|| = \sigma^2. \quad (5.2.2.2-8)$$

Thus,

$$\epsilon = \sqrt{||E||^2 + ||F||^2} = \sqrt{2} \sigma^2. \quad (5.2.2.2-9)$$

For $\epsilon \ll 0$, the bound on the chordal metric becomes

$$\chi(\lambda_1, \tilde{\lambda}_1) \leq \sigma^2 \sqrt{\frac{2}{((y_1^H M x_1)^2 + (y_1^H N x_1)^2)}} \quad (5.2.2.2-10)$$

5.2.2.3 Linear Array: Non-Overlapping Doublets Case

In this case two non-overlapping subarrays Y_1 and Y_2 are generated from the data received at the sensor array. Assuming m to be even, Y_1 and Y_2 are given by

$$Y_1 = [y_1 \ y_3 \ \dots \ y_{(m-1)}]^T \quad (5.2.2.3-1)$$

$$\underline{Y}_2 = [y_2 \ y_4 \ \dots \ y_m]^T. \quad (5.2.2.3-2)$$

As shown in chapter 3

$$E[\underline{Y}_1 \underline{Y}_1^H] = A_3 B S B^H A_3^H + \sigma^2 I_{(m/2)} \quad (5.2.2.3-3)$$

$$E[\underline{Y}_1 \underline{Y}_2^H] = A_1 B S \Phi^H B^H A_1^H. \quad (5.2.2.3.4)$$

Let

$$\tilde{M} = E[\underline{Y}_1 \underline{Y}_1^H]$$

$$\tilde{N} = E[\underline{Y}_1 \underline{Y}_2^H]$$

$$M = A_3 B S B^H A_3^H$$

$$E = \sigma^2 I_m$$

$$N = A_1 B S B^H \Phi^H A_1^H$$

$$F = 0.$$

Thus

$$\tilde{M} = M + \Delta M = M + E$$

$$\tilde{N} = N + \Delta N = N + F.$$

$||E||$ and $||F||$ are evaluated as before. Since $E = \sigma^2 I_m$ and $F = 0$, $E^H E = \sigma^4 I_{(m/2)}$ and $F^H F = 0$. The largest eigenvalue of these matrices are σ^4 and 0. Therefore,

$$||E|| = \sigma^2 \quad (5.2.2.3-5)$$

and

$$||F|| = 0. \quad (5.2.2.3-6)$$

Thus,

$$\epsilon = \sqrt{||E||^2 + ||F||^2} = \sigma^2. \quad (5.2.2.3-7)$$

In this case, the bound on the chordal metric becomes

$$\chi(\lambda_i, \tilde{\lambda}_i) \leq \frac{\sigma^2}{\sqrt{((\underline{y}_i^H M \underline{x}_i)^2 + (\underline{y}_i^H N \underline{x}_i)^2)}}. \quad (5.2.2.3-8)$$

5.2.3 COMPUTER SIMULATION

A computer simulation was carried out to demonstrate the applicability of the upper bounds derived for the chordal metric. It should be pointed out that few adjustments had to be made in order to exactly use the derived bounds. The bounds involve the matrices M and N and their corresponding eigenvalues and eigenvectors, the latter being of dimension $((m-L) \times 1)$. However, from previous sections, we have seen that the dimensions of M and N are reduced to the order needed (d , the number of sources) so that only the signal eigenvalues are estimated. The IMSL routine EIGZC called to do this will return eigenvectors of dimension $d \times 1$. There exists methods to obtain the desired eigenvectors from the returned set. We opt for the following. Recall that the original problem involved solving the equation

$$M\underline{x} = \lambda N\underline{x}. \quad (5.2.3-1)$$

The singular value decomposition (SVD) of the matrix N results in

$$N = U_n S_n V_n^H.$$

Let N^+ be the pseudo inverse of N . N^+ satisfies the Moore Penrose equations. It is clear that N^+ is given by

$$N^+ = V_n (S_n)^{-1} U_n^H,$$

where $(S_n)^{-1}$ consists on the inverse of the non zeros singular values. Premultiplying both sides of equation (5.2.3-1) by N^+ results in

$$N^+ M \underline{x} = \lambda N^+ N \underline{x}. \quad (5.2.3-2)$$

Noting that $N^+ N$ is the identity matrix provided that \underline{x} is in the range of N , solution of equation (5.2.3-1) is equivalent to solving the equation

$$N^+ M \underline{x} = \lambda \underline{x}. \quad (5.2.3-3)$$

The eigenvalues and eigenvectors obtained in this fashion would be of

dimension $(m-L) \times 1$.

The scenario used for the simulation consisted of a linear array of 8 sensors uniformly spaced at a distance Δ . 2 incoherent sources are present and are located at angles $\theta_1=16^\circ$ and $\theta_2=24^\circ$. The incoherent case was chosen so as to give a fair comparison to ESPRIT. The additive noise was generated as white Gaussian with zero mean and unit variance. The perturbed angles of arrival of the sources are obtained using the upper bound, the chordal metric and the perturbed eigenvalue. Tables 5.1 to 5.6 show the sample mean of the angle estimates obtained from 50 runs where 100 snapshots were considered in each run. Note from these tables that the bounds derived in this section perform quite well compared to the exact value of the chordal metric. In some instances, the bound is even smaller. This due to the bias that exists in the magnitude of the eigenvalue.

Moving Window

Angle=24°

SNR (dB)	$\bar{\theta}$ obtained from Bound	$\bar{\theta}$ obtained from chordal metric	$\bar{\theta}$ obtained from λ
10	24.26962	24.56922	24.13065
9	24.45502	24.65348	24.14139
8	24.71086	24.73565	24.15029

Table 1
(Sample Mean)

Angle=16°

SNR (dB)	$\bar{\theta}$ obtained from Bound	$\bar{\theta}$ obtained from chordal metric	$\bar{\theta}$ obtained from λ
10	16.56222	16.48074	16.00914
9	16.99071	16.54831	16.01596
8	17.41588	16.61207	16.02609

Table 2
(Sample Mean)

ESPRIT: Linear Overlapping Case

Angle=24°

SNR (dB)	$\bar{\theta}$ obtained from Bound	$\bar{\theta}$ obtained from chordal metric	$\bar{\theta}$ obtained from λ
10	24.26761	24.41945	24.13898
9	24.41869	24.47776	24.15929
8	24.68307	24.53942	24.18203

Table 3
(Sample Mean)

Angle=16°

SNR (dB)	$\bar{\theta}$ obtained from Bound	$\bar{\theta}$ obtained from chordal metric	$\bar{\theta}$ obtained from λ
10	16.33276	16.36528	15.97328
9	16.52749	16.41086	15.97049
8	16.81625	16.45882	15.96841

Table 4
(Sample Mean)

ESPRIT: Linear Non Overlapping Case
& ESPRIT: General Case

Angle=24°

SNR (dB)	$\bar{\theta}$ obtained from Bound	$\bar{\theta}$ obtained from chordal metric	$\bar{\theta}$ obtained from λ
10	24.51770	25.58454	24.04759
9	24.82163	25.94506	24.03446
8	24.30935	26.38912	24.01111

Table 5
(Sample Mean)

Angle=16°

SNR (dB)	$\bar{\theta}$ obtained from Bound	$\bar{\theta}$ obtained from chordal metric	$\bar{\theta}$ obtained from λ
10	16.67917	17.54183	16.04165
9	17.07774	17.88994	16.11396
8	17.70301	18.31548	15.22606

Table 6
(Sample Mean)

5.3 PERTURBATION DUE TO SENSOR SPACING

In this case we assume the environment to be noise free. However, each sensor is assumed to be perturbed from its ideal position.

5.3.1 MOVING WINDOW

Consider a linear array of m identical sensors spaced a distance $D + \Delta D_i$ where ΔD_i is the uncertainty in the spacing between the i -th and the $(i+1)$ -th sensors. Assume there are d ($d < m$) narrowband sources located at azimuthal angles θ_k ; $k=1, 2, \dots, d$, which are impinging on the array as plane waves and whose signal complex envelopes are denoted by $s_k(t)$. The signal received at the i -th sensor is modeled as

$$\tilde{y}_i(t, \theta) = \sum_{k=1}^d s_k(t) \tilde{a}_i(\theta_k) ; i=1, 2, \dots, m \quad (5.3.1-1)$$

where " $\tilde{\cdot}$ " denotes the response of the perturbed array and $\tilde{a}_i(\theta_k)$ is the perturbed relative response of the i -th sensor to the k -th source. Note that

$$\begin{aligned} \tilde{a}_i(\theta) &= a(\theta) e^{j(\omega/c)((i-1)D + \Delta D_i) \sin(\theta)} \\ &= a(\theta) e^{j(i-1)D(\omega/c) \sin(\theta)} e^{j(\omega/c)\Delta D_i \sin(\theta)} \end{aligned} \quad (5.3.1-2)$$

where $a(\theta)$ is the gain of the sensor in the angular direction θ . To a first order approximation

$$\begin{aligned} e^{j(\omega/c)\Delta D_i \sin(\theta)} &\approx 1 + j(\omega/c)\Delta D_i \sin(\theta) \\ &\approx 1 + j(2\pi\Delta D_i/\delta) \sin(\theta) \end{aligned} \quad (5.3.1-3)$$

where δ is the wavelength of the signal wavefront. Thus, $\tilde{a}_i(\theta)$ can be written as

$$\begin{aligned} \tilde{a}_i(\theta) &= a(\theta) e^{j(i-1)D(\omega/c) \sin(\theta)} \\ &\quad + j(2\pi\Delta D_i/\delta) e^{j(i-1)D(\omega/c) \sin(\theta)} \sin(\theta) a(\theta). \end{aligned} \quad (5.3.1-4)$$

For simplicity, let $a_k = a(\theta_k)$. Then

$$\begin{aligned} \bar{y}_i(t, \underline{\theta}) = & \sum_{k=1}^d a_k s_k(t) (e^{j(i-1)D(\omega/c) \sin(\theta_k)} \\ & + j(2\pi\Delta D_i/\delta) \sum_{k=1}^d a_k s_k(t) (e^{j(i-1)D(\omega/c) \sin(\theta_k)} \sin(\theta_k)); \quad i=1, \dots, m. \end{aligned} \quad (5.3.1-5)$$

Notice that the first part of equation (5.3.1-5) is just the unperturbed quantity y_i . Dropping the argument $(t, \underline{\theta})$ in equation (5.3.1-5), it can be written as

$$\bar{y}_i = y_i + \Delta y_i = y_i + e_i. \quad (5.3.1-6)$$

$(m-L+1)$ vectors $\bar{\underline{Y}}_n$ of length L are then formed where $\bar{\underline{Y}}_n$ is given by

$$\bar{\underline{Y}}_n = \{ \bar{y}_n \bar{y}_{n+1} \dots \bar{y}_{n+L-1} \}^T.$$

$\bar{\underline{Y}}_n$ can be written as

$$\bar{\underline{Y}}_n = \underline{Y}_n + \underline{E}_n. \quad (5.3.1-7)$$

From chapter 2 it is shown that \underline{Y}_n can be expressed in the form

$$\underline{Y}_n = \underline{A} \underline{B} \underline{\phi}^{(n-1)} \underline{S} \quad (5.3.1-8)$$

where \underline{A} , \underline{B} , $\underline{\phi}$ and \underline{S} are

$$\begin{aligned} \underline{A} &= [\underline{a}_1 \quad \underline{a}_2 \quad \dots \quad \underline{a}_d] \\ \underline{a}_i &= [1 \quad e^{j\phi_i} \quad \dots \quad e^{j(L-1)\phi_i}] \\ \underline{B} &= \text{diag} \{ a_1 \quad a_2 \quad \dots \quad a_d \} \\ \underline{\phi} &= \text{diag} [e^{j\phi_1} \quad e^{j\phi_2} \quad \dots \quad e^{j\phi_d}] \\ \phi_k &= (\omega\Delta/c) \sin(\theta_k), \quad k=1, 2, \dots, d \\ \underline{S} &= [s_1 \quad s_2 \quad \dots \quad s_d]^T. \end{aligned} \quad (5.3.1-9)$$

Similarly \underline{E}_n can be expressed as

$$\underline{E}_n = j(2\pi/\delta) [\Delta D]_n \underline{A} \underline{B} \underline{G} \underline{\phi}^{(n-1)} \underline{S}, \quad (5.3.1-10)$$

where \underline{A} , \underline{B} , $\underline{\phi}$ and \underline{S} are given by equation (5.3.1-9) and \underline{G} and $[\Delta D]_n$ are

$$\begin{aligned} \underline{G} &= \text{diag} \{ \sin(\theta_1) \quad \sin(\theta_2) \quad \dots \quad \sin(\theta_d) \} \\ [\Delta D]_n &= \text{diag} \{ \Delta D_n \quad \Delta D_{(n+1)} \quad \dots \quad \Delta D_{(n+L-1)} \}. \end{aligned}$$

The two matrices \underline{M}_1 and \underline{N}_1 are then formed in the usual way where

$$M_1 = [\tilde{Y}_1 \tilde{Y}_2 \dots \tilde{Y}_L]$$

$$N_1 = [\tilde{Y}_2 \tilde{Y}_3 \dots \tilde{Y}_{(L+1)}]$$

Consider the matrices $E[M_1^H M_1]$ and $E[N_1^H M_1]$. An element $m_{k,h}$ of $E[M_1^H M_1]$ is

$$m_{k,h} = E[\tilde{Y}_k^H \tilde{Y}_h]$$

where H denotes conjugate transpose and $E[\cdot]$ denotes expectation. Utilizing equation (3.3.1-7), $m_{k,h}$ becomes

$$m_{k,h} = E[Y_k^H \cdot Y_h] + E[Y_k^H \cdot E_h] + E[E_k^H \cdot Y_h] + E[E_k^H \cdot E_h] \quad (5.3.1-11)$$

$E[Y_k^H \cdot Y_h]$ can be obtained in closed form as

$$E[Y_k^H \cdot Y_h] = \sum_{q=1}^d \sum_{p=1}^d S_{pq} a_{pq} F_{pq} e^{-j(k-1)\phi_q} e^{j(h-1)\phi_p} \quad (5.3.1-12)$$

where

$$S_{pq} = E[s_q^* s_p] \quad (5.3.1-13)$$

$$a_{pq} = a_q^* a_p \quad (5.3.1-14)$$

$$F_{pq} = \sum_{i=1}^L e^{j(i-1)(\phi_p - \phi_q)} \quad (5.3.1-15)$$

Similarly, $E[Y_k^H E_h]$ can be expressed as

$$E[Y_k^H \cdot E_h] = j(2\pi/\delta) \sum_{q=1}^d \sum_{p=1}^d \{ S_{pq} a_{pq} F_{pq}^h e^{-j(k-1)\phi_q} \times e^{j(h-1)\phi_p} \sin(\theta_p) \} \quad (5.3.1-16)$$

where

$$F_{pq}^h = \sum_{i=h}^{h+L-1} \Delta \theta_i e^{j(i-h)(\phi_p - \phi_q)} \quad (5.3.1-17)$$

In a similar manner, $E[E_k^H Y_h]$ is

$$E[\underline{E}_k^H \cdot \underline{Y}_h] = j(2\pi/\delta) \sum_{q=1}^d \sum_{p=1}^d \{ S_{pq} a_{pq} F_{pq}^k e^{-j(k-1)\phi_q} \times e^{j(h-1)\phi_p \sin(\theta_q)} \} \quad (5.3.1-18)$$

where

$$F_{pq}^k = \sum_{i=k}^{k+L-1} \Delta D_i e^{j(i-k)(\phi_p - \phi_q)} . \quad (5.3.1-19)$$

Finally, following the same approach, $E[\underline{E}_k^H \underline{E}_h]$ can be written as

$$E[\underline{E}_k^H \cdot \underline{E}_h] = j(2\pi/\delta)^2 \sum_{q=1}^d \sum_{p=1}^d \{ S_{pq} a_{pq} F_{pq}^{hk} e^{-j(k-1)\phi_q} \times e^{j(h-1)\phi_p \sin(\theta_q) \sin(\theta_p)} \} \quad (5.3.1-20)$$

where

$$F_{pq}^{hk} = \sum_{r=0}^{L-1} \Delta D_{r+h} \Delta D_{r+k} e^{j(r-k)(\phi_p - \phi_q)} . \quad (5.3.1-21)$$

Note that the matrices $E[M_1^H M_1]$ and $E[N_1^H M_1]$ can be written as

$$E[M_1^H M_1] = M + E$$

and

$$E[N_1^H M_1] = N + F,$$

where the kh -th element of M and N are given by $E[\underline{Y}_k^H \cdot \underline{Y}_h]$ and $E[\underline{Y}_{k+1}^H \cdot \underline{Y}_h]$,

respectively. The kh -th element of E and F are given by

$$E[\underline{Y}_k^H \cdot \underline{E}_h] + E[\underline{E}_k^H \cdot \underline{Y}_h] + E[\underline{E}_k^H \cdot \underline{E}_h] \text{ and } E[\underline{Y}_{k+1}^H \cdot \underline{E}_h] + E[\underline{E}_{k+1}^H \cdot \underline{Y}_h] + E[\underline{E}_{k+1}^H \cdot \underline{E}_h],$$

respectively. Recall that $\|E\|$ and $\|F\|$ are given by the largest eigen-

values of $E^H E$ and $F^H F$, respectively. Note that this eigenvalue is always

less than or equal to the sum of all the eigenvalues. It is known that the

the sum of all eigenvalues of a matrix is equal to the trace of this

matrix. Recall that the matrix E is $(m-1) \times (m-1)$. Let $e_{k,h}$ be the kh -th ele-

ment of E . It can be shown that

$$\text{tr}(E^H E) = \sum_{k=1}^{(m-L)} \sum_{h=1}^{(m-L)} |e_{i,j}|^2 .$$

Note that the square root of $\text{tr}(D)$ is just the definition of the Frobenius norm of E defined as

$$\|E\|_f = \left\{ \sum_{k=1}^{(m-L)} \sum_{h=1}^{(m-L)} |e_{i,j}|^2 \right\} . \quad (5.3.1-24)$$

The hk^{th} element of E is of the the form

$$e_{h,k} = j(2\pi/\delta) \sum_{p=1}^d \sum_{q=1}^d \{ S_{pq} a_{pq} e^{-j(k-1)\phi_q} e^{j(h-1)\phi_p} \times \{ F_{pq}^h \sin(\theta_p) + F_{pq}^k \sin(\theta_q) + (j2\pi/\delta) F_{pq}^{hk} \sin(\theta_p) \sin(\theta_q) \} \} \quad (5.3.1-25)$$

Recall that if $a=bc$, then $|a| \leq |b| + |c|$. Thus,

$$|e_{h,k}| \leq (2\pi/\delta) \sum_{p=1}^d \sum_{q=1}^d |S_{pq}| |a_{pq}| \{ |F_{pq}^h| + |F_{pq}^k| + (2\pi/\delta) |F_{pq}^{hk}| \} \quad (5.3.1-26)$$

It is easy to see that

$$F_{pq}^h \leq \begin{cases} L | \Delta D_{\max} | & ; h \neq 1 \\ (L-1) | \Delta D_{\max} | & ; h = 1 \end{cases} \quad (5.3.3-27)$$

where ΔD_1 is assumed to be zero. Similarly, we can show that

$$F_{pq}^k \leq \begin{cases} L | \Delta D_{\max} | & ; k \neq 1 \\ (L-1) | \Delta D_{\max} | & ; k = 1 \end{cases} \quad (5.3.1-28)$$

and

$$F_{pq}^{hk} \leq \begin{cases} L |\Delta D_{\max}|^2 & ; h \neq 1 \text{ and } k \neq 1 \\ (L-1) |\Delta D_{\max}|^2 & ; h=1 \text{ or } k=1 \\ (L-2) |\Delta D_{\max}|^2 & ; h=1 \text{ and } k=1. \end{cases} \quad (5.3.1-29)$$

Because $(|\Delta D_{\max}|/\delta)^2$ is very small, F_{pq}^{hk} is negligible. Let R be the quantity

$$R = (2\pi/\delta) \sum_{p=1}^d \sum_{q=1}^d |S_{pq}| |a_{pq}|. \quad (5.3.1-30)$$

We can then show that

$$|e_{k,h}| \leq R \begin{cases} 2L |\Delta D_{\max}|^2 & ; h \neq 1 \text{ and } k \neq 1 \\ (2L-1) |\Delta D_{\max}|^2 & ; h=1 \text{ or } k=1 \\ 2(L-1) |\Delta D_{\max}|^2 & ; h=1 \text{ and } k=1. \end{cases} \quad (5.3.1-31)$$

Using equation (5.3.1-24), it can be shown that

$$||E||^2 \leq R^2 |\Delta D_{\max}|^2 [4(L-1)^2 + 2(m-L-1)(2L-1)^2 + (m-L-1)^2 4L^2]. \quad (5.3.1-32)$$

Similarly, it can be shown that

$$||F||^2 \leq R^2 |\Delta D_{\max}|^2 [(m-L)(2L-1)^2 + (m-L)(m-L+1)^2 4L^2]. \quad (5.3.1-33)$$

Therefore,

$$\begin{aligned} \varepsilon &= \sqrt{||E||^2 + ||F||^2} \\ &\leq R |\Delta D_{\max}| \{ [4(L-1)^2 + 2(m-L-1)(2L-1)^2 + (m-L-1)^2 4L^2] \\ &\quad + [(m-L)(2L-1)^2 + (m-L)(m-L+1)^2 4L^2] \}^{1/2} \end{aligned}$$

After some simplifications, it can be shown that

$$\varepsilon \leq R |\Delta D_{\max}| [8L^2(m-L)^2 + (m-L)(3-12L)+2]^{1/2}. \quad (5.3.1-34)$$

Let $K1 = [8L^2(m-L)^2 + (m-L)(3-12L)+2]^{1/2}$. The bound on the chordal metric then becomes

$$\chi(\lambda_1, \tilde{\lambda}_1) \leq \frac{2\pi(|\Delta D_{\max}|/\delta)K_1 \sum_{p=1}^d \sum_{q=1}^d |s_{pq}| |a_{pq}|}{\sqrt{(\underline{y}_1^H \underline{H}_{M\underline{x}_1})^2 + (\underline{y}_1^H \underline{H}_{N\underline{x}_1})^2}} \quad (5.3.1-35)$$

Note that the chordal metric is proportional to the correlation between the sources.

5.3.2 ESPRIT

5.3.2.1 General Case

Consider a planar array which consists of m matched sensor doublets whose elements are translationally separated by a displacement $D + \Delta D_i$ (ΔD_i is the uncertainty at one of the sensors of the i -th doublet). The signals received at the i -th doublet are

$$\tilde{x}_i(t, \underline{\theta}) = \sum_{k=1}^d s_k(t) a_i(\theta_k) \quad (5.3.2.1-1)$$

$$\tilde{y}_i(t, \underline{\theta}) = \sum_{k=1}^d s_k(t) a_i(\theta_k) e^{j(\omega/c)((i-1)D + \Delta D_i) \sin(\theta)}$$

To a first order approximation

$$\begin{aligned} e^{j(\omega/c)\Delta D_i \sin(\theta)} &\approx 1 + j(\omega/c)\Delta D_i \sin(\theta) \\ &\approx 1 + j(2\pi\Delta D_i/\delta)\sin(\theta), \end{aligned} \quad (5.3.2.1-2)$$

where δ is the wavelength of the signal wavefront. Then

$$\begin{aligned} e^{j(\omega/c)((i-1)D + \Delta D_i) \sin(\theta)} &= e^{j(i-1)D(\omega/c) \sin(\theta)} \\ &\quad + j(2\pi\Delta D_i/\delta) e^{j(i-1)D(\omega/c) \sin(\theta)} \sin(\theta) a(\theta). \end{aligned} \quad (5.3.2.1-3)$$

It follows that

$$\tilde{y}_i(t, \theta) = \sum_{k=1}^d a_i(\theta_k) s_k(t) (e^{j(i-1)D(\omega/c) \sin(\theta_k)}) \quad (5.3.2.1-4)$$

$$+ j(2\pi\Delta D_1/\delta) \sum_{k=1}^d a_i(\theta_k) s_k(t) (e^{j(i-1)D(\omega/c) \sin(\theta_k)} \sin(\theta_k)) ; i=1,2,\dots,m.$$

Equation (5.3.2.1-1) can be written as

$$\tilde{x}_i = x_i \quad (5.3.2.1-5)$$

$$\tilde{y}_i = y_i + \Delta y_i = y_i + e_i . \quad (5.3.2.1-6)$$

Let $\tilde{\underline{X}}$ and $\tilde{\underline{Y}}$ be the vectors

$$\tilde{\underline{X}} = \{ \tilde{x}_1 \ \tilde{x}_2 \ \dots \ \tilde{x}_m \}^T,$$

$$\tilde{\underline{Y}} = \{ \tilde{y}_1 \ \tilde{y}_2 \ \dots \ \tilde{y}_m \}^T.$$

It is easy to see that $\tilde{\underline{X}}$ and $\tilde{\underline{Y}}$ can be rewritten as

$$\tilde{\underline{X}} = \underline{X} \quad (5.3.2.1-7)$$

$$\tilde{\underline{Y}} = \underline{Y} + \underline{\Delta Y} \quad (5.3.2.1-8)$$

Previously, it was shown that \underline{X} and \underline{Y} have the following decompositions

$$\underline{X} = \underline{A}_1 \underline{S} \quad (5.3.2.1-9)$$

$$\underline{Y} = \underline{A}_1 \underline{\Phi S}. \quad (5.3.2.1-10)$$

Then

$$\tilde{y}_i(t, \theta) = \sum_{k=1}^d a_i(\theta_k) s_k(t) (e^{j(i-1)D(\omega/c) \sin(\theta_k)}) \quad (5.3.2.1-4)$$

$$+ j(2\pi\Delta D_1/\delta) \sum_{k=1}^d a_i(\theta_k) s_k(t) (e^{j(i-1)D(\omega/c) \sin(\theta_k)} \sin(\theta_k)) ; i=1,2,\dots,m.$$

Equation (5.3.2.1-1) can be written as

$$\tilde{x}_i = x_i \quad (5.3.2.1-5)$$

$$\tilde{y}_i = y_i + \Delta y_i = y_i + e_i . \quad (5.3.2.1-6)$$

Let $\tilde{\underline{X}}$ and $\tilde{\underline{Y}}$ be the vectors

$$\tilde{\underline{X}} = \{ \tilde{x}_1 \tilde{x}_2 \dots \tilde{x}_m \}^T,$$

$$\tilde{\underline{Y}} = \{ \tilde{y}_1 \tilde{y}_2 \dots \tilde{y}_m \}^T.$$

It is easy to see that $\tilde{\underline{X}}$ and $\tilde{\underline{Y}}$ can be rewritten as

$$\tilde{\underline{X}} = \underline{X} \quad (5.3.2.1-7)$$

$$\tilde{\underline{Y}} = \underline{Y} + \underline{\Delta Y} \quad (5.3.2.1-8)$$

Previously, it was shown that \underline{X} and \underline{Y} have the following decompositions

$$\underline{X} = A_1 \underline{S} \quad (5.3.2.1-9)$$

$$\underline{Y} = A_1 \phi \underline{S} \quad (5.3.2.1-10)$$

where A , ϕ and \underline{S} are

$$A_1 = [\underline{a}(\theta_1) \underline{a}(\theta_2) \dots \underline{a}(\theta_d)]$$

$$\underline{a}(\theta_i) = [a_1(\theta_i) a_2(\theta_i) \dots a_m(\theta_i)]$$

$$\phi = \text{diag} [e^{j\phi_1} e^{j\phi_2} \dots e^{j\phi_d}]$$

$$\underline{S} = \{ s_1 s_2 \dots s_d \}^T.$$

Similarly $\underline{\Delta Y}$ can be expressed as

$$\underline{\Delta Y} = j (2\pi/\delta) [\Delta D] A_1 G \phi \underline{S}, \quad (5.3.2.1-11)$$

where A , ϕ and \underline{S} have been defined earlier and G and $[\Delta D]$ are

$$G = \text{diag} \{ \sin(\theta_1) \sin(\theta_2) \dots \sin(\theta_d) \}$$

$$[\Delta D] = \text{diag} \{ \Delta D_1 \Delta D_2 \dots \Delta D_m \}.$$

Let \tilde{M} and \tilde{N} be the matrices

$$\tilde{M} = E[\tilde{\underline{X}} \tilde{\underline{X}}^H] = E[\underline{X} \underline{X}^H] = M \quad (5.3.2.1-12)$$

$$\tilde{N} = E[\tilde{\underline{X}} \tilde{\underline{Y}}^H] = E[\underline{X} (\underline{Y}^H + \underline{\Delta Y}^H)] = E[\underline{X} \underline{Y}^H] + E[\underline{X} \underline{\Delta Y}^H] = N + \Delta N. \quad (5.3.2.1-13)$$

The error matrices E and F are given by

$$E = 0 \quad (5.3.2.1-14)$$

$$F = \Delta N = E[\underline{X} \underline{\Delta Y}^H] = -j (2\pi/\delta) A_1 S \phi^H G^H A_1^H [\Delta D]^H. \quad (5.3.2.1-15)$$

Recall that

$$\epsilon = \sqrt{ ||E||^2 + ||F||^2 } = ||F|| \quad (5.3.2.1-16)$$

It is possible to show that the hk -th element of the matrix F is

$$f_{h,k} = -j(2\pi/\delta)\Delta D_h T_{h,k} \quad (5.3.2.1-17)$$

where

$$T_{h,k} = \sum_{p=1}^d \sum_{q=1}^d a_h(\theta_p) a_k^*(\theta_q) S_{pq} \sin(\theta_q) e^{-j\phi_q} \quad (5.3.2.1-18)$$

and

$$S_{pq} = E[s_p s_q^*].$$

Therefore,

$$|f_{h,k}| \leq (2\pi/\delta) |\Delta D_{\max}| \sum_{p=1}^d \sum_{q=1}^d |a_h(\theta_p)| |a_k^*(\theta_q)| |S_{pq}|. \quad (5.3.2.1-19)$$

For omni-directional sensors, $a(\theta)=1$, we get

$$|f_{h,k}| \leq (2\pi/\delta) |\Delta D_{\max}| \sum_{p=1}^d \sum_{q=1}^d |S_{pq}|. \quad (5.3.2.1-20)$$

The Frobenius norm of F is given by

$$\|F\| = \left\{ \sum_{h=1}^m \sum_{k=1}^m |f_{h,k}|^2 \right\}^{1/2}. \quad (5.3.2.1-21)$$

Thus,

$$\|F\| \leq (2\pi/\delta) |\Delta D_{\max}| \left\{ \sum_{h=1}^m \sum_{k=1}^m \sum_{p=1}^d \sum_{q=1}^d |S_{pq}|^2 \right\}^{1/2}. \quad (5.3.2.1-22)$$

which reduces to

$$\|F\| \leq (2\pi/\delta) |\Delta D_{\max}| m \left\{ \sum_{p=1}^d \sum_{q=1}^d |S_{pq}|^2 \right\}^{1/2}. \quad (5.3.2.1-23)$$

The bound on the chordal metric then becomes

$$\chi(\lambda_i, \tilde{\lambda}_i) \leq \frac{2\pi(|\Delta D_{\max}|/\delta)K^2 \sum_{p=1}^d \sum_{q=1}^d |S_{pq}|}{\sqrt{(\underline{y}_i^H \underline{M}_{X_i})^2 + (\underline{y}_i^H \underline{N}_{X_i})^2}}. \quad (5.3.2.1-24)$$

where

$$K^2 = m.$$

5.3.2.2 Linear Array: Overlapping Doublets Case

In this section we consider ESFRIT where a linear array composed of m sensors is used to solve for the angles of arrival. As for the case of the moving window, we assume that the i -th sensor is displaced by an amount ΔD_i with respect to the reference sensor which we assume as the first sensor. As seen in section 5.3.1, the received signal at the i -th sensor is given by

$$\begin{aligned} \tilde{y}_i(t, \underline{\theta}) = & \sum_{k=1}^d a_k s_k(t) (e^{j(i-1)D(\omega/c) \sin(\theta_k)}) \\ & + j(2\pi\Delta D_i/\delta) \sum_{k=1}^d a_k s_k(t) (e^{j(i-1)D(\omega/c) \sin(\theta_k)} \sin(\theta_k)) ; i=1, 2, \dots, m. \end{aligned} \quad (5.3.2.2-1)$$

Two arrays $\tilde{\underline{Y}}_1$ and $\tilde{\underline{Y}}_2$ are then formed from this data where

$$\begin{aligned} \tilde{\underline{Y}}_1 &= \{ \tilde{y}_1 \ \tilde{y}_2 \ \dots \ \tilde{y}_{m-1} \}^T \\ \tilde{\underline{Y}}_2 &= \{ \tilde{y}_2 \ \tilde{y}_3 \ \dots \ \tilde{y}_m \}^T. \end{aligned}$$

Recalling that \tilde{y}_i can be expressed as

$$\tilde{y}_i = y_i + e_i ; i=1, 2, \dots, m,$$

where y_i is the unperturbed data and e_i is the error in y_i . Therefore $\tilde{\underline{Y}}_1$ and $\tilde{\underline{Y}}_2$ are given by

$$\tilde{Y}_1 = Y_1 + E_1. \quad (5.3.2.2-2)$$

$$\tilde{Y}_2 = Y_2 + E_2. \quad (5.3.2.2-3)$$

Y_1 and Y_2 have the following decompositions

$$Y_1 = A_2 B S \quad (5.3.2.2-4)$$

$$Y_2 = A_2 B \phi S \quad (5.3.2.2-5)$$

where A , B , ϕ and S are

$$A_2 = [a_1 \ a_2 \ \dots \ a_d]$$

$$a_i = [1 \ e^{j\phi_1} \ \dots \ e^{j(m-2)\phi_1}]$$

$$B = \text{diag} \{ a_1 \ a_2 \ \dots \ a_d \}$$

$$\phi = \text{diag} [e^{j\phi_1} \ e^{j\phi_2} \ \dots \ e^{j\phi_d}]$$

and

$$\phi_k = (\omega\Delta/c) \sin(\theta_k), \quad k=1, 2, \dots, d. \quad (5.3.2.2-6)$$

Similarly E_1 and E_2 can be expressed as

$$E_1 = j (2\pi/\delta) [\Delta D]_1 A_2 B G S, \quad (5.3.2.2-7)$$

$$E_2 = j (2\pi/\delta) [\Delta D]_2 A_2 B \phi S, \quad (5.3.2.2-8)$$

where A , B , ϕ and S have been defined earlier and G , $[\Delta D]_1$ and $[\Delta D]_2$ are

$$G = \text{diag} \{ \sin(\theta_1) \ \sin(\theta_2) \ \dots \ \sin(\theta_d) \},$$

$$[\Delta D]_1 = \text{diag} \{ \Delta D_1 \ \Delta D_2 \ \dots \ \Delta D_{m-1} \},$$

$$[\Delta D]_2 = \text{diag} \{ \Delta D_2 \ \Delta D_3 \ \dots \ \Delta D_m \}.$$

Two matrices \tilde{M} and \tilde{N} are then formed where

$$\tilde{M} = E[\tilde{Y}_1 \ \tilde{Y}_1^H] = E[(Y_1 + E_1)(Y_1 + E_1)^H],$$

$$\tilde{N} = E[\tilde{Y}_1 \ \tilde{Y}_2^H] = E[(Y_1 + E_1)(Y_2 + E_2)^H].$$

These can be decomposed into

$$\tilde{M} = E[Y_1 \ Y_1^H] + E[Y_1 \ E_1^H] + E[E_1 \ Y_1^H] + E[E_1 \ E_1^H] = M + E, \quad (5.3.2.2-9)$$

$$\tilde{N} = E[Y_1 \ Y_2^H] + E[Y_1 \ E_2^H] + E[E_1 \ Y_2^H] + E[E_1 \ E_2^H] = N + F, \quad (5.3.2.2-10)$$

where

$$M = E[Y_1 \ Y_1^H],$$

$$N = E[\underline{Y}_1 \underline{E}^H_1] + E[\underline{E}_1 \underline{Y}^H_1] + E[\underline{E}_1 \underline{E}^H_1],$$

$$E = E[\underline{Y}_1 \underline{Y}^H_2],$$

$$F = E[\underline{Y}_1 \underline{E}^H_2] + E[\underline{E}_1 \underline{Y}^H_2] + E[\underline{E}_1 \underline{E}^H_2].$$

To obtain a bound on the chordal metric one needs to explicitly express ϵ in terms of the parameters of interest. One has thus to get the Euclidean norms of E and F . It can be shown that

$$E[\underline{Y}_1 \underline{E}^H_1] = -j(2\pi/\delta) A_2 B S B^H G^H A_2^H [\Delta D]_1^H,$$

$$E[\underline{E}_1 \underline{Y}^H_1] = E[\underline{E}_1 \underline{Y}^H_1]^H,$$

$$E[\underline{E}_1 \underline{E}^H_1] = (2\pi/\delta)^2 [\Delta D]_1 A_2 G B S B^H G^H A_2^H [\Delta D]_1^H,$$

$$E[\underline{Y}_1 \underline{E}^H_2] = -j(2\pi/\delta) A_2 B S B^H G^H A_2^H [\Delta D]_1^H,$$

$$E[\underline{E}_1 \underline{Y}^H_2] = j(2\pi/\delta) [\Delta D]_1 A_2 G B S B^H A_2^H,$$

$$E[\underline{E}_1 \underline{E}^H_2] = (2\pi/\delta)^2 [\Delta D]_1 A_2 G B S B^H G^H A_2^H [\Delta D]_2^H.$$

Consider the matrix $E[\underline{Y}_1 \underline{E}^H_1]$. The hk -th element of this matrix can be expressed as

$$-j(2\pi/\delta) \Delta D_h T_{hk},$$

where

$$T_{hk} = \sum_{p=1}^d \sum_{q=1}^d a_{pq} S_{pq} \sin(\theta_q) e^{j(h-1)\phi_p} e^{-j(k-1)\phi_q},$$

and a_{pq} and S_{pq} have been defined earlier. Since the matrix $E[\underline{E}_1 \underline{Y}^H_1]$ was shown to be $E[\underline{E}_1 \underline{Y}^H_1]^H$, the hk -th element of this matrix can be written as

$$j(2\pi/\delta) \Delta D_h T_{kh}^*.$$

Because the matrix $E[\underline{E}_1 \underline{E}^H_1]$ is given by $(2\pi/\delta)^2 [\Delta D]_1 A G B S B^H G^H A^H [\Delta D]_1^H$, a term of the form $(\Delta D/\delta)^2$ will be contained in all the elements of this matrix causing the matrix to be negligible. Therefore, the hk -th element of the matrix E is given by

$$e_{hk} = -j(2\pi/\delta) \Delta D_h T_{hk} + j(2\pi/\delta) \Delta D_h T_{kh}^*. \quad (5.3.2.2-11)$$

$$e_{hk} = j(2\pi/\delta)\Delta D_h (-T_{hk} + T_{kh}^*). \quad (5.3.2.2-12)$$

Therefore,

$$|e_{hk}| \leq 2(2\pi/\delta) |\Delta D_{\max}| \sum_{p=1}^d \sum_{q=1}^d |a_{pq}| |S_{pq}| \quad (5.3.2.2-13)$$

The Frobenius norm of E is given by

$$||E|| = \left\{ \sum_{h=1}^m \sum_{k=1}^m |e_{hk}|^2 \right\}^{1/2}. \quad (5.3.2.2-14)$$

Thus

$$||E|| \leq (2\pi/\delta) |\Delta D_{\max}| [2(m-2)(m-1)]^{1/2} \sum_{p=1}^d \sum_{q=1}^d |a_{pq}| |S_{pq}|. \quad (5.3.2.2-15)$$

The second step is to compute $||F||$. For this recall that

$$F = E[\underline{Y}_1 \underline{E}^H_2] + E[\underline{E}_1 \underline{Y}^H_2] + E[\underline{E}_1 \underline{E}^H_2],$$

where

$$E[\underline{Y}_1 \underline{E}^H_2] = -j(2\pi/\delta) A_2 B S B^H G^H \Phi A_2^H [\Delta D]_1^H,$$

$$E[\underline{E}_1 \underline{Y}^H_2] = j(2\pi/\delta) [\Delta D]_1 A_2 G B S B^H \Phi A_2^H,$$

$$E[\underline{E}_1 \underline{E}^H_2] = (2\pi/\delta)^2 [\Delta D]_1 A_2 G B S B^H G^H \Phi A_2^H [\Delta D]_2^H.$$

Because $E[\underline{E}_1 \underline{E}^H_2]$ will have a factor of $(\Delta D/\delta)^2$ which tends to zero, this term becomes negligible and is omitted in the computation of the matrix F.

An element hk -th of the matrix $E[\underline{Y}_1 \underline{E}^H_2]$ is of the form

$$-j(2\pi/\delta)\Delta D_h \sum_{p=1}^d \sum_{q=1}^d a_{pq} S_{pq} \sin(\theta_q) e^{j(h-1)\phi_p} e^{-jk\phi_q}.$$

The hk -th element of the matrix $E[\underline{E}_1 \underline{Y}^H_2]$ is of the form

$$j(2\pi/\delta)\Delta D_h \sum_{p=1}^d \sum_{q=1}^d a_{pq} S_{pq} \sin(\theta_p) e^{j(h-1)\phi_p} e^{-jk\phi_q}.$$

The hk -th element of the matrix F , f_{hk} , is given by

$$f_{hk} = j(2\pi/\delta)\Delta D_h \sum_{p=1}^d \sum_{q=1}^d a_{pq} S_{pq} e^{j(h-1)\phi_p} e^{-jk\phi_q} (\sin(\theta_p) + \sin(\theta_q)). \quad (5.3.2.2-16)$$

Therefore,

$$|f_{hk}| \leq (2\pi/\delta) |\Delta D_{\max}| \sum_{p=1}^d \sum_{q=1}^d |a_{pq}| |S_{pq}|, \quad (5.3.2.2-17)$$

and

$$|F| \leq 2\pi(|\Delta D_{\max}|/\delta) [(m-1)^2 + (m-1)(m-2)]^{1/2} \sum_{p=1}^d \sum_{q=1}^d |a_{pq}| |S_{pq}|. \quad (5.3.2.2-18)$$

Recall

$$\epsilon = \sqrt{||E||^2 + ||F||^2}$$

$$\epsilon \leq 2\pi(|\Delta D_{\max}|/\delta) [(m-1)^2 + (m-1)(m-2) + 2(m-2)(m-1)]^{1/2} \sum_{p=1}^d \sum_{q=1}^d |a_{pq}| |S_{pq}|.$$

$$\epsilon \leq 2\pi(|\Delta D_{\max}|/\delta) [(m-1)(4m-7)]^{1/2} \sum_{p=1}^d \sum_{q=1}^d |a_{pq}| |S_{pq}|. \quad (5.3.2.2-19)$$

Let $K_3 = [(m-1)(4m-7)]^{1/2}$. The bound on the chordal metric then becomes

$$\chi(\lambda_i, \tilde{\lambda}_i) \leq \frac{2\pi(|\Delta D_{\max}|/\delta) K_3 \sum_{p=1}^d \sum_{q=1}^d |S_{pq}| |a_{pq}|}{\sqrt{(\gamma_i^{H M X_i})^2 + (\gamma_i^{H N X_i})^2}}. \quad (5.3.2.2-20)$$

5.3.2.3 Linear Array: Non-Overlapping Doublets Case

In this section we assume that two adjacent sensors form a pair so that two non-overlapping arrays \bar{Y}_1 and \bar{Y}_2 are formed where

$$\bar{Y}_1 = \{ \bar{y}_1 \bar{y}_3 \dots \bar{y}_{m-1} \}^T$$

$$\bar{Y}_2 = \{ \bar{y}_2 \bar{y}_4 \dots \bar{y}_m \}^T.$$

m is assumed to be a multiple of 2. Recalling that \bar{y}_i can be expressed as

$$\bar{y}_i = y_i + e_i ; i=1, 2, \dots, m,$$

where y_i is the unperturbed data and e_i is the error in y_i . Therefore, \bar{Y}_1 and \bar{Y}_2 can be expressed as

$$\bar{Y}_1 = Y_1 + E_1.$$

$$\bar{Y}_2 = Y_2 + E_2.$$

Y_1 and Y_2 have the following decomposition

$$Y_1 = A_3 B S \quad (5.3.2.3-1)$$

$$Y_2 = A_3 B \phi S \quad (5.3.2.3-2)$$

where A_3 , B , ϕ and S are

$$A_3 = [\underline{a}_1 \ \underline{a}_2 \ \dots \ \underline{a}_d]$$

$$\underline{a}_i = [1 \ e^{j2\phi_i} \ \dots \ e^{j(m-2)\phi_i}]$$

$$B = \text{diag} \{ a_1 \ a_2 \ \dots \ a_d \}$$

$$\phi = \text{diag} [e^{j\phi_1} \ e^{j\phi_2} \ \dots \ e^{j\phi_d}]$$

and

$$\phi_k = (\omega \Delta / c) \sin(\theta_k) , k=1, 2, \dots, d.$$

Similarly E_1 and E_2 can be written as

$$E_1 = j (2\pi / \delta) [\Delta D]_1 A_3 B G S, \quad (5.3.2.3-3)$$

$$E_2 = j (2\pi / \delta) [\Delta D]_2 A_3 B \phi S, \quad (5.3.2.3-4)$$

where A_3 , B , ϕ and S have been defined earlier and G , $[\Delta D]_1$ and $[\Delta D]_2$ are

$$G = \text{diag} \{ \sin(\theta_1) \ \sin(\theta_2) \ \dots \ \sin(\theta_d) \},$$

$$[\Delta D]_1 = \text{diag} \{ \Delta D_1 \ \Delta D_3 \ \dots \ \Delta D_{m-1} \},$$

$$[\Delta D]_2 = \text{diag} \{ \Delta D_2 \Delta D_4 \dots \Delta D_m \}.$$

Two matrices \tilde{M} and \tilde{N} are then formed where

$$\tilde{M} = E[\tilde{Y}_1 \tilde{Y}_1^H] = E[(Y_1 + E_1)(Y_1 + E_1)^H],$$

$$\tilde{N} = E[\tilde{Y}_1 \tilde{Y}_2^H] = E[(Y_1 + E_1)(Y_2 + E_2)^H].$$

These can be decomposed into

$$\tilde{M} = E[Y_1 Y_1^H] + E[Y_1 E_1^H] + E[E_1 Y_1^H] + E[E_1 E_1^H] = M + E, \quad (5.3.2.3-5)$$

$$\tilde{N} = E[Y_1 Y_2^H] + E[Y_1 E_2^H] + E[E_1 Y_2^H] + E[E_1 E_2^H] = N + F, \quad (5.3.2.3-6)$$

where

$$M = E[Y_1 Y_1^H],$$

$$N = E[Y_1 Y_2^H] + E[E_1 Y_2^H] + E[E_1 E_2^H],$$

$$E = E[Y_1 E_1^H],$$

$$F = E[Y_1 E_2^H] + E[E_1 Y_2^H] + E[E_1 E_2^H].$$

It can be shown that

$$E[Y_1 E_1^H] = -j(2\pi/\delta) A_3 B S B^H G^H A_3^H [\Delta D]_1^H,$$

$$E[E_1 Y_1^H] = E[E_1 Y_1^H]^H,$$

$$E[E_1 E_1^H] = (2\pi/\delta)^2 [\Delta D]_1 A_3 G B S B^H G^H A_3^H [\Delta D]_1^H,$$

$$E[Y_1 E_2^H] = -j(2\pi/\delta) A_3 B S B^H G^H \Phi A_3^H [\Delta D]_1^H,$$

$$E[E_1 Y_2^H] = j(2\pi/\delta) [\Delta D]_1 A_3 G B S B^H \Phi A_3^H,$$

$$E[E_1 E_2^H] = (2\pi/\delta)^2 [\Delta D]_1 A_3 G B S B^H G^H \Phi A_3^H [\Delta D]_2^H.$$

Consider the matrix $E[Y_1 E_1^H]$. The hk -th element of this matrix can be expressed as

$$-j(2\pi/\delta) \Delta D_{2h-1} T_{hk}$$

where

$$T_{hk} = \sum_{p=1}^d \sum_{q=1}^d a_{pq} S_{pq} \sin(\theta_q) e^{j(2h-2)\phi_p} e^{-j(2-2)\phi_q}; \quad h, k = 1, 2, \dots, (m/2)$$

and a_{pq} and S_{pq} have been defined earlier. Since the matrix $E[E_1 Y_1^H]$ was

shown to be $E[\underline{E}_1 \underline{Y}_1^H]^H$, the hk -th element of this matrix can be written as

$$j(2\pi/\delta)\Delta D_{2h-1} T_{hk}^*$$

Because there will be a term $(\delta D/\delta)^2$ in the matrix $E[\underline{E}_1 \underline{E}_1^H]$ which tends to zero, the hk -th element of the matrix E is approximated by

$$e_{hk} = -j(2\pi/\delta)\Delta D_h T_{hk} + j(2\pi/\delta)\Delta d_h T_{kh}^*, \quad (5.3.2.3-7)$$

$$e_{hk} = j(2\pi/\delta)\Delta D_h (-T_{hk} + T_{kh}^*). \quad (5.3.2.3-8)$$

Therefore,

$$|e_{hk}| \leq 2(2\pi/\delta) |\Delta D_{\max}| \sum_{p=1}^d \sum_{q=1}^d |a_{pq}| |S_{pq}|. \quad (5.3.2.3-9)$$

The Frobenius norm of F is given by

$$||E|| = \left\{ \sum_{h=1}^{m/2} \sum_{k=1}^{m/2} |e_{hk}|^2 \right\}^{1/2}. \quad (5.3.2.3-10)$$

Thus

$$||E|| \leq (2\pi/\delta) |\Delta D_{\max}| [2(m/2-1)(m/2)]^{1/2} \sum_{p=1}^d \sum_{q=1}^d |a_{pq}| |S_{pq}|. \quad (5.3.2.3-11)$$

The second step is to compute $||F||$. Recall that

$$F = E[\underline{Y}_1 \underline{E}_2^H] + E[\underline{E}_1 \underline{Y}_2^H] + E[\underline{E}_1 \underline{E}_2^H].$$

The element $E[\underline{E}_1 \underline{E}_2^H]$ will be neglected because it will have a factor of $(\Delta D/\delta)^2$ which tends to zero. The hk -th element of the matrix $E[\underline{Y}_1 \underline{E}_2^H]$ is of the form

$$-j(2\pi/\delta)\Delta D_{2h} \sum_{p=1}^d \sum_{q=1}^d a_{pq} S_{pq} \sin(\theta_q) e^{j(2h-2)\phi_p} e^{-j(2k-1)\phi_q}.$$

The hk -th element of the matrix $E[\underline{E}_1 \underline{Y}_2^H]$ is of the form

$$j(2\pi/\delta)\Delta D_{2h-1} \sum_{p=1}^d \sum_{q=1}^d a_{pq} S_{pq} \sin(\theta_p) e^{j(2h-1)\phi_p} e^{-j(2k-2)\phi_q}.$$

Therefore,

$$|f_{hk}| \leq (2\pi/\delta) |\Delta D_{\max}| \sum_{p=1}^d \sum_{q=1}^d |a_{pq}| |S_{pq}|, \quad (5.3.2.3-12)$$

and

$$|F| \leq 2\pi (|\Delta D_{\max}|/\delta) [(m/2)^2 + (m/2-1)(m/2)]^{1/2} \sum_{p=1}^d \sum_{q=1}^d |a_{pq}| |S_{pq}|. \quad (5.3.2.3-13)$$

Recall

$$\epsilon = \sqrt{||E||^2 + ||F||^2}$$

$$\epsilon \leq 2\pi (|\Delta D_{\max}|/\delta) [(m/2)^2 + (m/2-1)(m/2) + 2(m/2)(m/2-1)]^{1/2} \sum_{p=1}^d \sum_{q=1}^d |a_{pq}| |S_{pq}|.$$

$$\epsilon \leq 2\pi (|\Delta D_{\max}|/\delta) [(m/2)(2m-3)]^{1/2} \sum_{p=1}^d \sum_{q=1}^d |a_{pq}| |S_{pq}|. \quad (5.3.2.3-14)$$

Let $K_4 = [(m/2)(2m-3)]^{1/2}$. The bound on the chordal metric then becomes

$$\chi(\lambda_i, \bar{\lambda}_i) \leq \frac{2\pi (|\Delta D_{\max}|/\delta) K_4 \sum_{p=1}^d \sum_{q=1}^d |S_{pq}| |a_{pq}|}{\sqrt{(\gamma_i^{H_{M_{X_i}}})^2 + (\gamma_i^{H_{N_{X_i}}})^2}}. \quad (5.3.2.3-15)$$

5.3.3 COMPUTER SIMULATION

In this section, we studied the effects of errors due to sensor spacing on the performance of the 3 algorithms discussed earlier. The model

used consisted of two incoherent ($d=2$) incident on a linear array consisting of eight sensors ($m=8$). The sources are assumed to be located at $\theta_1=16^\circ$ and $\theta_2=24^\circ$. For simplicity, the case of omnidirectional sensors was assumed for all three cases. In the simulation the case of perfect sensor spacing was first considered. 100 snapshots were used to obtain the matrices M and N . The process was repeated 50 times and the results averaged to obtain nominal values for λ_i , \underline{x}_i and \underline{y}_i ; $i=1,2$. A random perturbation with a maximum ΔD varying from $D/100$ to $D/1000$ was then introduced and the procedure used in the unperturbed case was repeated. D was assumed to be equal to half the wavelength so that $\omega\delta/c=\pi$ (δ being the wavelength). The computed results are shown in tables 5.7 to 5.14. If the error is small enough, then the bounds derived in this section give acceptable results. However, if the error large, then the conditions for which these bounds have been derived do not hold any more and therefore the bounds are not applicable.

Moving Window

Angle=24°

ΔD	$\bar{\theta}$ obtained from Bound	$\bar{\theta}$ obtained from chordal metric	$\bar{\theta}$ obtained from λ
D/100	26.47194	24.00648	24.00001
D/300	24.81639	24.00216	24.00001
D/500	24.48902	24.00130	24.00000
D/700	24.34906	24.00093	24.00000
D/1000	24.24422	24.00064	24.00000

Table 5.7
(Sample Mean)

Angle=16°

ΔD	$\bar{\theta}$ obtained from Bound	$\bar{\theta}$ obtained from chordal metric	$\bar{\theta}$ obtained from λ
D/100	20.68584	16.00554	16.00070
D/300	17.53180	16.00184	16.00024
D/500	16.91655	16.00110	16.00014
D/700	16.65397	16.00079	16.00010
D/1000	16.45743	16.00055	16.00007

Table 5.8
(Sample Mean)

ESPRIT: Linear Overlapping Case

Angle=24°

ΔD	$\tilde{\theta}$ obtained from Bound	$\tilde{\theta}$ obtained from chordal metric	$\tilde{\theta}$ obtained from λ
D/100	25.67951	24.00629	24.00038
D/300	24.55655	24.00210	24.00015
D/500	24.33357	24.00126	24.00009
D/700	24.23815	24.00090	24.00006
D/1000	24.16665	24.00063	24.00005

Table 5.9
(Sample Mean)

Angle=16°

ΔD	$\tilde{\theta}$ obtained from Bound	$\tilde{\theta}$ obtained from chordal metric	$\tilde{\theta}$ obtained from λ
D/100	18.17524	16.00500	16.00077
D/300	16.72113	16.00167	16.00021
D/500	16.43227	16.00100	16.00013
D/700	16.30865	16.00071	16.00009
D/1000	16.21599	16.00050	16.00006

Table 5.10
(Sample Mean)

ESPRIT: Linear Non Overlapping Case

Angle=24°

ΔD	$\bar{\theta}$ obtained from Bound	$\bar{\theta}$ obtained from chordal metric	$\bar{\theta}$ obtained from λ
D/100	25.76599	24.01485	24.00153
D/300	24.58539	24.00493	24.00053
D/500	24.35086	24.00296	24.00032
D/700	24.25051	24.00212	24.00023
D/1000	24.17530	24.00148	24.00016

Table 5.11
(Sample Mean)

Angle=16°

ΔD	$\bar{\theta}$ obtained from Bound	$\bar{\theta}$ obtained from chordal metric	$\bar{\theta}$ obtained from λ
D/100	18.25734	16.01279	16.00038
D/300	16.74875	16.00426	16.00012
D/500	16.44886	16.00255	16.00007
D/700	16.32050	16.00183	16.00005
D/1000	16.22420	16.00128	16.00003

Table 5.12
(Sample Mean)

ESPRIT: General Case

Angle=24°

ΔD	$\bar{\theta}$ obtained from Bound	$\bar{\theta}$ obtained from chordal metric	$\bar{\theta}$ obtained from λ
D/100	25.57809	24.01101	23.99986
D/300	24.52344	24.00366	23.99995
D/500	24.31377	24.00220	23.99997
D/700	24.22404	24.00157	23.99998
D/1000	24.15678	24.00110	23.99998

Table 5.13
(Sample Mean)

Angle=16°

ΔD	$\bar{\theta}$ obtained from Bound	$\bar{\theta}$ obtained from chordal metric	$\bar{\theta}$ obtained from λ
D/100	18.01733	16.01102	15.99943
D/300	16.66954	16.00368	15.99981
D/500	16.40142	16.00221	15.99989
D/700	16.28663	16.00158	15.99992
D/1000	16.20060	16.00111	15.99994

Table 5.14
(Sample Mean)

CHAPTER 6

CONCLUSION AND FUTURE RESEARCH

6.1 CONCLUSION

In this chapter we discuss the contributions of this work which dealt exclusively with the non search procedure known as the Matrix Pencil Approach. ESPRIT and the Moving Window are but two of the operators that can be used in the formulation of this approach which is based on the generalized eigenvalue decomposition of two matrices generated from the received data. Special attention is given to the Moving Window since it was shown to apply even in the case of fully correlated signals. However, the method as applied in [1] did not perform as was expected especially in cases of low signal to noise ratio. We have shown that the separation of the signal and noise subspaces is possible with the use of a window of length L with $d \leq L \leq (m-d)$ where m is the number of sensors and d is the number of sources. This, in turn, allowed us to consider only those eigenvalues which are related to the signal subspace by using a singular value decomposition (SVD). In [1] a window of length $L=m-d$ was recommended. We have explained why this choice is actually the worst one since it results in matrices of dimension $(d \times d)$ which do not permit recognition of the two subspaces.

Most of the proposed high resolution techniques in direction finding treat each sensor in the array as if it exists by itself. In practice however, mutual coupling exists and is very strong if the separation between the sensor is small. This can significantly alter the structure of the matrices involved in the formulation of the proposed algorithms which, in turn, drastically degrades their performance. In chapter 3 we have pro-

posed a model which takes into account the effects of mutual coupling between the sensor elements of the array. Under these conditions, we have studied the performance of the Matrix Pencil Approach and we have shown that the decompositions needed in this formulation are not possible. We proposed two methods to solve this problem. The first method consists of obtaining an estimate of the incident signal vector. A minimum mean-squared error estimation was then performed and an estimate was found. It was shown, through computer simulations, that the angles of arrival of the sources are well estimated using this estimate. In the second method, some pre-processing was needed in order to generate the desired incident signal vectors. This was referred to as the Direct Method. Several schemes have been proposed depending on the nature of the algorithm used. All schemes have been shown to be successful in estimating the angular locations of the sources.

The previous analysis dealt with narrowband signals. The modeling used there is not appropriate when dealing with wideband sources. Chapter 4 deals with signals of this nature. We have devised three techniques the first of which is original in the sense that the Matrix Pencil Approach is utilized with a signal model not used previously in other approaches. The signals are identified by their natural frequencies and their angles of arrival. This modeling is appropriate when the source signals are non stationary. Three matrix pencils have been generated from the data. The rank reducing values of the first matrix pencil allows us to generate estimates of the natural frequencies. The rank reducing values of a second matrix pencil are shown to be related to both the angles of arrival and the natural frequencies of the sources. At this stage, it is not apparent which natural frequencies go with which angles of arrival. The rank reducing

values of a third matrix pencil are used to eliminate any ambiguities that could arise. The second method utilizes the same model used by Su and Morf. However, the array configuration used is similar to the first method. The sources are assumed to be linear systems driven by white noise sequences. A scheme was devised in which the angles of arrival could be solved for with the knowledge of the system poles. These poles are shown to be a mixture of the source poles and the sensor poles. The analysis is carried out on the unit circle by using a discrete Fourier transform on the data sequences. The third method makes use of the CSS of Wang and Kaveh. This method was used in conjunction with ESPRIT and the Moving Window. The method is shown to perform very well and the sample variances of the angle estimates are shown to closely follow the Cramer-Rao Lower Bound (CRLB).

Chapter 5 analyzes the effects of the noise and perturbations due to sensor spacing on the performance of ESPRIT and the Moving Window. A measure, termed the chordal metric, was introduced. The chordal metric is shown to be a function of the true and perturbed angles of arrival. Geometric upper bounds have been derived for the Moving Window and ESPRIT operators. The proposed bounds give insight into performance degradation when ideal modeling is not met.

6.2 FUTURE WORK

The Matrix Pencil Approach is based on exact knowledge of the number of sources. Several methods have been proposed in the case of Gaussian signals [40,41]. These methods are shown to be very effective with respect to some set criteria. Special efforts should be devoted to non Gaussian cases. Also, the wideband methods described in chapter 4 assume the number of natural frequencies (first method) and the number of poles (second meth-

od) are known. Significant distortion will arise if this number is underestimated. More effort is needed for this particular case.

We have studied the effects of mutual coupling between the array elements in the narrowband case where only a single carrier frequency is assumed. In the case of wideband sources, the mutual impedances become frequency dependent. This significantly changes the nature of the signal modeling. The method that we have used should be generalized to the case of wideband signals.

Notice also that the bounds derived for the chordal metric in chapter 5 are not very tight. This is mainly due to the procedures used in evaluating the Frobenius norms of the error matrices. There exist other techniques to evaluate these norms. One can certainly tighten these bounds in order to obtain more insight into performance degradation when ideal conditions are not met.

An interesting case arises when one mounts an array of sensors on an airplane. The vibrations of the airplane will cause the sensors to be displaced from their ideal positions. A two dimensional perturbation analysis is needed to evaluate the chordal metric. Also, one is expected to study the effects of the structure on the mutual impedances.

Finally H. Ouibrahim [1] proposed a third operator, called the summation operator, that can be used in the formulation of the matrix pencil. The work that we have developed here can be easily generalized using this operator.

APPENDIX

COMPUTATION OF THE CRLB

Consider a linear uniformly spaced array consisting of m wideband sensors and let there be d wideband sources ($d < m$) located in the far field and emitting signals arriving at the array from direction θ_i ; $i=1,2,\dots,d$. The observed data vector \underline{X} at a frequency ω_l can be expressed as

$$\underline{X}(\omega_l) = A(\omega_l)\underline{S}(\omega_l) + \underline{N}(\omega_l) ; l=1, 2, \dots, L \quad (\text{A.1})$$

where

A is the direction matrix

\underline{S} is the source vector

and

\underline{N} is the additive noise vector.

Assume the noise components to be statistically independent zero mean random variables with variance σ^2 . Assume also that \underline{S} is a zero mean random vector. Let R be the covariance matrix of the observed data vector \underline{X} . Let $\underline{\theta}$ denote a parameter vector whose elements consist of the angles of arrival and statistical parameters related to the signal and noise complex envelopes. The joint probability density function of \underline{X} given $\underline{\theta}$ is given by

$$f(\underline{X}/\underline{\theta}) = (2\pi)^{-(m/2)} \{\det(R)\}^{-1/2} \exp\{-(1/2)\underline{X}^H R^{-1} \underline{X}\}. \quad (\text{A.2})$$

Therefore,

$$\text{Log}\{f(\underline{X}/\underline{\theta})\} = -(m/2)\text{Log}(2\pi) - (1/2)\text{Log}(\det(R)) - (1/2)\underline{X}^H R^{-1} \underline{X}. \quad (\text{A.3})$$

Taking into account all the frequency components and assuming statistical independence from one band to the next, we obtain

$$\text{Log}\{f(\underline{X}/\underline{\theta})\} = C - (1/2) \sum_{l=1}^L \text{Log}(\det(R)) - (1/2) \sum_{l=1}^L \underline{X}^H R^{-1} \underline{X}. \quad (\text{A.4})$$

where C is a constant. Let $\hat{\underline{\theta}}$ be an unbiased estimator of $\underline{\theta}$. It is known that

$$\text{Var}(\hat{\underline{\theta}}) \geq J^{-1}(\underline{\theta}) \quad (\text{A.5})$$

where J is the Fisher information matrix whose ij -th entry is

$$[J(\underline{\theta})]_{i,j} = E \{ (\partial \text{Log}(f(\underline{X}/\underline{\theta})) / \partial \theta_i) (\partial \text{Log}(f(\underline{X}/\underline{\theta})) / \partial \theta_j) \}. \quad (\text{A.6})$$

It has been shown [89] that

$$[J(\underline{\theta})]_{i,j} = (1/2) \text{Tr} \{ (R^{-1} \partial R / \partial \theta_i) (R^{-1} \partial R / \partial \theta_j) \} \quad (\text{A.7})$$

where $\text{Tr}(B)$ denotes the trace of the matrix B .

For the sake of clarity, assume that 2 correlated sources s_1 and s_2 impinge on the array from directions θ_1 and θ_2 , respectively. Let ρ be their correlation coefficient. Assuming that the noise components are independent zero mean random variables with variance σ_n^2 , the covariance matrix R can be written as

$$R = E [\underline{X} \underline{X}^H] = A S A^H + \sigma_n^2 I \quad (\text{A.8})$$

where I is the (mxm) identity matrix. The matrix S can be expressed as

$$S = \begin{bmatrix} \sigma_1^2 & \rho \sigma_1 \sigma_2 \\ \rho \sigma_1 \sigma_2 & \sigma_2^2 \end{bmatrix},$$

where the variances of s_1 and s_2 are denoted by σ_1^2 and σ_2^2 , respectively.

The signal to noise ratios SNR_1 and SNR_2 are defined as

$$\text{SNR}_1 = 10 \log \{ \sigma_1^2 / \sigma_n^2 \},$$

$$\text{SNR}_2 = 10 \log \{ \sigma_2^2 / \sigma_n^2 \}.$$

Therefore, σ_1^2 and σ_2^2 are given by

$$\sigma_1^2 = \sigma_n^2 10^{(\text{SNR}_1/10)},$$

$$\sigma_2^2 = \sigma_n^2 10^{(\text{SNR}_2/10)}.$$

The matrix S can be rewritten as

$$S = \begin{bmatrix} \sigma_n^2 10(\text{SNR}_1/10) & \rho \sigma_n^2 10(\text{SNR}_1+\text{SNR}_2)/20 \\ \rho \sigma_n^2 10((\text{SNR}_1+\text{SNR}_2)/20) & \sigma_n^2 10(\text{SNR}_2/10) \end{bmatrix}.$$

The matrix A is of the form

$$A = \begin{bmatrix} 1 & 1 \\ e^{j\phi_1} & e^{j\phi_2} \\ \vdots & \vdots \\ e^{j(m-1)\phi_1} & e^{j(m-1)\phi_2} \end{bmatrix},$$

where $\phi_i = (\omega\Delta/c)\sin(\theta_i)$. The parameter vector $\underline{\theta}$ is given by

$$\underline{\theta}^T = [\theta_1, \theta_2, \rho, \sigma_n^2, \text{SNR}_1, \text{SNR}_2].$$

Six derivatives have to be computed. They are

$$\partial R / \partial \theta_1 = (\partial A / \partial \theta_1) S A^H + A S (\partial A^H / \partial \theta_1),$$

$$\partial R / \partial \theta_2 = (\partial A / \partial \theta_2) S A^H + A S (\partial A^H / \partial \theta_2),$$

$$\partial R / \partial \rho = A (\partial S / \partial \rho) A^H,$$

$$\partial R / \partial (\sigma_n^2) = A (\partial S / \partial (\sigma_n^2)) A^H + I_m,$$

$$\partial R / \partial \text{SNR}_1 = A (\partial S / \partial \text{SNR}_1) A^H$$

$$\partial R / \partial \text{SNR}_2 = A (\partial S / \partial \text{SNR}_2) A^H$$

Note that

$$\partial S / \partial \rho = \sigma_n^2 10(\text{SNR}_1+\text{SNR}_2)/20 \begin{bmatrix} 0 & 1 \\ 1 & 0 \end{bmatrix},$$

$$\partial S / \partial (\sigma_n^2) = \begin{bmatrix} 10(\text{SNR}_1/10) & \rho 10(\text{SNR}_1+\text{SNR}_2)/20 \\ \rho 10(\text{SNR}_1+\text{SNR}_2)/20 & 10(\text{SNR}_2/10) \end{bmatrix}.$$

$$\partial S / \partial \text{SNR}_1 = \begin{bmatrix} ((\text{Ln}(10)/10) 10(\text{SNR}_1/10) & \rho((\text{Ln}(10)/20) 10(\text{SNR}_1+\text{SNR}_2)/20) \\ \rho((\text{Ln}(10)/20) 10(\text{SNR}_1+\text{SNR}_2)/20) & 0 \end{bmatrix}.$$

$$\partial S / \partial \text{SNR}_2 = \begin{bmatrix} 0 & \rho((\text{Ln}(10)/20) 10(\text{SNR}_1+\text{SNR}_2)/20) \\ \rho((\text{Ln}(10)/20) 10(\text{SNR}_1+\text{SNR}_2)/20) & ((\text{Ln}(10)/10) 10(\text{SNR}_1/10) \end{bmatrix}.$$

$$(\partial A / \partial \theta_1) = \begin{bmatrix} 0 & 0 \\ (\omega \Delta / c) \cos(\theta_1) e^{j \phi_1} & 0 \\ \vdots & \vdots \\ (m-1)(\omega \Delta / c) \cos(\theta_1) e^{j(m-1) \phi_1} & 0 \end{bmatrix},$$

and

$$(\partial A / \partial \theta_2) = \begin{bmatrix} 0 & 0 \\ 0 & (\omega \Delta / c) \cos(\theta_2) e^{j \phi_2} \\ \vdots & \vdots \\ 0 & (m-1)(\omega \Delta / c) \cos(\theta_2) e^{j(m-1) \phi_2} \end{bmatrix}.$$

Having defined all the above quantities, it is easy to do the multiplications needed in equation (A.7) and determine the CRLB.

REFERENCES

- [1]. H. Oubrahim, "A Generalized Approach to Direction Finding," Ph.D dissertation, Syracuse University, Dec. 1986.
- [2]. M. S. Bartlett, "Smoothing Periodograms from Time Series With Continuous Spectra," Nature, London, vol. 161, pp. 686-687, May 1948.
- [3]. R. H. Jones, "A Reappraisal of the Periodogram in Spectral Analysis," Technometrics, vol. 7, pp. 531-542, Nov. 1965.
- [4]. R. B. Blackman and J. W. Tukey, "The Measurement of Power Spectra from the Point of View of Communication Engineering," Dover Publications Inc., NY 1958.
- [5]. A. H. Nuttall and G. C. Carter, "Spectral Estimation Using Combined Time and Lag Weighting," Proc. IEEE, vol. 70, pp. 115-1125, Sept. 1982.
- [6]. S. L. Marple, "Digital Spectral Analysis With Applications," pp. 178-184, Prentice Hall Inc., NJ 1987.
- [7]. S. M. Kay, "Modern Spectral Estimation," Prentice Hall Inc., Englewood Cliffs, NJ 1987.
- [8]. J. P. Burg, "Maximum Entropy Spectral Analysis," Ph.D dissertation, Dept. of Geophysics, Stanford University, 1975.
- [9]. J. Makhoul, "Linear Prediction: A Tutorial Review," Proc. IEEE, vol. 63, pp. 561-580, April 1975.
- [10]. _____, "A Class of All Zeros Lattice Digital Filters; Properties and Applications," IEEE Trans. ASSP, vol. ASSP-26, pp. 304-314, Aug. 1978.
- [11]. A. Papoulis, "Maximum Entropy and Spectral Estimation: A Review," IEEE Trans. ASSP, vol. ASSP-29, pp. 1176-1186, Dec. 1981.
- [12]. J. P. Burg, "Maximum Entropy Spectral Analysis," Proc. 37th Meeting of the Society of Exploration Geophysicists, 1967.
- [13]. T. J. Ulrych and R. W. Clayton, "Time Series Modeling and Maximum Entropy," Phys. Earth Planet. Inter., vol. 12, pp. 188-200, Aug. 1976.
- [14]. A. H. Nuttall, "Spectral Analysis of a Univariate Process With Bad Data via Maximum Entropy and Linear Predictive Technique," Naval Underwater Systems Center, Technical Report TR-5303, New London, Conn., March 1976.
- [15]. D. W. Tufts and R. Kumaresan, "Frequency Estimation of Multiple Sinusoids: Making Linear Prediction Perform Like Maximum likelihood," Proc. IEEE, vol. 70, pp. 975-990, Sept. 1982.
- [16]. B. Widrow and S. E. Stearns, "Adaptive Signal Processing," Prentice Hall Inc. Englewood Cliffs, NJ 1985.
- [17]. L. Ljung and T. Soderstrom, "Theory and Practice of Recursive Iden-

tification," The MIT Press, Cambridge, Mass. 1983.

[18]. G. E. P. Box and G. M. Jenkins, "Time Series Analysis," Forecasting and Control, Holdenday Inc., San Francisco, 1970.

[19]. J. C. Chow, "On the Estimation of the Order of a Moving Average Process," IEEE Trans. Autom. Control, vol. AC-17, pp. 386-387, June 1972a.

[20]. J. A. Cadzow, "Autoregressive Moving Average Estimation: A Model Equation Error Procedure," IEEE Trans. Geosci. Remote Sensing, vol. GE-19, pp. 24-28, Jan. 1981.

[21]. _____, "Spectral Estimation: An Overdetermined Rational Model Equation Approach," Proc. IEEE, vol. 70, pp. 907-938, Sept. 1982.

[22]. R. Kumaresan, "On the Zeros of the Linear Prediction Filter for Deterministic Signals." IEEE Trans. ASSP, vol. ASSP-31, pp. 217-220, Feb. 1983.

[23]. B. DeProny, "Essai Experimental et Analytique ... etc.," J. E. Polytechnique, vol. 1, no. 2, pp. 24-76, 1795.

[24]. M. A. Rahman and K. B. Yu, "Improved Frequency Estimation Using Total Least Squares Approach," Proc. 1986 IEEE ICASSP, pp. 1397-1400, Tokyo, Japan, April 1986.

[25]. J. Capon, "High Resolution Frequency-Wavenumber Spectrum Analysis," Proc. IEEE, vol. 57, pp.1408-1418,

[26]. _____, "Maximum Likelihood Spectral Estimation." Chap. 5 in Non-linear Methods of Spectral Analysis, 2nd Ed, S. Haykin. ed., Spring-Verlag, NY 1983.

[27]. W. F. Gabriel, "Spectral Analysis and Adaptive Array Processing." Proc. IEEE, vol. 68, no. 6, pp.654-666, June 1980.

[28]. R. O. Schmidt, "A Signal Subspace Approach to Multiple Emitter Location and Spectral Estimation," Ph.D dissertation, Stanford University, Nov. 1981.

[29]. _____, "Multiple Emitter Location and Signal Parameter Estimation," IEEE Trans. Antennas Prop., vol. AP-34, pp. 276-280, March 1986.

[30]. G. Bienvenu, "Influence of the Spatial Coherence of the Background on High Resolution Passive Methods," Proc. IEEE ICASSP, pp. 306-309, Washington, D.C., April 1979.

[31]. T. J. Shan et al., "On Spatial Smoothing for Direction of Arrival Estimation of Coherent Signals." IEEE Trans. ASSP, vol. ASSP-33, no. 4, pp. 806-811, Aug. 1985.

[32]. A. J. Barabell, "Improving the Resolution Performance of Eigenstructure-Based Direction Finding Algorithms." Proc. IEEE ICASSP, pp.

336-339, Boston, 1983.

[33]. V. F. Pisarenko, "The Retrieval of Harmonics from a Covariance Function," Geophys. Tourn. Royal Astro. Soc., vol. 33, 1973.

[34]. H. Akaike, "A New Look at the Statistical Model Identification," IEEE Trans. Automat. Cont., vol. AC-19, pp. 716-723, Dec. 1974.

[35]. M. S. Bartlett, "A Note on the Multiplying factors for various κ^2 Approximations," J. Roy Stat. Soc., ser. B, vol. 16, pp. 296-298, 1954.

[36]. J. Rissanen, "Modeling by Shortest Data Description Length," Automatica, vol. 14, pp. 417-431, 1978.

[37]. _____, "Consistent Order Estimation of Autoregressive Process by Shortest Description of Data," in Analysis and Optimization of Stochastic Systems, ed. Jacobs et al., NY, Academic Press, 1980.

[38]. _____, "A Universal Prior for the Integers and Estimation by Minimum Description Length," Ann. of Stat., vol. 11, pp. 417-431, 1983.

[39]. M. Wax and T. Kailath, "Detection of Signals by Information Theoretic Criteria," IEEE Trans. ASSP, vol. ASSP-33, no. 2, pp. 387-392, April 1985.

[40]. L. C. Zhao et al., "Remarks on Certain Criteria for Detection of Number of Signals," IEEE Trans. ASSP, vol. ASSP-35, no. 2, pp. 129-132, Feb. 1987.

[41]. Y. Q. Yin and P. K. Krishnaiah, "On Some Non Parametric Methods for Detection of the Number of Signals," IEEE Trans. ASSP, vol. ASSP-35, no. 11, pp. 1523-1538, Nov. 1988.

[42]. V. Shahmirian and S. B. Kesler, "Detection of Signals by SVD-Based Information Theoretic Criteria," Proc. 30th Midwest Symposium on Circuits and Systems, pp. 567-570, Syracuse, NY, 1987.

[43]. A. Paulraj, R. Roy and T. Kailath, "Estimation of Signal Parameters via Rotation Invariance Technique-ESPRIT," Proc. 19th Asilomar Conf. Circuits, Syst. and Computers, pp. 83-89, Pacific Grove, CA, Nov. 1985.

[44]. R. Roy and T. Kailath, "ESPRIT-Estimation of Signal Parameters Via Rotational Invariance Techniques," IEEE Trans. ASSP, vol. ASSP-37, no. 7, pp. 984-995, July 1989.

[45]. R. Roy, "ESPRIT Estimation of Signal Parameters via Rotation Invariance Technique," Ph.D dissertation, Stanford University, August 1987.

[46]. H. Ouibrahim, "Prony, Pisarenko and the Matrix Pencil: A Unified Presentation," IEEE Trans. ASSP, vol. ASSP-37, no. 1, pp. 33-34, January 1988.

[47]. S. Mayrargue, "ESPRIT and TAM Are Theoretically Equivalent," Proc. IEEE ICASSP, pp. 2456-2459, New York 1988.

- [48]. _____, "On the Common Structure of Several Well Known Methods for Harmonic Analysis and Direction of Arrival Estimation Induced by a New Version of ESPRIT," Proc. 4th ASSP Workshop on Spectrum Estimation and Modeling, pp. 307-311, Minneapolis, Minnesota, Aug. 1988.
- [49]. S. Y. Kung et al., "State Space and Singular Value Decomposition-Based Approximation Methods for the Harmonic Retrieval Problem," Journal Opt. Soc. Am., vol. 73, no. 12, Dec. 1983.
- [50]. _____, "New State Space and SVD-Based Approximate Modeling Methods for Harmonic Retrieval," IEEE 2nd ASSP Workshop on Spectrum Estimation, pp. 266-271, Tampa, Florida, 1983.
- [51]. R. Kumaresan and D. Tufts, "Estimating the Parameters of Exponentially Damped Sinusoids and Pole-Zero Modeling in Noise," IEEE Trans. ASSP, vol. ASSP-30, no.6 pp. 833-840, Dec. 1982.
- [52]. _____, "Estimating the Angles of Arrival of Multiple Plane Waves," IEEE Trans. AES, vol. AES-19, no. 1, pp.134-139, Jan. 1983.
- [53]. G. Su and M. Morf, "Modal Decomposition Signal Subspace Algorithms," Proc. IEEE ICASSP, pp. 340-343, Boston, 1983.
- [54]. _____, "Modal Decomposition Signal Subspace Algorithms," IEEE Trans. ASSP, vol. ASSP-34, no. 3, pp. 585-602, June 1986.
- [55]. M. Wax et al., "Spatio-Temporal Spectral Analysis by Eigenstructure Methods," IEEE Trans. ASSP, vol. ASSP-32, no. 4, pp. 817-827, Aug. 1984.
- [56]. H. Wang and M. Kaveh, "Coherent Signal Subspace Processing for the Detection and Estimation of Angles of Arrival of Multiple Wideband Sources," IEEE Trans. ASSP, vol. ASSP-33, no. 4, pp. 823-831, June 1985.
- [57]. H. Hung et al., "Further Results on Coherent Signal-Subspace Processing," Proc. 3rd ASSP Workshop on Spectrum Estimation and Modeling, pp. 97-100, Nov. 1986.
- [58]. K. Buckley and L. J. Griffiths, "Broadband Signal-Subspace Spatial-Spectrum (BASS-ALE) Estimation," IEEE Trans. ASSP, vol. ASSP-36, no. 7, pp. 953-964, July 1988.
- [59]. _____, "Eigenstructure Based Broadband Source Location Estimation," Proc. IEEE ICASSP, pp. 1869-1872, Tokyo, Japan, 1986.
- [60]. A. K. Shaw and R. Kumaresan, "Estimation of Angles of Arrival of Broadband Signals," Proc. IEEE ICASSP, pp. 2296-2299, Dallas, TX, 1987.
- [61]. B. Ottersten and T. Kailath, "ESPRIT for Wideband Signals," Proc. 21st Asilomar Conf. Circuits, Syst. and Computers, pp. , Monterey, CA, Nov. 1987.
- [61]. _____, "Direction of Arrival Estimation for

Wideband Signals Using the ESPRIT Algorithm," IEEE Trans. ASSP, vol. ASSP-38, no. 2, pp. 317-327, Feb. 1990.

[62]. H. Hung and M. Kaveh, "Focussing Matrices for Coherent Signal Subspace Processing," IEEE Trans. ASSP, vol. ASSP-36, no. 8, pp. 1272-1281, Aug. 1988.

[63]. _____, "Coherent Wideband ESPRIT Method for Direction of Arrival of Multiple Wideband Sources," IEEE Trans. ASSP, vol. ASSP-38, no. 2, pp. 354-360, Feb. 1990.

[64]. H. Wang and M. Kaveh, "On the Performance of Signal Subspace Processing - Part II: Coherent Wideband Systems," IEEE Trans. ASSP, vol. ASSP-35, no. 11, pp. 1583-1591, Nov. 1987.

[65]. H. Wang and J-X. Zhu, "On Performance Improvement of Tone Frequency Estimation in Active Radar/Sonar Systems with non fluctuating Targets," IEEE Trans. ASSP, vol. ASSP-36, no. 10, pp. 1582-1591, Oct. 1988.

[66]. H. Wang and C. C. Li, "A Channel Efficient Method for High Resolution Active Direction Finding of Multiple Sources," IEEE Trans. ASSP, vol. ASSP-36, no. 8, pp. 1367-1369, Aug. 1988.

[67]. V. U. Reddy et. al., "Performance Analysis of the Optimum Beamformer in the Presence of Correlated Sources and Its Behavior Under Spatial Smoothing," IEEE Trans. ASSP, vol. ASSP-35, no. 7, pp. 927-936, July 1987.

[68]. T. J. Shan et. al., "On Rank Profile Tests in Eigenstructure Methods for Direction of Arrival Estimation," IEEE Trans. ASSP, vol. ASSP-35, no. 10, pp. 1377-1385, Oct. 1987.

[69]. Y. Hua and T. K. Sarkar, "Perturbation Analysis of T.K Method for Harmonic Retrieval Problems," IEEE Trans. ASSP, vol. ASSP-36, no. 2, pp. 228-240, Feb. 1988.

[70]. B. D. Rao, "Relationship between Matrix Pencil and State Space Based Harmonic Retrieval Methods," IEEE Trans. ASSP, vol. ASSP-38, no. 1, pp. 177-179, Jan. 1990.

[71]. _____, "Perturbation Analysis of an SVD-Based Linear Prediction Method for Estimating the Frequencies of Multiple Sinusoids," IEEE Trans. ASSP, vol. ASSP-36, no. 7, pp. 1026-1035, July 1988.

[72]. B. D. Rao and K. V. S. Hari, "Performance Analysis of Root MUSIC," IEEE Trans. ASSP, vol. ASSP-37, no. 12, pp. 1939-1949, Dec. 1989.

[72]. _____, "Performance Analysis of ESPRIT and TAM in Determining the Direction of Arrival of Plane Waves," IEEE Trans. ASSP, vol. ASSP-37, no. 12, pp. 1990-1995, Dec. 1989.

[73]. J. P. LeCadre, "Parametric Methods for Spatial Processing in the Presence of Unknown Colored Noise Fields," IEEE Trans. ASSP, vol. ASSP-37, no. 7, pp. 965-983, July 1989.

- [74]. M. Wax and I. Ziskind, "On unique Localization of Multiple Sources by Passive Sensor Arrays," IEEE Trans. ASSP, vol. ASSP-37, no. 7, pp. 996-1000, July 1989.
- [75]. _____, "Detection of the Number of Coherent Signals by the MDL Principle," IEEE Trans. ASSP, vol. ASSP-37, no. 8, pp. 1190-1196, Aug. 1989.
- [76]. Q. T. Zhang et. al., "Statistical Analysis of the Performance of Information Theoretic Criteria in the Detection of Signals in Array Processing," IEEE Trans. ASSP, vol. ASSP-37, no. 10, pp. 1957-1967, Oct. 1989.
- [77]. S. U. Pillai and F. Haber, "Statistical Analysis of a High Resolution Spatial Spectrum Utilizing an Augmented Covariance Matrix," IEEE Trans. ASSP, vol. ASSP-35, no. 11, pp. 1517-1523, Nov. 1987.
- [78]. R. T. Williams et. al., "An Improved Spatial Smoothing Technique for Bearing Estimation in a Multipath Environment," IEEE Trans. ASSP, vol. ASSP-36, no. 4, pp. 425-432, April 1988.
- [79]. P. Stoica and A. Nehorai, "MUSIC, Maximum Likelihood and Cramer-Rao Bound," IEEE Trans. ASSP, vol. ASSP-37, no. 5, pp. 720-741, May 1989.
- [80]. I. J. Gupta and A. A. Ksienski, "Effect of Mutual Coupling on the Performance of Adaptive Arrays," IEEE Trans. Antennas and Propagation, vol. AP-31, no. 5, pp. 785-791, Sept. 1983.
- [81]. C. C. Yeh and H. L. Leou, "Estimating Angles of Arrival in the Presence of Mutual Coupling," IEEE AP-S Int. Symposium, vol. 2, pp. 862-865, Blacksburg, VA, 1987.
- [82]. D. H. Shau, "Effects of Mutual Coupling on the Direction Finding Performance of a Linear Array in a Multiple Source Environment Using the Method of Moments," Ph.D dissertation, Syracuse University, May 1988.
- [83]. A. T. Adams, "An Introduction to the Method of Moments," RADDC, TR-73-217, vol. 1, Aug. 1974.
- [84]. R. F. Harrington, "Field Computation by Moment Methods," Macmillan, N.Y, 1968.
- [85]. G. W. Stewart, "Perturbation Theory For The Generalized Eigenvalue Problem," Recent Advances in Numerical Analysis, Ed. C.deBoor and G. H. Golub, Academic Press, N.Y. pp. 193-206, 1978.
- [86]. _____, "On The Sensitivity Of The Eigenvalue Problem $Ax = \lambda Bx$," SIAM J. Numer. Anal., vol. 9, pp. 669-686, 1972.
- [87]. _____, "Gershgorin Theory For The Generalized Eigenvalue problem $Ax = \lambda Bx$," Math. Comp., vol. 29, pp. 600-606, 1975
- [88]. G. H. Golub and C. F. Van Loan, "Matrix Computations," Baltimore, Maryland, The John Hopkins University Press, 1985.

[89]. B. Porat and B. Friedlander, "Computation of The Exact Information Matrix of Gaussian Time Series With Stationary Random Components," IEEE Trans. ASSP, vol. ASSP-34, no.1, pp.118-130, Feb. 1986.

BIOGRAPHY

NAME	Braham Himed
DATE AND PLACE OF BIRTH	January 21, 1961, Algiers, Algeria.
ELEMENTARY SCHOOL	Ecole Paul Doumer, Algiers, Algeria. Graduate 1972.
PRE HIGH SCHOOL	C.E.M. Chateauneuf, Algiers, Algeria. Graduate 1976.
HIGH SCHOOL	Lycee El-Mokrani, Algiers, Algeria. Graduate 1979.
COLLEGE	Ecole Nationale Polytechnique, Algiers, Algeria. Graduate 1984.
GRADUATE WORK	Syracuse University Syracuse, New York. Research Assistant: 1987-1989. Teaching Assistant: 1989-1990.



**MISSION
OF
ROME LABORATORY**

Rome Laboratory plans and executes an interdisciplinary program in research, development, test, and technology transition in support of Air Force Command, Control, Communications and Intelligence (C³I) activities for all Air Force platforms. It also executes selected acquisition programs in several areas of expertise. Technical and engineering support within areas of competence is provided to ESD Program Offices (POs) and other ESD elements to perform effective acquisition of C³I systems. In addition, Rome Laboratory's technology supports other AFSC Product Divisions, the Air Force user community, and other DOD and non-DOD agencies. Rome Laboratory maintains technical competence and research programs in areas including, but not limited to, communications, command and control, battle management, intelligence information processing, computational sciences and software producibility, wide area surveillance/sensors, signal processing, solid state sciences, photonics, electromagnetic technology, superconductivity, and electronic reliability/maintainability and testability.